THE UNIVERSITY *of* EDINBURGH

S-Nitrosylation in Immunity and Fertility: A General Mechanism Conserved in Plants and Animals

Krieng Kanchanawatee

Doctor of Philosophy

The University of Edinburgh

2012

Abstract

Post-translational modification is an intracellular process that modifies the properties of proteins to extend the range of protein function without spending energy in *de novo* peptide synthesis. There are many post-translational modifications, for example, phosphorylation, ubiquitination, and *S*-nitrosylation. *S*-Nitrosylation is a post-translational modification which adds nitric oxide (NO) to sulfhydryl groups at cysteine residues to form *S*-nitrosothiol (SNO), and is required for plant immunity and fertility. Cellular NO changes between a pool of free NO and bound SNO. During pathogen infection, nitrosative stress in plants is mainly controlled by *S*-nitrosothiolglutathione reductase (GSNOR) via the decomposition of GSNO. GSNOR is an alcohol dehydrogenase type 3 (ADH3) which has both GSNOR and formaldehyde dehydrogenase (FDH) activities. The roles of *S*-nitrosylation in mammals overlap with those in plants. This conservation led us to explore the relationship between *S*-nitrosylation, immune response, and fertility in *Drosophila melanogaster* as it might prove to be a good genetic model for further analysis of the role of *S*-nitrosylation in animals. I have identified *fdh* as the likely *gsnor* in *D. melanogaster* and have knocked this out using an overlapping deficiency technique in order to observe the effect on immunity and fertility. There are two main pathways in the *Drosophila* innate immune response, the Toll pathway for protecting against gram-positive bacteria and fungi, and the Imd pathway against gram-negative bacteria. I have investigated the effect of removing GSNOR on sensitivity to gram-negative bacteria (*Escherichia coli* and *Erwinia carotovora*) by septic and oral infection, and to fungi (*Beauveria bassiana*). Susceptibility to infection by the gram negative bacteria was similar to wild-type but susceptibility to *B. bassiana* was increased. This increase in susceptibility correlated with reduced anti-fungal antimicrobial peptide (AMP) production after *B. bassiana* infection. This suggests that GSNOR might be required for the normal activity of the Toll pathway or novel Toll-independent processes. We also observed that *gsnor* knockout impairs fertility and development of embryos.

Declaration

I hereby declare that the work presented here is my own and has not been submitted in any form for any degree at this or any other university.

Krieng Kanchanawatee

Acknowledgements

I would like to thank the Development and Promotion of Science and Technology Talents Project, The Royal Thai Government for financial support throughout my PhD.

I would not have come this far without superb support from both of my supervisor Prof. David Finnegan and Prof. Gary Loake.

Hi David, first of all thank you very much for introducing fruit flies to me, and making me fall in love with this adorable creature and realise how useful flies are as a genetic model. Thank you very much for always being there whenever I need. I am indebted for your guidance, knowledge, great vision and everything that you have given me. It is invaluable experience and my honour to work under your supervision. What I have learnt from you is not only in science, but more importantly how to be a good scientist.

Hi Gary, thank you for giving me an opportunity for studying PhD in your lab. Although my plant project did not go as we expected, I had still gained excellent support from you in my fly project. Thank you for giving me a freedom to design and plan my PhD project as well as always willing to help me every time I knock at your office door. Everything that I have learnt from you will certainly mould my future scientific career.

To Dr. Steven Spoel, thank you very much Steven for helping so many times. Without you I would not have succeeded in SNO experiment. You are incredibly talented man (with a cool hairstyle). I learn something every time I talk with you.

To Dr. Byung-Wook Yun, without you the beginning of my PhD would have been very difficult. Thanks for all the technical guidance that you have given me.

I would like to thank Dr. Matt Tinsley from University of Sterling for kindly providing the Beauveria strain and for a guidance of how to manipulate this fungi. Thank you for anti-Psh antibody as a kind gift from Dr. Dominique Ferrandon, University of Strasbourg, France and *Relish*, *Spaetzle* and *imd* flies from Prof. Bruno Lemaitre, Ecole polytechnique fédérale de Lausanne, Switzerland. Also thanks to Dr. Garry Blakely for kindly providing the *E. coil* strain.

Thanks to Prof. Hiro Ohkura and Prof. Mary Bownes for giving discussion about my fertility-related phenotypes. Thanks to Dr. Giusy Pennetta for kindly providing antibodies and eye-specific drivers. Also thanks to Dr. Ian Chamber for showing me how to search for regulatory sequences.

Thank you to all past and present members in Loake lab: Adil, Corin, Debbie, Eunjung, Hannah, James, John, Kerstin, Kirsti, Manda Michael, Minghui, Noor, Priya, Rabia, Rafael, Rumana, Saad, Suzy, Thomas, Usman, Yan and Yuan.

Special thanks to John Moore, my main man, for proofreading this thesis and always keeping me amused, and also Eunjung Kwon for always making a cheerful day in the lab.

I would like to thank Chaweewan Sapcharoenkun for being such a good company and always helping me in all kinds of situation. Thanks to Wanaruk Chaimayo and Pimsuda Sakolvipas for proofreading.

Finally, I would like to thank my parents and my brother for always supporting me, no matter what. Your advice and encouragement always keep me going forward.

Table of Contents

Abbreviations

[-]	No pretreatment
[SF, Hg]	with the SF and $HgCl_2$ pretreatment
[SF]	with the SF pretreatment
·OH	Hydroxyl radical
acetic/KI/$CuSO_4$	10 mg/mL potassium iodide and 4 mM copper (II) sulfate in 80 %v/v acetic acid at 70˚C
*Act*5C-*GAL4*	*Actin5C-GAL4*
ADH3	Type III alcohol dehydrogenase
AHb1	Arabidopsis class-1 haemoglobin
AMP	Antimicrobial peptide
APS	Ammonium persulfate
At-NOS1	*Arabidopsis thaliana* nitric oxide synthase
AtSABP3	*Arabidopsis thaliana* salicylic acid-binding protein 3
Att	Attacin
A_X	Absorbance at wavelength X nm
b	*black*
βGRP	β-glucan recognition protein
BH4	Tetrahydrobiopterin
biotin-HPDP	*N*-[6-(biotinamido)hexyl]-3'-(2'-pyridyldithio)propionamide
BSA	Bovine serum albumin
BST	Biotin switch technique
CDS	Coding sequence
Cec	Cecropin
cGMP	Cyclic guanosine monophosphate
CIAP	Calf intestinal alkaline phosphatase
CO_2	Carbon dioxide
CTE	C-terminal extension
CuCl	Copper (I) chloride
CuCl/Ascorbic acid	0.2 mM copper (I) chloride with 50 mM ascorbic acid at 37˚C
CuCl/Cys	Saturated copper (I) chloride and 1 mM cysteine at 50˚C
Cys	Cysteine
CysNO	*S*-Nitrosocysteine
DAF	24,5-Diaminofluorescein
DAF-2T	Triazolofluorescein
Da-GAL4	*Daughterless-GAL4*
DAP-PGN	Diaminopimelic acid type PGN

Def	Defensin
DEPC	Diethylpyrocarbonate
Df7305	*Df(3R)Exel7305*
Df7306	*Df(3R)Exel7306*
DIAP2	Drosophila inhibitor of apoptosis 2
DMSO	Dimethyl sulfoxide
dNTPs	Deoxynucleotide triphosphates
Dpt	Diptericin
Dro	Drosocin
Drs	Drosomysin
dsRNA	Double stranded RNA
DTT	Dithiothreitol
DUOX	Dual oxidase
*Ecc*15	*Erwinia carotovora* pv. *carotovora* 15
EDTA	Ethylenediaminetetraacetic acid
EMS	Ethylmethane sulfonate
eNOS	Endothelial nitric oxide synthase
EP-gsnor	*gsnor* with upstream and downstream non-coding regions
Evf	Erwinia virulence factor
FAD	Flavin adenine dinucleotide
fdh	*formaldehyde dehydrogenase*
FGSH	Formylglutathione
FMN	Flavin mononucleotide
GAPDH	Glyceraldehyde-3-phosphate dehydrogenase
GFP	Green fluorescent protein
GNBP-1	Gram-negative bacteria binding protein 1
GPX	Glutathione peroxidase
GS-FDH	Glutathione dependent formaldehyde dehydrogenase
GSH	Glutathione
GSNHOH	Semimercaptale
GSNO	*S*-Nitrosoglutathione
GSNOR	*S*-Nitrosoglutathione reductase
GSO_2H	Glutathione sulfinic acid
GSO_3H	Glutathione sulfonic acid
$GSONH_2$	Glutathione sulfanamide
GSSG	Glutathione disulfide
GST	Glutathione transferase
GTP	Guanosine-5'-triphosphate
H^+	Proton
HCl	Hydrochloric acid

HEPES	4-(2-hydroxyethyl)-1-piperazineethanesulfonic acid
Hg	Mercury
$HgCl_2$	Mercury (II) chloride
HMGSH	Hydroxymethylglutathione
HPLC	High-pressure liquid chromatography
HRP	Horseradish peroxidase
hsp70	Heat shock protein 70
Hu	*Humeral*
I_3^-	Triiodide ion
IgG	Immunoglobulin G
IκB	Inhibitor of nuclear factor-kappaB
IKKβ	IκB kinase β
imd	*immune deficiency*
iNOS	Inducible nitric oxide synthase
IPTG	Isopropyl β-D-1-thiogalactopyranoside
IRAK	IL-1R-associated kinase
JNK	Jun N-terminal kinases
K_2HPO_4	Potassium hydrogen phosphate
$K_3[Fe(CN)_6]$	Potassium ferricyanide
KI	Potassium iodide
KPi buffer	Potassium phosphate buffer
LB	Luria-Bertani
LC-MS	Liquid chromatography–mass spectrometry
LiCl	Lithium chloride
LPS	Lipopolysaccharide
LTP	Long term potentiation
Lys	Lysine
Lys-PGN	lysine-type PGN
$MgSO_4 \cdot 7H_2O$	Heptahydrated magnesium sulfate
MMTS	Methyl methanethiosulfonate
Mod-SP	Modular serine protease
MOPS	3-(*N*-morpholino)propanesulfonic acid
MSC	Multi-cloning sites
Mtk	Metchnikowin
mtNOS	Mitochondrial nitric oxide synthase
N_2O_3	Nitrous anhydride
Na_3VO_4	Sodium orthovanadate
NaCl	Sodium chloride
NADH	Nicotinamide adenine dinucleotide
NADPH	Reduced nicotinamide adenine dinucleotide phosphate

NaF	Sodium fluoride
$NaNO_2$	Sodium nitrite
NaPi buffer	Sodium phosphate buffer
NBT	Nitroblue tetrazolium
Nec	Necrotic
NED	*N*-1-Naphthylethylenediamin
NEM	*N*-Ethylmaleimide
NF-κB	Nuclear factor-kappaB
NH_2OH	Hydroxylamine
nNOS	Neuronal nitric oxide synthase
NO	Nitric oxide
NO_2^*	Excited NO_2
NO_2^-	Nitrite
NOA	Nitric oxide analyzer
NOA	Nitric oxide associated protein
NOS	Nitric oxide synthase
NPR1	Non-expressor of pathogenesis related gene 1
O_2	Oxygen
O_2^-	Superoxide
O_3	Ozone
OD	Optical density
OH^-	Hydroxyl ions
$ONOO^-$	Peroxynitrite
PAGE	Polyacrylamide gel electrophoresis
PBS	Phosphate buffered saline
PBS-T	Phosphate buffered saline with 0.1%v/v Tween-20
PDA	Potato dextrose agar
PGN	Peptidoglycan
PGRP	Peptidoglycan receptor protein
PHGPX	Phospholipid hydroperoxide glutathione peroxidase
PMS	Phenazine methosulfate
PMSF	Phenylmethanesulfonylfluoride
PO	Phenol oxidase
pr	*purple*
ProPO	Pro-phenol oxidase
PRR	Pathogen recognition receptor
Psh	Persephone
Pst	*Pseudomonas syringae* pv. tomato strain DC3000
PTM	Post-translational modification
qRT-PCR	Quantitative reverse transcription PCR

RbCl	Rubidium chloride
rcf	Relative centrifugal force
RE	Regulatory element
RHD	Rel homology domain
RHIM	Homotypic interaction motif
RIP	Receptor-interacting protein
RISC	RNA-inducing silencing
ROI	Reactive oxygen intermediate
ROS	Reactive oxygen species
Rp49	Ribosomal protein 49
rpm	Revolutions per minute
RT-PCR	Reverse transcription PCR
S	Sulfur
SAR	Systemic acquired resistance
SDS	Sodium dodecyl sulphate
SE	Standard error
SF	Sulfanilamide
SNO	*S*-Nitrosothiol
SNP	Sodium nitroprusside
SO_2H	Sulphinic acid
SO_3H	Sulphonic acid
SOH	Sulphenic acid
SPE	Spaetzle processing enzyme
Spz	Spaetzle
SS	Disulfide
SSCs	Spermathecal secretory cells
SUMO	Small ubiquitin-like modifier
TAE	Tris-acetate-EDTA buffer
TAG	Thoracic abdominal ganglion
Tb	*Tubby*
TEMED	*N*,*N*,*N*′,*N*′-tetramethylethylenediamine
TIR	Toll and interleukin-1 receptor
TLR	Toll-like receptor
tri-iodide	10 mg/mL KI and 6.5 mg/mL I_2 in acetic acid at 50˚C
Tris-HCl	Tris(hydroxymethyl)aminomethane adjusted pH by hydrochloric acid
Trx	Thioredoxin
TrxR	Thioredoxin reductase
Tub-GAL4	*Tubulin-GAL4*
Tween-20	Polysorbate 20

Tyr	Tyrosine
UAS	Upstream activation sequences
UAS-gsnor	UAS linked with *gsnor* coding sequence
UTR	Untranslated region
UV	Ultraviolet
X-gal	5-Bromo-4-chloro-indolyl-β-D-galactopyranoside
XNO	Metal nitrosylation

Chapter 1 Introduction

It is undeniable that well-being of human populations is one of the ultimate objectives for scientists to achieve. One of the aspects leading to this crucial goal is to understand how immunity works. If we understand the basic biology of immunity conserved throughout every organism, we will be able to harness this knowledge and apply it not only to cure and protect ourselves from diseases but also for livestock and agricultural crops. Moreover, understanding pathogen and pest immune responses allows us to control and eliminate infectious diseases of humans, crops and livestock. Nitric oxide (NO) is produced after an infection in both plants and animals (Nappi et al., 2000; Coleman, 2001) suggesting that the production of NO is a very important mechanism underlying plant and animal immunity.

1.1 Post-translational modification: a keystone mechanism for biological complexity

Post-translational modification (PTM) is a key mechanism underlying biological complexity. PTM is an intracellular process that modifies the properties of proteins to extend the range of protein function without adding new genes to the genome. Due to the fact that PTM modifies protein functions without *de novo* peptide synthesis, this allows an organism to have quicker and more flexible responses. It has been estimated that in human genome there is about 30,000 protein coding genes. Due to transcription initiation at alternative promoters, differential transcription termination, mRNA editing and alternative splicing, the number of different mRNAs is increased to five to six times (Jensen, 2004). Together with PTM which generates about eight to ten different modifications on a polypeptide, about 1,800,000 different protein species in total are generated (Jensen, 2004) (Figure 1-1).

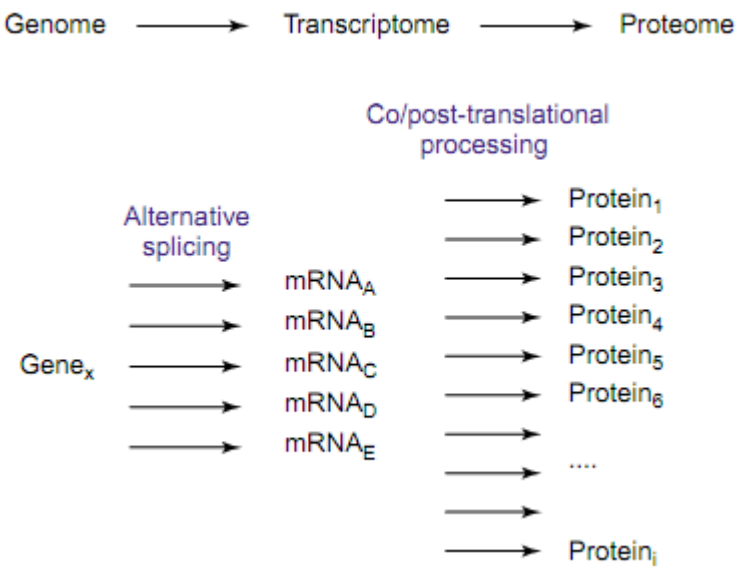

Figure 1-1. The increase in complexity from the genomic to the proteomic level based in humans. This figure is taken from Jensen (2004).

PTMs can be mainly categorised into cleavage of protein backbone, for example the activation of zymogens, and covalent modification (Walsh et al., 2005). The large number of modifications falls into the covalent modification category. However, it is noteworthy that the removal of PTM is equally important in regulating protein function. In this section, I will briefly describe the well known PTMs.

Phosphorylation is the addition of phosphate group to serine, threonine or tyrosine by a protein kinase. This is a reversible process which is controlled by a phosphatase. Phosphorylation is involved in many biological processes, such as cell cycle, cell growth, apoptosis and signal transduction processes (Tarrant and Cole, 2009).

Glycosylation is the addition of sugars to hydroxyl group of serine and threonine (*O*-linked glycosylation) and to amino group of asparagines (*N*-linked glycosylation). The added sugars range from a simple monosaccharide to a complex branched polysaccharide. The protein glycosylation affects a wide range of biological processes, from protein structural roles to molecular trafficking, self-recognition and clearance of unwanted proteins (Mariño et al., 2010).

Methylation is the addition of methyl group from the methyl donor *S*-adenosyl methionine to amino group of lysine and arginine by methyltransferase enzymes. Methylation increases the hydrophobicity of target proteins, and is a reversible process. The methylated lysine has been well studied in the aspect of the chromatin remodeling by histone methylation. The methylated arginine is a competitive inhibitor of nitric oxide synthase (NOS), the main enzyme for producing NO (which will be described in more details in the next section), so the function of arginine methylation shares some similarities with the function of NO, such as cell proliferation, signal transduction and protein-protein interaction. Chromatin remodeling and mRNA splicing are also affected by arginine methylation (Paik et al., 2007).

Acetylation is the addition of acetyl group to lysine residual of target proteins. The addition of acetyl group neutralizes the positive charge on the amino group resulting in the change of protein electrostatic properties. Acetylation is well

known for the decrease of chromatin condensation to promote transcription. However, acetylation targets also include transcription factor, cytoskeletal proteins, molecular chaperones and nuclear import factors. These targets are involved in a wide range of biological processes expanding the function of acetylation beyond the role in transcription regulation (Glozak et al., 2005).

Lipidation is the addition of lipids to target proteins which enhances the hydrophobicity resulting in the increased affinity toward organelles, vesicles and plasma membranes. The specific membrane affinity of lipidation depends on the lipids concerned. Some types of lipidation, such as *S*-palmitoylation, *S*-farnesylation and *S*-geranylgeranylation add lipid composed of 16, 15 and 20 carbons respectively, to cysteine residuals (Nadolski and Linder, 2007).

Ubiquitination and ubiquitin-like modification are the addition of ubiquitin or ubiquitin-like proteins to lysine residuals of target proteins; however, this modification can also occur with other amino acid residuals with less frequent, such as cysteine residuals. Ubiquitination and other ubiquitin-like modifications are generally regulated by specific activating enzymes, ubiquitin (or ubiquitin-like) -conjugating enzymes, and protein ligases (Kerscher et al., 2006). Ubiquitination may result in proteosome-mediated degradation or signal transduction (Kerscher et al., 2006). While ubiquitin-like proteins, such as small ubiquitin-like modifier (SUMO) are involved in protein localization, regulation of their target genes, and interactions with other molecules (Andreou and Tavernarakis, 2009).

Proteolysis or the cleavage of protein backbone can switch on its target protein by the proteolytic activation of zymogens or switch off by the degradation of unwanted proteins. Frequently, proteolysis is involved in protein conformational changes. This may affect protein localization and length of activity. Enzymes that cleave polypeptides are proteases. Most proteases fall into serine proteases, cysteine proteases, aspartic acid proteases, threonine proteases and metalloproteases (López-Otín and Overall, 2002).

S-Nitrosylation is the addition of NO to a thiol of cysteine residuals. This PTM will be described further in this chapter.

1.2 Nitric oxide production

NO is a lipophilic molecule with small Stoke's radius and neutral charge, allowing it to diffuse easily through cell membranes (Goretski and Hollocher, 1988). These properties indicate potential roles in cell signalling. NO influences many cellular functions because it reacts with cysteine in many proteins to form *S*-nitrosothiols (SNOs). This changes the functions of these target proteins (Stamler, 1994). The NO signalling process is among the earliest and the most conserved in evolution from prokaryotes to higher eukaryotes (Torreilles, 2001).

Post-translation modification by NO can be oxidative or transnitrosylative. Oxidative modification, in which electrons are removed from reactants, can occur between NO and reactants like thiols, transition metals, or superoxide (O_2^-) to form molecules with a -NO group (SNO, XNO (X refers to a transition metal), and peroxynitrite ($ONOO^-$) respectively). Transnitrosylation is a reaction in which a -NO group from one molecule is transferred to another molecule, such as the transfer of a -NO group from SNO to glutathione (GSH) to produce *S*-nitrosoglutathione (GSNO) (Guikema et al., 2005).

1.2.1 Nitric oxide production in animals

The main source of NO is from the nicotinamide adenine dinucleotide (NADH)-dependent conversion of L-arginine to L-citrulline by members of the NOS enzyme family (Figure 1-2), and NOS activity is found in bacteria, yeast, protozoa, and metazoa. In mammals, there are three well-described NOSs: inducible nitric oxide synthase (iNOS), neuronal nitric oxide synthase (nNOS), and endothelial nitric oxide synthase (eNOS). Also found in animals is mitochondrial nitric oxide synthase (mtNOS) (Finocchietto et al., 2009). Protein *S*-nitrosylation is seen in plants as well as in animals, but the mechanism of NO synthesis in plants is unclear (Torreilles, 2001).

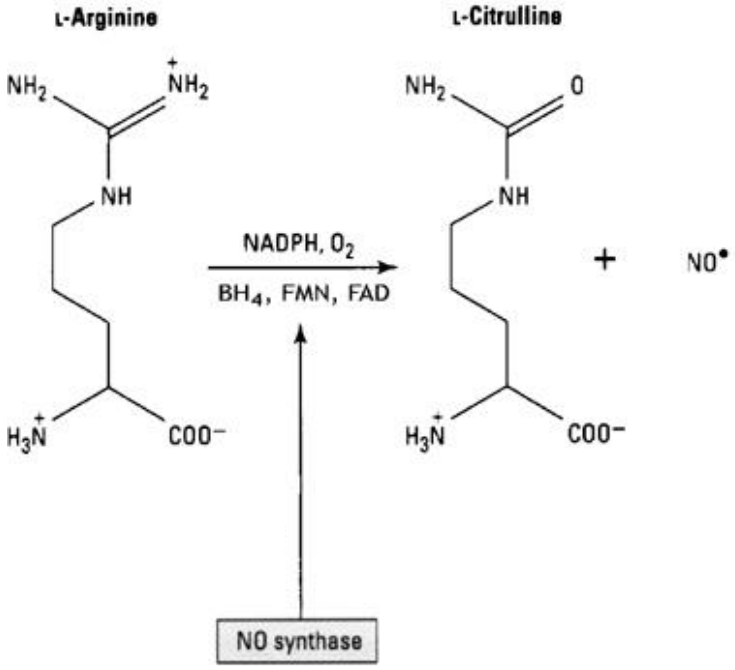

Figure 1-2. NO generation from L-arginine by NOS. NOS catalyses L-arginine to L-citrulline in the presence of O2 and the cofactors (reduced nicotinamide adenine dinucleotide phosphate (NADPH), tetrahydrobiopterin (BH4), flavin mononucleotide (FMN), and flavin adenine dinucleotide (FAD)). This figure is adapted from Ghalayini (2004).

NO can also be produced from nitrite (NO_2^-). This mechanism has been proposed as a backup source of NO, if NOS is impaired, such as in hypoxic condition. NO_2^- is more stable than NO, and NO_2^- is more than NO about 100-500 times. NO_2^- comes from three major routes: 1) dietary, 2) oxidation of NO and 3) reduction of nitrate (NO_3^-) by commensal bacteria. NO_2^- can be converted to NO non-enzymatically in acidic condition. Deoxy-haemoglobin, mitochondrial cytochromes and xanthine oxidase can also catalyzed the conversion of NO_2^- to NO (Lundberg and Weitzberg, 2005).

1.2.2 Nitric oxide production in plants

The production of NO in plants has been well-researched and documented, and is the result of two production processes, nitrite-dependent NO synthesis and L-arginine-dependent synthesis (Gas et al., 2009). Reduction of NO_2^- to NO by the enzyme nitrate reductase is not an efficient method (Yamasaki et al., 1999). Nitrate reductase is more efficiently used in catalyzing NO_3^- to NO_2^-. However, further mechanisms might be required to reduce NO_2^- to NO as introduction of exogenous NO_2^- can increase the NO level in *Arabidopsis thaliana nia1* and *nia2* mutants (the reduced nitrate reductase activity mutants) (Modolo et al., 2005). These mutants show that NO production by nitrate reductase is required for some physiological and developmental processes, but not in response to pathogen infection (Zhang et al., 2003), salicylic acid treatment (Zottini et al., 2007), and mechanical stress (Garcês et al., 2001). NO is also produced non-enzymatically in the apoplast (Bethke et al., 2004) and plastids (Cooney et al., 1994), in acidic and reducing environments.

NOS has been found in organisms from bacteria to mammals, except in plants. Despite this, NOS activity has been observed in plants. An important enzyme in L-arginine-dependent NO synthesis was previously known as *A. thaliana* nitric oxide synthase (At-NOS1), based on the homology with snail (*Helix pomatia*) NOS (Huang et al., 1997). The enzyme At-NOS1 seemed to explain NOS activity in *A. thaliana*, and so it seemed that NOS might also be present in other plants. Overexpression of At-NOS1 in *A. thaliana* enhanced the level of NOS activity and, in the same way, the loss-of-function mutant lowered the level of NOS activity (Guo et al., 2003). NOS1, however, has been re-named to nitric oxide associated protein

(NOA1) for three main reasons. 1) NOS1 is likely to produce NO for only some stimuli (Bright et al., 2006). 2) Exogenous NO complementation does not allow a *nos1* mutant to recover the wild-type phenotype (Flores-Pérez et al., 2008). 3) Bacteria homolog exhibits a lack of NOS activity (Sudhamsu et al., 2008).

NOA1 is similar in sequence to member of the P-loop guanosine-5'-triphosphate (GTP) binding protein family, which are involved in ribosome biosynthesis and translation (Leipe et al., 2002). The protein which is most similar to NOA1 is the YqeH protein of *Bacillus subtillis* which does not have NOS activity (Uicker et al., 2007). Interestingly, the entire protein complements the *noa1* mutant, while the GTP binding domain of the protein (without the C-terminal domain) does not. This suggests that both domains are required for NOA1 function and the GTP binding domain may not be involved in NO production, while the C-terminus, which functions in peptide and nucleic acid recognition for RNA binding, might be involved in NO production (Sudhamsu et al., 2008). In eukaryotes, NOA1 is found in mitochondria. This leads to the inference that NOA1 binds to ribosome and translates proteins in plastids (Zemojtel et al., 2006). Moreau et al. (2008) proposed that the NO synthesis from NOA1 may be a result from pleiotropic effects of defective plastids.

Aside from these processes, there are other pathways which might also contribute towards the production of NO. These include NO biosynthesis by xanthine oxidoreductase (Harrison, 2002), peroxidase (Boucher et al., 1992b), and cytochromes P450 (Boucher et al., 1992a).

1.3 Nitric oxide signalling via PTMs

1.3.1 Metal nitrosylation

Many proteins are nitrosylated at the transition metal atoms in their structure. One of the molecules believed to have a role in NO turnover is haeme, an iron (Fe) containing molecule. Haeme is prosthetic group of many proteins. In humans, haemes in haemoglobin have an important function in gas exchange. Nitrosylated haemes in haemoglobin play an important role in the regulation of vasodilation. NO can attach itself to deoxygenated haemes to form nitrosylated haemes. Together with

the transnitrosylation from nitrosylated haemes to cysteine (Cys) 93 on the β-chain of haemoglobin, NO is released from Cys 93 when oxygen (O_2) is released from haemoglobin. This released NO reduces vasodilation resulting in faster blood flow matching with low haemoglobin O_2 saturation which reflexes high tissue O_2 demand (Lima et al., 2010).

There are at least three types of plant haemoglobin which have been grouped as symbiotic (Appleby, 1984), nonsymbiotic (Dordas et al., 2003), and truncated (Watts et al., 2001). Nonsymbiotic haemoglobin is a ubiquitous molecule found in the plant kingdom that can be divided into two classes, class-1 and -2. Class-1 haemoglobin has a high affinity for O_2 and can be induced by hypoxia. Class-2 haemoglobin has a lower affinity for O_2 and can be induced by low temperature (Perazzolli et al., 2004). Class-1 haemoglobin in Arabidopsis (AHb1) can convert NO into NO_3^- with NADPH as the electron donor, especially in hypoxic stress, which enhances nitrate reductase activity to produce NO. However, the kinetics of this reaction are too slow to control the NO burst from events, such as hypersensitive response or pathogen invasion (Perazzolli et al., 2004).

In animals, guanylate cyclase is nitrosylated at the ferrous iron of haeme. This leads to a conformational change in the enzyme and enhances cyclic guanosine monophosphate (cGMP) production, the second signalling molecule. cGMP controls many cellular activities (Lucas et al., 2000). In plants, the NO-dependent guanylate cyclase remains unidentified. Studies show that cGMP is induced by NO signalling (Pfeiffer et al., 1994).

1.3.2 Tyrosine nitration

$ONOO^-$ can non-enzymatically react with the *o*-position of tyrosine to form a nitrotyrosine. In cell signalling, tyrosine nitration involves the introduction of a negative charge, which may alter the conformation of the target protein (Schopfer et al., 2003). This alteration is a biological marker for nitrosative stress (Corpas et al., 2008). Also, tyrosine nitration prevents tyrosine from being phosphorylated by tyrosine kinase (Schopfer et al., 2003).

To demonstrate that tyrosine nitration is important in plant immunity, a tobacco cell line treated with INF1, an elicitor secreted by *Phytophthora infestans*, causes an increase in $ONOO^-$ levels and nitrotyrosine production (Saito et al., 2006). Peroxiredoxin II E in Arabidopsis may be a detoxification enzyme for $ONOO^-$. A mutation in Peroxiredoxin II E contributes to an increase in tyrosine nitration (Romero-Puertas et al., 2007).

Tyrosine nitration is involved with animal immunity. In mammalian cells, the nuclear factor-kappaB (NF-κB) p65 is tyrosine nitrated at Tyr-66 and Tyr-152. This reduces the induction of defence related genes by increasing the association of NF-κB with its inhibitor IκB resulting in the sequestration of p65 in cytoplasm (Park et al., 2005).

1.3.3 *S*-Nitrosylation

S-Nitrosylation occurs when a cysteine thiol reacts with NO to form an SNO. SNO can be seen as one type of adaptation toward nitrosative and oxidative stress to prevent toxicity by cysteine NO-dependent electrophilic and oxidative modifications (Figure 1-3). The free thiol of cysteine is modified in order to control the cellular nitrosative and oxidative stress. The first level of the modifications is SNO. If the level of redox-related stress still increases, the SNO can progress into sulphenic acid (SOH)/disulfide (SS), sulphinic acid (SO_2H) and irreversible sulphonic acid (SO_3H). However, only the *S*-nitrosylation has been shown to be involved not only in redox homeostasis, but also in signal transduction (Hess et al., 2005).

S-Nitrosylation affects a wide array of protein functions. About a thousand *S*-nitrosylated proteins have been identified in all organisms (Xue et al., 2010). Human *S*-nitrosylated proteins are involved in a wide range of physiological functions (Seth and Stamler, 2011). In Arabidopsis, Lindermayr et al. (2005) identified a total of 105 proteins as candidates for *S*-nitrosylation. These were characterised into stress-related, redox-related, signalling/regulating, cytoskeleton, and metabolic proteins.

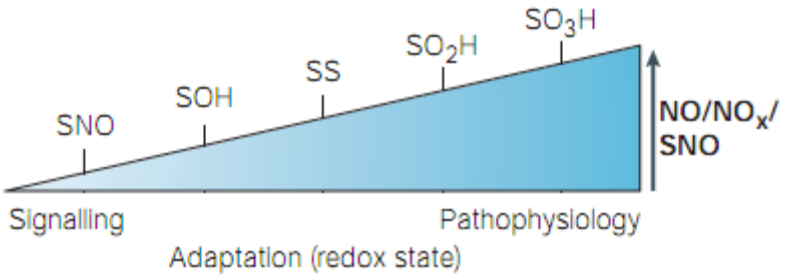

Figure 1-3. The homeostasis of redox-related stress by cysteine NO-dependent electrophilic and oxidative modifications. Redox-related stress, which leads to cellular toxicity, is controlled by graded cysteine modifications. The progression of SNO to SOH/SS, SO_2H and SO_3H is due to the increase in redox-related stress. Taken from Hess et al. (2005).

1.3.4 Denitrosylation

Denitrosylation is the removal of the NO group from cysteine in SNO. Denitrosylation should not merely be considered as the reverse process of nitrosylation. This process can be considered as a method of cellular signalling. For example, in the caspase protein family, human caspase-3 remains *S*-nitrosylated at the active site and becomes inactive. Thioredoxin 1 (Trx1) denitrosylates and activates this enzyme, triggering apoptosis (Mannick et al., 1999). Apoptotic regulation of this type is also present in plants. Arabidopsis metacaspase 9 is *S*-nitrosylated at the active site Cys-147 suggesting conservation of NO function between plants and animals (Belenghi et al., 2007).

Denitrosylation is also required in the defence response in plants. Non-expressor of PR1 (NPR1) is a major control of salicylic acid-dependent genes. After an increase in salicylic acid and the change in redox stress by pathogen induction, thioredoxins (Trxs), denitrosylate NPR1, causing it to change from an oligomer to a monomer. This monomer translocates into the nucleus, where it induces expression of salicylic acid-dependent genes. The addition of GSNO, a NO donor, enhances the oligomerization by *S*-nitrosylation. This oligomerization does not occur when hydrogen peroxide or the NO donor sodium nitroprusside (SNP) is present (Tada et al., 2008). This demonstrates *S*-nitrosylation of NPR1 required the NO donor GSNO.

A. thaliana salicylic acid-binding protein 3 (AtSABP3) is another example of a protein that undergoes *S*-nitrosylation. AtSABP3 has two functions: it is involved in salicylic acid binding and exhibits carbonic anhydrase activity. Wang et al. (2009) demonstrated that AtSABP3 is *S*-nitrosylated *in vitro* by GSNO and controlled *in vivo* by the GSH/GSNOR system, which will be further described in Section 1.3.4.3. *S*-nitrosylation of AtSABP3 negatively regulates the plant defence system because SNO-AtSABP3 formation reduces both salicylic acid binding and carbonic anhydrase activity. Therefore, denitrosylation is required for exhibiting normal immune responses.

In mammals, *S*-nitrosylation has been shown to be closely involved with immune signalling via the Toll-like receptor (TLR) signalling pathway. *S*-

Nitrosylated MyD88 reduces TLR-mediated responses by reducing its translocation to the cell membrane where it interacts with its partners TIRAP and TRAF6, and induces of IκB degradation by phosphorylation (Into et al., 2008). Phosphorylation of IκB is directly controlled by *S*-nitrosylation. The *S*-nitrosylation of IκB kinase β (IKKβ) inhibits its ability to inactivate IκB by phosphorylation resulting in the inhibition of NF-κBs. NF-κBs are also S-nitrosylated and this inhibits DNA binding of NF-κBs preventing them from transcribing TLR responsive genes (Marshall et al., 2004). The multiple levels of mammalian defence signalling are inhibited by *S*-nitrosylation, therefore denitrosylation, the inverse process of *S*-nitrosylation, is required for activating those defence-related target proteins.

SNO is normally stable under physiological condition but can be non-enzymatically degraded by heat, light or a redox reaction. Metal ions also rapidly affect decomposition of SNO; however in the cellular environment, these ions are sequestered by proteins. A slight change in the redox status of the cell is not enough to trigger denitrosylation signalling (Benhar et al., 2009), so it is inferred that enzymatic systems are crucial in the regulation of denitrosylation.

Enzymes that could be responsible for the regulation of SNOs include protein disulfide isomerase (Sliskovic et al., 2005), xanthine oxidase (Trujillo et al., 1998), superoxide dismutase (Jourd'heuil et al., 1999), and carbonyl reductase (Bateman et al., 2008), thioredoxin (Trx) (Stoyanovsky et al., 2005), glutathione peroxidase (GPX) (Hou et al., 1996), and GSNOR (Staab et al., 2008).

1.3.4.1 Thioredoxin/thioredoxin reductase system for denitrosylation

Trx, thioredoxin reductase (TrxR), and NADPH are key components in the Trx/TrxR denitrosylation system present in all organisms (Lillig and Holmgren, 2007). Active sites on Trx are at CXXC, where C is cysteine and X is any amino acid. Trx reduces both disulfide substrates (Carvalho et al., 2008) and SNOs, including small molecule SNOs and GSNO (Stoyanovsky et al., 2005; Sengupta et al., 2007). Denitrosylation happens in two steps: 1) Nucleophilic attack at the SNO substrate by the first cysteine of the CXXC motif leads to SNO formation there. 2) The reduction of the first cysteine by the second cysteine causes the formation of a

disulfide bond between the two cysteines. As a result, the SNO substrate is reduced to free thiol, while the Trx with disulfide bonds between cysteines is converted to the initial form by TrxR (Stoyanovsky et al., 2005). These steps are illustrated in Figure 1-4. Denitrosylation of caspase-3 and NPR1 by the Trx/TrxR system supports the role of Trx/TrxR in SNO regulation.

1.3.4.2 Glutathione peroxidase system for denitrosylation

GPX has been proposed to have a function in controlling reactive oxygen species (ROS) level. With GSH as an electron donor, GPX catalyzes hydrogen peroxide into glutathione disulfide (GSSG) and H_2O (Margis et al., 2008). The substrates of this enzyme can also be organic hydroperoxides and lipid peroxides (Ursini et al., 1995). Moreover, GPX catalyzes the decomposition of GSNO and SNO *in vitro* by converting GSNO (or SNO) into GSSG and NO (Hou et al., 1996). This suggests that GPX plays a part in regulating SNO level.

Most of the GPX genes in plants are similar to phospholipid hydroperoxide glutathione peroxidases (PHGPXs) in animals. Seven GPX genes in Arabidopsis (AtGPX) express peptides ranging from 169 to 236 amino acids long. Among those AtGPXs, AtGPX7 displays the greatest similarity to PHGPX. The core peptides of each of the seven AtGPX are conserved, but the N-termini are varied – this may indicate the differences in transit peptides of the different AtGPXs. These AtGPXs can be found in different compartments in the cell. For example, AtGPX2, 4, and 6 can be found in cytosol (AtGPX6 has another isoform occurring in mitochondria). The seven genes respond differently to stress and plant hormones (Miguel et al., 2003). AtGPX2 and 6 are the only two AtGPXs which respond greatly to biotic stresses (Winter et al., 2007). This result concurs with the response of these genes to salicylic acid and the predicted upstream cis-acting element, a W-box (Miguel et al., 2003), which is over-represented in salicylic acid-regulated genes.

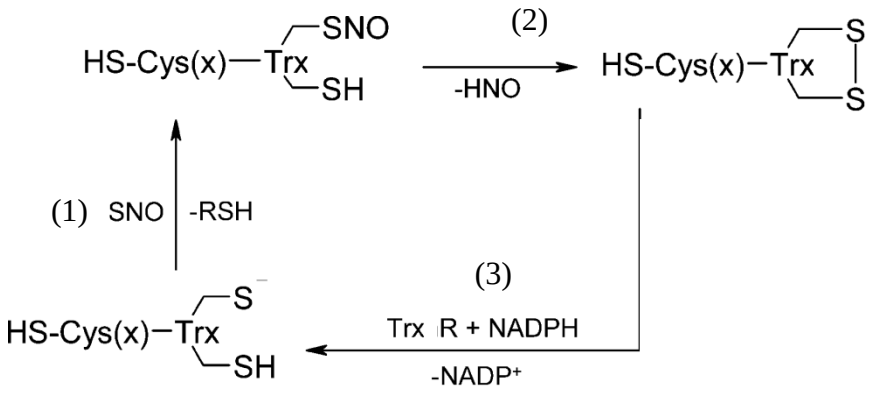

Figure 1-4. Trx mechanisms of denitrosylation and Trx turnover. (1) The nucleophillic attack by the first cysteine results in denitrosylated substrate and *S*-nitrosylated of the first cysteine of Trx. (2) The reduction from the second cysteine creates disulfide bond Trx and HNO. (3) The turnover of Trx by TrxR and NADPH converts Trx back to normal form and produced $NADP^+$. Adapted from Stoyanovsky et al. (2005).

1.3.4.3 Glutathione/*S*-nitrosoglutathione reductase system for denitrosylation

GSH is a tripeptide composed of cysteine, glutamic acid, and glycine. The cysteine in GSH can be *S*-nitrosylated by free NO (oxidation) or accepts NO that is transferred from other SNOs (transnitrosylation) to yield GSNO. GSNO can act as a NO donor by transferring NO to free thiols generating other SNOs, or be removed by *S*-nitrosoglutathione reductase (GSNOR). As a result, GSNOR can indirectly denitrosylate protein using GSH as an intermediate (Figure 1-5).

GSNOR, type III alcohol dehydrogenase (ADH3), is a bifunctional enzyme conserved from prokaryotes to eukaryotes. This suggests that the enzyme has essential roles in life forms (Danielsson et al., 1994). Aside from 'GSNOR', this enzyme has many aliases: glutathione dependent formaldehyde dehydrogenase (GS-FDH), octanol dehydrogenase, xx alcohol dehydrogenase, class 3 alcohol dehydrogenase, and, in humans, alcohol dehydrogenase 5 (Staab et al., 2008). It is expressed ubiquitously in mammals, and is important in the detoxification of endogenous and exogenous formaldehyde, ethanol metabolism, retinoic acid formation, and NO regulation (Staab et al., 2008). It has a dimeric structure with two zinc atoms, and is part of the medium chain alcohol dehydrogenase/reductase family (Figure 1-6).

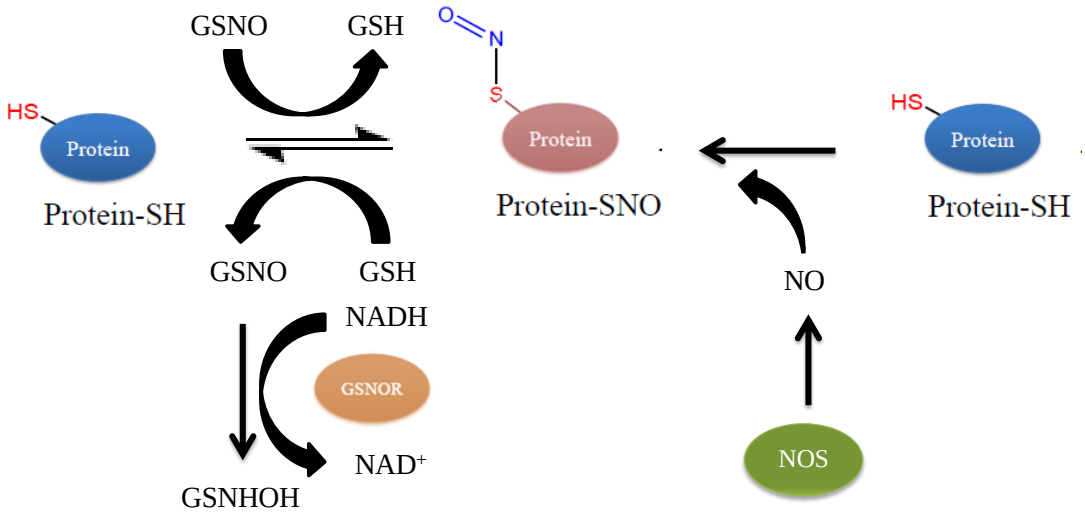

Figure 1-5. A schematic showing protein *S*-nitrosylation by NO produced by NOS or transnitrosylation and denitrosylation by the GSH/GSNOR system.

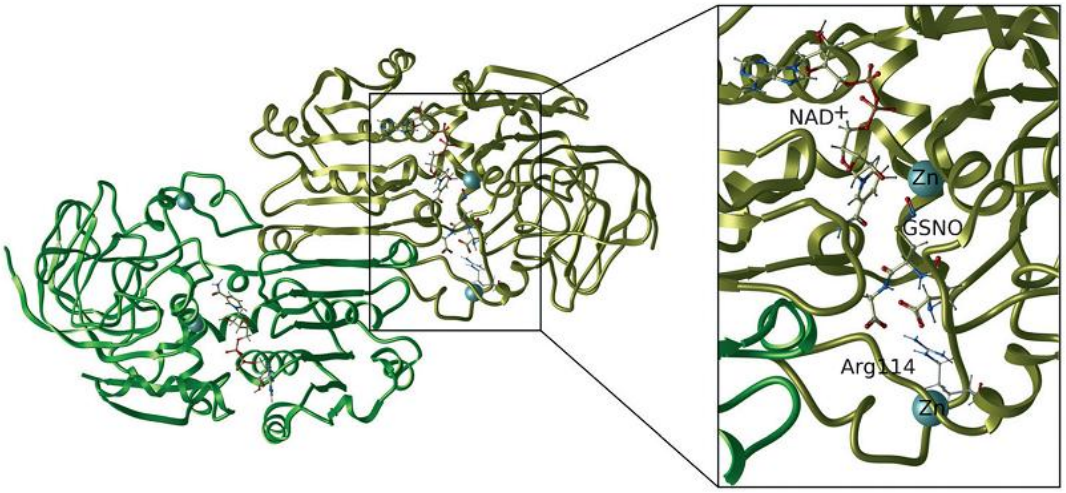

Figure 1-6. The conformation of dimeric ADH3 (green and yellow; left). At the active sites, NAD^+ and GSNO were docked into ADH3. Arginine-114 functions to bind substrates in the correct orientation. Two zinc atoms (cyan) function in structural/mechanical support and chemical activation of substrates (right). Taken from Staab et al. (2008).

ADH3 takes part in two kinds of reactions, oxidation and reduction. In oxidation, ADH3 catalyzes hydroxymethylglutathione (HMGSH) (produced spontaneously from GSH and formaldehyde) to form formylglutathione (FGSH) and NADH. NADH is then used to reduce GSNO to form a semimercaptale (GSNHOH), an intermediate which reacts further to form either glutathione sulfanamide ($GSONH_2$) or GSSG. The presence of GSH reduces the catalytic rate of ADH3 and drives the reaction toward the production of GSSG. However with infection, a reduced presence of GSH leads to the rearrangement of GSNHOH to become $GSONH_2$. After pathogen invasion, ROS accumulation leads to the spontaneous hydrolysis of $GSONH_2$ into glutathione sulfinic acid (GSO_2H). GSO_2H is then oxidized to form glutathione sulfonic acid (GSO_3H). Notably, $GSONH_2$, GSO_2H, and GSO_3H, inhibit the activities of glutathione transferase (GST) (Figure 1-7), which are responsible for the detoxification of xenobiotics (Staab et al., 2008). This inhibition contributes to the increase in the of GSH pool.

Among the enzymes proposed to be major regulators of GSNO levels, GSNOR exhibits three properties that suggest it could be the most important candidate. Firstly, GSNOR is the only enzyme that catalyzes the destruction of GSNO, yielding non-NO products. This removes NO from the cellular NO pool. Secondly, GSNOR has the highest k_{cat}/K_m ratio (a measure of enzyme efficiency) among other known candidates (Table 1-1). Finally, as the aforementioned reaction of GSNOR, type of product formed by GSNOR corresponds to the size of the GSH pool (Staab et al., 2008). GSNO, a mobile reservoir of NO activities, causes the formation of SNOs through transnitrosylation. Hence, the GSH/GSNOR system indirectly controls SNOs by catalyzing GSNO to either GSSG or hydroxylamine (NH_2OH) or $GSONH_2$

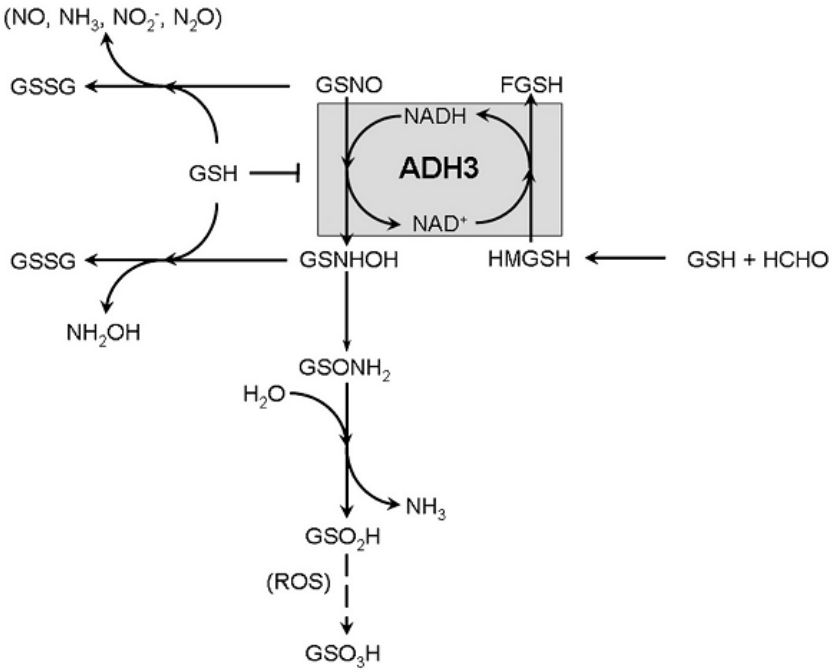

Figure 1-7. Mechanisms of ADH3's two functions. HMGSH is produced in the oxidative reaction between NADH and FGSH. GSNO and NADH are coupled in the reduction reaction, which produces the intermediate GSNHOH and NH_2OH, depending on the GSH concentration. GSNHOH can be converted into $GSONH_2$ or GSSG. Some of the GSNO is non-enzymatically converted into GSSG through reacting with various nitric species. Taken from Staab et al. (2008).

Table 1-1. Activities of enzymes that turnover GSNO in humans. This table is from Staab et al. (2008).

Table 1. Human GSNO converting enzymatic activities (see also note added in proof).

Enzyme	kinetic parameters	Reaction products
ADH3 [64]	$K_m = 11$ μM $k_{cat} = 1200$ min^{-1} $k_{cat}/K_m = 110$ min^{-1} μM^{-1}	GSNHOH[a] as intermediate which can be: a) rearranged to form $GSONH_2$ [12, 15, 64] or b) intercepted by GSH to form GSSG and NH_2OH [12, 64]
Cu/Zn superoxide dismutase [82]	$K_m = 5.6$ μM $k_{cat} = 0.3$ min^{-1} $k_{cat}/K_m = 0.05$ min^{-1} μM^{-1}	GSSG and NO
Glutathione peroxidase [83]	ND[b]	GSSG and NO
Thioredoxin system [84]	$K_m = 60$ μM $k_{cat} = 36$ min^{-1} $k_{cat}/K_m = 0.6$ min^{-1} μM^{-1}	GSH, NO and O_2^{-}[c]
Xanthine oxidase [85]	ND[b]	GSH, NO and O_2[d]

[a] Reaction is NADH-dependent.
[b] ND, not determined.
[c] Reaction is oxygen-dependent.
[d] Reaction is dependent on xanthine oxidase-mediated formation of O_2.

1.4 Nitric oxide signalling in immunity

1.4.1 Nitric oxide signalling in plant immunity

In a plant, the defence system after pathogen recognition involves many signalling molecules. There is ongoing research into the interactions among these molecules and how they actually fit into defence signalling in plants. This report focuses on NO signalling because NO is induced by pathogen challenge, and because it plays many important roles in a plant's defence.

1.4.1.1 Nitric oxide in plant hypersensitive response

Directly after pathogens are detected in plants, NO and reactive oxygen intermediate (ROI) levels increase. NO reacts with O_2 to produce $ONOO^-$, which has cytotoxic effects (Bonfoco et al., 1995). $ONOO^-$ is also believed to trigger the hypersensitive response, a response resembling programmed cell death in animals, to restrict pathogen growth. However, compared to animal cells, plant cells can tolerate higher concentrations of $ONOO^-$ (Delledonne et al., 2001). Hence it is proposed that the hypersensitive response is initiated by the interaction of NO and hydrogen peroxide. Hydrogen peroxide is generated by the conversion of O_2^- (produced by NADH oxidase) to hydrogen peroxide by pathogen inducible superoxide dismutase (Delledonne et al., 2001).

1.4.1.2 Nitric oxide in systemic acquired resistance (SAR)

As aforementioned, salicylic acid is a crucial molecule in eliciting SAR. NO affects salicylic acid accumulation, which in turn modulates SAR. In tobacco, the addition of NO enhances the accumulation of salicylic acid, which causes the induction of pathogenesis-related protein 1 (Durner et al., 1998). NO, in the form of SNO, has also been proposed to act as a long-distance mobile molecule in SAR. This is shown in the increase of SNO during SAR in both initial and distal tissues (Rustérucci et al., 2007). GSNO, the tripeptide SNO, was discovered to induce SAR against tobacco mosaic virus infection (Durner et al., 1998; Song and Goodman, 2001). Overexpression of GSNOR compromises SAR. Therefore, it has been hypothesized that GSNOR might regulate SAR via vascular tissues (Rustérucci et al.,

2007). On the other hand Feechan et al. (2005), following a genetic approach rather than employing pharmacological agents, found that the gain-of-function *gsnor1-1* mutation, which exhibits low levels of SNO and GSNO, promoted disease resistance in Arabidopsis. In support of these findings, recent data has shown that increased GSNO levels in the *gsnor1-3* mutant enhances *S*-nitrosylation of NPR1 and promotes NPR1 oligomer formation in the cytosol, compromising the induction of SAR (Tada et al., 2008). However, a cycle of NPR1 monomer-to-oligomer formation underpins the development of this defence mechanism. Thus, lower levels of SNOs are required to maintain this signalling system. Therefore, *S*-nitrosylation of NPR1 appears to function in both activation and repression of SAR.

1.4.2 Nitric oxide signalling in *Drosophila melanogaster* immunity

While a large amount of current research is devoted to NO signalling in insects. There are few studies of its role in the defence systems of insects. The important downstream signalling molecule is cGMP (produced by NO-triggered guanylate cyclase). cGMP activates many other components, such as cGMP-dependent protein kinase, which is a major effector of cGMP (Davies, 2000).

In insects, it has been proposed that at low concentrations NO acts as a signalling molecule, while at high concentrations NO has direct toxicity. As a signalling molecule, NO mediates defence signalling in order to produce antimicrobial peptides (AMPs) (Nehme et al., 2007). Toxicity is initiated when a high concentration of NO interacts with defence-triggered O_2^- to form $ONOO^-$ (Nappi et al., 1995), and with hydrogen peroxide to produce the very reactive hydroxyl radical (·OH) (Nappi and Vass, 1998). Evidence backing these proposed uses of NO in insects can be found in studies conducted by Nappi et al. (2000) who found that the defence response of *D. melanogaster* and *D. teissieri* of larvae challenged by parasitoid wasps was found to include an enhanced production of NO and the AMP Diptericin (Dpt). The pattern of NO concentration was clearly shown in *D. paramelanica* infected with parasitoid wasps. The NO concentration increased within less than one minute and then in four hours decreased to below the normal level. High NO concentrations are directly toxic for the pathogen while at low concentration NO acts as a defence signalling molecule (Carton et al., 2009).

More recently, Eleftherianos et al. (2009) have shown, using RNA silencing to inhibit NOS expression in the gut of moth *Manduca sexta*, that NOS protects against oral bacteria infection. NOS does not protect against septic infection, even though NOS expression is induced in haemocytes and fatbody by septic infection. Moreover, the NOS-induced gut defence is likely to restrict the spreading of bacteria from the gut.

Foley and O'Farrell (2003) proposed that NO is a beneficial molecule that is produced in *D. melanogaster* gut epithelia and then transfers signals through haemocytes before triggering the systemic expression of AMPs in the fat body. Take the study conducted by Broderick et al. (2006) for example, it has contradicted the Foley and O'Farrell's paper. The study showed that cobinamide, a NO scavenger, enhances the survival of *D. melanogaster* because, hypothetically, NO triggers guanylate cyclase to produce more cGMP, hence leading to the elicitation of diseases such as impaired cardiac system, hypotension, and decreased systemic vascular resistance.

1.5 GSNOR in immunity

1.5.1 GSNOR in plant immunity

The chief roles of GSNOR in plants are best shown in the study conducted on Arabidopsis by Feechan et al. (2005). The loss-of-function Arabidopsis *gsnor* mutant *gsnor1-3* exhibited the following: higher SNO levels, diminished *R* gene-mediated, basal and non-host disease resistance, repressed expression of *pathogenesis-related gene 1* (the marker of salicylic acid-dependent genes), and decreased salicylic acid level in pathogenic conditions. On the other hand, specimens with the gain-of-function mutant *gsnor1-1* illustrated inverse results (Feechan et al., 2005).

1.5.2 GSNOR in animal immunity

The role of GSNOR in animal immunity is unclear. *gsnor* knockout mice have a wild-type morphological phenotype but have increased arterial pressure which is correlated with elevated SNO levels in blood. The knockout mice show increased lethality and liver SNO levels in response to endotoxic shock generated by a

peritoneal injection of lipopolysaccharide (LPS). Their response to pathogen infection was not tested, however, the concentration of LPS injected was extremely high. Therefore, the increment of liver SNOs may not represent the actual situation from pathogen infection (Liu et al., 2004).

GSNOR has been shown to be involved in asthma. In patients suffering from asthma, GSNOR activity from bronchoalveolar lavage is significantly higher than normal correlating with decreased SNO levels (Que et al., 2009). In mice, asthma was modelled by injection of the allergen ovalbumin. This resulted in an increase in GSNOR activity. *gsnor* knockout mice treated in the same way showed a higher SNO level than wild-type mice suggesting that GSNOR controls SNOs in the event of asthma (Que et al., 2005).

1.6 *gsnor* knockout contributes to a loss of apical dominance phenotype in Arabidopsis.

gsnor knockout (*gsnor1-3*) contributes to a loss of apical dominance. Moreover, mutant plants tend to grow slower and produce more yellowish leaves than wild type (Figure 1-8). This might demonstrate the functions of *gsnor* in the regulation of phytohormone auxin or in cell proliferation regulation.

1.7 Motivation and research aims

In Arabidopsis, it is well established that the function of GSNOR is pivotal for effective plant disease resistance by modulating protein *S*-nitrosylation (Feechan et al., 2005). However it remains unclear whether this enzyme has any function in the defence system of other organisms and particularly in animals. Drosophila is a powerful genetic model and has been widely used as a model organism for studying innate immune responses. Drosophila immunity has been shown to have some conserved characteristics with mammal innate immune responses. By harnessing these advantages, we strongly believed that Drosophila will offer us a great opportunity for studying the role of GSNOR in animal immunity which could also be applied to mammal immunity. If successful this transferability will undoubtedly not only help elucidate the animal and plant defence system but also improve our

understanding about primitive immunity and the evolution of a system that relies on NO. The experiments reported in this thesis were designed to investigate the role of GSNOR in Drosophila immunity.

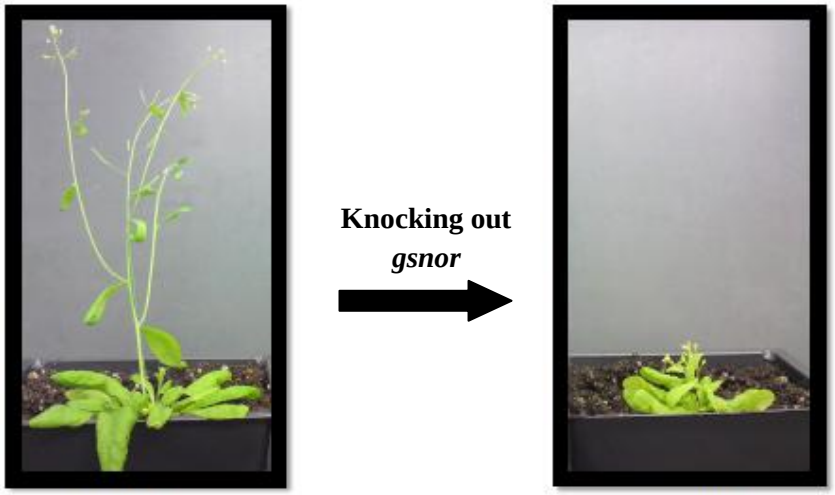

Figure 1-8. *gsnor1-3* shows a distinctive morphological phenotype. *gsnor1-3* plants possess a T-DNA knockout insertion within the *A. thaliana gsnor* gene. This insertion results in a loss of apical dominance and yellowish leaves.

Chapter 2 Materials and Methods

All chemicals and oligonucleotides were purchased from Sigma-Aldrich, unless otherwise stated.

2.1 Drosophila stocks and maintenance

All Drosophila lines were grown at 25 ℃ on standard yeast-cornmeal-agar medium. This was changed as a matter of routine every two weeks. Drosophila lines are listed in Table 2-1.

2.2 General techniques

2.2.1 Drosophila DNA extraction and purification

The protocol was adapted from the method presented by the Johnston lab, Columbia University, NY. Initially 30 flies were frozen (-70℃) for a period in excess of five minutes and then ground in 400 μL of 100 mM Tris-HCl (tris(hydroxymethyl)aminomethane adjusted pH by hydrochloric acid (HCl)) pH 7.5, 100 mM EDTA (ethylenediaminetetraacetic acid), 100 mM sodium chloride (NaCl), and 0.5 % sodium dodecyl sulphate (SDS) with a disposable plastic grinder until homogenization occurred. The homogenate was incubated at 65℃ for 30 minutes and then 800 μL of 1.67 M potassium acetate and 4 M LiCl were added, followed by incubation on ice for 10 minutes and a subsequent centrifugation at 14,000 revolutions per minute (rpm) for 15 minutes. Equal volumes of the supernatant were transferred to two new clean tubes, and ethanol precipitation perform by adding 700 μL isopropanol followed by centrifugation at 14,000 rpm for 15 minutes. The pellet was resuspended in 100 μL sterile distilled water.

Table 2-1.The list of *D. melanogaster* lines

Stock number	Name	Genotype and description	Origin
OR	Oregon-R	Wild type	Finnegan lab stocks
679		w^{1118}; $P\{GT1\}Fdh^{BG00983}$ - P element *P{GT1}* insertion upstream of *gsnor* gene	Bloomington stock centre (stock No. 12524)
680		Fdh^{nNC1}/*TM6* - Possibly *fdh* null allele	Bloomington stock centre (stock No. 4038)
681	*Relish*	Rel^{E20} - *Relish* loss of function mutation causing sensitivity to gram-negative bacteria.	Bruno Lemaitre
682	*Spaetzle*	spz^{rm7}/*TM6C* - *Spaetzle* loss of function mutation causing sensitivity to gram- positive bacteria.	Bruno Lemaitre
683		P-element imprecise excision from 679	Hannah Barton
684		P-element imprecise excision from 679	Hannah Barton
727	*Df7305*/ *TM6B*	*Df(3R)Exel7305*/*TM6B*, Tb^3, Hu^4 - Genomic deletion which has breakpoint on *gsnor*	Bloomington stock centre (stock No. 7956)
728	*Df7306*/ *TM6B*	*Df(3R)Exel7306*/*TM6B*, Tb^3, Hu^4 - Genomic deletion which has breakpoint on *gsnor*	Bloomington stock centre (stock No. 7957)
738	*imd*	b^1, pr^2, *imd* - *imd* loss of function mutation causing sensitivity to gram-negative bacteria	Bruno Lemaitre
787	*UAS-gsnor*; *Df7305*/ *TM6B*	*UAS-gsnor*/*UAS-gsnor*; *Df(3R)Exel7305*/*TM6B*, Tb^3, Hu^4	The cross between *UAS-gsnor* and *Df7305*/*TM6B*

Stock number	Name	Genotype and description	Origin
788	*act*5C-*GAL4*, *Df7306*/*TM6B*	*P{Act5C-GAL4}17bFO1*, *Df(3R)Exel7306*/*TM6B*, Tb^3, Hu^4	The cross between *act5C-GAL4*/*TM6B* and *Df7306*/*TM6B*
789	*EP-gsnor*; *Df7305*/*TM6B*	*EP-gsnor*/*EP-gsnor*; *Df(3R)Exel7305*/*TM6B*, Tb^3, Hu^4	The cross between *EP-gsnor* and *Df7305*/*TM6B*
790	*EP-gsnor*; *Df7306*/*TM6B*	*EP-gsnor*/*EP-gsnor*; *Df(3R)Exel7306*/*TM6B*, Tb^3, Hu^4	The cross between *EP-gsnor* and *Df7306*/*TM6B*
791	*act*5C-*GAL4*/*TM6B*	*P{Act5C-GAL4}17bFO1*/*TM6B*, Tb^1, Hu^2 - *GAL4* controlled by *Actin5C* promoter (*Actin5C-GAL4*)	Bloomington stock centre (stock No. 3954)
792	*UAS-gsnor*	*UAS-gsnor*/*UAS-gsnor*; +/+ - *gsnor* CDS linked with *UAS*	This study
793	*EP-gsnor*	*EP-gsnor*/*EP-gsnor*; +/+ - *gsnor* gene with the endogenous promoter	This study
	Df7305/*Df7306*	*Df(3R)Exel7305*/*Df(3R)Exel7306* - Overlapping deletion on *gsnor*	The cross between *Df7305*/*TM6B* and *Df7306*/*TM6B*
	Df7306/*Df7305*	*Df(3R)Exel7306*/*Df(3R)Exel7305* - Overlapping deletion on *gsnor*	The cross between *Df7306*/*TM6B* and *Df7305*/*TM6B*
	act5c:*UAS-gsnor*; *Df7305*/*Df7306*	*UAS-gsnor*/+; *Df(3R)Exel7305*/*P{Act5C-GAL4}17bFO1*, *Df(3R)Exel7306* - Complementation by expressing GSNOR under control of *Actin5C* promoter	The cross between *UAS-gsnor*; *Df7305*/*TM6B* and *act5C-GAL4*, *Df7306*/*TM6B*

Stock number	Name	Genotype and description	Origin
	act5c:*UAS-gsnor*; *Df7306*/ *Df7305*	+/*UAS-gsnor*; *P{Act5C-GAL4}17bFO1*, *Df(3R)Exel7306*/ *Df(3R)Exel7305* - Complementation by expressing GSNOR under control of *Actin5C* promoter	The cross between *act5C-GAL4*, *Df7306*/*TM6B* and *UAS-gsnor*; *Df730*5/*TM6B*
	EP-gsnor/ *EP-gsnor*; *Df7305*/ *Df7306*	*EP-gsnor*/*EP-gsnor*; *Df(3R)Exel7305*/ *Df(3R)Exel7306* - Complementation by *gsnor* with the endogenous promoter	The cross between *EP-gsnor*; *Df7305*/*TM6B* and *EP-gsnor*; *Df7306*/*TM6B*
	EP-gsnor/ *EP-gsnor*; *Df7306*/ *Df7305*	*EP-gsnor*/*EP-gsnor*; *Df(3R)Exel7306*/ *Df(3R)Exel7305* - Complementation by *gsnor* with the endogenous promoter	The cross between *EP-gsnor*; *Df7306*/*TM6B* and *EP-gsnor*; *Df7305*/*TM6B*

[1]*Black* (*b*)

[2]*Purple* (*pr*)

[3]*Tubby* (*Tb*)

[4]*Humeral* (*Hu*)

Further purification was done using the phenol/chloroform method. Initially phenol was added to the solution following by vortexing and centrifugation at 14,000 rpm for 15 minutes. The supernatant was transferred to the new clean tube and 150 mL (25:24:1) phenol: chloroform: isoamyl alcohol was added followed by centrifugation at 14,000 rpm for 15 minutes. The supernatant was once again transferred to a clean tube and 150 mL (24:1) chloroform: isoamyl alcohol added. Samples were again centrifugated at 14,000 rpm for 15 minutes and supernatant decanted into a fresh tube. 1/10 volume of 3 M sodium acetate (pH 5.2) and 2 volumes of 100 % ethanol were added to the supernatant in order to precipitate DNA following by centrifugation at 14,000 rpm for 15 minutes. The pellet DNA was washed with 70 % ethanol and air dried before being resuspended in 100 µL of sterile distilled water.

2.2.2 Total RNA extraction, DNase treatment, and RNA quantification

The protocol used to extract total RNA was adapted from Bogart & Andrews (2006). 25 adult flies were frozen in liquid nitrogen (N_2) and subsequently ground in 500 µL of Trizol (Invitrogen) using a bead mill (Qiagen). The homogenate was either used immediately or stored at -70℃ (maximum of two months). The homogenate was left at room temperature for 5 minutes followed by centrifugation at 12,000 relative centrifugal force (rcf) for 10 minutes at 4℃. The supernatant was transferred to a new microcentrifuge tube. 100 µL of chloroform was added to each tube. The homogenate and chloroform were mixed vigorously by hand followed by incubation at room temperature for 3 minutes and centrifugation at 10,000 rcf for 15 minutes at 4℃. The upper phase was transferred to a new microcentrifuge tube. From this step, RNase contamination was avoided by using RNase-free pipette tips and microcentrifuge tubes and removing contaminating RNase present on experimental equipment using RNaseZap (Sigma). 250 µL of isopropanol was added to each tube followed by incubation at room temperature for 10 minutes and centrifugation at 12,000 rcf for 10 minutes at 4℃. The supernatant was replaced with 0.5 mL of 75 % ethanol followed by centrifugation at 7,500 rcf for 5 minutes at 4℃. The supernatant was removed, and the RNA pellet was dried in a laminar flow cabinet. The pellet was resuspended in 50 µL of diethylpyrocarbonate (DEPC) -treated water.

The RNA extract was treated with TURBO DNase (Ambion). 5 µL of 10 x TURBO DNase buffer and 1 µL of 2 units/µL TURBO DNase were added to the 50 µL of the RNA extract. The solution was mixed and incubated at 37℃ for 30 minutes. After the incubation, 5 µL of DNase inactivation reagent was added, and the solution was mixed occasionally for 5 minutes at room temperature. The sample was then centrifuged at 10,000 rcf for 1.5 minutes at room temperature and the resultant supernatant transferred to a new RNase-free microcentrifuge tube.

The concentration of RNA was quantified using a NanoDrop spectrophotometer ND 1000. The DECP-treated water usedin the RNA samples, the TURBO DNase buffer and DNase inactivation reagent were used as blank controls.

2.2.3 Agarose electrophoresis

All experiments requiring agarose electrophoresis were carried out using 1 % agarose in 1 x Tris-acetate-EDTA buffer (TAE) (40 mM Tris, 20 mM Acetic acid and 1 mM EDTA). The gels were prestained with 0.5 µg/ml ethidium bromide and visualized using an ultraviolet (UV) imaging system.

2.2.4 Bradford protein quantification

100 µL of bovine serum albumin (BSA) at different concentration (0, 10, 20, 40, 60, 80 and 100 µg/mL) were added to a new microcentrifuge tube in order to generate a standard curve (at 0 µg/mL was used as blank). 100 µL of the respective protein sample at an appropriate dilution was added to a new microcentrifuge tube. To this 1 mL of working concentration of protein assay dye reagent (Biorad) was added to each microcentrifuge tube. After gentle mixing to avoid foaming, the solution was transferred to a disposable cuvette and the absorbance at 595 nm (A_{595}) measured using a spectrophotometer.

The concentration of samples was obtained by comparing A_{595} value to the standard curve and conversion using the dilution factor.

2.2.5 Plasmid extraction by alkaline lysis

Plasmids were selected by growing transformed bacteria under antibiotic selection pressure for 16-24 hours. Initially a 5 mL culture was pelleted by centrifugation at 13,000 rpm for 2 minutes. The pellet was then resuspended in 250 µL 50 mM glucose, 25 mM Tris-Cl pH 8.0, 10 mM EDTA pH 8.0 and 50 µg/mL RNaseA and transferred to a 1.5 mL microcentrifuge tube. 250 µL of 0.2 N sodium hydroxide and 1% SDS was added to the cell suspension. The tube was inverted rapidly 4-5 times. 350 µL of ice-cold 3 M potassium acetate and 5 M acetic acid was added followed by several tube inversions. The mixture was stored on ice for 5 minutes followed by centrifugation at 15,000 rpm for 5 minutes at 4℃. The supernatant was transferred to a new microcentrifuge tube and absolute ethanol added to the maximum capacity of the tube, followed by mixing and incubating at room temperature for 2 minutes. The tube was centrifuged at 15,000 rpm for 5 minutes at 4℃. The pellet was washed with 1 mL 70 % ethanol and centrifuged at 15,000 rpm for 1 minute at 4℃. The pellet was air dried and resuspended with 50 µL of sterile distilled water.

2.3 Sequencing of the *fdh*/gsnor gene of strain 680

2.3.1 PCR for amplifying fragment used in sequencing

PCR to generate product possessing an A overhang at the 3'termini necessary for sequencing was performed using Ex Taq (TaKaRa Biotechnology) DNA polymerase (0.025 unit/µL Ex Taq, 1 x Ex Taq Buffer, 0.2 mM dNTPs (deoxynucleotide triphosphates), 0.5 µM primer 1 and 2 (Table 2-2; Figure 2-1), using 2 %v/v of Drosophila DNA (extracted by the protocol described in Section 2.2.1) as a template and mixed to the final volume of 200 µL (4 x 50 µL reaction)). PCR cycles include initial denaturation at 94℃ for 5 minutes followed by denaturation at 94℃ for 30 seconds, annealing at 55℃ for 30 seconds, and extension at 72℃ for 2 minutes for 30 cycles, and final extension at 72℃ for 15 minutes.

2.3.2 Cloning and transformation for Drosophila *gsnor* for sequencing

The amplified *gsnor* gene fragments of 680 (Table 2-1) were pooled and purified using a solid phase PCR purification kit (QIAquick PCR Purification Kit, Qiagen) in accordance with the manufacturer instructions. The purified PCR product was ligated into pGEM T-easy vertor (Promega) (Figure 2-2). Ligation reactions of 20 μL were performed using the following conditions: 1 x rapid ligation buffer (Promega), 0.3 unit/μL T4 DNA ligase, and preheated 3:1 PCR product: vector molar ratio. Samples were incubated at 4℃ overnight. After incubation, about 15 ng of plasmid in the ligation solution was mixed in 50 μL of DH5α *Escherichia coli* competent cells previously prepared using rubidium chloride (RbCl) method (Hanahan, 1983). Then heat shock transformation was done by first incubating on ice for 30 minutes followed by a heat shock step at 42℃ for 45 seconds and then allowed to cool on ice for 2 minutes. After the addition of 950 mL Luria-Bertani (LB) the cells were incubated at 37℃ with shaking at 275 rpm for 1 hour, samples were spread on LB medium plates supplemented with 100 μg/mL ampicillin, 0.003 %wt/v X-gal (5-bromo-4-chloro-indolyl-β-D-galactopyranoside), and 60 μM IPTG (isopropyl β-D-1-thiogalactopyranoside). Blue/white colour selection was used to detect successful transformants

A single white colony was inoculated in 5 mL LB broth with ampicillin and shaken at 275 rpm at 37℃ overnight. The recombinant plasmid was extracted and purified by alkaline lysis and solid phase purification kit (QIAprep Spin Miniprep Kit, Qiagenin accordance with the manufacturer instructions. 3 μL of purified plasmid and 1 μL of 10 μM T7 promoter primer or SP6 promoter primer were sent for sequencing at the GenePool sequencing centre, University of Edinburgh.

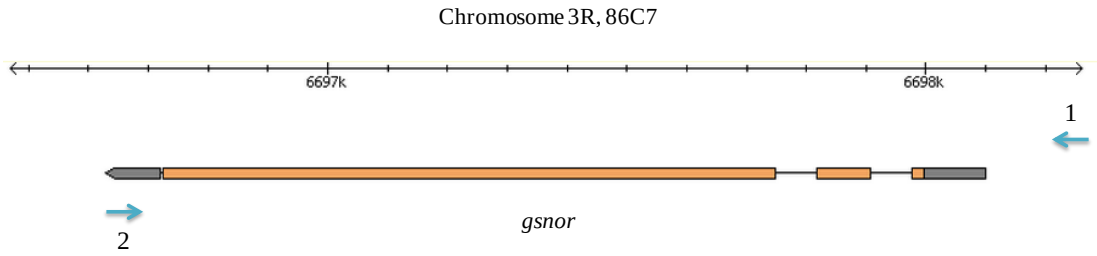

Figure 2-1. The position and orientation of primers for the amplification of *gsnor* from genomic DNA. Numbers designate primer number, details of which, can be found in Table 2-2.

Table 2-2. The list of primers for the amplification of *gsnor* from genomic DNA for sequencing.

Number	Name	Position[1]	Sequence
1	5' *gsnor* - 141	141 base pair upstream of the *gsnor* gene	atttcaaatgtagtttcaaaagacaagaaa
2[2]	3' *gsnor* 1418	At base pair number 1418 in *gsnor* gene	aaaaagtgaaaagcaaagaattgttatctc

[1]The position of primers count from the number of base that 5' of each primer anneal to.

[2]This primer was designed by Hannah Barton.

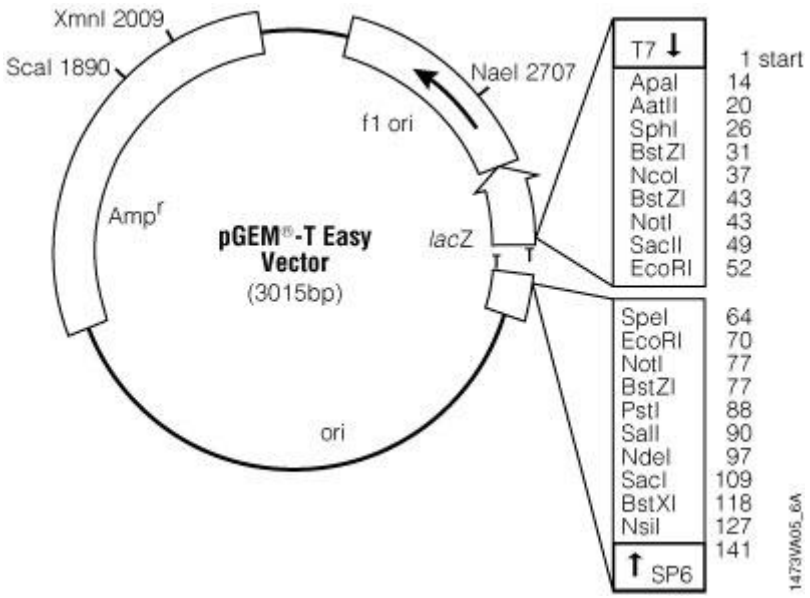

Figure 2-2. The map of pGEM-T Easy plasmid (Promega). An Adenine (A)-overhang DNA fragment is inserted at thymine (T) overhangs of the vector. The insertion abolishes *lacZ* expression resulting in white-coloured colonies, when grown on LB plates with ampicilin, X-gal and IPTG. Taken from www.promega.com.

2.4 GSNOR and GS-FDH activity assays

2.4.1 Protein extraction for *D. melanogaster* and *A. thaliana*

Either 50 flies or ~ 0.5g *A. thaliana* fresh leaf weight were homogenized in 500μL extraction buffer (50 mM HEPES (4-(2-hydroxyethyl)-1-piperazineethanesulfonic acid) pH 7.4, 5 mM EDTA pH 7.4, 5 mM dithiothreitol (DTT), 10mM sodium fluoride (NaF), 10 mM sodium orthovanadate (Na_3VO_4), 50 mM β–glycerophosphate, and 1 mM phenylmethanesulfonylfluoride (PMSF)). The homogenate was centrifuged at 14,000 rpm at 4℃ for 20 minutes with the resulting supernatant being collected.

2.4.2 GS-FDH in gel activity assay

A.thaliana gsnor 1-3 and Col-0 ecotype were used as negative and positive controls, respectively. Col-0, *atgsnor 1-3*, and extracted Drosophila protein were quantified with Bradford micro assay. 50 μg of protein were loaded onto 7.5 % native 29:1 acrylamide : bisacrylamide polyacrylamide gel and run at 20-25 mA at 4℃ until the bromophenol blue stain reach the bottom of the gel.

After polyacrylamide gel electrophoresis (PAGE), the gel was incubated in 0.1 mM sodium phosphate buffer (NaPi buffer) pH 7.0 for one minute.The gel was then incubated again in activity staining solution (0.1 mM sodium phosphate (NaPi) buffer pH 7.0, 0.1mM NAD^+, 0.1 mM nitroblue tetrazolium (NBT), 0.1mM phenazine methosulfate (PMS), 1 mM reduced glutathione, and 1 mM formaldehyde) until the bands appeared.

2.4.3 GSNOR in gel activity assay

The sample preperation and PAGE were performed as described in 2.4. For the assay, the gel was incubated in 0.1 M potassium phosphate buffer pH 8.0 and 1 mM NADH for 15 minutes at 4℃. The staining solution was discarded, and the gel was covered with filter paper soaked with 3 mM GSNO for 15 minutes. The stained gel was visualized using a UV imaging system.

2.4.4 Spectophotometric assay for GSNOR activity measurement

The extracted protein was quantified using a Bradford micro assay (Section 2.2.4). The samples were added to assay the solution to obtain the final concentration of 250 µg in 20 mM Tris-Cl pH 8.0, 0.5 mM EDTA pH 8.0, and 0.2 mM NADH. A similar quatity of the sample was also added to the assay solution without 0.2 mM NADH. This served as a blank control and accordingly every sample has its own individual blank. The solution was transferred to a disposable UV cuvette. At t=1 minute, a final concentration of 400 µM GSNO was added to the solution. The conversion of NADH to NAD^+ was measured using a spectrophotometer at A_{340} at one-minute interval for a total of 11 minutes at room temperature.

2.5 Generation of Drosophila *gsnor* knockdown using RNAi

2.5.1 PCR of the RNAi target on genomic DNA

The cDNA fragments corresponding to base pair number 112-511 and 603-1002 of *gsnor* mRNA were amplified using Phusion DNA polymerase (Finnzymes) (0.01 unit/µL Phusion DNA polymerase, 1 x Phusion HF buffer, 0.2 mM dNTPs, 0.5 µM primers (number 3 and 4 for the 112-511 fragment, and 5 and 6 for 603-1002 fragment) (Figure 2-3; Table 2-3), and 0.5 %v/v wild-type Drosophila cDNA (extracted according to Section 2.2.2) were mixed to the final volume of 200 µL reaction (4 x 50 µL reaction)). PCR cycles for the 112-511 fragment were set to initial denaturation at 98℃ for 3 minutes followed by denaturation at 98℃ for 10 seconds, annealing at 64℃ for 30 seconds, and extension at 72℃ for 10 seconds for 5 cycles. Then the cycles were set to denaturation at 98℃ for 10 seconds, and annealing included extension at 72℃ for 10 seconds for 30 cycles, and final extension at 72℃ for 10 minutes. Similar cycles were performed for the 603-1002 fragment, apart from that the annealing which was changed from 64℃ to 68℃.

The PCR fragments were pooled and purified by solid phase PCR purification kit (QIAquick PCR Purification Kit, Qiagen) in accordance with manufacturers' instructions.

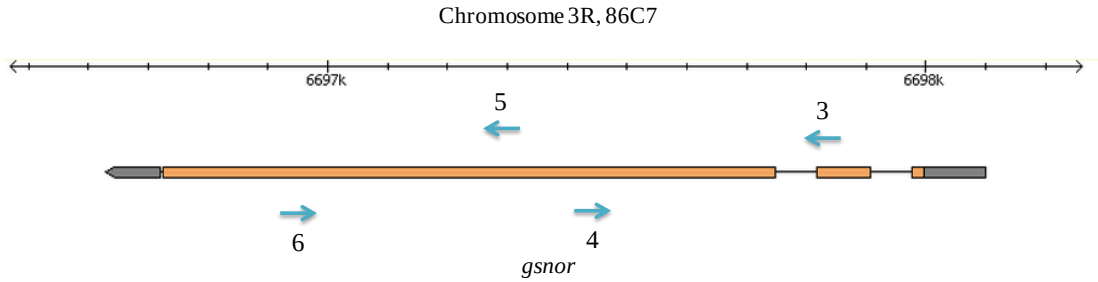

Figure 2-3. The position and orientation of primers for the amplification of fragments from *gsnor* mRNA required for generating RNAi. Numbers designate primer number, details of which, can be found in Table 2-3.

Table 2-3. The list of primers for RNAi generation

Number	Name	Position[1] and restriction site	Sequence
3	5'*XbaIgsnor* c112	Anneals to base pair number 112 in *gsnor* mRNA and contains *Xba*I site at 5'	aaaatctagagctaccgagggcaaggttat
4	3'*XbaIgsnor* c511	Anneals to base pair number 511 in *gsnor* mRNA and contains *Xba*I site at 5'	aaaatctagatgcagctgagacggga
5	5'*XbaIgsnor* c603	Anneals to base pair number 603 in *gsnor* mRNA and contains *Xba*I site at 5'	aaaatctagaggcgccgctggagaaa
6	3'*XbaIgsnor* c1002	Anneals to base pair number 1002 in *gsnor* mRNA and contains *Xba*I site at 5'	aaaatctagacactccgatcaccaccgaag

[1]The position of primers count from the number of base that 5' of each primer anneal to.

2.5.2 Two-step cloning to pWIZ

The first step required the digestion of pWIZ using the restriction enzyme *Nhe*I at 37 ℃ for 12-16 hours (New England Biolabs) (0.2 unit/µL *Nhe*I, 1 x NEBuffer 2, 1 x BSA, and 15 µL of pWIZ plasmid from QIAprep Spin Miniprep Kit were incubated at 37℃ overnight followed by heat inactivation at 65℃ for 20 minutes). To prevent self ligation, the digested pWIZ was dephosphorylated by adding the final concentration of 0.0008 unit/µL calf intestinal alkaline phosphatase (CIAP) (Promega) and 1 x CIAP buffer at 37℃ for 30 minutes. The dephosphorylation process was repeated again by adding the same amount of CIAP and incubated at 37℃ for a further 30 minutes. Both PCR fragments were digested at 37℃ for 12-16 hours with *Xba*I restriction enzyme (Promega) (0.2 unit/µL *Xba*I, 1 x Buffer D, 1 x BSA, and total purified PCR fragments from QIAquick PCR Purification Kit were incubated at 37℃ overnight).

The digested pWIZ and each PCR fragment were ligated together using T4 DNA ligase (Promega) using ligation reactions comprising of 10 µL with 1 x rapid ligation buffer (Promega), 0.3 unit/µL T4 DNA ligase, and preheated 3:1 PCR product: vector molar ratio. Samples were incubated at 16℃ for 3 hours. After the incubation, the transformation was performed as described at Section 2.3.2 with the exception that the transformed *E. coli* DH5α were spread on LB medium plates supplemented with 100 µg/mL ampicillin.

The insert was confirmed by colony PCR using primer 7 and 8 (Figure 2-4; Table 2-4). Restriction enzyme double digestion at 37℃ for 12-16 hours with *Xba*I (Promega) and *Xho*I (Promega) (0.2 unit/µL *Xba*I, 0.2 unit/µL *Xho*I, 1 x Buffer D, 1 x BSA, and 4 µL of plasmid extracted by alkaline lysis without solid-phase purification (Section 2.2.5) were incubated at 37℃ overnight) was also performed to confirm the presence of the insert. The confirmed recombinant plasmid was extracted and purified by alkaline lysis and the solid phase purification kit (QIAprep Spin Miniprep Kit, Qiagenin accordance with manufacturers' instructions. 3 µL of purified plasmid and 1 µL of 10 µM the primer number 7 or primer number 8 (Figure 2-4; Table 2-4) were sequenced at the GenePool sequencing centre, University of Edinburgh.

The second step cloning essentially mirrored the first step, except the restriction enzyme *Avr*II was used instead of *Nhe*I in order to insert the fragment in the reverse orientation to the other end of the *white* intron 2 (Figure 2-4). After transformation, the correct recombinant plasmids which have the *white* intron 2 flanked by inverted repeats of 112-511 and 603-1002 fragments were screen by the amount of plasmid produced from the similar amount of bacteria cells. Recombinant plasmids from 5 mL overnight cultures of each colony were extracted by alkaline lysis and solid phase purification kit (QIAprep Spin Miniprep Kit, Qiagen) in accordance with manufacturers' instructions. The extracted plasmids were digested at 37 ℃ overnight with *Xba*I (Promega) and *Xho*I (Promega) and then agarose electrophoresis (Section 2.2.3) was performed to observe the plasmid concentration. The plasmids at low relative concentration (compared to other plasmids) with a correct insert size were selected for further experimentation.

2.5.3 Transfer of the inverted repeats to pUASTattB

The selected plasmids were double digested at 37 ℃ overnight by *Xba*I (Promega) and *Xho*I (Promega) (0.2 unit/µL *Xba*I, 0.2 unit/µL *Xho*I, 1 x Buffer D, 1 x BSA, and 50 µL of plasmid extracted and purified by alkaline lysis and solid-phase purification were incubated at 37℃ overnight) in order to remove the inverted repeat insert present in pWIZ. The plasmid and insert were separated by agarose electrophoresis, and under UV light, the area of agarose containing the insert was cut and purified using a QIAquick gel extraction kit (Qiagen). The purified insert was ligated with pUASTattB also previously double digested at 37℃ overnight with *Xba*I (Promega) and *Xho*I (Promega) (0.2 unit/µL *Xba*I, 0.2 unit/µL *Xho*I, 1 x Buffer D, 1 x BSA, and 15 µL of plasmid extracted (Figure 2-5) and purified by alkaline lysis and solid-phase purification were incubated at 37℃ overnight) as described in the previous section. The recombinant pUASTattB containing the correct insert was first confirmed by double digestion with *Xba*I (Promega) and *Xho*I (Promega) followed by sequencing using primer number 10 and 11 (Figure 2-5; Table 2-5).

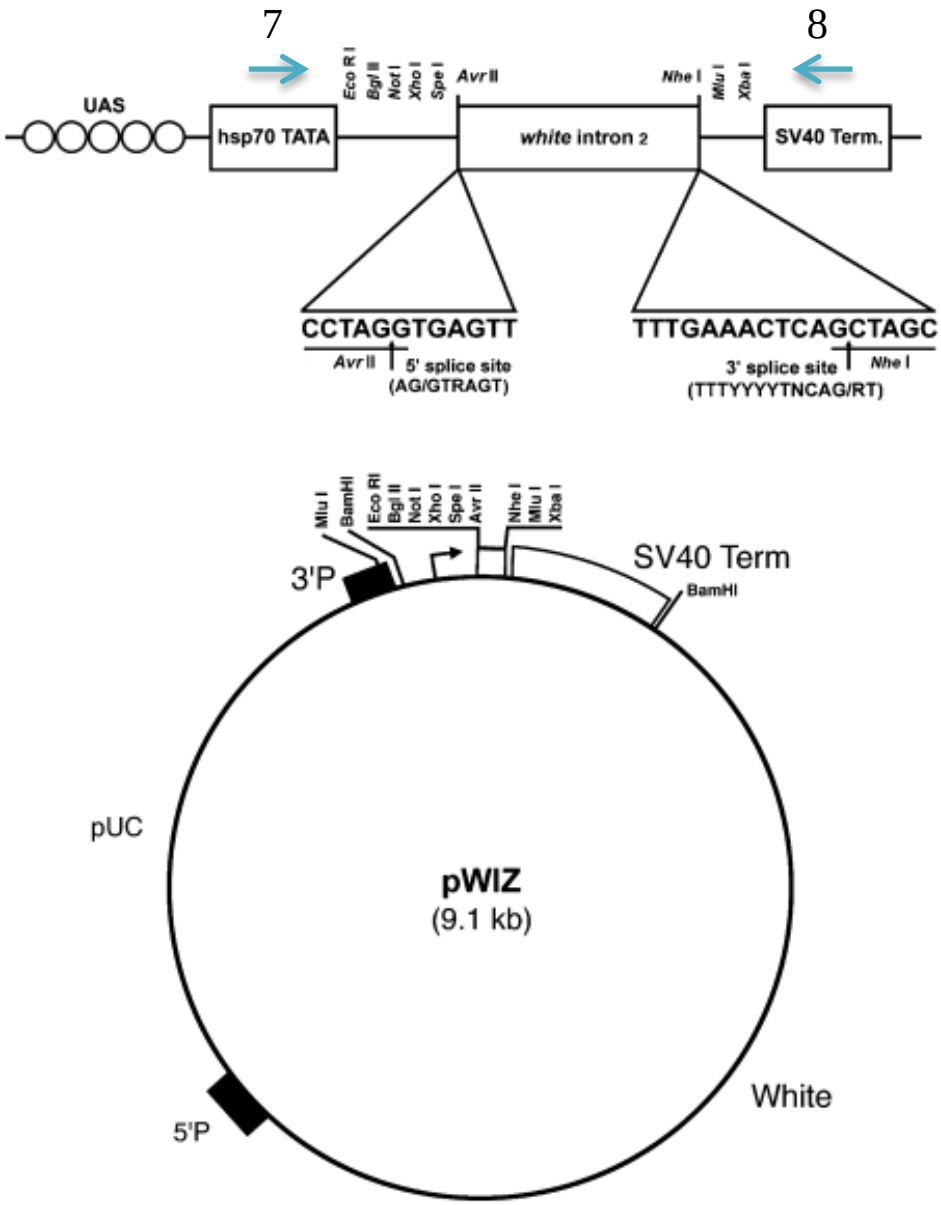

Figure 2-4. The position and orientation of primers for the amplification and sequencing of inserted DNA positioned in the pWIZ multi-cloning sites (MSC). Numbers designate primer number, details of which, can be found in Table 2-4. Adapted from Sik Lee & Carthew (2003).

Table 2-4. The list of primers for amplifying and sequencing inserts in pWIZ

Number	Name	Position[1]	Sequence
7	5’ pWIZ 3311	At base pair number 3311 in pWIZ plasmid sequence	aaagtgaatcaattaaaagtaacca
8	3’ pWIZ 3698	At base pair number 3698 in pWIZ plasmid sequence	agaatcagtagtttaacacattatacactta

[1]The position of primers count from the number of base that 5’ of each primer anneal to.

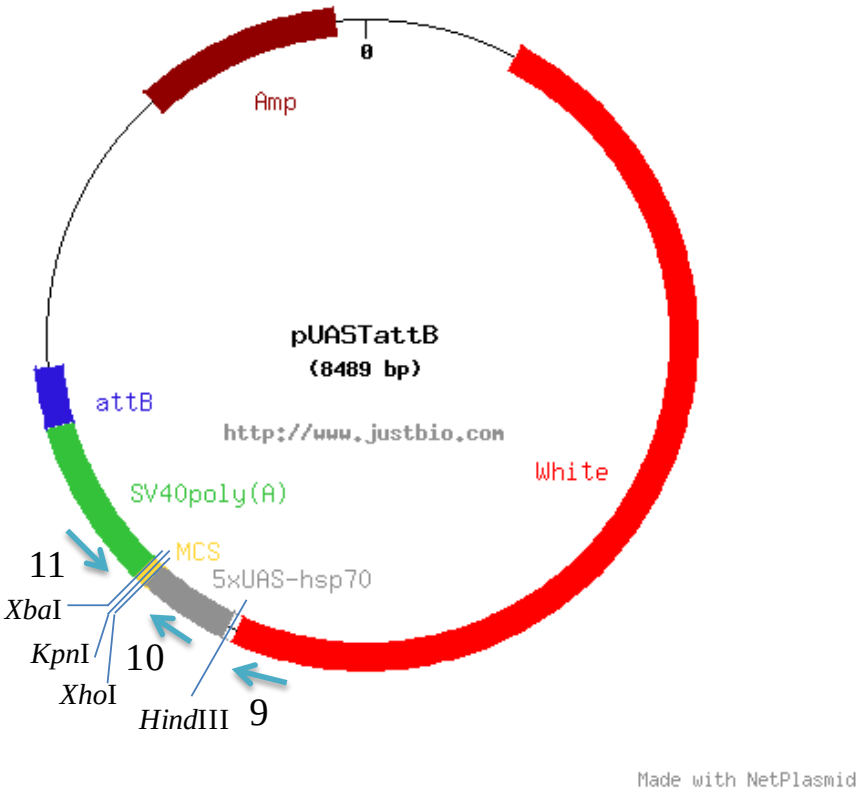

Figure 2-5. The position and orientation of primers for the amplification and sequencing of inserted DNA at pUASTattB MCS (primer number 10 and 11). If five upstream activation sequences (UAS) with heat shock protein 70 promoter (5 x UAS-hsp70) is removed, the primer number 9 and 11 are used for amplifying and sequencing the inserted DNA at MCS. Numbers designate primer number, details of which, can be found in Table 2-5.

Table 2-5. The list of primers for amplifying and sequencing inserts in pUASTattB

Number	Name	Position[1]	Sequence
9	5’ pUASTattB 4765	At base pair number 4756 in pWIZ plasmid sequence	atttaatttagaaaatgcttgg
10	5’ pUASTattB 5118	At base pair number 5118 in pWIZ plasmid sequence	aagtgcaagttaaagtgaa
11	3’ pUASTattB 5405	At base pair number 5405 in pWIZ plasmid sequence	tcagtagtttaacacattatacac

[1]The position of primers count from the number of base that 5’ of each primer anneal to.

QIAfilter plasmid midi kit (Qiagen) was used to purify the recombinant plasmids in accordance to the manufacturers' instructions. The concentration of plasmid was quantified using a NanoDrop spectrophotometer ND 1000 with a final amount consisting of 50 µg sent to Genetic Services Inc for efficient transformation into the attP40 site of the recipient Drosophila line, through a process of co-microinjection with phiC31 integrase (Markstein et al., 2008).

2.6 Measurement of *gsnor* transcript level of RNAi flies

2.6.1 Reverse transcription PCR (RT-PCR) for measuring *gsnor* mRNA

2 µg of total RNA (detailed in Section 2.2.2) extracted from 3-4 day old Drosophila grown at 28℃ was synthesized to cDNA using a PrimeScript RT-PCR Kit (TaKaRa Biotechnology) in accordance to the manufacturers' instructions. The *gsnor* cDNA was amplified by *TaKaRa Ex Taq* HS (TaKaRa Biotechnology) (0.05 unit/µL *TaKaRa Ex Taq* HS, 1 x PCR Buffer II, 0.4 mM dNTPs, 0.2 µM primer 12 and 13 (Figure 2-6; Table 2-6), and 5 %v/v cDNA). The PCR cycles for ampiflication and detection of *gsnor* cDNA were set to an initial denaturation at 94℃ for 1 minute followed by 30 cycles of 94℃ for 30 seconds, 55℃ for 30 seconds and 72℃ for 20 seconds.

To normalize the amount of *gsnor* transcript from each sample, the housekeeping gene *Rp49* transcript was used as an internal control. *Rp49* cDNA was amplified using *TaKaRa Ex Taq* HS (TaKaRa Biotechnology) (0.05 unit/µL *TaKaRa Ex Taq* HS, 1 x PCR Buffer II, 0.4 mM dNTPs, 0.2 µM primer 14 and 15 (Figure 2-7; Table 2-7), and 0.05 %v/v cDNA). The PCR cycles of *gsnor* cDNA were set to an initial denaturation at 94 ℃ for 1 minute followed by 30 cycles of 94 ℃ for 30 seconds, 60 ℃ for 30 seconds and 72 ℃ for 30 seconds. The amplified *gsnor* and *Rp49* fragments were visualized according to Section 2.2.3.

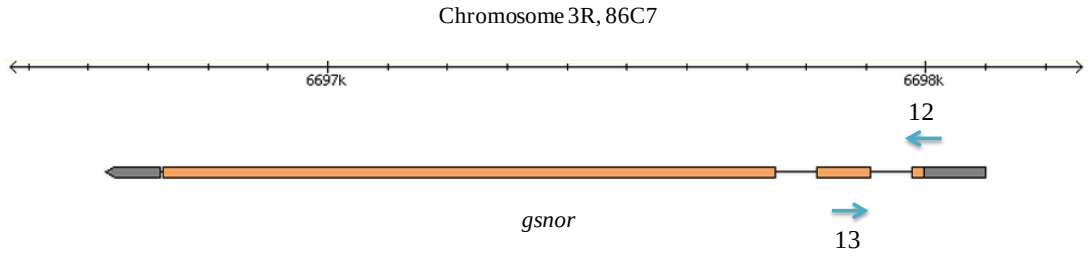

Figure 2-6. The position and orientation of primers for RT-PCR and qRT-PCR measuring *gsnor* mRNA levels. Numbers designate primer number, details of which, can be found in Table 2-6.

Table 2-6. The list of primers for RT-PCR and qRT-PCR measuring *gsnor* mRNA level

Number	Name	Position[1]	Sequence
12	5'*gsnor* 87	At base pair number 87 in *gsnor* gene	aataaaccatactgcaaagatgtctgctac
13	3' *gsnor* 231	At base pair number 231 in *gsnor* gene	ctcgatgaccagcggtttctt

[1]The position of primers count from the number of base that 5' of each primer anneal to.

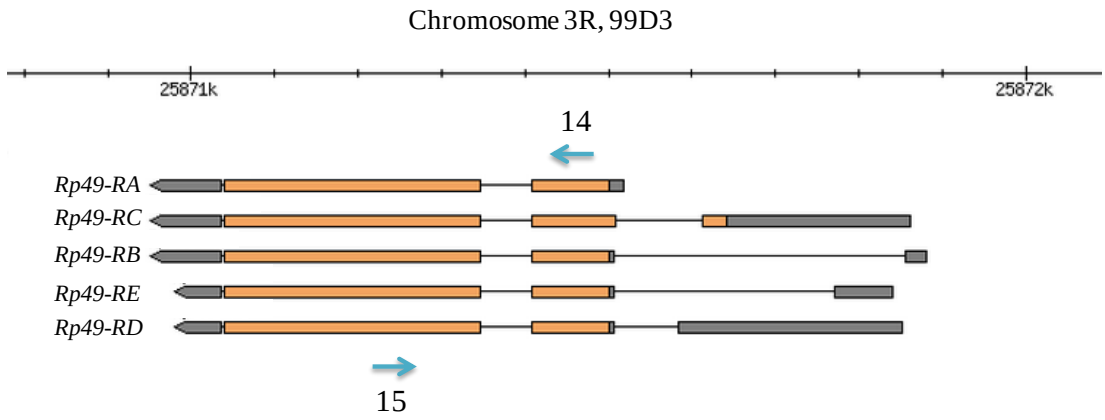

Figure 2-7. The position and orientation of primers for RT-PCR and qRT-PCR measuring *Rp49* mRNA level. Numbers designate primer number, details of which, can be found in Table 2-7.

Table 2-7. The list of primers for RT-PCR and qRT-PCR measuring *Rp49* mRNA level

Number	Name	Position[1]	Sequence
14[2]	5'*Rp49*	At base pair number 407 in *Rp49* gene	agatcgtgaagaagcgcaccaag
15[2]	3' *Rp49*	At base pair number 675 in *Rp49* gene	caccaggaacttcttgaatccgg

[1]The position of primers count from the number of base that 5' of each primer anneal to.

[2]These primers were designed by Koganezawa and Shimada (2002).

2.6.2 Quantitative reverse transcription PCR (qRT-PCR) for measuring *gsnor* mRNA

cDNA synthesized from Section 2.6 was quantified by qRT-PCR using SYBR Green JumpStart *Taq* ReadyMix (Sigma-Aldrich) (1 x SYBR Green JumpStart *Taq* ReadyMix, 0.3 µM primer 12 and 13 (Figure 2-6; Table 2-6) and 1 %v/v cDNA were mixed to produce the end volume of 15 µL). The cycles of qPCR were set to an initial denaturation at 94 ℃ for 2 minutes followed by 45 cycles of 94 ℃ for 15 seconds, 60 ℃ for 20 seconds and 72 ℃ for 20 seconds. The correct size of the PCR product was confirmed by melting curve analysis (temperature was increased from 72 ℃ to 95 ℃ by 1 ℃ increment with 5 second hold in each temperature). DNA-incorporated SYBR green was obtained at the end of every 72 ℃ extension step and continuously from 72 ℃ to 95 ℃ in the melting analysis.

All samples in this experiment were compared to the same standard curve obtained from the same OR cDNA pool. The standard curve was generated from OR cDNA at 0, 10, 10^2, 10^3 and 10^4 fold dilutions. Each sample and standard dilution was measured in three independent replicates (using the cDNA from the same pool). The mean from the three replicates was used to represent the mRNA level from each sample and standard. The *gsnor* transcript level of each sample was normalized with the *Rp49* transcript level of that sample (using the similar condition with the quantification of *gsnor* transcript) with primer set 14 and 15 (Figure 2-7; Table 2-7) were used). The result is the ratio of *gsnor*/*Rp49* transcript levels. The qPCR was performed using a Corbett Rotor-Gene 3000 real-time PCR machine. The measurement of light intensity by incorporated SYBR green dye and all the calculations were done by Corbett Rotor-Gene 3000 Application Software, version 6.1.

2.7 Generation of *gsnor* knockout and complementation of Drosophila

2.7.1 Generation of UAS linked with *gsnor* CDS (UAS-gsnor)

The CDS *of gsnor* from wild-type cDNA (method described in Section 2.2.2) was amplified using Phusion DNA polymerase (Finnzymes) (0.01 unit/µL Phusion

DNA polymerase, 1 x Phusion HF buffer, 0.2 mM dNTPs, 0.5 μM primers number 16 and 17 (Figure 2-8; Table 2-8), and 0.5 %v/v OR cDNA was mixed to the final volume of 200 μL (4 x 50 μL reaction)). PCR cycles were set to an initial denaturation at 98℃ for 3 minutes followed by 5 cycles of 98℃ for 10 seconds, 65℃ for 30 seconds, and 72℃ for 1 minute. Cycles were then set to 25 cycles of 98℃ for 10 seconds, and 72℃ for 1 minute followed by the final extension at 72℃ for 10 minutes.

The amplified *gsnor* CDS fragment was pooled and purified using a solid phase PCR purification kit (QIAquick PCR Purification Kit, Qiagen) in accordance to the manufacturers' instructions. In order to insert the fragment into pUASTattB at the MCS (Figure 2-5), both the amplified fragment and pUASTattB were double digested at 37 ℃ for 12-16 hrs with *Kpn*I (New England Biolabs) and *Xba*I (New England Biolabs) (0.24 unit/μL *Kpn*I, 0.4 unit/μL *Xba*I, 1 x Buffer 2, 1 x BSA, and the total volume of the purified *gsnor* CDS fragment or 15 μL of pUASTattB from QIAprep Spin Miniprep Kit (Qiagen). The digested fragment and plasmid were ligated together using T4 DNA ligase (Promega) in a ligation reaction comprising of 10 μL with 1 x rapid ligation buffer (Promega), 0.3 unit/μL T4 DNA ligase, and preheated 3:1 PCR product: vector molar ratio. Samples were incubated at 16℃ for 3 hours. After the incubation, the transformation was performed as described in Section 2.3.2 except that the transformed *E. coli* DH5α were spread on LB medium plates supplemented with only 100 μg/mL ampicillin.

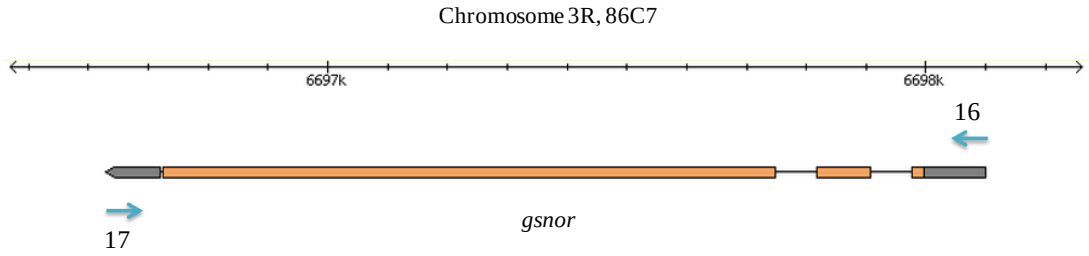

Figure 2-8. The position and orientation of primers for the amplification of full length *gsnor* CDS. Numbers designate primer number, details of which, can be found in Table 2-8.

Table 2-8. The list of primers for amplifying full length *gsnor* CDS

Number	**Name**	**Position[1] and restriction site**	**Sequence**
16	5' *Kpn*I *gsnor* 1	Anneals to the start of *gsnor* gene and contains *Kpn*I at 5'	tttggtacctttcccgcctgctcttctt
17	3' *Xba*I *gsnor* full	Anneals to the end of *gsnor* gene and contains *Xba*I at 5'	gggtctagatacatatacactgggattg ccaacttg

[1]The position of primers count from the number of base that 5' of each primer anneal to.

The colonies which were able to survive ampicillin selection were screened for the correct recombinant plasmids. The screening was performed by colony PCR using the primer 10 and 11 (Figure 2-5; Table 2-5). Double digestion at 37℃ for 12-16 hrs with *Kpn*I (New England Biolabs) and *Xba*I (New England Biolabs) (0.24 unit/µL *Kpn*I, 0.4 unit/µL *Xba*I, 1 x Buffer 2, 1 x BSA, and 4 µL of plasmids extracted by alkaline lysis without solid phase purification (Section 2.2.5)) was performed to identify correct recombinant plasmids. Recombinant plasmid was extracted and purified by alkaline lysis and solid phase purification kit (QIAprep Spin Miniprep Kit, Qiagen) in accordance with the manufacturers' instructions. 3 µL of purified plasmid and 1 µL of 10 µM the primer number 10 or primer number 11 (Figure 2-5; Table 2-5) were sent for sequencing at the GenePool sequencing centre, University of Edinburgh.

The plasmid identified as being correct was purified using a QIAfilter plasmid midi kit (Qiagen) in accordance with the manufacturers' instructions. The plasmids were quantified using a NanoDrop spectrophotometer ND 1000 and 50 µg of the plasmid was sent to Genetic Services Inc for efficient transformation into attP40 site of the recipient Drosophila through a process of co-microinjection with phiC31 integrase (Markstein et al., 2008).

2.7.2 Generation of *gsnor* with the endogenous regulatory sequence (*EP-gsnor*)

Phusion DNA polymerase (Finnzymes) (0.01 unit/µL Phusion DNA polymerase, 1 x Phusion HF buffer, 0.2 mM dNTPs, 0.5 µM primers number 18 and 19 (Figure 2-9; Table 2-9), and 0.5 %v/v OR genomic DNA was mixed to the final volume of 200 µL (4 x 50 µL reaction)) was used to amplify the *gsnor* gene with upstream and downstream non-coding regions using genomic DNA (method describe in the Section 2.2.1) extracted from wild-type Drosophila PCR cycles were set to an initial denaturation at 98℃ for 3 minutes followed by 5 cycles of 98℃ for 10 seconds, 67℃ for 30 seconds, and 72℃ for 1 minute and 40 seconds. Then the cycles were set to 25 cycles of 98℃ for 10 seconds, and 72℃ for 1 minute and 40 seconds followed by the final extension at 72℃ for 10 minutes.

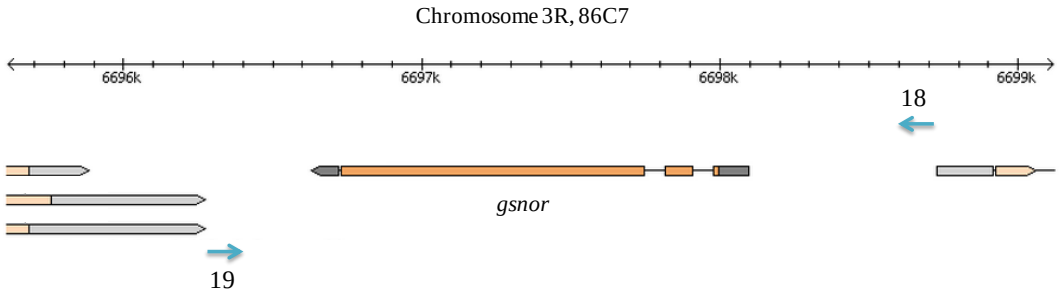

Figure 2-9. The position and orientation of primers for the amplification of the *gsnor* gene with upstream and downstream non-coding sequences present in genomic DNA. Numbers designate primer number, details of which, can be found in Table 2-9.

Table 2-9. The list of primers for amplifying *gsnor* CDS with upstream and downstream non-coding sequences

Number	Name	Position[1] and restriction site	Sequence
18	5'*Hind*III *gsnor* -625	Anneals to the 625 base pair upstream of *gsnor* gene and contains *Hind*III at 5'	aaaaaagcttgaatttgcgttcattggcgt
19	3'*Xba*I *gsnor* +394	Anneals to the 394 base pair downstream of *gsnor* gene and contains *Xba*I at 5'	aaaatctagaaacgttgttgtagtgcgtatttaaatacaggc

[1]The position of primers count from the number of base that 5' of each primer anneal to.

The amplified fragment was pooled and purified by solid phase PCR purification kit (QIAquick PCR Purification Kit, Qiagen) in accordance with the manufacturers' instructionsl. The 5 x UAS-hsp70 in pUASTattB was removed by digestion with *Hind*III and *Xba*I (Figure 2-5), and replaced with the amplified fragment. Both the amplified fragment and pUASTattB were double digested at 37℃ for 12-16hrs with *Hind*III (New England Biolabs) and *Xba*I (New England Biolabs) (0.4 unit/μL *Hind*III, 0.4 unit/μL *Xba*I, 1 x Buffer 2, 1 x BSA, and the total volume of the purified *EP-gsnor* fragment or 15 μL of pUASTattB from QIAprep Spin Miniprep Kit (Qiagen)). The digested fragment and plasmid were ligated together using T4 DNA ligase (Promega) in a ligation reaction comprising 10 μL with 1 x rapid ligation buffer (Promega), 0.3 unit/μL T4 DNA ligase, and preheated 3:1 PCR product: vector molar ratio. Samples were incubated at 16℃ for 3 hours. After the incubation, the transformation was performed as described in Section 2.3.2 with the exceptionthat the transformed *E. coli* DH5α were spread on LB medium plates supplemented with only 100 μg/mL ampicillin.

The colonies able to survive under ampicillin selection were screened for the presence of the correct recombinant plasmid. The screening was performed by colony PCR using the primer 9 and 11 (Figure 2-5; Table 2-5). Double digestion at 37 ℃ for 12-16 hrs with *Hind*III (New England Biolabs) and *Xba*I (New England Biolabs) (0.4 unit/μL *Xba*I, 0.4 unit/μL *Xho*I, 1 x Buffer 2, 1 x BSA, and 4 μL of plasmids extracted by alkaline lysis without solid phase purification (Section 2.2.5)) was also performed to confirm the the presence of a insert in recombinant plasmids. Those recombinant plasmids identified as being correct were extracted and purified by alkaline lysis and the use of a solid phase purification kit (QIAprep Spin Miniprep Kit, Qiagen). 3 μL of purified plasmid and 1 μL of 10 μM the primer number 9 or primer number 11 (Figure 2-5; Table 2-5) were sent for sequencing at the GenePool sequencing centre, University of Edinburgh.

The plasmid identified as being correct was purified using a QIAfilter plasmid midi kit (Qiagen) in accordance with the manufacturers' instructions. The plasmids were quantified using a NanoDrop spectrophotometer ND 1000 with 50 μg of the plasmid being sent to Genetic Services Inc for efficient transformation into the

attP40 site of the recipient Drosophila line through a process of co-microinjection with phiC31 integrase (Markstein et al., 2008).

2.8 Confirmation of *gsnor* knockout by PCR and RT-PCR

2.8.1 PCR to detect full length *gsnor* gene

In order to confirm the presence or absence of *gsnor* genomic DNA, the full length *gsnor* gene was amplified to PCR saturation phase using *TaKaRa Ex Taq* HS DNA polymerase (TaKaRa Biotechnology) (0.05 unit/μL *TaKaRa Ex Taq* HS, 1 x *Ex Taq* Buffer, 0.2 mM dNTPs, 0.2 μM primer 16 and 17 (Figure 2-8; Table 2-8), and 5 %v/v genomic DNA extracted using Section 2.2.1 procedure). The PCR cycles were set to an initial denaturation at 94℃ for 1 minute followed by 5 cycles of 94℃ for 30 seconds, 60℃ for 30 seconds, and 72℃ for 2 minutes and 30 seconds. Then the cycles were set to 25 cycles of 94℃ for 30 seconds, and 68℃ for 2 minutes and 30 seconds. After the amplification, DNA was visualized as stipulated in Section 2.2.3.

2.8.2 RT-PCR to detect *gsnor* mRNA

The presence or absence *of gsnor* mRNA was determined by RT-PCR. Total RNA from Drosophila was extracted according to Section 2.2.2 and then cDNA was produced according to Section 2.6.1. The *gsnor* cDNA was amplified to PCR saturation phase using *TaKaRa Ex Taq* HS (TaKaRa Biotechnology) (0.05 unit/μL *TaKaRa Ex Taq* HS, 1 x PCR Buffer II, 0.4 mM dNTPs, 0.2 μM primer 12 and 13 (Figure 2-6; Table 2-6), and 5 %v/v cDNA). The PCR cycles for ampiflication of *gsnor* cDNA were set to an initial denaturation at 94℃ for 1 minute followed by 35 cycles of 94℃ for 30 seconds, 55℃ for 30 seconds and 72℃ for 20 seconds. The amplified DNA was visualized according to Section 2.2.3.

Rp49 mRNA level was used to normalize the amount of *gsnor* mRNA. The procedure for amplifying *Rp49* mRNA is detailed at Section 2.6.1.

2.9 Fertility measurement

2.9.1 Arabidopsis seed production

The weight (g) of seed per plant was multiplied by the number of seeds counted from 0.1 g seeds and was then multiplied by 10 in order to get the number of seeds per plant. For each sample, three biological replicates were performed and the the standard error (SE) was calculated from the SE from weighting seeds per plant and counting seeds per plant.

2.9.2 Drosophila egg production and percentage of Drosophila eggs that hatch

3-4 day old virgin females and males were used in this experiment. 50 female flies were crossed with about 100 males for 3 days at 25℃. The flies were transferred to grape juice agar containing yeast supplement for 18 hours at 25℃ in order to collect resultant eggs. Following these 18 hours, the flies were removed and the agar was incubated for a further 24 hours at 25℃ in order to determine the hatching frequency.

2.9.3 Photography of Drosophila ovaries and eggs

The ovaries from 3-4 day old virgin females previously crossed with wild-type males as per Section 2.9.2 were dissected in phosphate buffered saline (PBS) (137 mM sodium chloride (NaCl), 2.7 mM potassium chloride (KCl) and 10 mM phosphate buffer) solution. The photographs were taken under a stereo microscope (Nikon SMZ 1500) with a microscope camera attached (Leica DFC425 C).

Eggs were collected using the procedure described at Section 2.9.2, with the exception that eggs were collected for 4 hours following introduction onto grape juice agar containing yeast supplement. The photographs of the 0-4 hour old eggs in PBS solution were taken using a compound microscope (Nikon Eclipse E600) with an microscope camera attached (Leica DFC425 C).

2.9.4 Testing the eggshell properties in preventing desiccation and restricting permeability

Eggs were collected using the procedure described at Section 2.9.2, with eggs collected for 4 hours. The 0-4 hour old eggs were gently transferred to PBS solution. Then the PBS was aspirated through absorption with tissue paper, and the eggs were left to air dry for 15 minutes. 5 mg/mL neutral red dye in PBS solution was added to the eggs for 1 hour and following this the eggs were washed three times with PBS. The photographs were taken in every step using a stereo microscope (Nikon SMZ 1500) with a microscope camera attached (Leica DFC425 C).

2.10 Infection assay

2.10.1 Arabidopsis infection assay

Pseudomonas syringae pv. tomato strain DC3000 (*Pst*) diluted to OD value 0.0002 in 10 mM $MgCl_2$ (diluted from 5 mL King's B medium (20 g/L peptone, 1.5 g/L potassium hydrogen phosphate (K_2HPO_4), 1.5 g/L heptahydrated magnesium sulfate ($MgSO_4 \cdot 7H_2O$), and 15 g/L bacteriological agar) with 50µg/mL rifampicin) from fresh overnight cultures grown at 28℃ with shaking at 225 rpm was infiltrated into the abaxial side of three and a half week old Arabidopsis plants (before bolting occurs) using a 1 mL syringe. After five days, the inoculated leaves were punched with a standard in order to obtain leaf tissue of identical area and sizes. Samples were ground in 10 mM $MgCl_2$ and the number of *Pst* colonies identified from appropriate serial dilutions (in 10 mM $MgCl_2$) plated on King's B agar plates supplemented with 50µg/mL rifampicin incubated at 28℃ (until colonies appeared). From this data the colony forming unit per cm^2 leaf tissue was calculated.

2.10.2 Drosophila septic infection assay

This assay was completed using adult female flies harvested three to four days after eclosion. For each line ~ 30 flies were anaesthetized with carbondioxide (CO_2) and pierced with a sterile tungsten needle dipped in *E. coli* strain MG1655 culture (a pellet of 5 mL LB overnight culture grown at 37℃ with shaking at 275 rpm) with sterile LB acting as the mock control experiment. Fly vials were put on

their side in order to prevent the infected flies falling onto the food at the bottom of the vial. In order to keep infected flies adequately hydrated, a sterile water-soaked dental roll was put in each vial. Vials were kept at 29℃ and the number of surviving flies recorded twice a day, each day forten days post inoculation

2.10.3 Drosophila oral infection assay

A *Erwinia carotovora* pv. *carotovora* 15 (*Ecc*15) culture was obtained by inoculating 500 mL LB with 10 mL *Ecc*15 previously grown for 12-16 hours at 28℃ with shaking at 225 rpm. The bacteria pellet was collected in a 15 mL falcon tube with an equal volume of 10 % sucrose added to the pellet (final concentration is 5 % sucrose).

Prior to the experiment, about 30 3-4 day old female flies were starved for 2 hours. The flies were transferred to a new empty vial containing a dental roll soaked with half a pellet concentration of *Ecc*15. The dental roll was rehydrated using the bacteria solution once per day. Vials were kept at 29℃ and the number of survivors recorded twice a day until no flies remained viable.

2.10.4 Drosophila fungal infection assay

Beauveria bassiana spores were grown on potato dextrose agar (PDA) medium supplemented with 50 μg/mL chloramphenicol at 29℃ until the fugal mycelium had fully covered the plate. To induct spore formation, the plate was protected from light and left in a fume hood until completely desiccated. The dried plate was stored in the dark at 4℃.

About 30 female flies aged 3-4 day old were anaesthetized by chilling on ice. Once fully anaesthetized, the flies were transferred to a 2 mL microcentrifuge tube containing about a one quarter plate amount of *B. bassiana* spores and mycelium. The flies were shaken by hand for 2 minutes. Spores inactivated by autoclaving were used as a control to confirm any observation was not due to wounding (as a result of shaking the flies). Vials containing fungal infected flies were kept at 29℃ and the number of survivors recorded twice a day for a total of 10 days.

2.11 Measurement of antimicrobial peptide (AMP) transcript level by qRT-PCR

cDNA was synthesized from total RNA (extracted as detailed in Section 2.2.2) using PrimeScript RT reagent kit (Perfect Real Time; TaKaRa Biotechnology) (1 x PrimeScript buffer (Perfect Real Time), 5 %v/v PrimeScript RT enzyme mix I, 2.5 μM oligo dT primer, 5 μM random 6 mers and 500 ng RNA) in a total volume of 10 μL. The mixture was incubated at 37℃ for 15 minutes followed by heat inactivation of the reverse transcriptase for 5 seconds at 85℃.

The cDNA was quantified by qRT-PCR using LightCycler 480 DNA SYBR Green I Master (Roche) (1 x Master Mix, 0.5 μM primers of *Dpt*, *Drs*, *Def* and *Mtk* (Figure 2-10; Table 2-10), and 0.05 %v/v cDNA from infected flies or 0.5 %v/v from uninfected flies were mixed to produce a final volume of 20 μL). The cycles of qPCR were set to an initial denaturation at 95℃ for 5 minutes followed by 45 cycles of 95℃ for 10 seconds, 60℃ for 20 seconds and 72℃ for 20 seconds. The correct size of PCR products was confirmed by melting curve analysis (temperature was increased to 95℃ for 5 seconds and decreased 65℃ for 1 minute followed by the increment from 65℃ to 97℃). The ramp rate was set to 4.4℃/second except for when the temperature was decreased to 60℃ in the qPCR cycles and 65℃ in the melting analysis (the ramp rate was at 2.2℃/second), and when the temperature increase from 65℃ to 97℃ in the melting analysis (the ramp rate was at 1.1℃/second). DNA-incorporated SYBR green was obtained at the end of every 72℃ extension step and continuously from 65℃ to 97 ℃ in the melting analysis

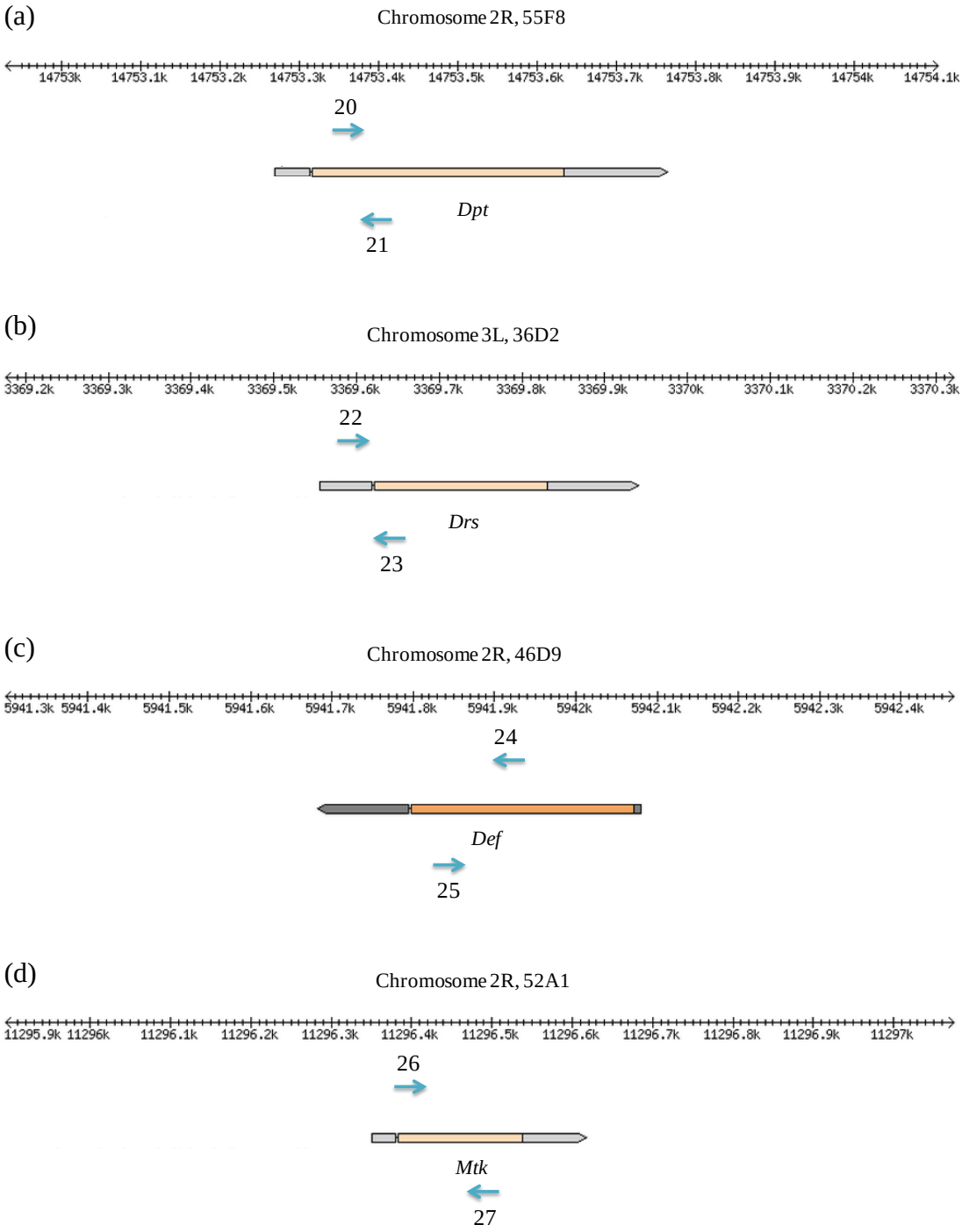

Figure 2-10. The position and orientation of primers used in qRT-PCR of AMP mRNA (**a**) *Diptericin* (*Dpt*), (**b**) *Drosomysin* (*Drs*), (**c**) *Defensin* (*Def*), and (**d**) *Metchnikowin* (*Mtk*). Numbers designate primer number, details of which, can be found in Table 2-10.

Table 2-10. The list of primers for amplifying AMP mRNA

Number	Name	Position[1]	Sequence
20[2]	5’ *Dpt* 76	Anneals to the 76 base pair of *Dpt* gene	gctgcgcaatcgcttctact
21[2]	3’ *Dpt* 143	Anneals to the 143 base pair of *Dpt* gene	tggtggagtgggcttcatg
22[2]	5’ *Drs* 32	Anneals to the 32 base pair of *Drs* gene	cgtgagaacctttccaatatgatg
23[2]	3’ *Drs* 110	Anneals to the 110 base pair of *Drs* gene	tcccaggaccaccagcat
24[3]	5’ *Def* 143	Anneals to the 143 base pair of *Def* gene	tgcagcatagccgccagaa
25[3]	3’ *Def* 257	Anneals to the 257 base pair of *Def* gene	ttgcagtagccgcctttgaacc
26	5’ *Mtk* 30	Anneals to the 30 base pair of *Mtk* gene	gatgcaacttaatcttggagcg
27	3’ *Mtk* 162	Anneals to the 162 base pair of *Mtk* gene	ttaataaattggacccggtcttggttgg

[1]The position of primers count from the number of base that 5’ of each primer anneal to.

[2]These primers are taken from Romeo and Lemaitre (2008).

[3]These primers are taken from Ryu et al. (2008).

All samples in this experiment were compared with the same standard curve obtained from the *Df7305*/*TM6B* cDNA pool. The standard curve was generated from *Df7305*/*TM6B* cDNA with 10, 10^2, 10^3 and 10^4 fold dilutions used. Each sample and standard dilution was measured in three dependent replicates (using the cDNA from the same pool). The mean from the three replicates represent the mRNA level from each sample and standard. The AMP transcript level of each sample was normalized to the *Rp49* transcript level of that sample (using the similar condition with the quantification of AMP transcript) with primer 14 and 15 (Figure 2-7; Table 2-7)). The result was reported as a ratio of AMP/*Rp49* transcript level. The qPCR was performed using a LightCycler 480 real-time PCR machine (Roche). The measurement of light intensity by incorporated SYBR green dye and all the calculations were done using LightCycle 480 Software release 1.5.0 (Roche).

2.12 GSNO synthesis

GSNO was synthesized in accordance to the method described by Hart (1985) with slight modifications. As such, 13 mL of acetone followed by 40 minute stirring was used rather that 10 mL of acetone followed by 10 minute stirring. To wash the GSNO powder, 1 x 5 mL of ice-cold water was used instead of 5 x 1 mL ice-cold water washes.

After the GSNO synthesis, 20 mL of water was added to dissolve the powder. The GSNO concentration was calculated via the Lambert-Beer law ($A = \varepsilon Cd$ where A = absorbance, ε = molar extinction coefficient ($M^{-1}.cm^{-1}$), C = concentration (M), and d = light path length (cm)). The millimolar extinction coefficient of GSNO is 0.92 $mM^{-1}.cm^{-1}$ at 335 nm. The GSNO solution was aliquoted and stored at -70℃.

2.13 Biotin switch technique (BST)

The BST was conducted as per the method described by Forrester et al. (2009) with some modifications. For the sample preparation, about 70 flies were ground with a disposable plastic grinder in HEN buffer pH 8.0 (100 mM HEPES, 1 mM EDTA and 0.1 mM neocuproine) with 1% SDS, 0.5 mM PMSF and working concentration of protease inhibitors (Roche). The protein concentration from each

sample was quantified using the Bradford protein assay (Section 2.2.4). The maximum amount of protein that could be obtained in equal amounts from each sample was diluted into 1.8 ml volume with HEN buffer. OR protein extract was used as positive and negative control. For the positive control, a final concentration of 0.5 mM GSNO was added to the extract and incubated for 20 minutes. For the negative control, the protein extract was transferred to a UV cuvette and placed in UV light for 5 minutes. In the pull down step, 30 µL of prewashed NeutrAvidin agarose suspension (Pierce) was applied to each sample followed by 18 hour rotating incubation at 4℃. In the elution step, 30 µL of elution buffer was used to release the pulled down protein from the agarose bead. If SDS-PAGE (explained in the next section) was not performed within 12-24 hours the eluted protein and input control protein were stored in 1 x Laemmli loading buffer (explained in the next section) at -20℃.

2.14 SDS-PAGE

Protein samples in 1 x Laemmli loading buffer (62.5 mM Tris-Cl pH 6.8, 2 %wt/v SDS, 5 %v/v β-mercaptoethanol, 10 %v/v glycerol, and 0.002 %wt/v bromophenol blue) (stored at -20℃, if β-mercaptoethanol is added) were denatured at 95℃ for 5 minutes. The protein sample was then loaded into polyacrylamide gels previously cast and containing a resolving gel (10 %wt/v 29:1 acrylamide:*N*,*N*′-Methylenebisacrylamide, 375 mM Tris-Cl pH 8.8, 0.1 %wt/v SDS, 0.05 %wt/v ammonium persulfate (APS), and 0.05 %v/v *N*,*N*,*N*′,*N*′-tetramethylethylenediamine (TEMED)) and about 1 cm of stacking gel (4 %wt/v 29:1 acrylamide:*N*,*N*′-Methylenebisacrylamide, 125 mM Tris-Cl pH 6.8, 0.1 %wt/v SDS, 0.05 %wt/v APS, and 0.1 %v/v TEMED). The gels were run in 0.3 %wt/v Tris, 1.44 %wt/v glycine and 0.1 %wt/v SDS. Initially samples were run at a constant 100 volt which was then increased to 120 - 150 volt once the dye had entered the resolving gel. The electrophoresis was stopped after the bromophenol blue margin had reached the end of resolving gel.

2.15 Western blot

The protein from the SDS-PAGE (the previous section) was transferred to PVDF membrane (activated by incubating in methanol for 30 seconds, then rinsing with water, and equilibrating with transfer buffer (25 mM Tris, 192 mM glycine, 10% methanol) for at least 10 min) in transfer buffer at 22 volt, 4℃ for 12-16 hrs using a Trans-Blot Cell system (Bio-Rad).

The membrane was incubated in about 15 mL of blocking buffer (PBS with 5% non-fat dry milk and 0.1% Tween-20) on a rocking platform at room temperature for 2 hour. Following this the membrane is briefly rinsed in blocking buffer before being incubated in a dilution of appropriate primary antibody (500 fold dilution for antiserum of Psh polyclonal antibody (Ferrandon Lab, University of Strasbourg), 100 fold dilution for tissue culture supernatant of Cactus monoclonal antibody (The Developmental Studies Hybridoma Bank, Universiy of Iowa) and 1000 fold dilution for purified GAPDH monoclonal antibody (Imgenex) in 5 mL the blocking buffer) in a 50 mL sterile falcon tube, and incubated on a rocker and roller mixer either at 4℃ overnight or room temperate for 2 hours. The membrane was then washed two times for 10 minutes each with an excess of PBS with 0.1% Tween-20 (PBS-T) on a rocking platform at room temperature. If a polyclonal antibody was used the PBS-T was supplemented with 5% non-fat dry milk

Following the washing steps, the membrane was incubated with an appropriate dilution of horseradish peroxidase (HRP)-linked secondary antibody (2,000 fold dilution for goat anti-rabbit immunoglobulin G (IgG) for the polyclonal primary antibody (Cell Signaling Technology) and 2,000 fold dilution for horse anti-mouse IgG for the monoclonal primary antibodies (Cell Signaling Technology) in 5 mL of the blocking buffer) in a 50 mL sterile falcon tube, and incubated on a rocker and roller mixer at room temperate for 1 hour. The membrane was then washed three times on a rocking platform at room temperature for 10 minutes with about 15 mL of PBS with 0.1% Tween-20 for the monoclonal antibodies or PBS with 5% non-fat dry milk and 0.1% Tween-20 for the polyclonal antibody.

To detect the signal from the secondary antibodies, the washing solution was replaced with ECL Prime Western blotting detection reagent (Amersham) in accordance with the manufacturers' instructions. The membrane was exposed using X-ray films for a period of time optimized to the strength of the signal. The exposed X-ray film was developed using a film processor (Konica SRX-101A) in accordance with the manufacturers' instructions.

If it was necessary to reprobe with a different antibody, the membrane was striped using 62.5 mM Tris-Cl pH 6.7, 2 % SDS and 100 mM β-mercaptoethanol for 30 minutes. The membrane was then washed two times in PBS for 10 minutes on a rocking platform. The washed membrane was then blocked and incubated with an appropriate pair of antibodies.

2.16 Silver staining

The proteins separated by SDS-PAGE (Section 2.14) was silver-stained in accordance to the short silver nitrate staining method described by Chevallet et al. 2006.

.

Chapter 3 The Generation and Morphological Phenotype of *gsnor* Loss-of-Function Mutant

3.1 Introduction

In order to investigate if GSNOR plays important roles in Drosophila, the generation of a loss-of-function *gsnor* mutant is crucial. There are many methods for compromising the function of a target gene. For example, P element insertion, P element imprecise excision, RNAi knockdown, and overlapping deficiencies. In this chapter, I will describe methods that were used to create a loss-of-function *gsnor* mutant and complementation of the loss-of-function *gsnor* mutant by the GAL4/UAS system.

We performed BLAST analysis (more details can be found in http://blast.ncbi.nlm.nih.gov) to search for *A. thaliana gsnor* in the *D. melanogaster* genome using the CDS of *A. thaliana gsnor* as an input template. Two regions of *A. thaliana gsnor* gene (which are about 40 % coverage) were found to have a similarity only with *D. melanogaster formaldehyde dehydrogenase* (*fdh*) (Figure 3-1a). The first conserved region (highlighted with yellow colour) has a score of 48.2 bits, an expect value of $5x10^{-4}$, identities of 119/176 (68 %), and gaps of 6/176 (3 %) (Figure 3-1b). The second conserved region (highlighted with purple colour) has a score of 102 bits, an expect value of $3x10^{-20}$, identities of 214/315 (68 %), and gaps of 8/315 (3 %) (Figure 3-1b). BLAST analysis using the amino acid sequence of *A. thaliana* GSNOR as an input template was performed to ascertain the potential of *D. melanogaster* FDH as the homolog of Arabidopsis GSNOR. The total amino acid sequence of *A. thaliana* GSNOR was found to have the highest similarity with *D. melanogaster* FDH (a score of 497 bits, an expect value of $1x10^{-174}$, identities of 245/388 (63 %), positives = 299/388 (77 %) and gaps of 15/388 (4 %)) (Table 3-1; Figure 3-2).

The score indicates how well the two regions are aligned. In brief, the score is the similarity between compared regions denoted by gaps or miss matches, therefore

the higher this number the higher quality of the alignment. The expected value indicates the number of hits that by chance can be observed in a particular size. This value illustrates a background of each BLAST analysis, so if expect value is near to zero, it means that it is very likely for BLAST to give a significant result. Positives in protein BLAST analysis indicate the number of amino acid residuals that are in the same group based on the BLOSUM62 substitution matrix (more details can be found in http://www.ncbi.nlm.nih.gov) (Madden, 2002).

Because *D. melanogaster fdh* was found to have the highest similarity with *A. thaliana gsnor*, the previous publications about *fdh* were reviewed. FDH is actually a class III ADH which previously has been shown to have GSNOR activity in mammals (Luque et al., 1994; Jensen et al., 1998). In this study, we therefore exploited *fdh* to study GSNOR function in Drosophila. In this thesis, *fdh* is called *gsnor* in order to make it synchronised with Arabidopsis *gsnor* and also to emphasize on GSNOR activity of this enzyme.

(a)

GACCGGATAATTACATTTGTAGCTATGAGAAGAAAAAGAAGACCACACTACTCTCTCTATCT

CTCTTTCTCTCTATCTCTCTCTATCTCTCTCATTTCTTCCTGCGTCAATGGCGACTCAAGGT

CAGGTTATCACTTGCAAAGGTACCTTTATCCTCGATCCTCGCACTCTCACTATCTCTGCGGT

GGCTTACGAGCCGAACAAGCCTCTGGTCATCGAAGATGTGCAAGTGGCTCCACCTCAAGCTG

GTGAGGTTCGGATCAAGATCCTCTACACTGCTCTTTGTCACACCGACGCTTACACTTGGAGC

GGCAAGGATCCTGAAGGTCTCTTTCCTTGTATTCTAGGTCATGAGGCTGCTGGGATTGTTGA

GAGTGTTGGTGAAGGAGTAACTGAAGTTCAAGCTGGAGATCATGTTATCCCTTGTTATCAAG

CTGAGTGTCGTGAATGCAAGTTTTGCAAATCTGGGAAGACTAACCTTTGTGGCAAGGTGAGA

TCTGCTACTGGTGTTGGGATTATGATGAATGACCGTAAGTCGAGGTTCTCGGTTAATGGGAA

ACCCATTTATCACTTCATGGGTACTTCCACGTTTAGTCAGTATACTGTTGTTCATGATGTTA

GCGTCGCCAAAATTGATCCTACTGCTCCTTTGGATAAAGTTTGCCTTCTTGGATGTGGTGTT

CCCACTGGCCTTGGAGCAGTTTGGAATACTGCAAAAGTAGAACCAGGGTCAAATGTTGCCAT

TTTCGGTCTTGGCACTGTTGGACTTGCTGTTGCCGAGGGTGCGAAAACAGCTGGTGCTTCAA

GGATCATTGGCATTGACATCGATAGCAAGAAGTATGAAACTGCAAAGAAGTTTGGTGTTAAC

GAATTTGTGAACCCAAAGGATCACGACAAGCCAATTCAGGAAGTGATTGTCGATCTCACTGA

TGGCGGTGTTGACTACAGCTTTGAGTGCATCGGGAATGTCTCCGTGATGAGAGCTGCATTGG

AGTGCTGTCACAAGGGATGGGGAACTTCGGTCATAGTTGGTGTTGCAGCATCAGGACAAGAG

ATATCAACTCGTCCGTTCCAACTCGTGACTGGCCGTGTGTGGAAAGGAACAGCTTTTGGTGG

TTTCAAGAGTCGAACCCAAGTGCCTTGGCTTGTAGAAAAGTACATGAACAAGGAGATAAAAG

TGGATGAATACATAACACACAACTTGACCTTGGGAGAAATCAATAAGGCTTTCGATCTATTG

CACGAAGGTACTTGCCTTCGTTGTGTCCTCGATACCAGCAAATGACTATATGGGTCCTCTCT

GCTTTAATCTATGTGTTCTTGTGACTTTCGTCTTTTATCGGTATTGACATTTCCTAAGAGCA

ACAGACTACTCTACTCGTGTGTGTCTCGTTTCTATCTTATGCTTCAATAAAATATCAATTAA

GACCGAAACCATCA

(b)

```
gsnor 143      AGGTTCGGATCAAGATCCTCTACACTGCTCTTTGTCACACCGACGCTTACACTTGGAGCG  202
               |||| || |||||||||      ||| |    | || ||||| || || | |||    |||||
fdh   6697749  AGGTGCGCATCAAGATCACGGCCACGGGCGTCTGCCACACGGATGCCTTCACCCTGAGCG  6697690

gsnor 203      GCAAGGATCCTGAAGGTCTCTTTCC--TTGTATTCTAGGTCATGAGGCTGCTGGGATTGT  260
               |     ||||| || || || || ||  | || ||   || |||||||  || || || ||
fdh   6697689  GTGCCGATCCGGAGGGCCTGTTCCCAGTGGTGTTG--GGACATGAGGGCGCCGGCATCGT  6697632

gsnor 261      TGAGAGTGTTGGTGAAGGAGTAACTGAAGTTCAA-GCTGGAGATCATGTTATCCCT  315
                ||||| || || || || || ||  || ||||| ||||| || ||||| ||| ||
fdh   6697631  GGAGAGCGTCGGCGAGGGCGTGAC-CAACTTCAAGGCTGGCGACCATGTCATCGCT  6697577


gsnor 685      GCTGGTGCTTCAAGGATCATTGGCATTGACATCGATAGCAAGAAGTATGAAACTGCAAAG  744
               ||||||||    | ||||   |||||||||||| ||  | | |||| |||    || |||
fdh   6697210  GCTGGTGCCGGCAAGATCTACGGCATTGACATCAATCCCGACAAGTTTGAGCTGGCCAAG  6697151

gsnor 745      AAGTTTGGTGTTAACGAATTTGTGAACCCAAAGGATCA---CGACAAGC---CAATTCAG  798
               ||||| ||  | | ||| ||||| ||||| ||||||     |||||||    | || |||
```

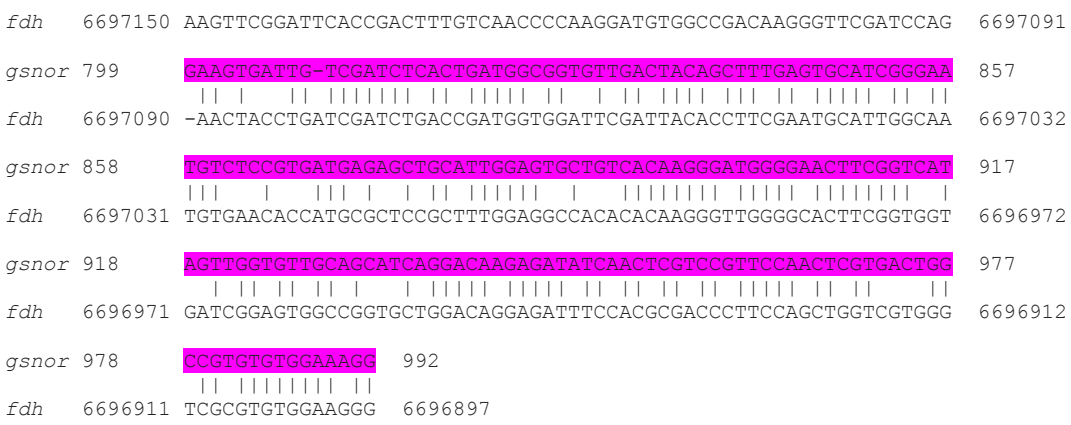

Figure 3-1. (**a**) The *A. thaliana gsnor* CDS used as a template for the BLAST analysis. The yellow and purple highlight the regions that were found to be conserved in *D. melanogaster* by the BLAST analysis (40 % coverage). (**b**) The alignment of the two conserved areas between *A. thaliana gsnor* gene and *D. melanogaster fdh* which was selected by the BLAST analysis. The *gsnor* yellow region has a score of 48.2 bits, an expect value of $5x10^{-4}$, identities of 119/176 (68 %), and gaps of 6/176 (3%). The *gsnor* purple region has a score of 102 bits, an expect value of $3x10^{-20}$, identities of 214/315 (68 %), and gaps of 8/315 (3 %). The numbers on *gsnor* panel indicate a base pair position on *A. thaliana gsnor* CDS. The numbers on *fdh* panel indicate a base pair position on the Drosophila third chromosome.

Table 3-1. The protein BLAST results showing *D. melanogaster* proteins that can significantly align with to *A. thaliana* GSNOR

Drosophila proteins	**Score (bits)**	**Coverage**	**Expect value**	**Identities**	**Positives**	**Gaps**
Formaldehyde dehydrogenase	497	98 %	$1x10^{-174}$	245/388 (63 %)	299/388 (77 %)	15/388 (4 %)
Sorbitol dehydrogenase 1	79.3	85 %	$5x10^{-16}$	89/339 (26 %)	135/339 (40 %)	36/339 (11 %)
LP12301p	78.2	85 %	$1x10^{-15}$	92/339 (27 %)	136/339 (40 %)	36/339 (11 %)
Sorbitol dehydrogenase 2	68.2	85 %	$3x10^{-12}$	84/339 (25 %)	128/339 (38 %)	34/339 (10 %)
CG4836 isoform E	53.9	91 %	$2x10^{-7}$	80/369 (22 %)	134/369 (36 %)	58/369 (16 %)
CG4836 isoform B	53.5	91 %	$3x10^{-7}$	80/369 (22 %)	134/369 (36 %)	58/369 (16 %)
CG4836 isoform C	53.5	91 %	$2x10^{-7}$	80/369 (22 %)	134/369 (36 %)	58/369 (16 %)
CG16935	42.7	19 %	$5x10^{-4}$	27/78 (35 %)	41/78 (53 %)	1/78 (1 %)
AT25977p	42.0	19 %	$6x10^{-4}$	27/78 (35 %)	41/78 (53 %)	1/78 (1 %)
MIP20337p	29.3	17 %	10.0	20/75 (27 %)	31/75 (41 %)	5/75 (7 %)

```
GSNOR 2   ATQGQVITCKGTFILDPRTLTISAVAYEPNKPLVIEDVQVAPPQAGEVRIKILYTALCHTDAYTWSGKDP  71
          AT+G+VITCK            +AVA+E  KPLVIED++VAPP+A EVRIKI  T +CHTDA+T SG DP
FDH   3   ATEGKVITCK------------AAVAWEAKKPLVIEDIEVAPPKAHEVRIKITATGVCHTDAFTLSGADP  60

GSNOR 72  EGLFPCILGHEAAGIVESVGEGVTEVQAGDHVIPCYQAECRECKFCKSGKTNLCGKVRSATGVGIMMNDR  141
          EGLFP +LGHE AGIVESVGEGVT  +AGDHVI  Y  +C ECKFCKSGKTNLC K+R   G G+M  +
FDH   61  EGLFPVVLGHEGAGIVESVGEGVTNFKAGDHVIALYIPQCNECKFCKSGKTNLCQKIRLTQGAGVM-PEG  129

GSNOR 142 KSRFSVNGKPIYHFMGTSTFSQYTVVHDVSVAKIDPTAPLDKVCLLGCGVPTGLGAVWNTAKVEPGSNVA  211
           SR S  G+ ++HFMGTSTF++YTVV D+S+ KI+  APL+KVCLLGCG+ TG GA  NTAKVE GS  A
FDH   130 TSRLSCKGQQLFHFMGTSTFAEYTVVADISLTKINEKAPLEKVCLLGCGISTGYGAALNTAKVEAGSTCA  199

GSNOR 212 IFGLGTVGLAVAEGAKTAGASRIIGIDIDSKKYETAKKFGVNEFVNPKD-HDK-PIQEVIVDLTDGGVDY  279
          ++GLG VGLAV  G K AGA +I GIDI+  K+E AKKFG  +FVNPKD  DK  IQ  ++DLTDGG DY
FDH   200 VWGLGAVGLAVGLGCKKAGAGKIYGIDINPDKFELAKKFGFTDFVNPKDVADKGSIQNYLIDLTDGGFDY  269

GSNOR 280 SFECIGNVSVMRAALECCHKGWGTSVIVGVAASGQEISTRPFQLVTGRVWKGTAFGGFKSRTQVPWLVEK  349
          +FECIGNV+ MR+ALE  HKGWGTSV++GVA +GQEISTRPFQLV GRVWKG+AFGG++S + VP LVE
FDH   270 TFECIGNVNTMRSALEATHKGWGTSVVIGVAGAGQEISTRPFQLVVGRVWKGSAFGGWRSVSDVPKLVED  339

GSNOR 350 YMNKEIKVDEYITHNLTLGEINKAFDLLHEGTCLRCVL  387
          Y+ K++ VDE+ITH L L +IN+AFDL+H+G  +R ++
FDH   340 YLKKDLLVDEFITHELPLSQINEAFDLMHKGESIRSII  377
```

Figure 3-2. The amino acid alignment between *A. thaliana* GSNOR and *D. melanogaster* FDH, the likely homolog of *A. thaliana* GSNOR (Table 3-1). The numbers on the GSNOR panel indicate an amino acid position on *A. thaliana* GSNOR (in total of 391 amino acids). The numbers on the FDH panel indicate an amino acid position on *D. melanogaster* FDH (in total of 379 amino acids). The letters between both panels indicate positions with identical amino acid residuals in *A. thaliana* GSNOR and *D. melanogaster* FDH. + indicates positions where there is an amino acid from the same group in *A. thaliana* GSNOR and *D. melanogaster* FDH (based on BLOSUM62 substitution matrix) (Madden, 2002).

3.2 Possible *gsnor* null allele and P element imprecise excision flies

This experiment was necessary to determine if Drosophila lines 680 (*Fdh*^{nNC1}/TM6; possible *gsnor* null allele), 683 (P element excision), and 684 (P element excision) were knockout lines of the *gsnor* gene (or not). 680 was ordered from Bloomington stock centre (stock number: 4038). 683 and 684 were generated by Hannah Barton by the induction of P element imprecise excision from 679 (the P element insertion upstream of *gsnor* gene) (Barton, 2008). Sequence analysis and in gel activity assays were performed in order to examine whether these lines are a knockout of *gsnor*.

3.2.1 Sequencing of *gsnor* gene in 680 (possibly null allele) does not show a significant loss-of-function mutation.

The genomic sequence exhibited two adjacent point mutations which change from thymine (T) and guanine (G) to cytosine (C) and adenine (A), respectively. These mutations presumably represent polymorphism within the population of Drosophila from which strain 680 was derived (Voelker et al., 1980). These mutations result in valine (V) to alanine (A) changes (Figure 3-3), both of these residues are in the same group of nonpolar amino acids. This amino acid sequence was checked for the amino acids required for GSNOR activities with the reported GSNOR protein conformation in *Antrodia camphorate* (fungi) GSNOR (Huang et al., 2009) and horse liver GSNOR (Eklund and Ramaswamy, 2008). This revealed that line 680 might not be a knockout for *gsnor*.

(a)
CTTTTAGGGTTTTTTATCGATCGCTGTCTGGTCACACTGCGCTAACCGGCCTTTTCCCGCCT
GCTCTTCTTCCTTATCATCATTCATTTTCCAGTCGTTCTCCATTCGCCAATTGGACCTTGTC
GCTAAACTTTCCAATAAACCATACTGCAAAGATGTCTGCTACCGAGGGCAAGGTGAGTGCAG
CAACTGGAATTTTAATTAGCAGAAACACACCCAGGCTGTCAATCAACAATCAATCACAGGTT
ATCACATGCAAGGCCGCCGTCGCTTGGGAGGCAAAGAAACCGCTGGTCATCGAGGATATCGA
GGTGGCGCCGCCCAAGGCTCATGAGGTTAGTTCAGTTCGGAATGTGTCAAATGTGACAGATT
TAACTAATTACCATGATGGCATGACTTCAAAAGGGGCACCTCCCGTCTCAGCTGCAAGGGAC
AGCAGTTGTTCCACTTCATGGGCACCTCCACCTTCGCAGAGTACACCGTGGTGGCCGACATT
TCGCTGACAAAGATCAACGAAAAGGCGCCGCTGGAGAAAGTCTGCCTGCTGGGGTGCGGCAT
TTCCACAGGCTACGGAGCCGCCCTCAACACTGCCAAGGCAGAAGCCGGTAGCACCTGCGCTG
TTTGGGGCTTGGGAGCTGTGGGCTTGGCCGTGGGTTTGGGCTGCAAGAAGGCTGGTGCCGGC
AAGATCTACGGCATTGACATCAATCCCGACAAGTTTGAGCTGGCCAAGAAGTTCGGATTCAC
CGACTTTGTCAACCCCAAGGATGTGGCCGACAAGGGTTCGATCCAGAACTACCTGATCGATC
TGACCGATGGTGGATTCGATTACACCTTCGAATGCATTGGCAATGTGAACACCATGCGCTCC
GCTTTGGAGGCCACACACAAGGGTTGGGGCACTTCGGTGGTGATCGGAGTGGCCGGTGCTGG
ACAGGAGATTTCCACGCGACCCTTCCAGCTGGTCGTGGGTCGCGTGTGGAAGGGTTCCGCCT
TCGGAGGCTGGCGCTCCGTTTCCGATGTTCCCAAATTGGTGGAGGACTACCTGAAGAAGGAT
CTGCTGGTGGACGAGTTCATCACCCACGAGCTGCCGCTGTCGCAGATCAACGAGGCATTCGA
TCTGATGCACAAGGGCGAGAGTATCCGATCCATTATTAAGTAC

(b)
V R I K I T A T G V C H T D A F T L S G A D P E G L F P V V L G H E
G A G I V E S V G E G V T N F K A G D H V I A L Y I P Q C N E C K F
C K S G K T N L C Q K I R L T Q G A G V Met P E G T S R L S C K G Q
Q L F H F Met G T S T F A E Y T V V A D I S L T K I N E K A P L E K
V C L L G C G I S T G Y G A A L N T A K A E A G S T C A V W G L G A
V G L A V G L G C K K A G A G K I Y G I D I N P D K F E L A K K F G
F T D F V N P K D V A D K G S I Q N Y L I D L T D G G F D Y T F E C
I G N V N T Met R S A L E A T H K G W G T S V V I G V A G A G Q E I
S T R P F Q L V V G R V W K G S A F G G W R S V S D V P K L V E D Y
L K K D L L V D E F I T H E L P L S Q I N E A F D L Met H K G E S I
R S I I K Y (Stop)

Figure 3-3. (**a**) *gsnor* sequence of 680 (possible *gsnor* null allele) showing two adjacent point mutations (marked with red colour). 'XXXX', 'XXXX' and 'XXXX' represent mRNA sequence, CDS and intron sequence, respectively. (**b**) The translation of the third exon. The mutated amino acids are marked in red.

3.2.2 In gel activity assays revealed that possible null allele 680, P element excision 683 and 684 are not gsnor knockouts.

Wild type OR, 679 (the P element insertion upstream of *gsnor* gene), 680 (possibly null allele), Relish (the impaired Imd pathway), Spaetzle (the impaired Toll pathway), 683 (the P element excision), 684 (the P element excision), *gsnor 1-3* (the loss-of-function *gsnor*; the negative control) and wild-type Arabidopsis (the positive control) were tested for both GS-FDH and GSNOR activities of the GSNOR protein. The in gel GS-FDH activity assay was performed by staining the native polyacrylamide gel (preloaded with total protein extracts) with substrates (GSH, formaldehyde and NAD^+) and chemicals for visualization (NBT and PMS). The PMS is an intermediate electron carrier by coupling NADH to the reduction of NBT to produce coloured formazans (Worsfold et al., 1976). Initially it appears that GS-FDH activity is absent in lines 680, 681 and 682 (the top bands; Figure 3-4a). We thought that 680 was a null allele, and also in lines 681and 682. However, due to the dual function of the enzyme, GS-FDH and GSNOR, an in gel GSNOR assay was performed by staining the native polyacrylamide gel with GSNO and NADH. The gel then visualized with a UV transilluminator. Because NADH can be excited by UV light (340nm) leading to a visible light emission (455nm), areas that GSNOR activity was present were indicated by an absence of emitted visible light (McComb et al., 1976). The results from the GSNOR in gel activity assay show the position of actual enzyme activities (indicated by the band between 80 kDa and 58 kDa markers) (black arrows; Figure 3-4a and b). This reveals that the top bands of GS-FDH activity are not the activity from the GSNOR protein. This is because GS-FDH and GSNOR activity (the band between 80 kDa and 58 kDa markers) were present in all of the Drosophila lines, none of them are a true knockout of the *gsnor* gene. We are unsure about which types of enzymes produce the top and the bottom bands in the GS-FDH assay, but presumably they could be enzymes producing NADH or other chemicals which can act as an electron donor leading to detection by PMS and NBT.

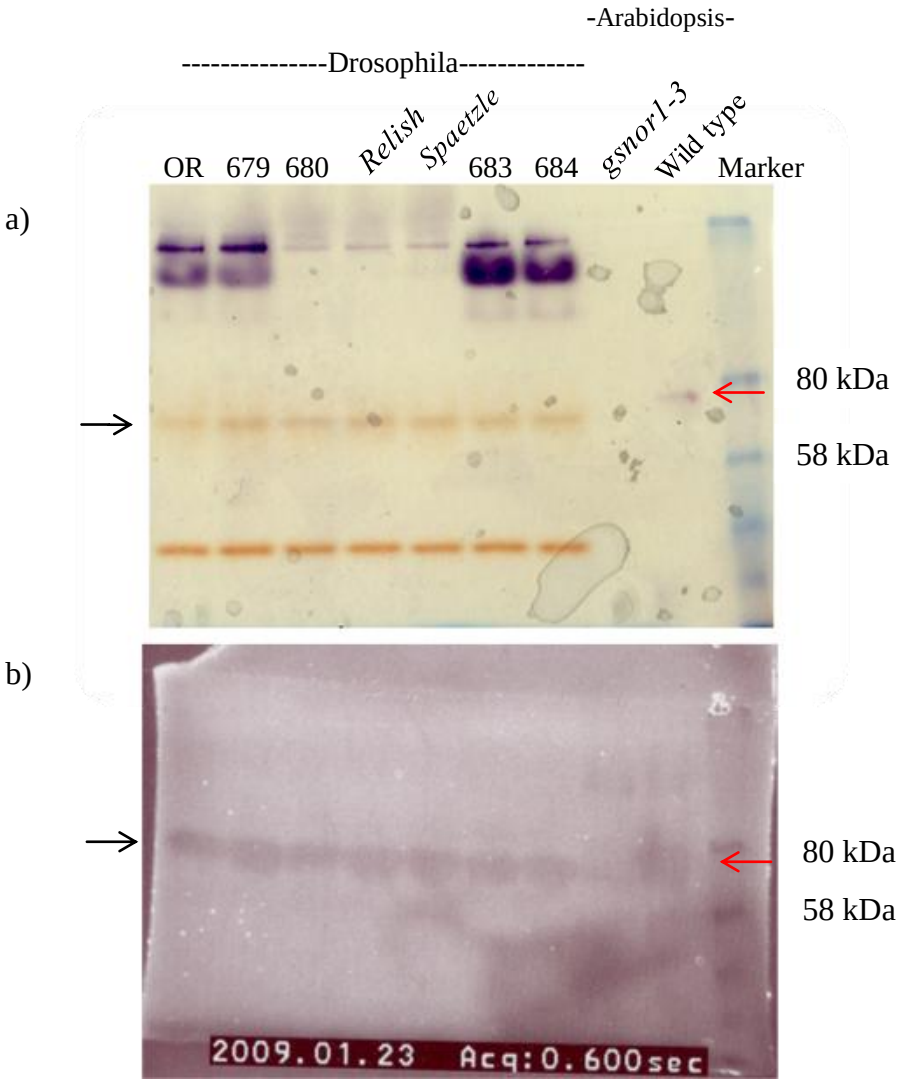

Figure 3-4. In gel activity assays were undertaken on native polyacrylamide gels by staining with substrates and detection chemicals. Native polyacrylamide gels were loaded with total protein extracts from wild type OR, 679 (the P element insertion upstream of *gsnor* gene), 680 (possibly null allele), the impaired Imd pathway *Relish*, the impaired Toll pathway *Spaetzle*, 683 (the P element excision), 684 (the P element excision), *gsnor 1-3* (the loss-of-function *gsnor*) and wild-type Arabidopsis. *gsnor 1-3* and wild-type Arabidopsis were used as a negative and positive controls, respectively. (**a**) The GS-FDH activity staining was performed with GSH,

formaldehyde and NAD^+ as substrates, and NBT and PMS for NADH visualization. (**b**) The replica of (a) staining for GSNOR activity. The gel was stained with NADH and GSNO as substrates and then bands were detected by a UV transilluminator. The black arrows show the Drosophila GS-FDH (a) and GSNOR (b) activities. The red arrows show the Arabidopsis GS-FDH (a) and GSNOR (b) activities. The bands indicated by black and red arrows in GS-FDH (a) and GSNOR (b) activity assays were in the same position of both gels.

3.3 Using a RNA interference (RNAi) approach for targeting *gsnor* gene knockdown

Since the previous experiments had shown that 680, 683, and 684 Drosophila lines were not *gsnor* knockouts, the next experiment was to generate a loss-of-function *gsnor* through RNAi manipulation.

3.3.1 Introduction to RNAi and a GAL4/UAS system

RNAi is defined as the introduction of double stranded RNA (dsRNA) that leads to the degradation of target mRNA and abortion of translation. In brief, the RNAi mechanism has two main steps: firstly, the RNAse III enzyme Dicer processes dsRNA into about 20 to 30 bp with two-nucleotide overhangs usually on the 3' end. Secondly, one strand of the processed RNA (guide RNA) is incorporated into RNA-inducing silencing (RISC) complex. The agonaute component of the RISC complex then uses the guide RNA to target complementary mRNA (Nowotny and Yang, 2009).

A construct expressing dsRNA can be transcribed under the control of the GAL4/UAS. In yeast *Saccharomyces cerevisiae*, GAL4 regulates the transcription of *GAL10* and *GAL1* genes by binding to the 17 bp UAS. This gene-activation ability is not limited to yeast but also functions in *D. melanogaster*. In Drosophila, this system has two components: a GAL4 containing line or 'driver' and UAS containing line or 'responder'. This system allows us to control gene expression in both space and time. To control spatial expression, *GAL4* can be placed after regulatory elements which drive expression in a specific tissue, hence GAL4 only activates UAS followed by a gene of interest in that tissue (Figure 3-5) (Gustafson and Boulianne, 1996; Duffy, 2002). For temporal regulation, GAL4 can be linked with a hormone receptor, such as the estrogen receptor or progesterone receptor. GAL4 can therefore only bind the UAS in the presence of estrogen or progesterone, which can be applied exogenously (Osterwalder et al., 2001; Duffy, 2002).

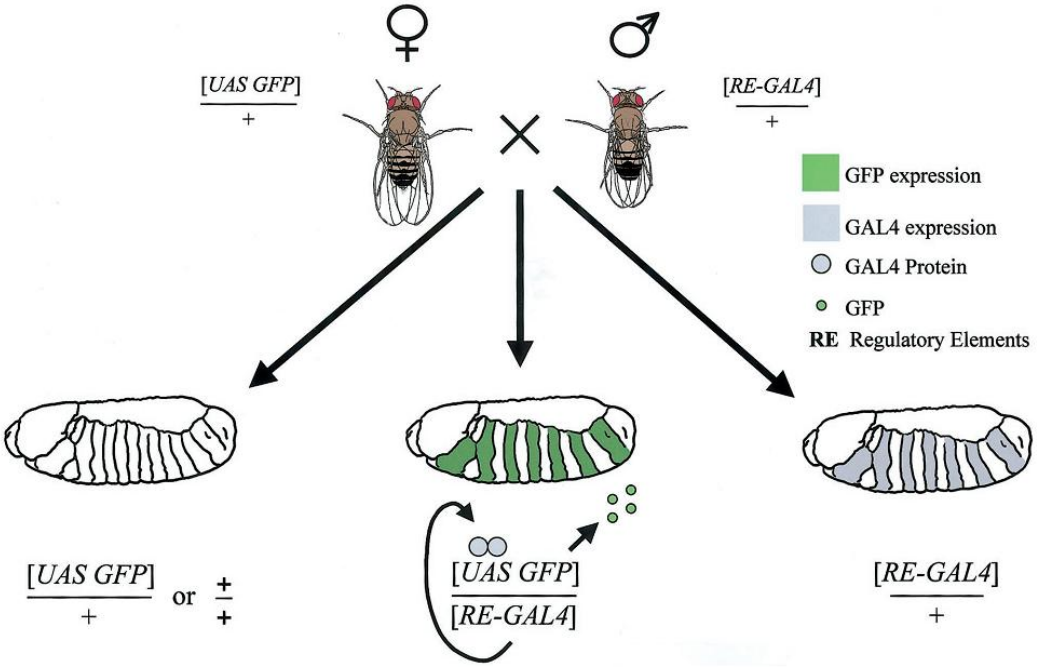

Figure 3-5. The schematic description of the GAL4/UAS system in spatial control of expression. The responder (containing UAS followed by green fluorescent protein (GFP) gene) and driver (containing GAL4 after a regulatory element (RE)) are crossed together to produce progenies that have both UAS and GAL4. In these progenies, GAL4 is transcribed in specific tissue depending on RE. As a result UAS is also activated in this specific tissue. Taken from Duffy (2002).

3.3.2 Generation of Drosophila RNAi lines

One of the crucial things to consider about making RNAi is the 'off-target silencing effect' caused by unexpected pairing between generated guide RNA and non-target mRNA. In order to minimize the off-target effect, this experiment used 'dsCheck' program because it is one of a few programs available for designing long RNAi which covers all of possible generated guild RNAs. This program chose fragments by dicing the long dsRNA into every possible 19-nucleotide piece, for example, a 500-bp fragment is diced into 482 pieces of 19 nucleotides. Each piece was then compared with the mRNA database and fragments which have the lowest mismatch to other mRNAs are identified (Naito et al., 2005).

Two 400-bp fragments at base pair number 112-511 (*RNAi1*) and 603-1002 (*RNAi2*) of *gsnor* mRNA were chosen as they exhibited the lowest match to other non-target mRNAs. The reason why two fragments were chosen is to confirm each other in order to prevent an off-target effect.

3.3.2.1 PCR and two step cloning to pWIZ

The RNAi containing organisms are made of inverted repeats which are integrated into host DNA. After transcription, the inverted repeats will form hairpin dsRNA. However, a problem of plasmid constructs with long inverted repeats (palindrome) is that it often provokes cruciform DNA leading to replication abortion or elimination of cruciform DNA (David, 1994). It is noticeable that a plasmid with long inverted repeats has a lower yield when compared to typical plasmid preparations.

In order to overcome this problem, plasmid pWIZ was chosen for this experiment. pWIZ is an efficient plasmid for making an RNAi construct in *E. coli*. This is due to the presence of the *white* intron 2 that once efficiently removed from mature mRNA locates between the inverted repeats (Figure 3-6) (Sik Lee and Carthew, 2003).

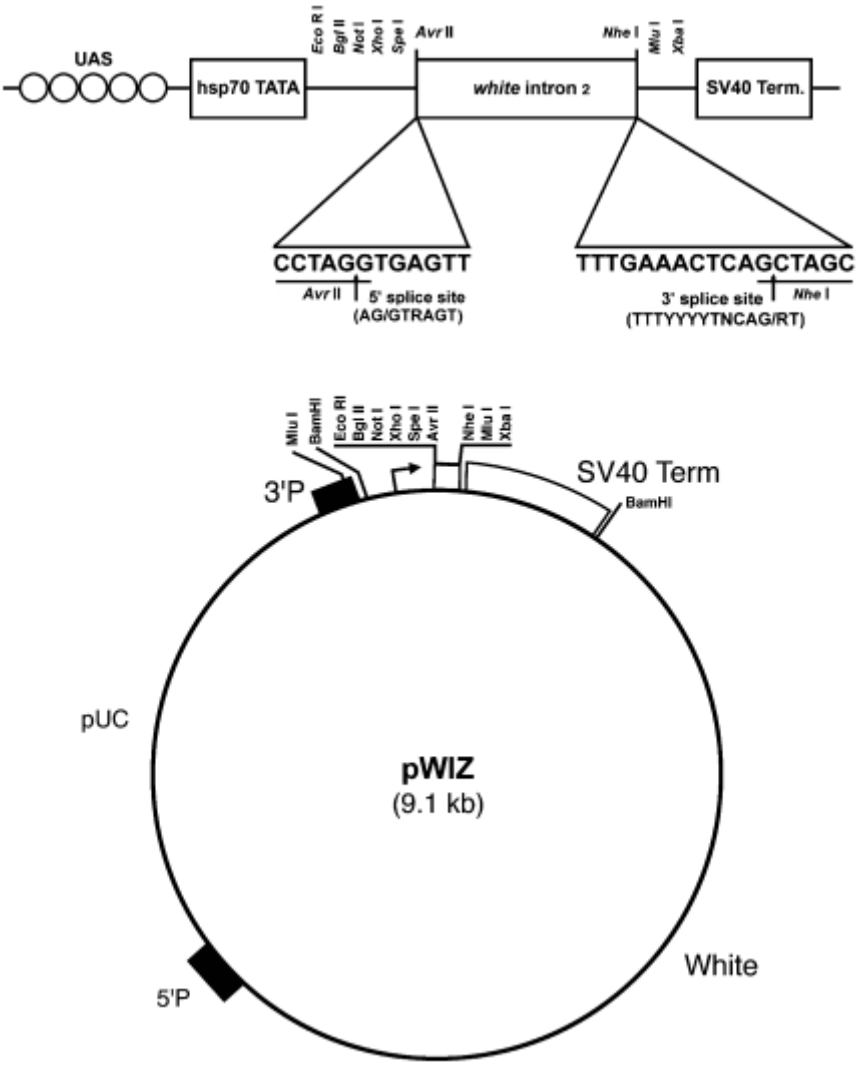

Figure 3-6. The structure of pWIZ. This is a pUC-derived plasmid containing the white intron 2 between a multiple cloning site for inverted repeat insertion. *Avr* II and *Nhe* I are the respective restriction sites, compatible with *Xba* I in primers, which are used for insertions before and after the *white* intron 2. Taken from Sik Lee and Carthew (2003).

For constructing an RNAi construct in pWIZ, a two step cloning strategy was employed. Initially, both high fidelity PCR fragments (112-511 and 603-1002), amplified by Phusion DNA polymerase (Finnzyme), were separately inserted into plasmid pWIZ. The two recombinant plasmids were transformed into DH5α competent cells. The plasmid-containing cells were selected and cultured to increase the plasmid yield. The recombinant plasmids were then purified and checked by sequencing. Plasmids containing the correct insert were then used to perform the second cloning stage. It is possible that the second insert can be oriented either in the same direction as the first insert or in the desired opposite orientation. In order to select the correct orientation, the recombinant plasmids were extracted and concentration differences were ascertained. Because of the instability of long inverted repeats, RNAi-containing plasmids are likely to have a lower concentration and this can be detected in an ethidium bromide stained agarose gel (Figure 3-7). Here, the orientation is 5' to 3' for the first fragment and 3' to 5' for the second fragment. After screening for differences in plasmid concentration, the constructs were again confirmed by sequencing. However, due to the complex structure of inverted repeats, only 200 bp sequences can be typically obtained at the beginning and end of this fragment (Figure 3-8).

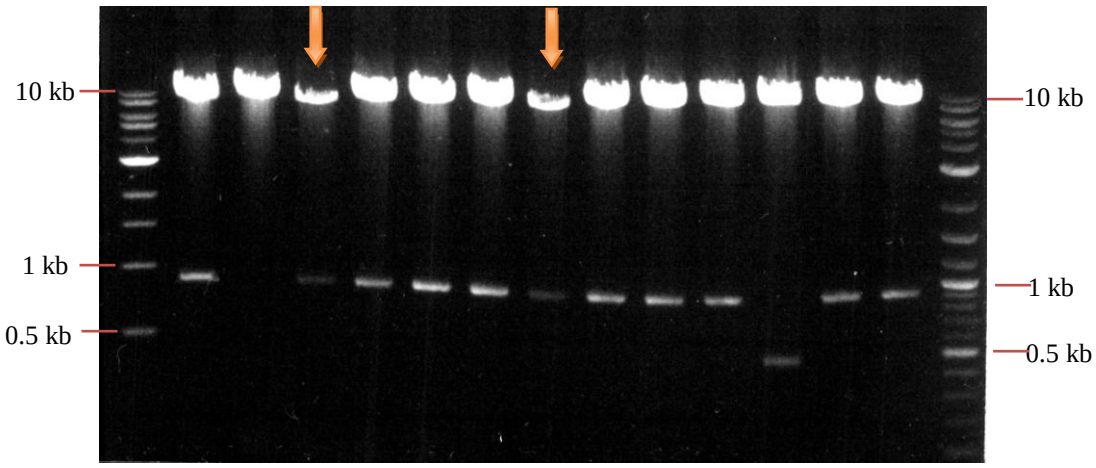

Figure 3-7. Agarose gel electrophoresis with plasmid DNA digested with *Xho*I and *Xba*I and then stained with ethidium bromide. The orange arrows show lower concentrations of plasmid, compared to other lanes. This may potentially indicate plasmids containing a successful RNAi construct.

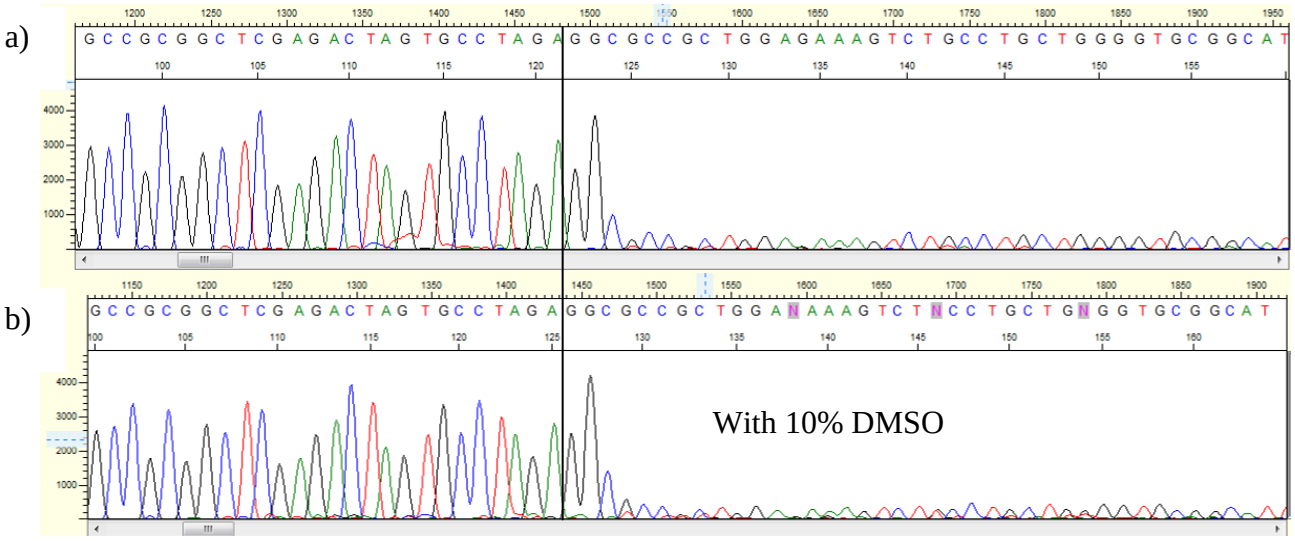

Figure 3-8. (**a**) The DNA sequencing chromatogram shows a highly reduced signal after entering RNAi inverted repeats (black line). (**b**) The addition of 10% dimethyl sulfoxide (DMSO), which aids the denaturation of template, did not improve this signal.

3.3.2.2 Transfering RNAi fragments to pUASTattB for site-specific tranformation

The main problem in using P elements to integrate the exogenous DNA is that transgenes are randomly integrated into the recipient's genome and the expression level of the transgene is then altered by its location on the recipient's genome, a process known as 'position effect'. Therefore, the transformants need to be screened for optimum expression. Not only does the position effect reduce the efficiency of transformation but the screening process is extremely labour intensive.

To overcome the position effect, a targeted integration approach is adopted. In Drosophila, phage phi31 site-specific integration system is used for the integration between attB (in phage) and attP (in bacteria) site. There are over 100 attP sites randomly inserted into the Drosophila genome. To identify the optimal attP site, Markstein et al. (2008) placed the luciferase gene under the control of the UAS and integrated this transgene into 20 attP sites. Luciferase activity was then monitored directly and was found to be highest at the attP 40 integration site (flanked by CG14035 and Msp-300). This location also resulted in the highest expression when driven with the tissue-specific GAL4 driver in the fat body, the major organ in Drosophila defense system. Thus, attP 40 was chosen as an integration site for *gsnor* RNAi line.

The RNAi fragments were cut out and purified. Then the fragments were ligated to the pUASTattB plasmid which has an attB site for integration and UAS site for GAL4 driver (Bischof et al., 2007) (Figure 3-9). The RNAi pUASTattB constructs were confirmed again by sequencing.

The *gsnor* RNAi pUASTattB constructs were sent to Genetic Services Inc for efficient transformation into Drosophila through a process of co-microinjection with phiC31 integrase. Three independent transformed lines were generated for each construct (*RNAi1-1*, *RNAi1-2* and *RNAi1-3*, and *RNAi2-1*, *RNAi2-2* and *RNAi2-3*).

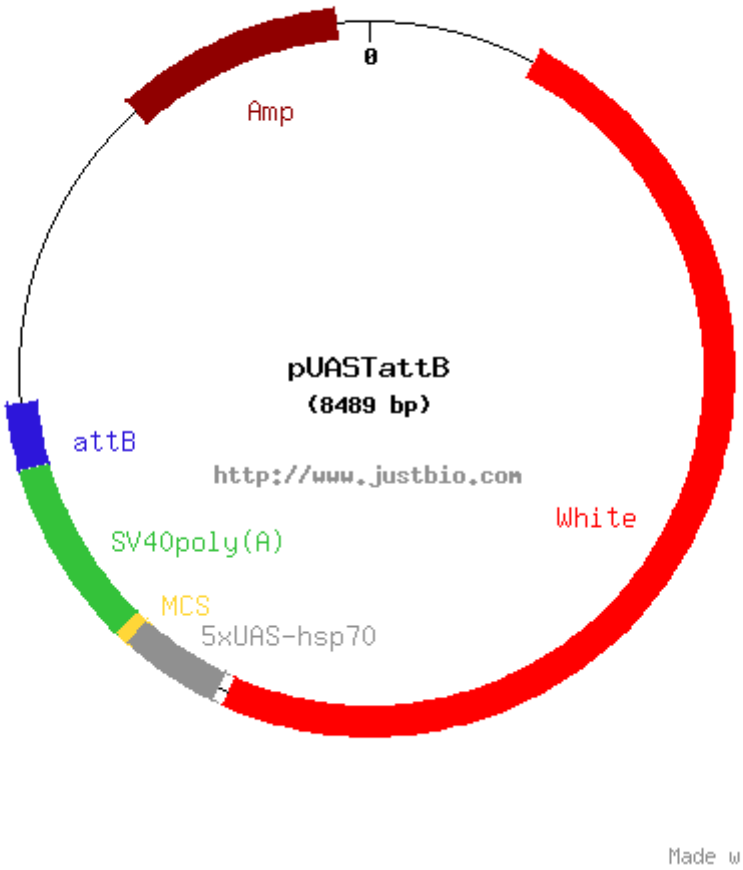

Figure 3-9. The structure of pUASTattB (Bischof et al., 2007). The RNAi inverted repeats with *white* intron 2 in between were cut from pWIZ (Figure 3-6) and inserted into MCS in order to create a construct with the attB site for Drosophila site-specific transformation. This figure was made by NetPlasmid online tool (www.justbio.com) based on GenBank sequence database (accession number: EF362409) (www.ncbi.nlm.nih.gov/genbank).

3.3.3 RNAi constructs did not strongly knockdown *gsnor* transcript levels.

After crossing *UAS-RNAi1* and *2* together with *Tubulin-GAL4* (*Tub-GAL4*, the strong whole body-expressed GAL4) and *Daughterless-GAL4* (*Da-GAL4*, the moderate whole body-expressed GAL4) (Figure 3-10), we observed that the progenies from *Da-GAL4*, and *UAS-RNAi1* and *2* (*Da-GAL4*/*UAS-RNAi1* and *Da-GAL4*/*UAS-RNAi2*) were viable, however the progenies from *Tub-GAL4* and *UAS-RNAi2* (*Tub-GAL4*/*UAS-RNAi2*), but not with *UAS-RNAi1*, were completely lethal in the pupa stage. This effect can be also observed partially in *Da-GAL4*/*UAS-RNAi1*, *Da-GAL4*/*UAS-RNAi2*, and *Tub-GAL4*/*UAS-RNAi1*. Drosophila can develop to a complete adult stage, but become trapped inside their pupa cases (Figure 3-11). We think that this is an off-target interference effect which is stronger in *RNAi2* compared to *RNAi1* containing lines (because increased GAL4 expression by using *Tub-GAL4* leads to complete lethality only in the *RNAi2* flies). For the viable flies, we then performed RT-PCR to measure *gsnor* mRNA levels. Only slightly lower *GSNOR* transcript levels were detected when comparing *Da-GAL4*/*UAS- RNAi* or *Tub-GAL4*/*UAS-RNAi* with the recipient flies crossed with *Da-GAL4* or *Tub-GAL4* (*Da-GAL4*/+ or *Tub-GAL4*/+) (Figure 3-12). In order to see a more accurate mRNA level of the RNAi effect, qRT-PCR was performed. We found that the *GSNOR* transcript levels of *Da-GAL4*/*UAS-RNAi1*, *Da-GAL4*/*UAS-RNAi2*, and *Tub-Gal4*/*UAS-RNAi1* decrease to approximately 50 percent of the recipient controls (Figure 3-13a and b). We reasoned that the 50 percent reduction is unlikely to be sufficient to observe the phenotypic effect from the *gsnor* RNAi knockdown. Further, enhanced RNAi production by increasing the temperature or using stronger expressed GAL4 is also unlikely to improve the knockdown efficiency because these procedures also increase the off-target effect.

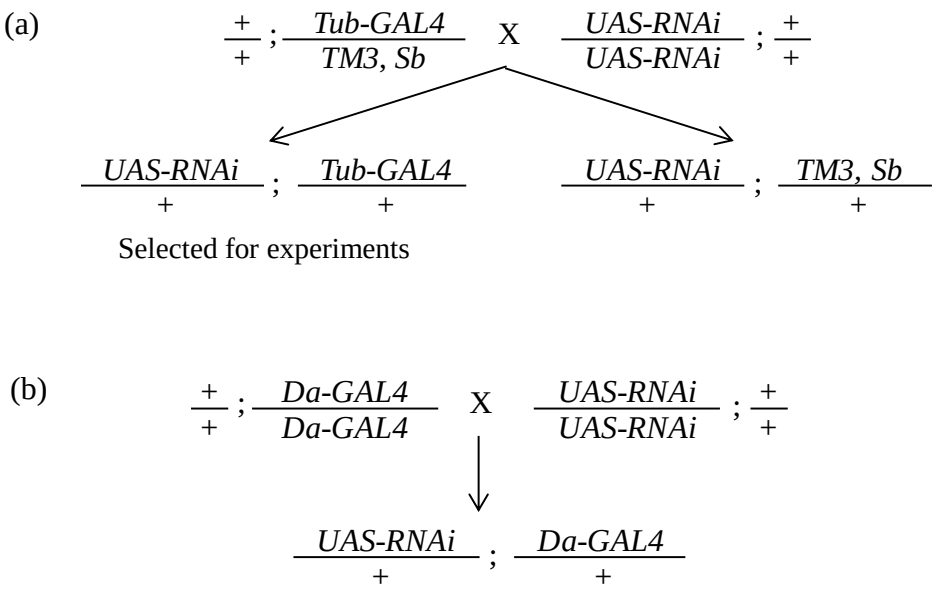

Figure 3-10. Crossing schemes to generate *gsnor* knockdown flies by GAL4 driving RNAi expression. (**a**) *Tub-GAL4* flies were used for generating whole body strong expression RNAi Drosophila. (**b**) *Da-GAL4* flies were used for generating whole body moderate expression RNAi Drosophila.

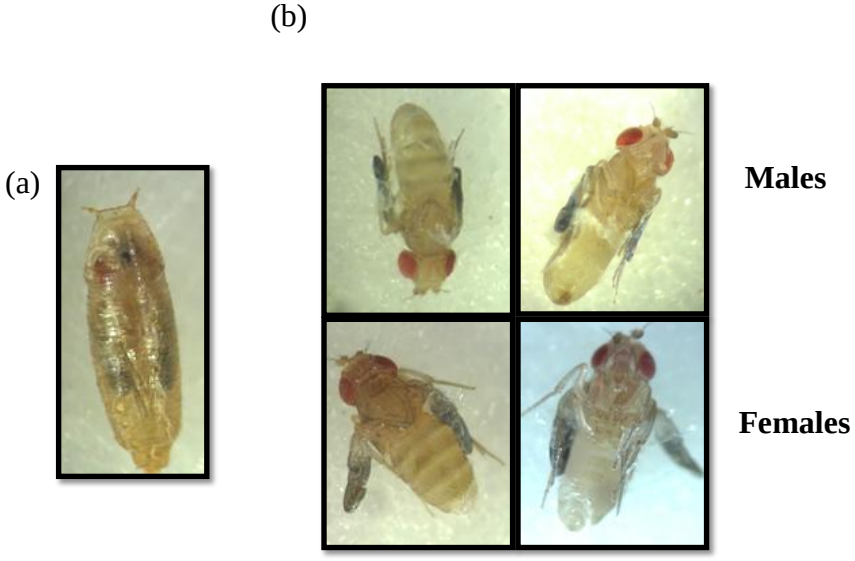

Figure 3-11. (**a**) The pictures of *Tub-GAL4*/*UAS-RNAi2* adult fly trapped in its pupa case and (**b**) *Tub-GAL4*/*UAS-RNAi2* male and female adults which pupa cases were removed. The complete morphological development was shown in adults trapped in pupa cases.

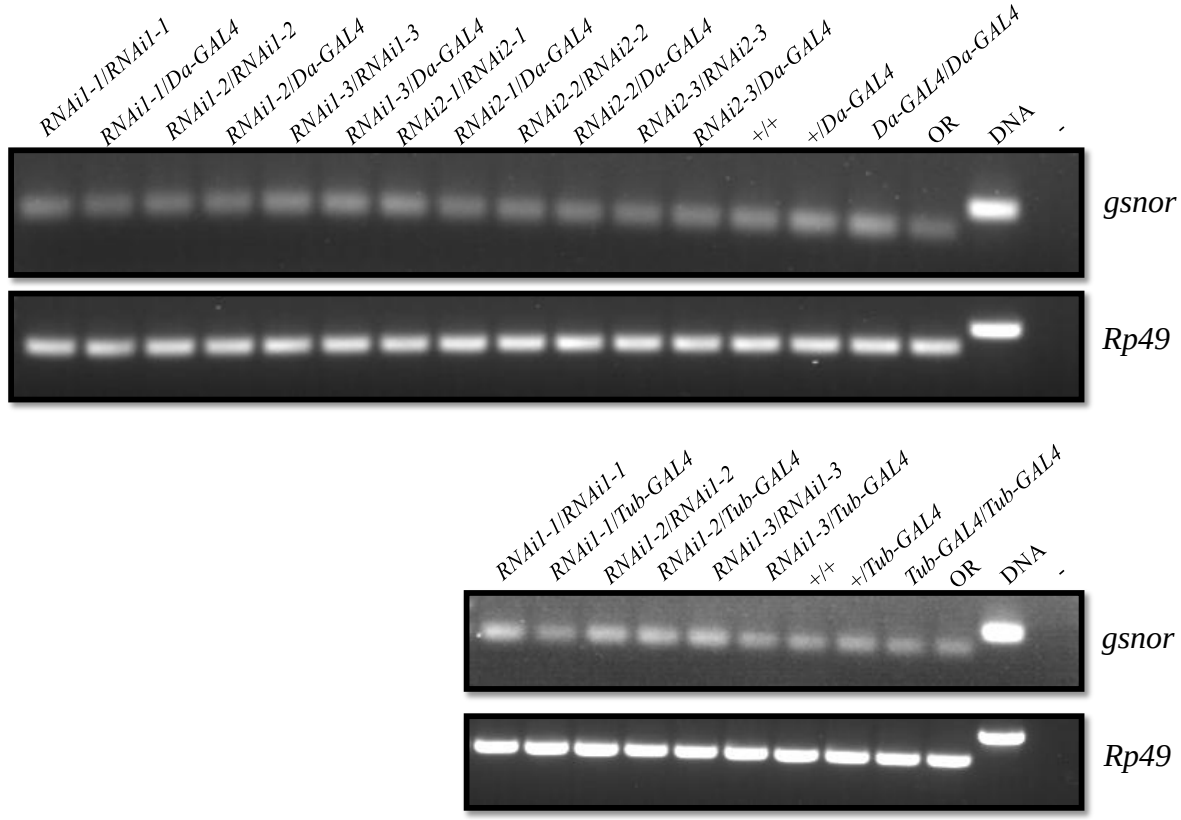

Figure 3-12. RT-PCR measurement of *gsnor* and house-keeping *ribosomal protein 49* (*Rp49*) transcript for semi-quantification. Each RNAi construct has three independent transformed lines (*RNAi1-1*, *RNAi1-2* and *RNAi1-3* for the first construct, and *RNAi2-1*, *RNAi2-2*, *RNAi2-3* for the second construct). The '+' indicates the wild-type genotype in the RNAi construct recipient background. The '-' indicates non-template controls.

(a)

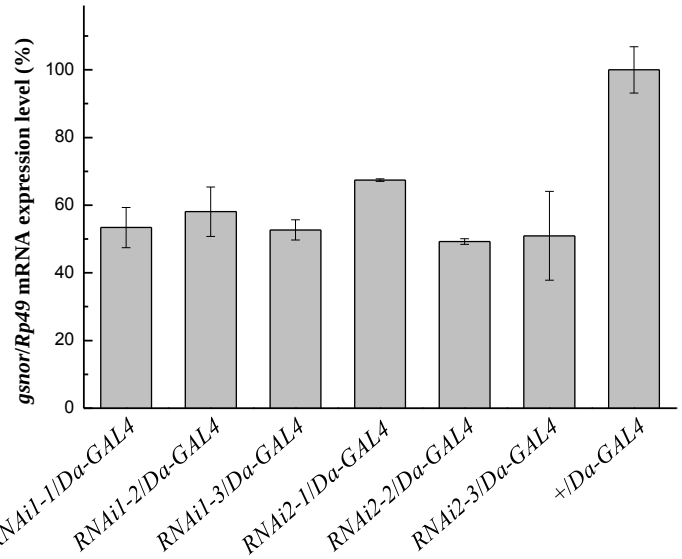

(b)

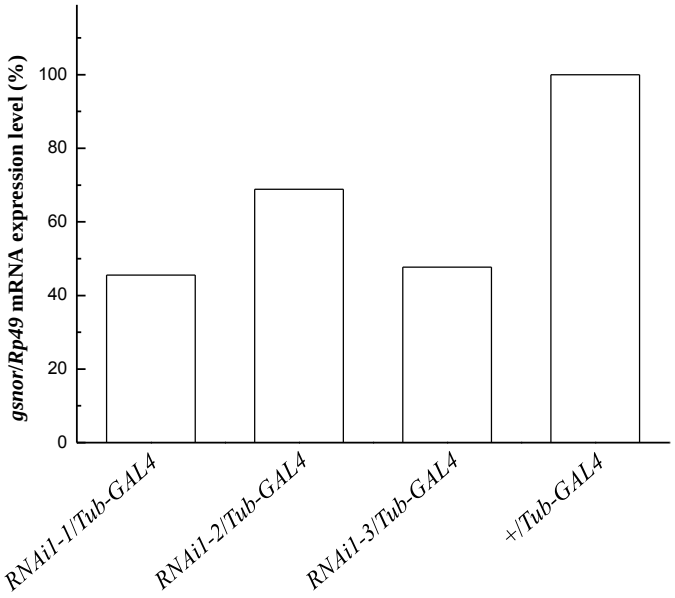

Figure 3-13. qRT-PCR measuring the relative *gsnor* transcript level normalized to the level of *Rp49* mRNA. The relative transcript levels of (**a**) +/*Da-GAL4* and (**b**) +/*Tub-GAL4* were calibrated to 100 percent indicating the normal relative level of *gsnor* mRNA. The data in graph (a) represents a mean of two independent experiments. The error bars in graph (a) indicate standard error (SE). Only one experiment was done for graph (b).

3.4 *gsnor* knockout mutant generation by overlapping deletion technique

As we could not generate RNAi knockdown of *GSNOR*, we searched through the Drosophila database in Flybase (www.flybase.org) in order to find Drosophila strains containing a deletion of the *gsnor* gene region which we could use together with RNAi lines to increase the knockdown effect or to use them as an overlapping deficiency to delete the *gsnor* gene. The overlapping deficiency is a technique to generate a knockout mutant by crossing two deficiency lines which have genomic deletions that both include the gene of interest.

We found two deficiency lines (*Df(3R)Exel7305*/*TM6B* (called '*Df7305*/*TM6B*' in this thesis) and *Df(3R)Exel7306*/*TM6B* (called '*Df7306*/*TM6B*' in this thesis)) with breakpoints that overlap within *gsnor* (Figure 3-14a). This collection has been generated by trans-recombination between two FRT elements in a chromosome resulting in a genomic deletion between those two FRT elements (Parks et al., 2004). The two deficiency lines were crossed, and their overlapping progenies (*Df7305*/*Df7306*) were collected for further experiments (Figure 3-14b). To verify that there is no maternal effect involved in *Df7305*/*Df7306* and also to confirm the results from *Df7305*/*Df7306*, most of the experiments were undertaken using both *Df7305*/*Df7306* and its reciprocal cross (*Df7306*/*Df7305*) (Figure 3-14c).

In order to ensure that phenotypes observed in the overlapping deficiency are from the absence of GSNOR, complementation lines were generated by introduction of UAS linked with the CDS of *gsnor* (*UAS-gsnor*) into *Df7305*/*TM6B* (shown by the crossing scheme in Figure 3-15a) and *act5C-GAL4* into *Df7306*/*TM6B* (shown by the crossing scheme in Figure 3-15b). Therefore, GSNOR will be highly expressed in the overlapping deficiency containing both *UAS-gsnor* and *act5C-GAL4* (*UAS-gsnor*/+; *Df7305*/*act5C-GAL4*, *Df7306* or *act5c*:*UAS-gsnor*; *Df7305*/*Df7306*) (Figure 3-15c). A construct containing the endogenous promoter of *gsnor* was also generated by introduction of the endogenous *gsnor* gene with upstream and downstream non-gene regions between the *gsnor* gene and the adjacent genes (*EP-gsnor*) into *Df7305*/*TM6B* (shown by the crossing scheme in Figure 3-16a) and *Df7306*/*TM6B* (shown by the crossing scheme in Figure 3-16b). Therefore, the overlapping deficiency will contain two copies of the transgene (*EP-gsnor*/*EP-gsnor*;

Df7305/*Df7306*) (Figure 3-16c). These non-gene regions were predicted by http://www.ensembl.org using the Biotiffin regulatory motif database, and these regions should contain all the regulatory sequences needed to regulate *gsnor* (Figure 3-16e).

3.5 The overlapping deficiency on *gsnor* results in a *gsnor* knockout.

Loss of *gsnor* in flies with the overlapping deletions was confirmed by PCR to detect *gsnor* gene, RT-PCR to detect *gsnor* mRNA and activity assays to detect both GSNOR and GS-FDH activities (using the same method as described in Section 1.2 in this chapter). *gsnor* DNA (the amplified fragment between 87th and 595th base pair of *gsnor* gene) (Figure 3-17a; red arrows), *gsnor* mRNA (the amplified fragment between 87th and 231st base pair of *gsnor* gene) (Figure 3-17a; blue arrows) and GSNOR and GS-FDH activities cannot be detected for the *Df7305*/*Df7306* (Figure 3-17b and c). This indicates that *Df7305*/*Df7306* is a *gsnor* knockout generated by overlapping defiency. For the *act5c*:*UAS-gsnor*; *Df7305*/*Df7306*, GSNOR and GS-FDH activities are greatly increased (Figure 3-17b). This indicates that *act5c*:*UAS-gsnor*; *Df7305*/*Df7306* is a GSNOR overexpressor which can be used for the complementation of *Df7305*/*Df7306*. However, the activities of *EP-gsnor*/*EP-gsnor*; *Df7305*/*Df7306* are lower than that of wild-type OR (Figure 3-17c). This is possibly because the selected endogenous promoter region does not have enough essential regulatory sequences. The level of transcript may also be reduced because of a position effect, although the transformation was directed to the specific site, which has been shown to have high expression (attP40) (Markstein et al., 2008) by site-specific recombination between cloned attP and attB sites.

To generate further evidence, an alternative enzyme assay for GSNOR was undertaken for each Drosophila genotype. This assay measures the absence of NADH at wavelength of 340 nm by spectrophotometry after an addition of GSNO. *Df7305*/*Df7306* cannot utilize NADH after adding GSNO. This therefore confirms that there is no detectable GSNOR activity in *Df7305*/*Df7306*. The GSNOR activity of *act5c*:*UAS-gsnor*; *Df7305*/*Df7306* can oxidize NADH at a much higher level compared to the wild type. However, *EP-gsnor*/*EP-gsnor*; *Df7305*/*Df7306* only can slowly oxidize a small amount of NADH with the presence of GSNO (Figure 3-18).

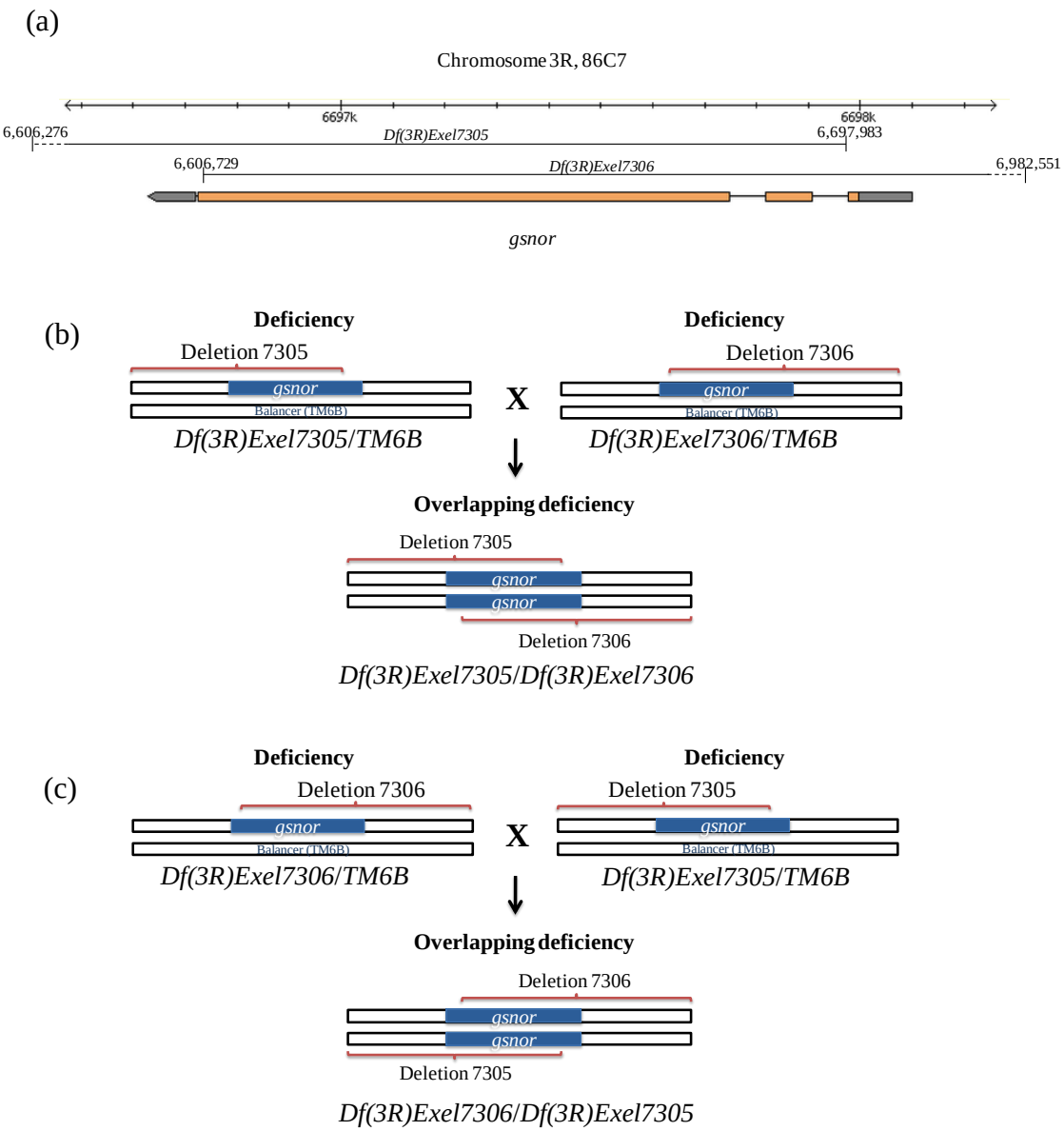

Figure 3-14. (**a**) Genomic region of the *gsnor* locus. *gsnor* locates in 86C7. It has three exons that can be translated into a 379 amino acid protein. *Df7305* and *Df7306* overlap mostly within *gsnor*. Orange colour indicates CDS of *gsnor*. Dark gray colour indicates 5' and 3' untranslated region (5' and 3' UTR). (**b**) Crossing scheme of making the overlapping deficiency *Df7305*/*Df7306* from parent strains *Df7305*/*TM6B* females and *Df7306*/*TM6B* males. (**c**) Crossing scheme of making the reciprocal cross of *Df7305*/*Df7306* (*Df7306*/*Df7305*) from parent strains *Df7306*/*TM6B* females and *Df7305*/*TM6B* males.

(a)

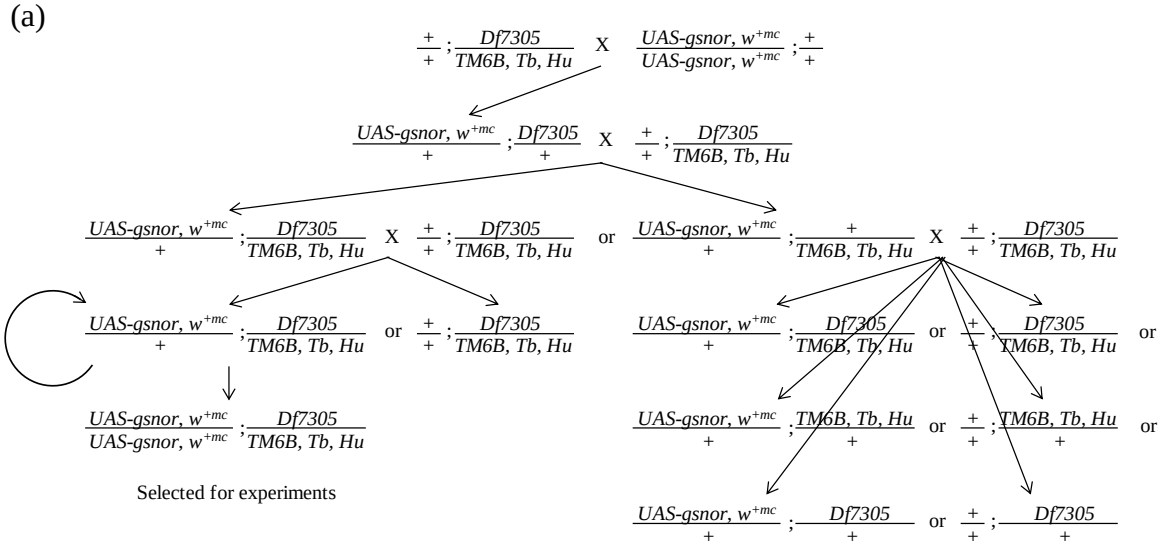
+/+ ; Df7305/TM6B, Tb, Hu X UAS-gsnor, w+mc/UAS-gsnor, w+mc ; +/+
UAS-gsnor, w+mc/+ ; Df7305/+ X +/+ ; Df7305/TM6B, Tb, Hu
UAS-gsnor, w+mc/+ ; Df7305/TM6B, Tb, Hu X +/+ ; Df7305/TM6B, Tb, Hu or UAS-gsnor, w+mc/+ ; +/TM6B, Tb, Hu X +/+ ; Df7305/TM6B, Tb, Hu
UAS-gsnor, w+mc/+ ; Df7305/TM6B, Tb, Hu or +/+ ; Df7305/TM6B, Tb, Hu
UAS-gsnor, w+mc/UAS-gsnor, w+mc ; Df7305/TM6B, Tb, Hu
Selected for experiments
UAS-gsnor, w+mc/+ ; Df7305/TM6B, Tb, Hu or +/+ ; Df7305/TM6B, Tb, Hu or
UAS-gsnor, w+mc/+ ; TM6B, Tb, Hu/+ or +/+ ; TM6B, Tb, Hu/+ or
UAS-gsnor, w+mc/+ ; Df7305/+ or +/+ ; Df7305/+

(b)

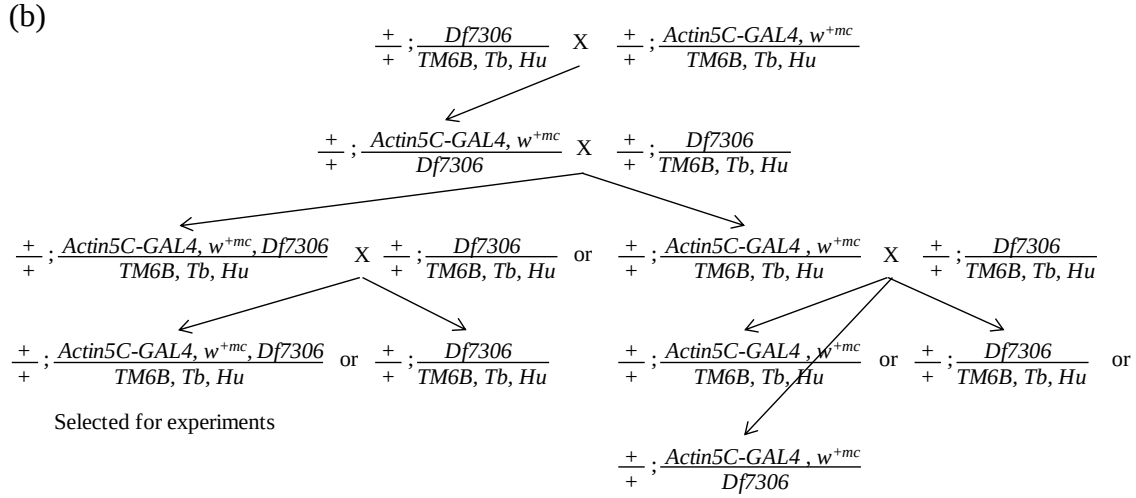
+/+ ; Df7306/TM6B, Tb, Hu X +/+ ; Actin5C-GAL4, w+mc/TM6B, Tb, Hu
+/+ ; Actin5C-GAL4, w+mc/Df7306 X +/+ ; Df7306/TM6B, Tb, Hu
+/+ ; Actin5C-GAL4, w+mc, Df7306/TM6B, Tb, Hu X +/+ ; Df7306/TM6B, Tb, Hu or +/+ ; Actin5C-GAL4 , w+mc/TM6B, Tb, Hu X +/+ ; Df7306/TM6B, Tb, Hu
+/+ ; Actin5C-GAL4, w+mc, Df7306/TM6B, Tb, Hu or +/+ ; Df7306/TM6B, Tb, Hu
Selected for experiments
+/+ ; Actin5C-GAL4 , w+mc/TM6B, Tb, Hu or +/+ ; Df7306/TM6B, Tb, Hu or
+/+ ; Actin5C-GAL4 , w+mc/Df7306

(c)

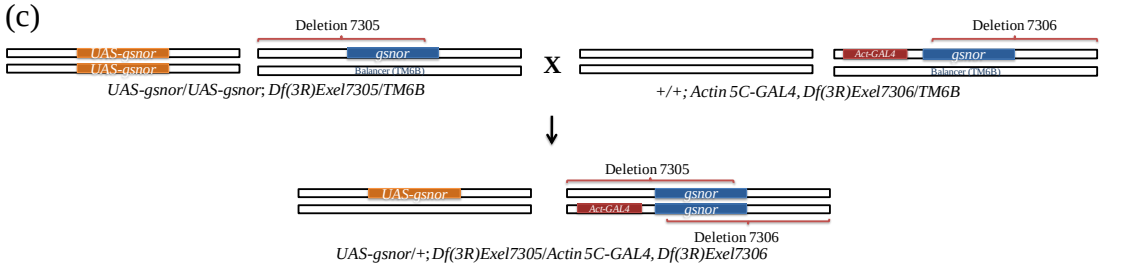
Deletion 7305
UAS-gsnor
UAS-gsnor
gsnor
Balancer (TM6B)
UAS-gsnor/UAS-gsnor; Df(3R)Exel7305/TM6B
X
Deletion 7306
Act-GAL4
gsnor
Balancer (TM6B)
+/+; Actin 5C-GAL4, Df(3R)Exel7306/TM6B
Deletion 7305
UAS-gsnor
Act-GAL4
gsnor
gsnor
Deletion 7306
UAS-gsnor/+; Df(3R)Exel7305/Actin 5C-GAL4, Df(3R)Exel7306

(d)

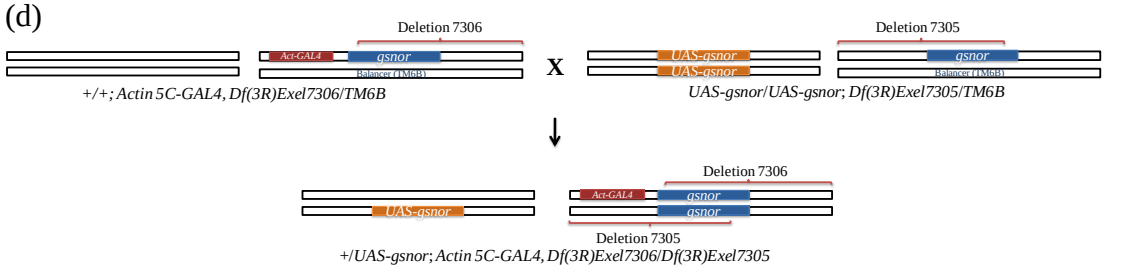
Deletion 7306
Act-GAL4
gsnor
Balancer (TM6B)
+/+; Actin 5C-GAL4, Df(3R)Exel7306/TM6B
X
Deletion 7305
UAS-gsnor
UAS-gsnor
gsnor
Balancer (TM6B)
UAS-gsnor/UAS-gsnor; Df(3R)Exel7305/TM6B
Deletion 7306
UAS-gsnor
Act-GAL4
gsnor
gsnor
Deletion 7305
+/UAS-gsnor; Actin 5C-GAL4, Df(3R)Exel7306/Df(3R)Exel7305

Figure 3-15. (**a**) A crossing scheme of *UAS-gsnor*/*UAS-gsnor*; +/+ and +/+; *Df7305*/*TM6B* to generate *UAS-gsnor*/*UAS-gsnor*; *Df7305*/*TM6B*. To distinguish *UAS-gsnor*, w^{+mc}/+; *Df7305*/*TM6B* from *UAS-gsnor*, w^{+mc} /+; +/*TM6B*, flies were crossed with +/+; *Df7305*/*TM6B*. Only *UAS-gsnor*, w^{+mc} /+; *Df7305*/*TM6B* can produce all progenies with *Tubby* (*Tb*) and *Humeral* (*Hu*). (**b**) A crossing scheme of +/+; *act5C-GAL4*/*TM6B* and +/+; *Df7306*/*TM6B* to generate +/+; *act5C-GAL4*, *Df7306*/*TM6B*. To distinguish +/+; *act5C-GAL4*, w^{+mc}, *Df7306*/*TM6B* from +/+; *act5C-GAL4*, w^{+mc}/*TM6B*, flies were crossed with +/+; *Df7306*/*TM6B*. Only +/+; *act5C-GAL4*, w^{+mc}, *Df7306*/*TM6B* can produce all progenies with *Tb* and *Hu*. (**c**) A crossing diagram to generate a GAL4/UAS system based complementation by crossing *UAS-gsnor*/*UAS-gsnor*; *Df7305*/*TM6B* and +/+; *act5C-GAL4*, *Df7306*/*TM6B* to produce *act5c*:*UAS-gsnor*; *Df7305*/*Df7306*. (**d**) A crossing diagram to produce a reciprocal cross of (c) (*act5c*:*UAS-gsnor*; *Df7306*/*Df7305*).

(a)

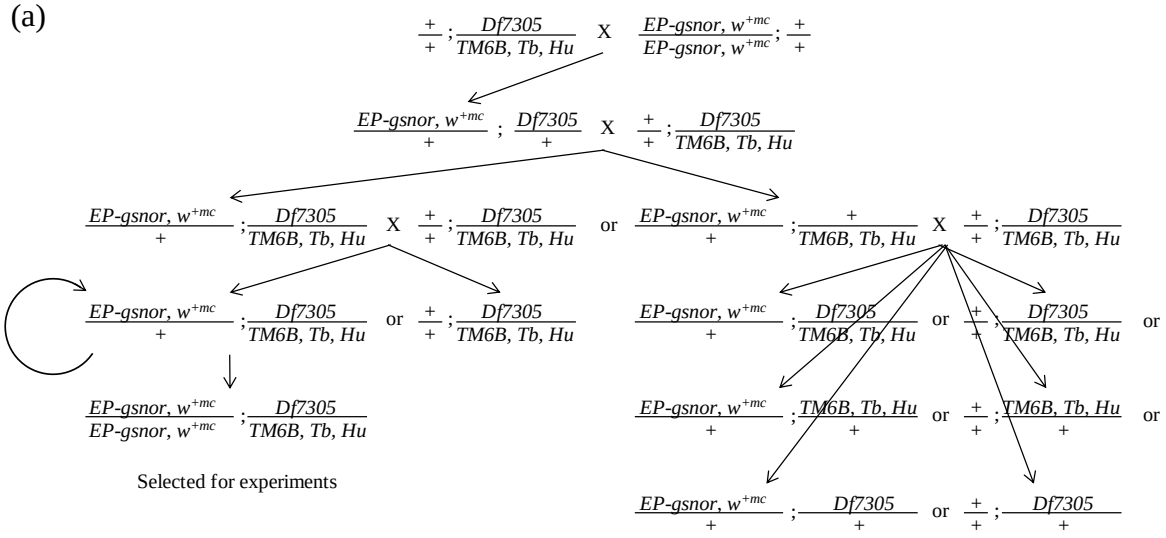
+/+ ; Df7305/TM6B, Tb, Hu X EP-gsnor, w+mc/EP-gsnor, w+mc ; +/+
EP-gsnor, w+mc/+ ; Df7305/+ X +/+ ; Df7305/TM6B, Tb, Hu
EP-gsnor, w+mc/+ ; Df7305/TM6B, Tb, Hu X +/+ ; Df7305/TM6B, Tb, Hu or EP-gsnor, w+mc/+ ; +/TM6B, Tb, Hu X +/+ ; Df7305/TM6B, Tb, Hu
EP-gsnor, w+mc/+ ; Df7305/TM6B, Tb, Hu or +/+ ; Df7305/TM6B, Tb, Hu
EP-gsnor, w+mc/+ ; Df7305/TM6B, Tb, Hu or +/+ ; Df7305/TM6B, Tb, Hu or
EP-gsnor, w+mc/+ ; TM6B, Tb, Hu/+ or +/+ ; TM6B, Tb, Hu/+ or
EP-gsnor, w+mc/+ ; Df7305/+ or +/+ ; Df7305/+
EP-gsnor, w+mc/EP-gsnor, w+mc ; Df7305/TM6B, Tb, Hu
Selected for experiments

(b)

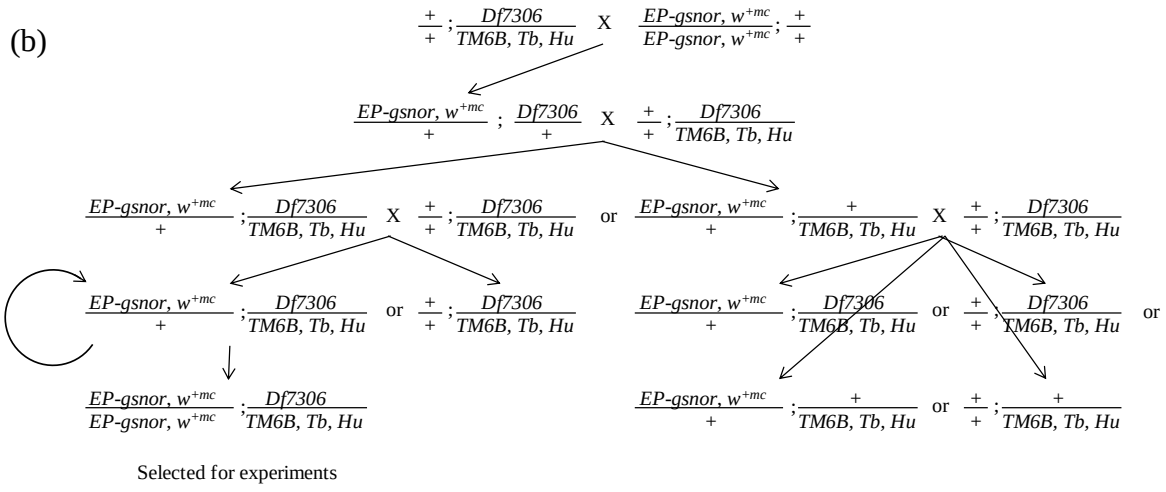
+/+ ; Df7306/TM6B, Tb, Hu X EP-gsnor, w+mc/EP-gsnor, w+mc ; +/+
EP-gsnor, w+mc/+ ; Df7306/+ X +/+ ; Df7306/TM6B, Tb, Hu
EP-gsnor, w+mc/+ ; Df7306/TM6B, Tb, Hu X +/+ ; Df7306/TM6B, Tb, Hu or EP-gsnor, w+mc/+ ; +/TM6B, Tb, Hu X +/+ ; Df7306/TM6B, Tb, Hu
EP-gsnor, w+mc/+ ; Df7306/TM6B, Tb, Hu or +/+ ; Df7306/TM6B, Tb, Hu
EP-gsnor, w+mc/+ ; Df7306/TM6B, Tb, Hu or +/+ ; Df7306/TM6B, Tb, Hu or
EP-gsnor, w+mc/+ ; +/TM6B, Tb, Hu or +/+ ; +/TM6B, Tb, Hu
EP-gsnor, w+mc/EP-gsnor, w+mc ; Df7306/TM6B, Tb, Hu
Selected for experiments

(c)

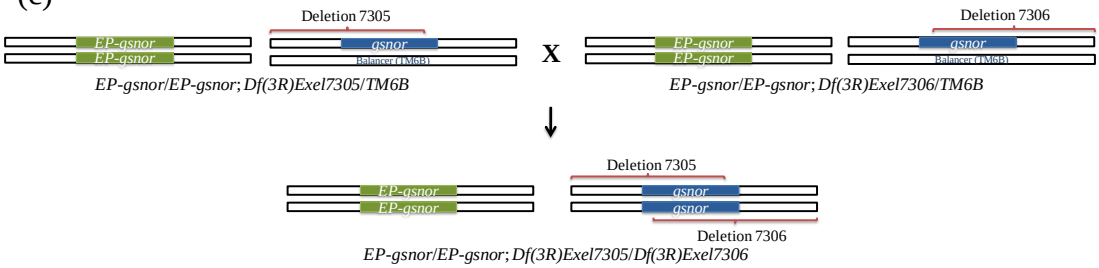

EP-gsnor/EP-gsnor; Df(3R)Exel7305/TM6B x *EP-gsnor/EP-gsnor; Df(3R)Exel7306/TM6B*

EP-gsnor/EP-gsnor; Df(3R)Exel7305/Df(3R)Exel7306

(d)

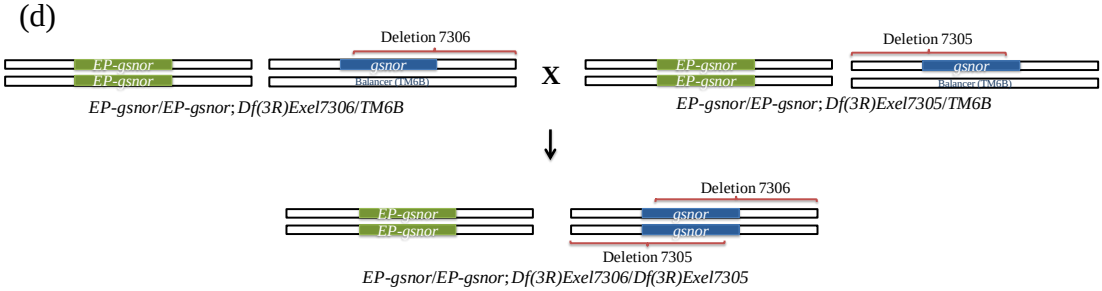

EP-gsnor/EP-gsnor; Df(3R)Exel7306/TM6B x *EP-gsnor/EP-gsnor; Df(3R)Exel7305/TM6B*

EP-gsnor/EP-gsnor; Df(3R)Exel7306/Df(3R)Exel7305

(e)

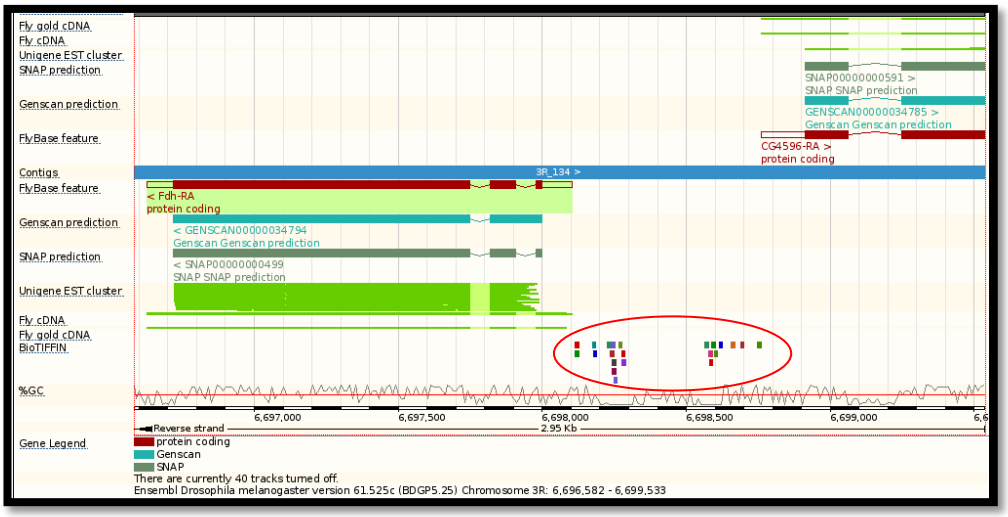

Figure 3-16. (**a**) A crossing scheme of *EP-gsnor*/*EP-gsnor*; +/+ and +/+; *Df7305*/*TM6B* to generate *EP-gsnor*/*EP-gsnor*; *Df7305*/*TM6B*. To distinguish *EP-gsnor*, w^{+mc} /+; *Df7305*/*TM6B* from *UAS-gsnor*, w^{+mc} /+; +/*TM6B*, flies were crossed with +/+; *Df7305*/*TM6B*. Only *UAS-gsnor*, w^{+mc} /+; *Df7305*/*TM6B* can produce all progenies with *Tb* and *Hu*. (**b**) A crossing scheme of *EP-gsnor*/*EP-gsnor*; +/+ and +/+; *Df7306*/*TM6B* to generate *EP-gsnor*/*EP-gsnor*; *Df7306*/*TM6B*. To distinguish *EP-gsnor*, w^{+mc} /+; *Df7306*/*TM6B* from *UAS-gsnor*, w^{+mc} /+; +/*TM6B*, flies were crossed with +/+; *Df7306*/*TM6B*. Only *UAS-gsnor*, w^{+mc} /+; *Df7306*/*TM6B* can produce all progeny with *Tb* and *Hu*. (**c**) A crossing diagram to generate a complementation line by the *gsnor* gene with endogenous upstream and downstream non-gene regions by crossing *EP-gsnor*/*EP-gsnor*; *Df7305*/*TM6B* and *EP-gsnor*/*EP-gsnor*; *Df7306*/*TM6B* to produce *EP-gsnor*/*EP-gsnor*; *Df7305*/*Df7306*. (**d**) A crossing diagram to produce a reciprocal cross of (c) (*EP-gsnor*/*EP-gsnor*; *Df7306*/*Df7305*). (**e**) The predicted regulatory sequences by www.ensembl.org using the Biotiffin regulatory motif database. The predicted regulatory sequences (red circle) are in a non-coding sequence between *gsnor* and the upstream adjacent gene *CG4596*. This area together with *gsnor* gene was cloned to generate a construct containing endogenous promoter linked with *gsnor*.

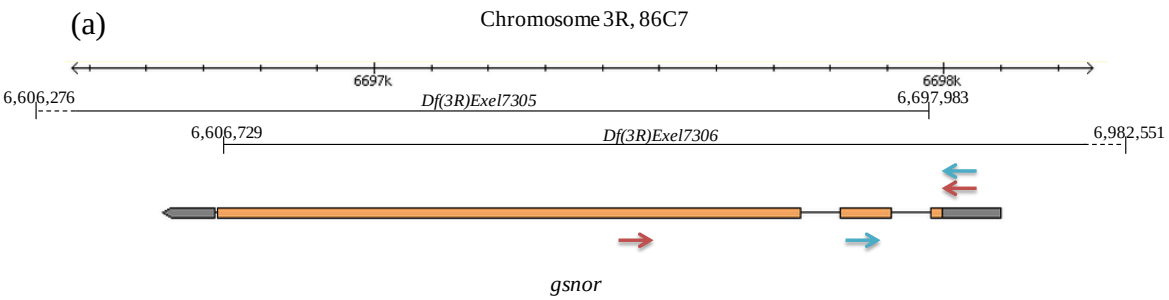
(a)
Chromosome 3R, 86C7
6697k
6698k
6,606,276
Df(3R)Exel7305
6,697,983
6,606,729
Df(3R)Exel7306
6,982,551
gsnor

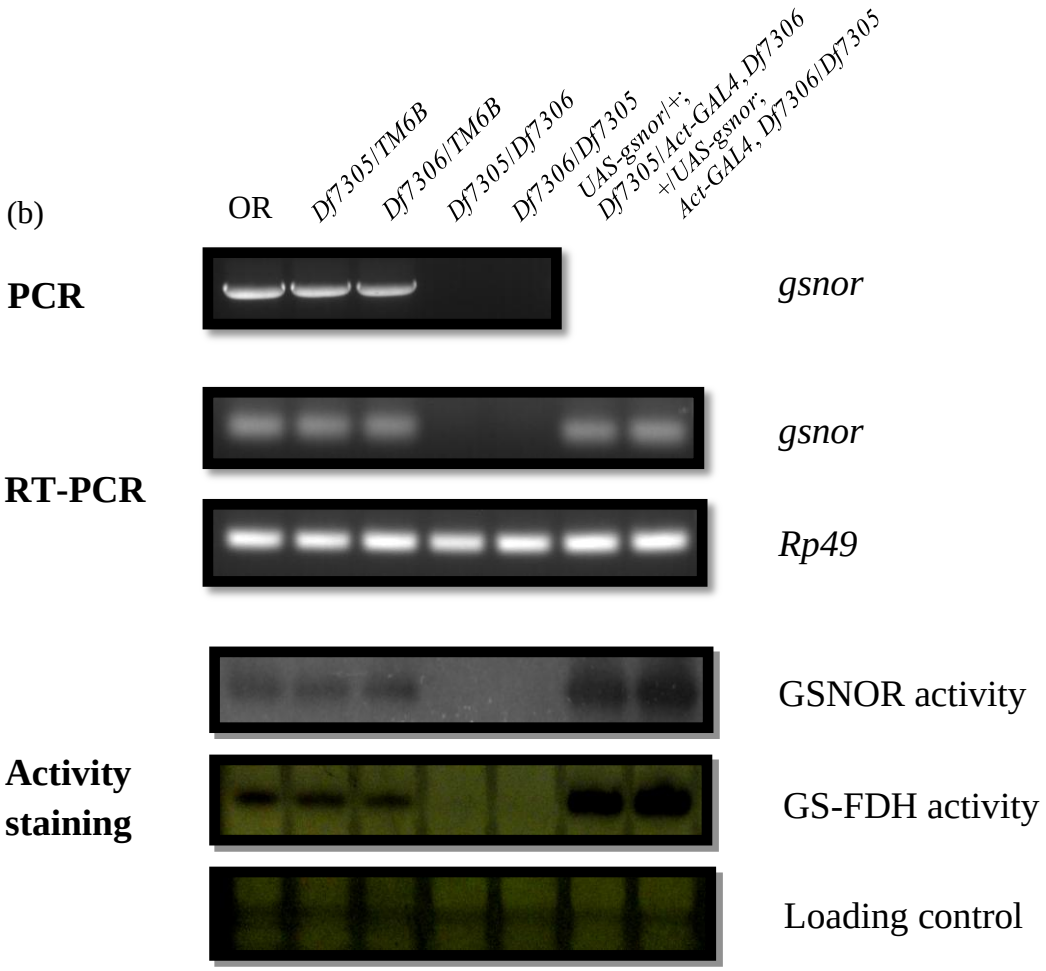
(b)
OR
Df7305/TM6B
Df7306/TM6B
Df7305/Df7306
Df7306/Df7305
UAS-gsnor/+;
Df7305/Act-GAL4, Df7306
+/UAS-gsnor;
Act-GAL4, Df7306/Df7305
PCR
gsnor
RT-PCR
gsnor
Rp49
Activity staining
GSNOR activity
GS-FDH activity
Loading control

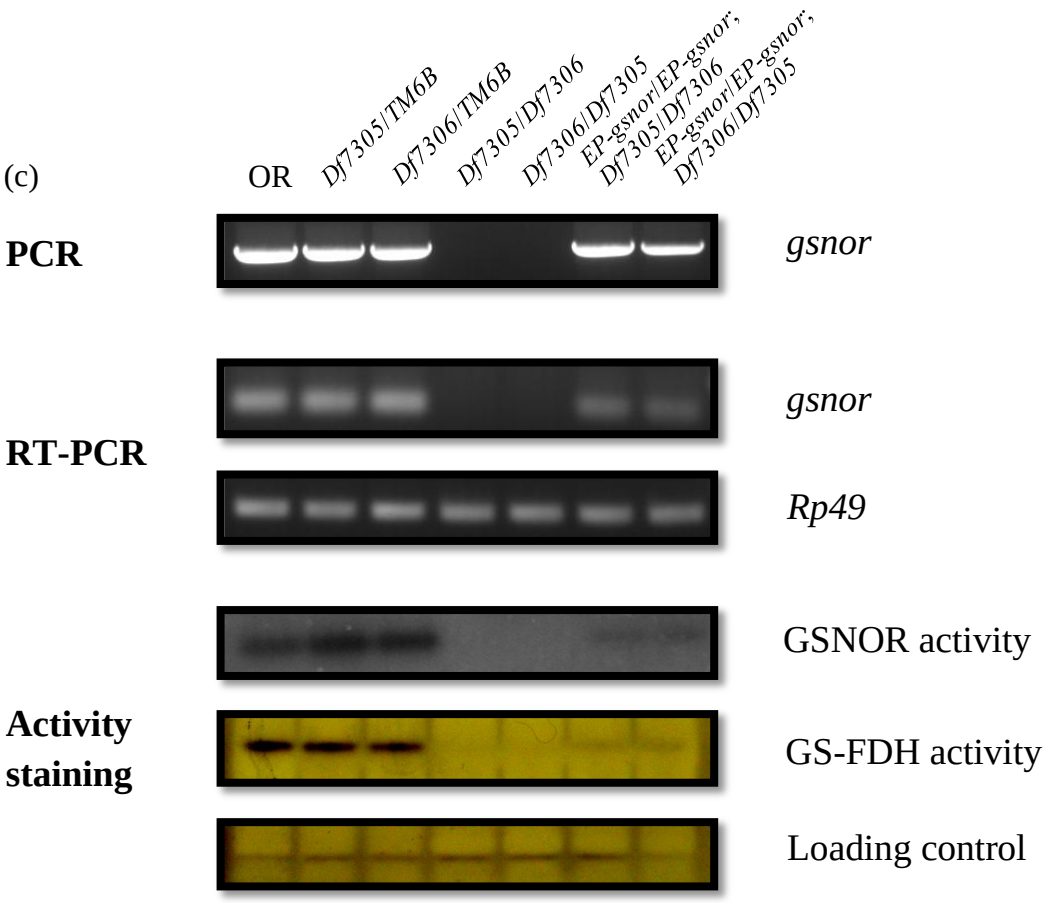

Figure 3-17. (**a**) The map of primers used to confirm the loss of *gsnor* in *Df7305*/*Df7306*. The red arrows indicate forward and reverse primers for genomic DNA amplification. The blue arrows indicate forward and reverse primers for cDNA amplification by RT-PCR (from 87th to 231st base pair of *gsnor* gene). Orange colour indicates CDS of *gsnor*. Dark gray colour indicates 5' and 3' UTR. The *gsnor* knockout and complementation confirmation by PCR of *gsnor* gene, RT-PCR of *gsnor* mRNA, GSNOR activity staining and GS-FDH activity staining. Two independent experiments were performed in order to confirm the presence or absence of *gsnor* genomic DNA, mRNA and protein activities of each genotype. (**b**) OR, *Df7305*/*TM6B*, *Df7306*/*TM6B*, *Df7305*/*Df7306*, *Df7306*/*Df7305*, *act5c*:*UAS-gsnor*; *Df7305*/*Df7306*, and *act5c*:*UAS-gsnor*; *Df7306*/*Df7305* were tested for the present of 1) *gsnor* gene by genomic DNA PCR, 2) *gsnor* mRNA by RT-PCR, and 3) GSNOR and GS-FDH activities by the same method described in the Section 3.2.2 in this chapter. (**c**) Similar to (b), but *EP-gsnor*/*EP-gsnor*; *Df7305*/*Df7306* and *EP-gsnor*/*EP-gsnor*; *Df7306*/*Df7305* were used instead of *act5c*:*UAS-gsnor*; *Df7305*/*Df7306* and *act5c*:*UAS-gsnor*; *Df7306*/*Df7305*.

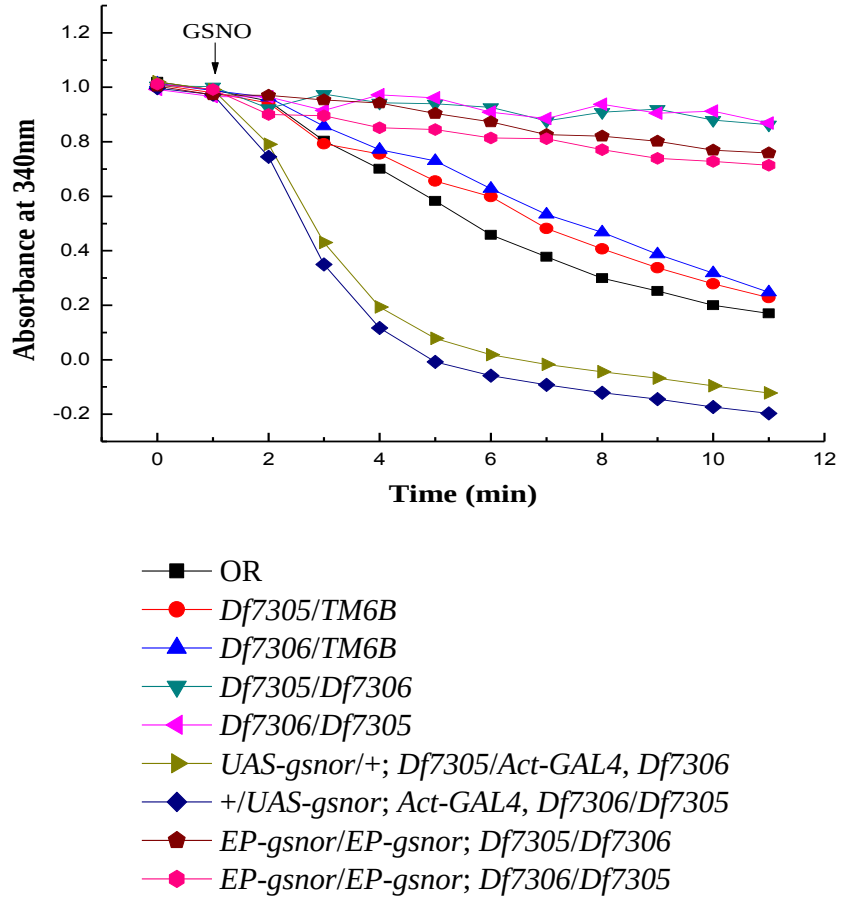

Figure 3-18. GSNOR activity was measured by the rate of oxidation from NADH to NAD^+ after GSNO addition. The NADH concentration was continuously measured at A_{340} by a spectrophotometer for 10 minutes. The arrow indicates the addition of GSNO.

3.6 Morphological phenotypes of gsnor knockout mutants

A morphological phenotype observed in *Df7305*/*Df7306* is the absence or malformation of tergites, mostly the fourth and the fifth tergites. However, the degree of the phenotype is variable. We have divided the tergite phenotype into five categories (Table 3-2; Figure 3-19a).

Although the deficiency parents *Df7305*/*TM6B* and *Df7306*/*TM6B* exhibit a mild tergite phenotype (about 20-30 % in females and 10-20 % in males), the *Df7305*/*Df7306* and *Df7306*/*Df7305* dramatically increase both the percentage of the phenotype (70-80% in females and 60 % in males) and the degree of phenotype. The complementation *act5c*:*UAS-gsnor*; *Df7305*/*Df7306* and *EP-gsnor*/*EP-gsnor*; *Df7305*/*Df7306* rescue both percent of the phenotype (50 % in females and 30-40 % in males, and 35-40 % females and 20 % in males, respectively) and the degree of the phenotype (Figure 3-19b). This confirms that the tergite phenotype observed in *Df7305*/*Df7306* is the effect of the *gsnor* knockout. The reasons why *act5c*:*UAS-gsnor*; *Df7305*/*Df7306* and *EP-gsnor*/*EP-gsnor*; *Df7305*/*Df7306* cannot completely rescue the phenotype is possibly because of an atypical GSNOR expression level (too high in *act5c*:*UAS-gsnor*; *Df7305*/*Df7306* and too low in *EP-gsnor*/*EP-gsnor*; *Df7305*/*Df7306*) and/or a haploid inefficient effect from *Df7305*/*Df7306* which contains a large number of haploid genes, which might synergistically cause the tergite effect, from both deletions of *Df7305* and *Df7306*.

Table 3-2. Symbols indicate the degree of the absence or malformation of the tergite phenotype.

Symbols	Tergite phenotype
0	No tergite phenotype
+	The phenotype occurs in a single tergite with a area equal or less than a quarter of the fifth tergite
++	The phenotype occurs in a multiple tergites with a total area equal or less than a quarter of the fifth tergite
+++	The phenotype occurs in a single or multiple tergites (normally multiple tergites observed) with a total area more than a quarter but equal or less a half of the fifth tergite
++++	The phenotype occurs in a single or multiple tergites (normally multiple tergites observed) with a total area more than a half of the fifth tergite

(a)

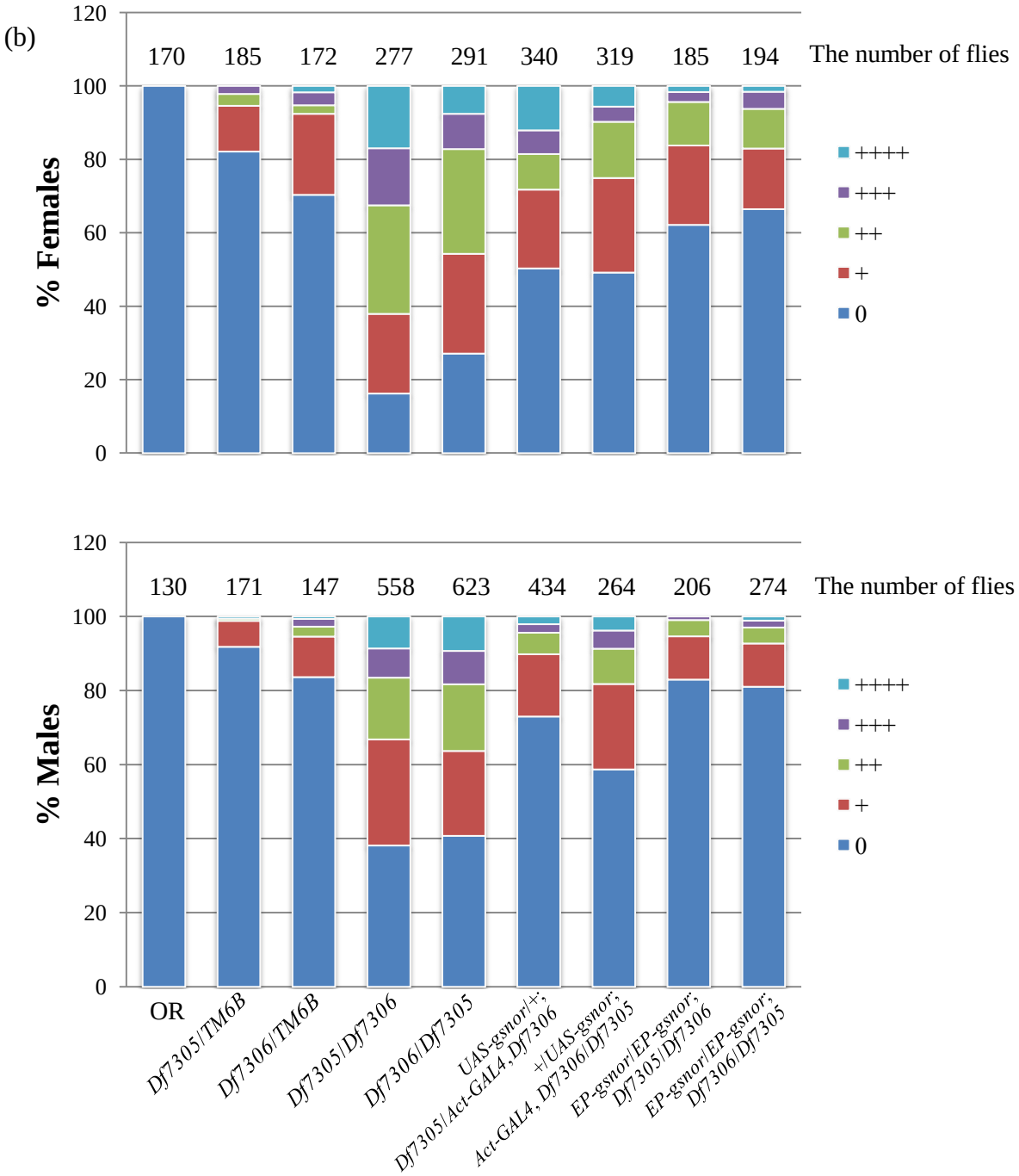

Figure 3-19. The effect of the loss of GSNOR function on tergite-related phenotypes. (**a**) The tergite phenotype has been divided into five categories according to Table 3-2. (**b**) Female and Male Drosophila were divided into five groups by their tergite phenotype (Table 3-2) (a) and the number of files in each category was calculated into a percentage. The numbers above each bar indicates the total number of flies counted.

Surprisingly, the low GSNOR expression of *EP-gsnor*/*EP-gsnor*; *Df7305*/*Df7306* is enough to rescue the majority of tergite phenotype, and the rescue is even better than GSNOR overexpression *act5c*:*UAS-gsnor*; *Df7305*/*Df7306*. This phenomenon may be implied that in order to elicit a normal biological function a level of GSNOR activity possibly has to be at a certain level – too low or too high GSNOR activity (which reflects *S*-nitrosylation level) may alter the normal biological function (the tergite formation in this case). In addition, *EP-gsnor*/*EP-gsnor* was not able to rescue the disease phenotype while *act5c*:*UAS-gsnor*; *Df7305*/*Df7306* was (This will be described in Section 6.4). This also supports the previous implication that each biological process requires an appropriate level of *S*-nitrosylation.

Due to a large body of evidence describing the ability of NO to inhibit cell growth, including cancer cells, NO is well established as a cell proliferation inhibitor (Cui et al., 2005; Villalobo, 2006). NO is also involved in cell cycle arrest. In G1/S checkpoint, NO ceases the progression of S phase by increasing the nuclear localization of p21 and p27 the inhibitor of cyclin-dependent kinase (CDK) 2 (Wedgwood and Black, 2003). CDK2 enhances the release of retinoblastoma protein (pRb) from transcription factor E2F by the phosphorylation of pRb. The inhibition of CDK2 by p21 and p27 results in binding between pRb and E2F preventing E2F to transcribe essential genes for progressing to the S phase (Ciani et al., 2004). NO has a direct effect to induce hypophosphorylation of pRb increasing binding with the transcription of E2F (Pervin et al., 2001). The treatment of NO also decreases the synthesis of Cyclin D (Pervin et al., 2001) and Cyclin A (Sharma et al., 1999).

In Drosophila, NO is also a cell proliferation inhibitor. Larvae injected with NO inhibitors show oversized legs, tergites, sternites, genital structures, and wings after become adults. Ectopic expression of a mouse NOS controlled by a heat-shock promoter reduces the size of limbs in adults (Enikolopov et al., 1999). In contrast, eye size remains constant after treated with NO inhibitors. Interestingly, after apoptosis is removed by expressing baculovirus p35 protein in eyes, a reduced NO level can trigger oversized eyes by increasing the number of ommatidia which is the repeat unit in Drosophila compound eyes. This phenomenon reveals that the size of

some organs is regulated by a balance between cell proliferation and apoptosis (Poluha et al., 1997).

We believe that the cellular NO regulator GSNOR might also affect cell proliferation. In a *gsnor* loss-of-function line, the total cellular level of NO in both bound forms (*S*-nitrosylated proteins) and free forms should be elevated and this may lead to the tergite phenotype. However, other phenotypes, such as undersized legs (the most obvious phenotype described in Enikolopov et al. (1999)) should also have been observed. Because undersized tergites are the only phenotype observed in the *gsnor* knockout, we hypothesize that there is a specificity of the GSNOR system. This could lie in the interaction between *S*-nitrosylated proteins and GSH (not all *S*-nitrosylated proteins could transfer NO to GSH).

Another possible source of a tissue specific response could be tissue or cell specific recruitment of GSNOR to perform the denitrosylation process, akin to that which occurs with nNOS. In mammals, the specificity of *S*-nitrosylation has been shown to be controlled by an adapter protein. CAPON forms a complex with nNOS and Dexras1. This allows nNOS to produce NO which in turn specifically *S*-nitrosylates the proximal Dexras1 (Fang et al., 2000). A similar phenomenon might appear in denitrosylation mediated by GSNOR.

3.7 Conclusion

We have discovered that Drosophila FDH has high similarity to the Arabidopsis GSNOR. FDH is a class III ADH which has been previously shown in mammals to possess GSNOR activity (Luque et al., 1994; Jensen et al., 1998). Recently, *fdh* has been shown to be a homolog of the mammalian *gsnor* (Hou et al., 2011). In this thesis, we name *fdh* as *gsnor* in order to synchronize with Arabidopsis and also to emphasize the GSNOR activity of this enzyme.

Many strategies for compromising *gsnor* were performed. We have confirmed that the null *fdh* allele 680 is not a real null allele, due to the lack of mutation that can alter the protein function and the normal production of GSNOR activity. The P element imprecise excision 683 and 684 (Barton, 2008) were shown to have a normal GSNOR activity. Both RNAi targeting *gsnor* lines were able to

knock the transcript of *gsnor* down to approximately 50 % of the normal level. The increment of the knockdown level by elevating temperate and using the stronger GAL4 driver lines aggravated the off-target effect by increasing the number of flies trapped in pupa cases instead of enhancing the knockdown level.

The complete *gsnor* knockout Drosophila was obtained from the cross between two deficiency lines (*Df7305*/*TM6B* and *Df7306*/*TM6B*) which have breakpoints overlapping within *gsnor* to generate the overlapping deficiency (*Df7305*/*Df7306*). Two complementation flies were generated by the addition of *UAS-gsnor* driving by *act5C-GAL4* into *Df7305*/*Df7306* (*act5c*:*UAS-gsnor*; *Df7305*/*Df7306* or *act5c*:*UAS-gsnor*; *Df7305*/*Df7306*) and the addition of the endogenous *gsnor* gene and its regulatory sequences into *Df7305*/*Df7306* (*EP-gsnor*/*EP-gsnor*; *Df7305*/*Df7306*). The *Df7305*/*Df7306* and *act5c*:*UAS-gsnor*; *Df7305*/*Df7306* was confirmed to be a complete knockout of *gsnor* and the true complement of *gsnor* knockout (due to the overexpression of GSNOR activity), respectively. The *EP-gsnor*/*EP-gsnor*; *Df7305*/*Df7306* also expressed a low level of GSNOR activity, we think that the expression level is not adequate for using in complementation.

The *gsnor* knockout *Df7305*/*Df7306* showed the absence and malformation of tergites; however, the degree of the phenotype is variable. The tergite phenotype of *Df7305*/*Df7306* can vary from normal tergites to more than a half of tergites disappeared. The phenotype in females is stronger than in males. About 80 % of female *gsnor* knockouts showed the tergite phenotype whereas in males the percentage decreased to approximately 60 %. The complementation *act5c*:*UAS-gsnor*; *Df7305*/*Df7306* partially rescued the phenotype to approximately 50 % in females and 30-40 % in males. Surprisingly, *EP-gsnor*/*EP-gsnor*; *Df7305*/*Df7306* was able to rescue the phenotype even better than *act5c*:*UAS-gsnor*; *Df7305*/*Df7306* (35-40 % females and 20 % in males), even though it has less GSNOR activity. This might indicate that in each biological process the appropriate level of *S*-nitrosylation is crucial. Too much or too low *S*-nitrosylation might not be suitable for a particular biological process.

To explain the tergite phenotype, NO has been previously shown to be a cell proliferation inhibitor by arresting cell cycles at the G1/S checkpoint (Villalobo, 2006). It is very likely that the increment of NO in both bound and free forms from the loss of GSNOR activity (as reported in the Arabidopsis *gsnor* knockout (Feechan et al., 2005)) inhibits cell proliferation leading to the absence and malformation of tergites. However, there is a specificity of the denitrosylation process of GSNOR, because the phenotype only exhibits at tergites, but not other organs.

Chapter 4 A Conserved Function of GSNOR in Fertility between Arabidopsis and Drosophila

4.1 GSNOR is important for Arabidopsis fertility.

Defective fertility is one of the obvious phenotypes observed in *gsnor* knockout Arabidopsis. It is very noticeable that siliques from *gsnor* knockout Arabidopsis are considerably undersized compared with wild type, and seeds are rarely found in each silique (Figure 4-1a). The number of seeds per plant in a *gsnor* knockout is greatly reduced to about five times lower than wild type (Figure 4-1b). This discovery leads us to question whether or not GSNOR is required for fertility in Drosophila.

4.2 Introduction to Drosophila oogenesis

An adult Drosophila ovary has about 14-16 ovarioles surrounded by a peritoneal sheath containing a network of muscle (Figure 4-2). The peritoneal sheath is believed to be involved with oviposition and egg development by assisting the movement of haemolymph around ovaries to provide sufficient nutrients and O_2, for oogenesis (Spradling, 1993; Middleton et al., 2006). Each ovariole is a progressive string of different stages of egg development starting with a germarium at the anterior end and ending with stage-14 egg chambers at the posterior end which are ready to be fertilised and laid (Figure 4-3). Each germarium contains 2-3 germline stem cells near the tip. In the process of oogenesis, a germline stem cell goes through four mitotic cell divisions resulting in the increment of the cell number to 16 cells. One of them will become oocyte, and the rest 15 cells will turn into nurse cells (Koch and King, 1966; King et al., 1968; Wu et al., 2008). Later on this 16 cell cyst is surrounded by precursor follicle cells produced by two follicle cell stem cells (Margolis and Spradling, 1995). About 16 cells of the precursor follicle cells from the total precursor follicle cells separate the 16 cell cyst from the other cysts and become pre-polar cells. These pre-polar cells will become stalk cells and polar cells. The rest of precursor follicle cells surrounding the cyst develop into the epithelial

follicle cell layer which is required for establishment of an egg chamber. The differentiation of pre-polar cells to stalk cells assists the egg chamber to gradually move out of the germarium (Wu et al., 2008).

The egg chamber grows larger by follicle cell proliferation, enlargement of nurse cells and oocyte at the same rate until stage 7, and at stage 8 oocyte by the deposition of yolk protein (vitellogenins) by follicle cells making oocyte to become the largest cell in the egg chamber (Richard et al., 2001). From stage 9 to stage 10, there are extensive changes in follicle cell organization. Firstly, the most anterior cells migrate centripetally through the nurse cells to oocyte and develop into border cells. Secondly, the follicle cells overlying the oocyte change their cell shape from cuboidal to columnar. Thirdly, the follicle cells covering nurse cells convert into squamous epithelium. Finally, in stage 10B, follicle cells at the anterior end of oocyte move inward between nurse cells and the oocyte (Spradling, 1993).

(a)

Wild type *gsnor1-3*

(b)

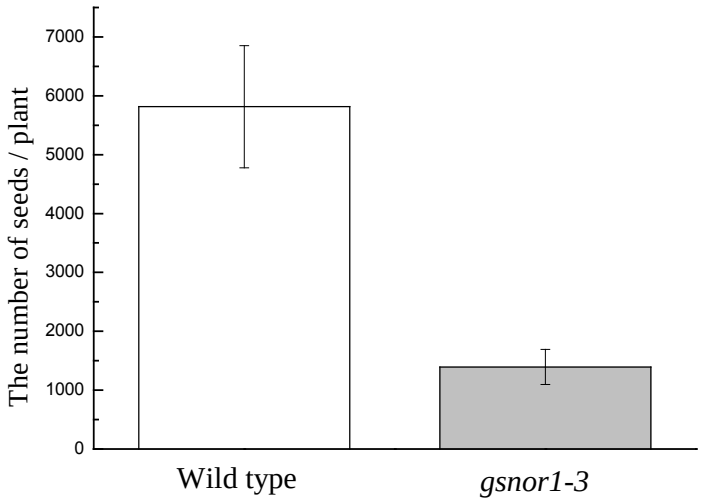

Figure 4-1. (**a**) Arabidopsis GSNOR functions in fertility shown by smaller siliques and (**b**) reduced the number of seeds produced per plant. The data represents a mean of three independent experiments (±SE).

(a)

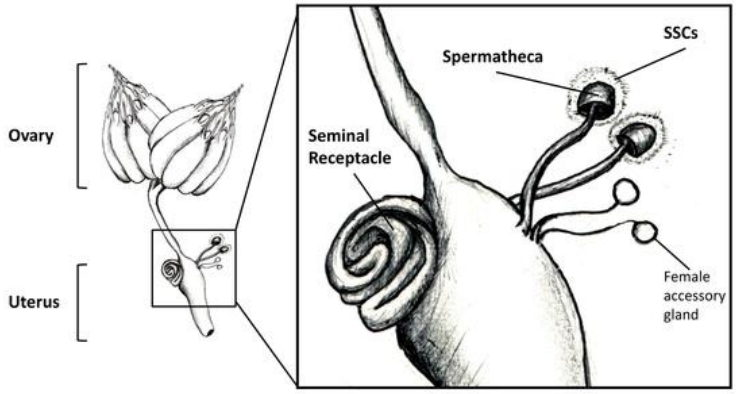

(b)

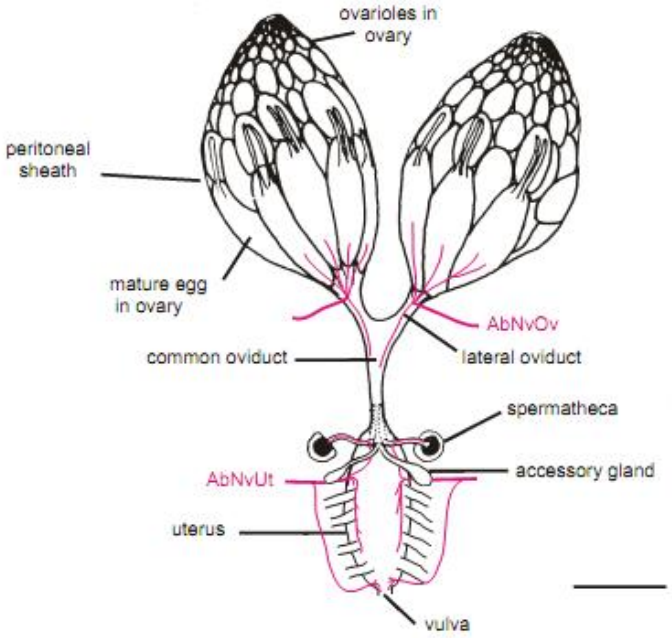

Figure 4-2. The *D. melanogaster* female reproductive system. (**a**) Unfertilised mature eggs produced from ovaries are transferred along oviducts and uterus. Once the eggs reside in uterus, they are fertilised by sperm stored in the spermatheca and seminal receptacle. Spermathecal secretory cells (SSCs) assists sperm storage and female accessory glands are believed to have a secretory function (taken from Wolfner 2011). (**b**) The *D. melanogaster* female reproductive system similar to (a) with two pairs of nerve innervations. The AbNvOv (abdominal nerve to the ovary) and AbNvUt (abdominal nerve to the uterus) branch from the 5th pair of nerves emerging from the abdominal ganglion of the central nervous system. Taken from Middleton et al. (2006).

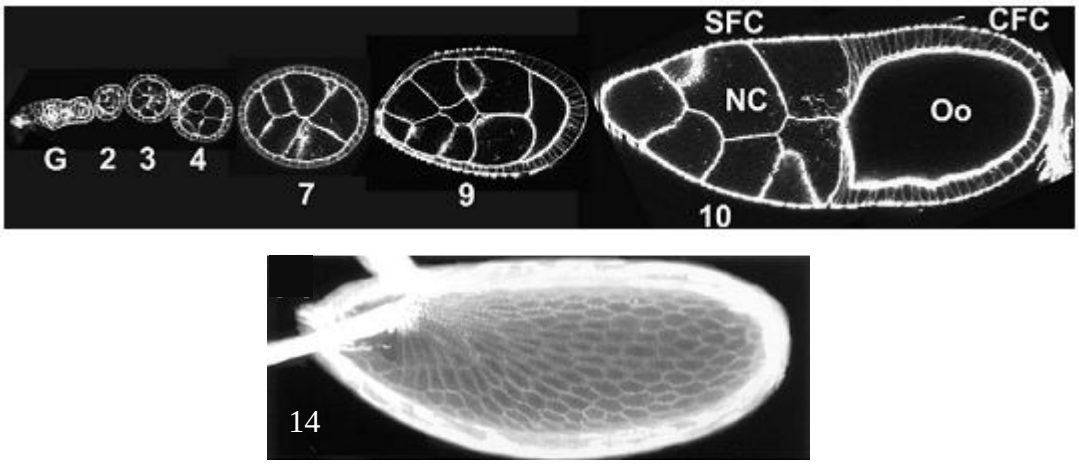

Figure 4-3. Development of Drosophila eggs starting from a single germline stem cell in the germarium (G) to the stage 14 egg chamber. From the stem cell, it commits four mitotic cell divisions to become one oocyte (Oo) and 15 nurse cells (NC). Before stage 7 both the nurse cells and the oocyte grow at the same rate, but after stage 7 the growth rate of the oocyte is accelerated due to the deposition of yolk protein. In stage 10, changes in cell shape of follicle cells from cuboidal to squamous follicle cells (SFC) (on cells surrounding nurse cells) and cuboidal to columnar follicle cells (CFC) (on cells surrounding the oocyte), and the inward movement of follicle cells in between nurse cells and oocyte are observed. From stage 10 to stage 14, the columnar follicle cells produce eggshell, respiratory appendages, operculum, collar and micropyle. Nurse cells dump their cytosolic contents. Follicle and nurse cells undergo apoptosis leaving only the mature egg. Taken from Wu et al. (2008) and Nilson and Schüpbach (1998).

From stage 10B to stage 14, eggshell is produced by columnar follicle cells to cover the oocyte and terminate the transfer of yolk proteins from the follicle cells. The eggshell consists of five layers. The first layer of eggshells produced by the follicle cells is the vitelline membrane. The vitelline membrane also acts as a reservoir of chorion proteins for the subsequent chorion layers. The second layer is the wax layer which is a multilayered hydrophobic plate. Then, the innermost chorion layer, which is composed of a crystalline lattice, is the third layer. The fourth layer is endochorion which has a similar structure to the floor, pillars and roof of a building. The fifth layer is the outermost exochorion layer (Figure 4-4) (Margaritis et al., 1980). Nurse cells take over a role in transfering yolk proteins produced from fatbody into oocyte (Richard et al., 2001) and dumping their cytosol. This dumping process is actin cytoskeleton dependent. The dumped cytosol contains large quantities of RNAs and proteins required for early embryogenesis (McNeil et al., 2004). At the anterior end, follicle cells construct appendages (for respiration), an operculum (embryo escape hatch), a collar (a hinge for the operculum) and a micropyle (for sperm entry). When oogenesis is complete, nurse cells and follicle cells undergo apoptosis leaving the shelled oocyte, as a mature egg, to travel along the oviduct (Berg, 2005).

Muscle contraction is required for mature eggs to move along the lateral oviducts and common oviduct (Figure 4-2). The muscle contraction is a pivotal mechanism in Drosophila female fertility, because the inhibition of oviduct muscle contraction by tetanus toxin results in female sterile phenotype (Rodríguez-Valentín et al., 2006). The oviduct is innervated by an abdominal nerve from the thoracic abdominal ganglion (TAG) (Middleton et al., 2006) (Figure 4-2). There are three neurotransmitters working together for regulating oviduct contraction and relaxation: glutamate and proctoline for oviduct muscle contraction, and octopamine for relaxation (Rodríguez-Valentín et al., 2006). Once the mature egg reaches the uterus (ovulation), the egg is fertilised by sperm previously stored in the seminal receptacle and spermatheca (if the female has a successful copulation) by entering the micropyle (Wolfner, 2011). The egg is passed through a vulva and then laid by an ovipositor, a specialised organ for laying eggs. Normally, a healthy female produces two mature eggs per ovariole per day (Bownes, 1986).

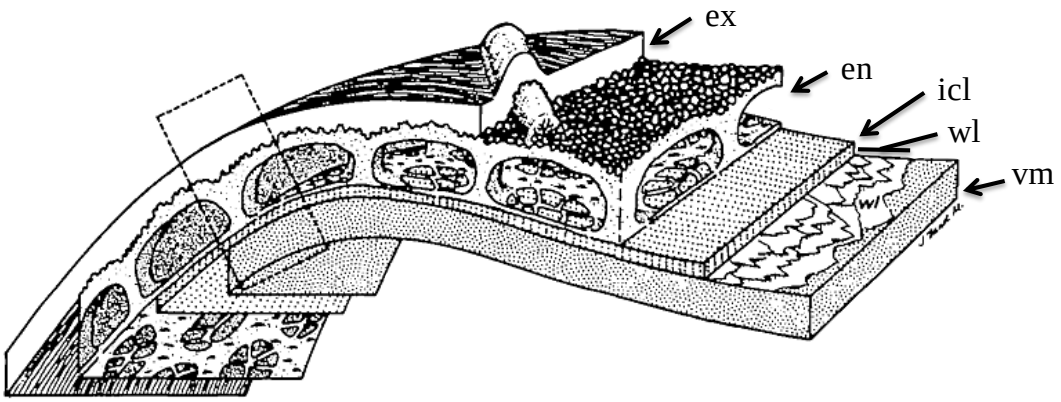

Figure 4-4. The structure of eggshells showing five separate layers. The innermost layer is the vitelline membrane (vm) which is the first layer built. The multiple wax layers (wl) for the protection against water is the second layer followed by three chorion layers: the innermost chorion layer (icl), endochorion (en) (which has the similarity to the floor, pillars and roof) and exochorion (ex), respectively. Adapted from Margaritis et al. (1980).

4.3 The loss of GSNOR function results in an egg retention phenotype in Drosophila.

After the cross between *Df7305*/*TM6B* and *Df7306*/*TM6B* to generate *Df7305*/*Df7306*, males and females *Df7305*/*Df7306* were selected to generate *gsnor* knockout lines. This attempt was not successful, because either males or females were infertile. To investigate further, either male or female *Df7305*/*Df7306* flies were crossed with OR, and eggs laid by 50 females during 18 hours with yeast supplement were collected and counted. *Df7305*/*Df7306* females and females from the reciprocal cross *Df7306*/*Df7305* laid approximately 10 times fewer than *Df7305*/*TM6B* and *Df7306*/*TM6B* females. Complementation of the *gsnor* knockout by *act5c*:*UAS-gsnor* partially rescued the phenotype (about 50% recovery) confirming that the observed effect of *Df7305*/*Df7306* was due to the loss of GSNOR (Figure 4-5a).

Possibilities for the observed infertile phenotype could be because 1) eggs were produced but could not be laid or 2) eggs were not produced so nothing laid. In order to observe these possibilities, we then investigated by mating *Df7305*/*Df7306*, OR, *Df7305*/*TM6B*, *Df7306*/*TM6B* and *act5c*:*UAS-gsnor*; *Df7305*/*Df7306* with an excess number of OR males with yeast supplement. After three days, ovaries were dissected out and compared. The ovaries of *Df7305*/*Df7306* females were considerably larger than those of OR, *Df7305*/*TM6B* and *Df7306*/*TM6B* females; however, we did not observe a complete recovery from *act5c*:*UAS-gsnor*; *Df7305*/*Df7306* ovaries which were just slightly smaller than *Df7305*/*Df7306* (Figure 4-5b). This can be explained that *Df7305*/*Df7306* can still produce eggs, but the eggs are retained inside their ovaries.

The main machinery controlling egg retention in female Drosophila is likely to be nervous system. This is because the nervous system links the extrinsic factors, such as low temperature, humidity and food availability to its responded reaction, such as muscle contraction and relaxation. *gsnor* knockout might also affect the muscle contraction and relaxation; however, we think that it is unlikely, because *gsnor* knockout Drosophila does not show any defect in movement. There is strong evidence to link neurotransmission with egg retention. For example, knocking out

tyrosine decarboxylase and tyramine β-hydroxylase, enzymes required for producing an invertebrate neurotransmitter octopamine, results in egg retention (Monastirioti, 2003; Cole et al., 2005), as the mutation in the gene coding for the octopamine receptor (OAMB) (Lee et al., 2003). A population of nerve cells expressing octopamine is found in the abdominal ganglion which innervates ovaries and oviducts (Monastirioti, 2003). Octopamine has been later shown to involve in oviduct muscle relaxation (Rodríguez-Valentín et al., 2006). In humans, NO has been long known to associate with learning, memory, and behavior (Garthwaite et al., 1989; Duncan and Heales, 2005). NO functions as a co-transmitter in long term potentiation (LTP) which is a form of synaptic plasticity for learning and memory. Unlike other neurotransmitters, NO is produced from post-synaptic neurons and diffuses back to pre-synaptic neurons in order to increase and prolong the production of the neurotransmitter from the pre-synaptic neuron (Arancio et al., 1996). Moreover, recently the NO regulator GSNOR has been shown to play an important role in visual pattern memory in *D. melanogaster* (Hou et al., 2011). This is important evidence that associates GSNOR together with neurotransmission. Possibly, the loss of GSNOR may lead to egg retention due to a defect in neuronal signalling within the ovary.

4.4 Loss of GSNOR function produces malformed eggs with low hatching frequency.

Although *Df7305*/*Df7306* females retained their eggs they did lay a low number of eggs (approximately 50 eggs per 50 females per 18 hours), so they should produce some viable progeny. We thus hypothesized that *Df7305*/*Df7306* eggs may be defective. Eggs were again collected from 50 females of each genotype previously mated with an excess number of OR males for 18 hours, and then after 24 hours incubation eggs were counted for the hatched and unhatched eggs. Only 1-2 % of eggs laid by *Df7305*/*Df7306* and *Df7306*/*Df7305* females hatched (Figure 4-6) while in *Df7305*/*TM6B* or *Df7306*/*TM6B* females 60-80 % of eggs hatched. The complementation *act5c*:*UAS-gsnor*; *Df7305*/*Df7306* again could not fully rescue the phenotype back to *Df7305*/*TM6B* or *Df7306*/*TM6B* (about 50 % recovery); however, this confirms that the dramatic reduction in percentage hatched of *Df7305*/*Df7306* is

due to the loss of GSNOR. For *Df7305*/*Df7306* males, after crossed with OR females the percentage hatched was similar to OR females crossed with OR males (about 90% hatched) meaning that *Df7305*/*Df7306* males were fully fertile (Figure 4-6).

Eggs laid by *Df7305*/*Df7306* female were studied under a compound microscope compared with eggs from OR and *act5c*:*UAS-gsnor*; *Df7305*/*Df7306* flies. Eggs from *Df7305*/*Df7306* females look different from OR eggs. In wild-type eggs, the pattern on the eggshells created by the follicle cells fully covers the eggs. This pattern is entirely absent in *Df7305*/*Df7306* eggs, but it is partially restored in eggs laid by *act5c*:*UAS-gsnor*; *Df7305*/*Df7306* female where it is present but does not completely cover the eggs (Figure 4-7). This pattern is due to overproduction of exochorion at the boundary between follicle cells. With high magnification this pattern appears as ridges (Margaritis et al., 1980). Because the pattern is created by follicle cells, this phenomenon might indicate a function of GSNOR in follicle cells.

Another obvious defect on *Df7305*/*Df7306* eggs is distorted and diminutive dorsal appendages compared with those of OR and *act5c*:*UAS-gsnor*; *Df7305*/*Df7306* (Figure 4-7). Because appendages are also produced by follicle cells (Margaritis et al., 1980), this phenotype highlights on the role of GSNOR in follicle cell formation or function.

The number of eggs laid by OR female mated with *Df7305*/*Df7306* or *Df7306*/*Df7305* male, the proportion of these eggs that hatched, was not significantly different to the number of eggs laid by OR female mated to OR male or the proportion of these that hatched (Figure 4-5a and 4-6). This indicates that GSNOR is not required for male fertility.

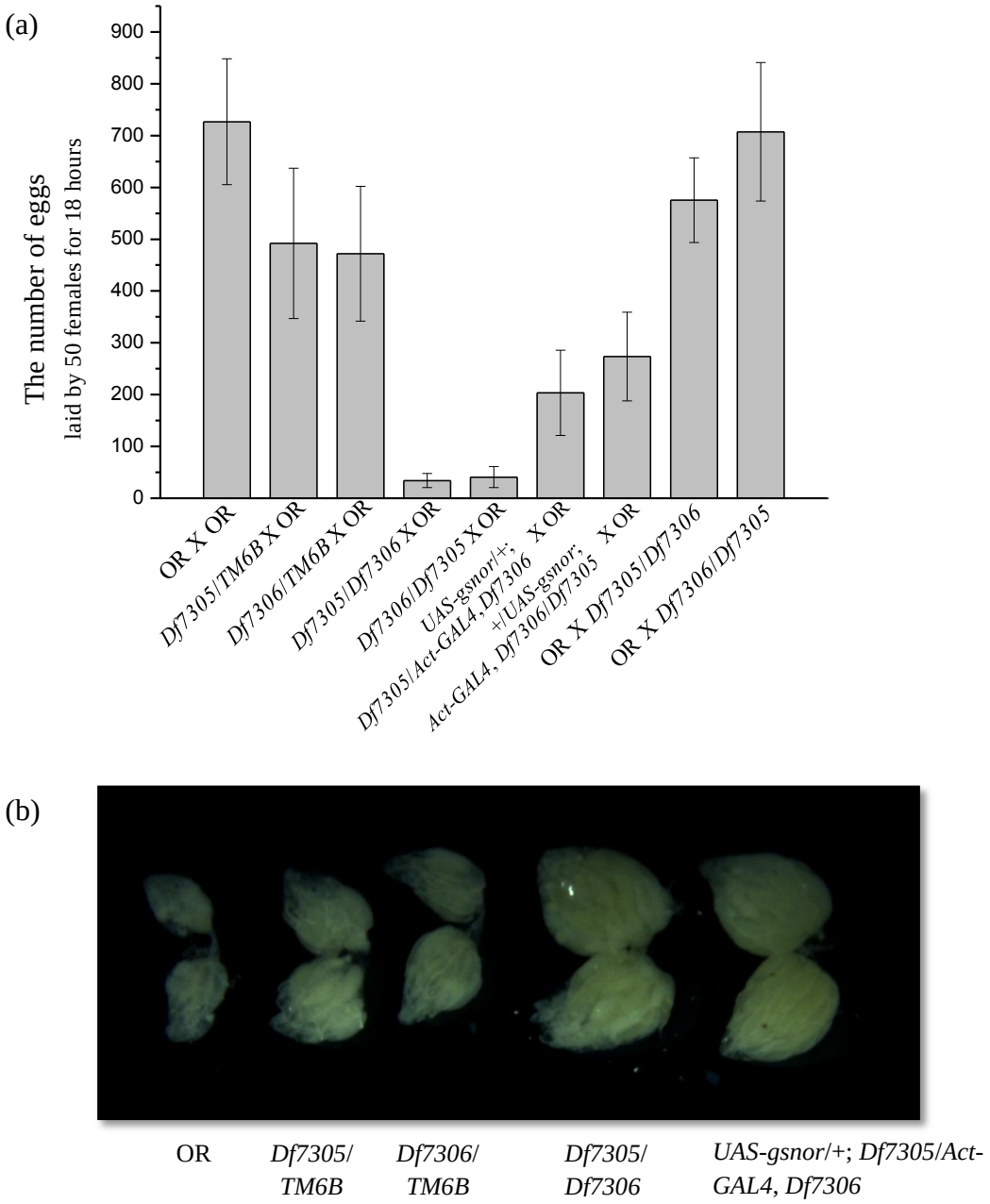

Figure 4-5. Drosophila fertility measured by the ability in egg laying (**a**) The number of eggs laid by 50 females during 18 hours with yeast supplement. The data represents a mean from three independent experiments (±SE). (**b**) Ovaries from 6-7 day old females grown in an environment with an excess number of OR males and with yeast supplement.

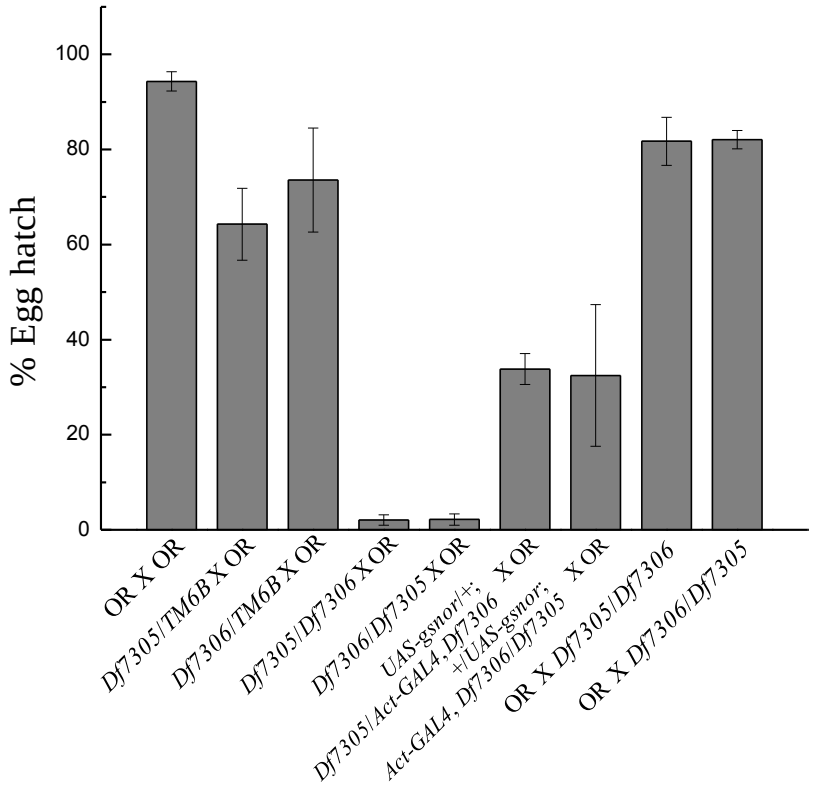

Figure 4-6. Drosophila fertility measured by the percentage of hatched eggs from the eggs laid by 50 females for 18 hours with yeast supplement. The number of eggs used in this experiment indicates in Figure 4-5a.The data represents a mean from three independent experiments (±SE).

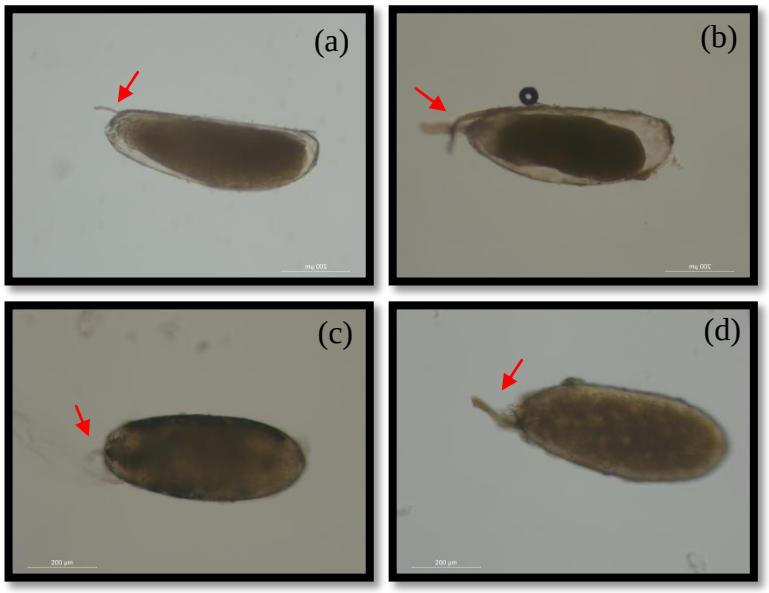

Df7305/*Df7306*

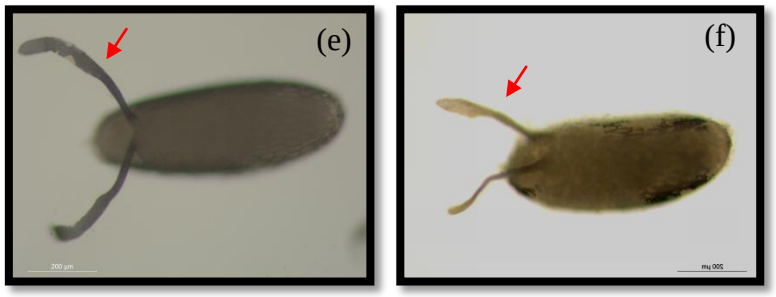

OR

UAS-gsnor/+; *Df7305*/*Act-GAL4*, *Df7306*

Figure 4-7. Drosophila egg morphology of (**a-d**) Drosophila *Df7305*/*Df7306* eggs compared with (**e**) wild-type eggs and (**d**) complementation eggs at the similar magnification. Eggs were collected within 4 hours after being laid. Red arrows indicate dorsal appendages.

4.5 GSNOR functions in the integrity of eggshells.

Since the discovery that GSNOR may relate to follicle cell formation, a further experiment to examine the integrity of eggshells, which is the product of follicle cells, was performed. The eggshell of a wild-type egg prevents desiccation and restricts permeability. We tested whether or not these characteristics are affected in *Df7305*/*Df7306* eggs. Wild-type, *Df7305*/*Df7306*, and *act5c*:*UAS-gsnor*; *Df7305*/*Df7306* eggs laid within 4 hours were collected in PBS solution. We noticed that the eggs from *Df7305*/*Df7306* were extremely fragile. Immediately after the PBS solution was dried, the majority of *Df7305*/*Df7306* eggs collapsed suggesting that the eggs might not be able to restrain water inside eggs, while OR and *act5c*:*UAS-gsnor*; *Df7305*/*Df7306* eggs were still normal. After drying for 15 minutes, all *Df7305*/*Df7306* eggs were collapsed and completely dried out; however, wild-type eggs were still entirely able to protect the loss of water. The complementation *act5c*:*UAS-gsnor*; *Df7305*/*Df7306* eggs were also able to prevent the desiccation; however, there was one egg that showed a partial desiccation (marked by red arrows; Figure 4-8). This again indicates the partial recovery of *act5c*:*UAS-gsnor*; *Df7305*/*Df7306*.

Neutral red dye in PBS was used to test the eggshell permeability. After adding the neutral red to eggs for one hour and washed three times with PBS, the dye was able to penetrate into every *Df7305*/*Df7306* egg, but was unable to penetrate into wild-type eggs. For *act5c*:*UAS-gsnor*; *Df7305*/*Df7306* eggs, most of the eggs were able to prevent the dye penetration; however the egg that showed partially desiccation was penetrated by the neutral red dye (red arrows; Figure 4-8).

This experiment suggests that the main functions of the eggshell, the product of follicle cells, in preventing desiccation and restricting permeability were absent in *gsnor* knockout Drosophila, and emphasizes the previous observation that GSNOR might be involved in follicle cell formation or function (Section 4.4).

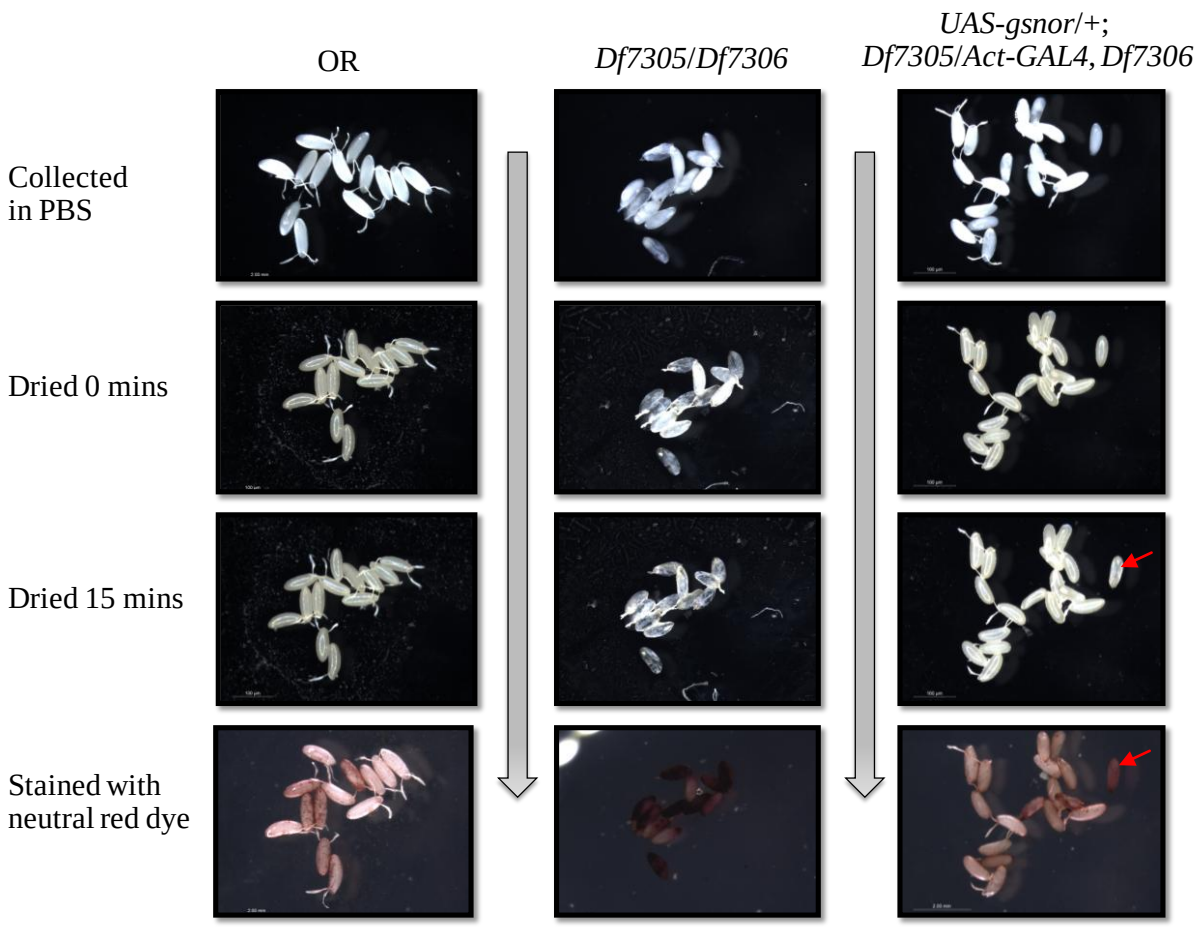

Figure 4-8. The eggshell properties in preventing desiccation and restricting permeability were tested in OR, *Df7305*/*Df7306*, and *act5c*:*UAS-gsnor*; *Df7305*/*Df7306*. In the first row, 0-4 hours eggs were collected on grape juice agar plates and then transferred to PBS solution. The photographs in the second row were taken immediately after the eggs had been dried. The eggs were allowed to dry for 15 minutes (the third row). The property of eggshell integrity was observed by how long the eggs can withstand desiccation. Neutral red dye in PBS solution was used to stain the eggs for one hour. After three time washes by PBS, photographs were taken (the fourth row) and the ability to restricting permeability was observed by whether the dye was able to penetrate into the eggs or not.

The defect in follicle cell formation or activity may also contribute to the egg retention phenotype. Based on the example of Drosophila M6 protein, transmembrane glycoprotein of the proteolipid protein family, the down-regulated M6 protein results in an absence of cell shape change of the follicle cells surrounding the oocyte from cuboidal to columnar, and disrupts follicle epithelium formation. The eggs laid by the down-regulated M6 flies exhibit similar phenotypes in water loss protection and permeability restriction as the eggs laid by *gsnor* knockout flies (but with less severity). Interestingly, the down-regulated M6 Drosophila also produces the low number of eggs (Zappia et al., 2011). This suggests that potentially there might be an association between egg development and egg retention; therefore, the effect of egg retention in *gsnor* knockout Drosophila is possibly a subsequent effect of the impaired follicle cell formation.

4.6 Conclusion

Arabidopsis *gsnor* loss-of-function mutation *gsnor1-3* exhibited decreased fertility measured by the number of seeds produced per plant, the *gsnor* knockout Drosophila also showed the reduced fertility. The total number of eggs laid was dramatically compromised due to egg retention. Of those eggs that were laid, the percentage that hatched in *gsnor* knockout Drosophila was also reduced. The eggs laid by *gsnor* knockout flies had abnormal dorsal appendages, defect eggshell pattern and increased permeability. Both appendages and eggshells are produced by the epithelial follicle cells. We believe that GSNOR is required for egg laying and follicle cell formation. The defect in egg laying could simply be due to a follicle defect as suggested by the M6 mutation (Zappia et al., 2011).

GSNOR is required for follicle cell formation and function, possibly because NO inhibits cell proliferation. Therefore, impaired GSNOR, the enzyme that regulates NO function, might contribute to the defect in cell proliferation as observed in *gsnor* knockout follicle cells and tergites (Section 3.6). Another possibility is that GSNOR might be required for egg laying because NO is involved in neurosignalling.

Chapter 5 Optimization of *S*-Nitrosothiol Measurement By Chemiluminescence Assay and Its Deployment to Determine *S*-Nitrosothiol Levels of *D. melanogaster*

5.1 Introduction

In Arabidopsis, the *gsnor* loss-of-function mutation *gsnor1-3* exhibits elevated SNO basal levels. This increase in SNO level is higher with an infection (Feechan et al., 2005) pointing out the role of GSNOR as a regulator of the cellular SNO level. There is therefore a potential that the total *S*-nitrosylation level in *gsnor* knockout Drosophila might increase as occurred in Arabidopsis *gsnor1-3*. However, the SNO level of Drosophila has never been reported. In order to observe the Drosophila SNO level, the method for measuring the SNO level has to be developed. In this chapter, I will describe how we developed and optimized the method for measuring Drosophila SNO level based on a chemiluminescence assay.

5.1.1 The properties of SNOs.

NO is a small and lipophilic molecule that can move freely in intercellular and intracellular environments. NO is an active molecule. It can react with molecules with unpaired electrons, such as O_2^- and hydroxyl ions (OH^-), transition metals, and thiols. When NO reacts with thiols of cysteine amino acid residues, it forms SNOs. This PTM often alters protein function. Although the NO in SNOs is labile, there is a large body of evidences indicating that in physiological condition SNO does not release NO (Hogg, 2002). For example, many proteins are constitutively *S*-nitrosylated, such as human caspase-3 (Mannick et al., 1999), endothelial isoform of nitric-oxide synthase (eNOS) (Erwin et al., 2005), and IκB kinase (IKK) (Reynaert et al., 2004). Although, protein SNOs are stable in cellular conditions, once the proteins are extracted, attached NO is prone to be displaced by exogenous heat, light, reducing agents or nucleophilic compounds (Benhar et al., 2009) making SNOs difficult to be accurately measured.

Technique for detecting *S*-nitrosylated proteins uses two approaches either the detection of sulfur (S) atoms of SNOs or NO molecules released from SNOs.

5.1.2 SNO measurement by the detection at S atoms

SNOs from biological samples can be directly quantified by liquid chromatography–mass spectrometry (LC-MS); however, only known SNOs can be measured by matching with S-^{15}NO internal controls (Tsikas et al., 1999). In order to be able to identify SNOs together with quantification, the total cellular SNOs can be isolated by the BST followed by streptavidin pull down.

In the BST first the total proteins are extracted and the free thiols are blocked by chemicals that can react with free thiols, such as methyl methanethiosulfonate (MMTS) or *N*-ethylmaleimide (NEM). The SNO groups are reduced by mild reducing agents, such as ascorbate which reduces only SNO groups but not di-sulfide bonds. The reduced SNOs produce free thiols which later form di-sulfide bonds with *N*-[6-(biotinamido)hexyl]-3'-(2'-pyridyldithio)propionamide (biotin-HPDP) replacing SNO with S-biotin (Jaffrey et al., 2001) (Figure 5-1). The purified protein-SNOs can be detected and identified by MS/MS (Zaman et al., 2006). or Western blot followed by probing with specific antibodies (Jaffrey et al., 2001). If only the level of *S*-nitrosylation without any identification is required, the total protein-SNOs can be visualized by SDS-PAGE followed by silver staining or by Western bloting with anti-biotin antibody prior to the streptavidin pull down.

5.1.3 SNO measurement by the detection at NO molecules

The detection of NO molecules is often used to quantify the total level of SNOs or to observe the *S*-nitrosylation level of target proteins. The main principal of this approach is to induce the release of NO from SNOs and detect the released NO.

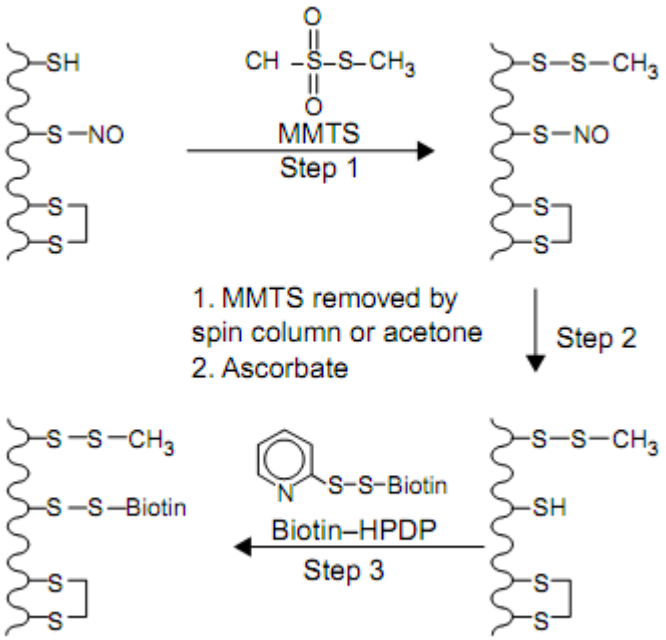

Figure 5-1. A schematic diagram illustrates BST process. Step 1, a free thiol of a hypothetical protein is block with MMTS. Step 2, the excess MMTS is removed by using a spin column or acetone precipitation. Ascorbate is added to reduce and remove NO from SNO. Step 3, biotin-HPDP is added to form di-sulfide bond with the free thiol which has just been reduced with ascorbate. The final product shows that NO of SNO is replaced with biotin. This figure is taken from Jaffrey et al. (2001)

5.1.3.1 4,5-Diaminofluorescein (DAF-2) fluorescence assay

DAF-2 can be used to indicate the amount of NO by reacting with nitrous anhydride (N_2O_3) which is a product of the reaction between NO and O_2 (Planchet and Kaiser, 2006). The DAF-2 reaction yields a fluorescent triazolofluorescein (DAF-2T) which can be excited at 485 nm to emit light at 520 nm. The NO from SNOs can be released by mercury (Hg) or UV photolysis and then detected by DAF-2. The detection by DAF-2 can be performed on microtiter plates for the total SNO level (Doctor et al., 2005) or on SDS-PAGE to observe *S*-nitrosylation of the expected molecular weight (King et al., 2005). The detection of this method is at low nM, and if gel-based is used the detection is above 3 µM (Gow et al., 2007).

5.1.3.2 The Saville assay

The Saville assay is a classic method for detecting SNOs. NO in SNOs is displaced with Hg^{2+} from mercury (II) chloride ($HgCl_2$) releasing NO^+. In the presence of O_2, NO^+ is spontaneously converted to NO_2^- (Bryan and Grisham, 2007). NO_2^- can irreversibly react with sulfanilamide (SF) to form a diazonium salt which can be coupled with *N*-1-naphthylethylenediamin (NED) to yield a coloured azo dye (measured at A_{540}) (Figure 5-2). Because the SF can react with NO_2^- that is also present in biological samples, the level of SNOs inmeasured from the difference between A_{540} with or without the addition of $HgCl_2$. However, this method is not sensitive (the limit of detection is at 500 nM) (Saville, 1958).

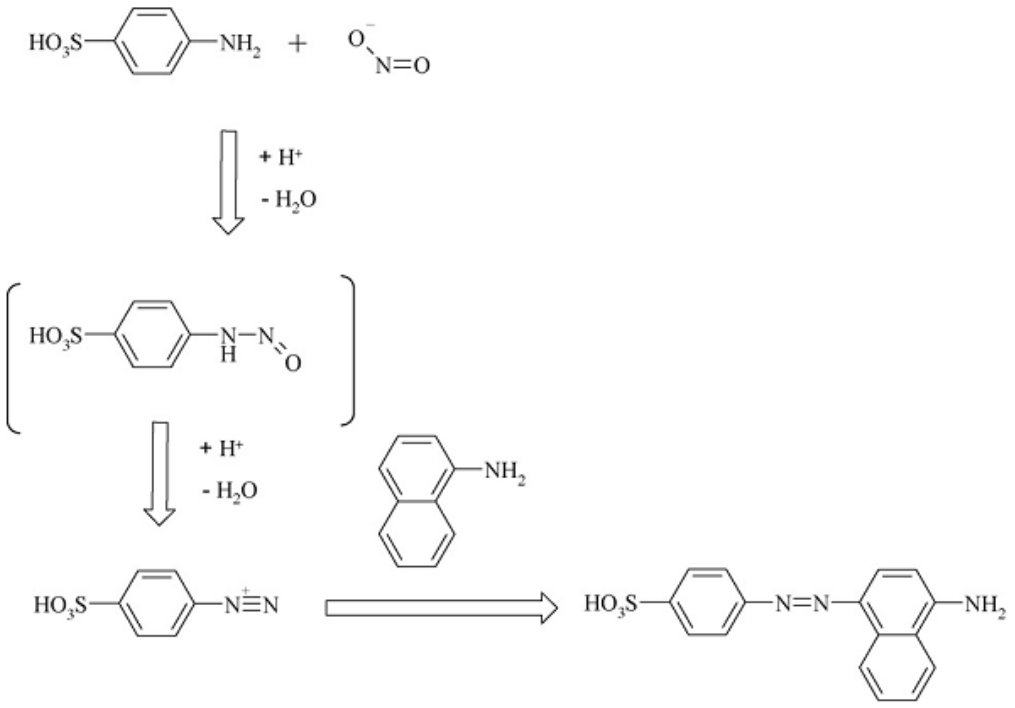

Figure 5-2. The Griess reaction followed by coupling with NED. SF reacts with NO_2^- the form a diazonium salt which is then coupled with NED to form a colourd azo dye. Taken from Tsikas (2007).

5.1.3.3 Chemiluminescence-based assays

Chemiluminescence-based assays for SNO measurement comprise three steps: sample preparation, NO displacement from SNOs, and the released NO detection. The extraction procedure is crucial in order to slow down the protein SNO degradation. pH in the extraction buffer directly affects the stability of SNO. A mildly basic buffer can prolong stability of SNOs (Hornyák et al., 2012). The type of buffer used is important as HEPES and MOPS (3-(*N*-morpholino)propanesulfonic acid) accelerate the decomposition of $ONOO^-$ to NO (Schmidt et al., 1998) which might contribute the over-estimation of SNO level. The addition of chelating agents, such as EDTA or neocuproine, helps decelerate the detachment of NO from SNOs by sequestering and preventing metal ions from reducing NO (Wang et al., 2009a). Preventing proteins from degradation is another aspect to be considered, because degraded SNO proteins might cause the release of NO and interfere protein quantification for normalizing NO signal with an amount of protein. Different types of protease inhibitors can be added to the extraction buffer. Strong detergents, such as SDS, also prevent protein degradation by denaturing proteases, and SDS also denatures other enzymes which may have roles in *S*-nitrosylation. Furthermore, immunoprecipitation or high-pressure liquid chromatography (HPLC) can be performed in this step, if only a particular protein SNO is measured (Gow et al., 2007).

For the second step, there are many methods for releasing NO from SNOs. Photolysis can be utilized for inducing NO disassociation from SNOs. UV light at 300-350 nm can induce the excitation of the oxygen atom in SNOs and light between 530-560 nm can excite the nitrogen atom of SNOs leading to instability and cleavage of NO from SNOs (Sexton et al., 1994). However, each SNO has different suitable excitation wavelength (Shishido et al., 2003); therefore, ideally samples should be treated with all wavelengths stated above . The conversion of NO_2^- to NO may occur at a wavelength below 300 nm or at low pH and a NO_2^- standard should be used in every experiment (Gow et al., 2007).

Many reducing agents have been reported to reduce NO from SNOs. Some reducing agents detect only SNOs without NO_2^- signal contamination. Saturated

copper (I) chloride (CuCl) and 1 mM cysteine in water at 50˚C (CuCl/Cys) (Fang et al., 1998; Doctor et al., 2005), 0.2 mM CuCl with excess amount of ascorbic acid (50 mM) at 37˚C (CuCl/Ascorbic acid) (Sengupta et al., 2007), and hydroquinone and quinone in Tris buffer (pH 10) at 60˚C (Samouilov and Zweier, 1998) are examples. The main advantage of the sole detection of SNOs is that only a single measurement is required. This is more convenient and has less error. However, the disadvantage is that how to make sure that the signal generated is due to SNOs and not NO_2^-. This is because NO_2^- is easily converted to NO. For example, protons (H^+), xanthine oxidase, or cytochromes can transform NO_2^- to NO and lead to a false positive signal (Lundberg and Weitzberg, 2005). In the complexity of the total protein extract, we think it is difficult to be confident that the signal detected is solely from SNOs.

Some reducing agents detect all together SNOs, XNOs and NO_2^-. For example, 10 mg/mL potassium iodide (KI) and 4 mM copper (II) sulfate ($CuSO_4$) in 80 %v/v acetic acid at 70˚C (acetic/KI/$CuSO_4$) (Marley et al., 2000), and 10 mg/mL KI and 6.5 mg/mL I_2 in acetic acid at 50˚C (tri-iodide) (Pinder et al., 2008). In order to obtain solely SNO level, the measurement with SF pretreatment followed by deduction with the measurement with SF and $HgCl_2$ pretreatment has to be performed. The advantage of these reducing agents is that NO_2^- is completely removed before the measurement begins; however due to the multiple measurement, the level of SNOs is likely to have more error than the direct SNO detection.

For the NO detection step, NO released by reducing agents is cooled down and filtered to remove contaminating liquid before entering the NOA. Inside the NOA, NO is reacted with ozone (O_3) to form excited NO_2 (NO_2^*) that emits light detected by the machine (Figure 5-3).

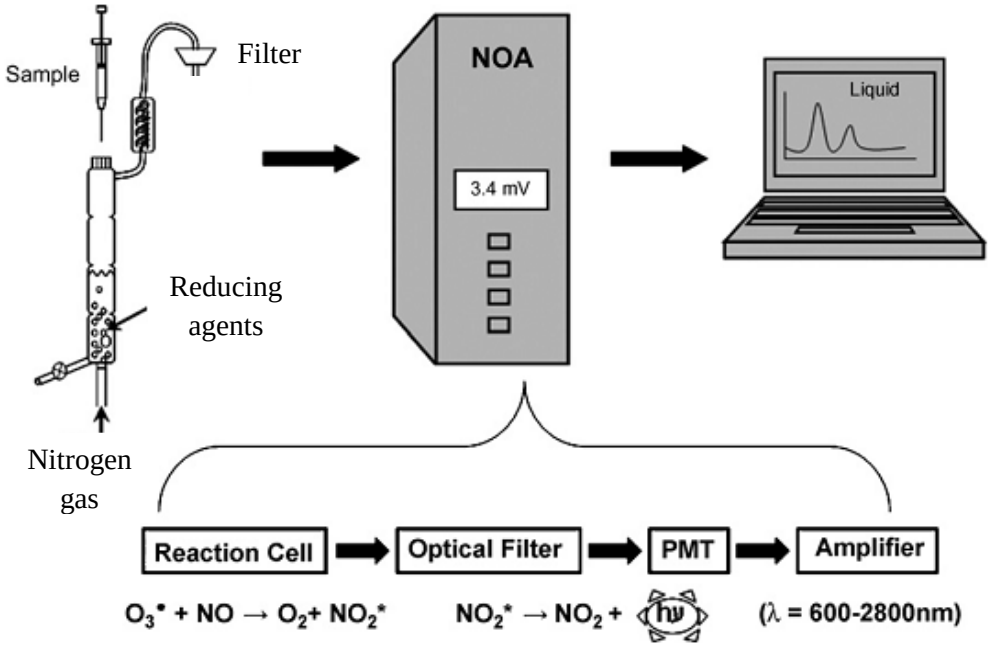

Figure 5-3. NO measurement from SNOs by the chemiluminescence method. The sample is injected into the temperature controlled reaction chamber containing reducing agents. NO from reduced SNOs is released and brought through condenser, hydrophobic filter, and nitric oxide analyzer (NOA) machine by continuous nitrogen flow. In the machine, NO reacts with O_3 producing excited NO_2^* which returns to its ground state and emits light ($h\upsilon$) at 600-1800 nm. This light signal is detected by a photomultiplier tube (PMT) and recorded by a data recording software. This figure is adapted from MacArthur et al. (2007).

For the total SNO level measurement, chemiluminescence-based assays are probably the method of choice. This is because this technique can detect SNOs in a pmole range (Gow et al., 2007) which is more sensitive than the Saville assay and DAF-2 fluorescence assay. However, an appropriate reducing agent and extraction buffer have to be optimized to match with the type of samples measured.

5.2 The chemiluminescence method used in Arabidopsis cannot successfully quantify SNO in Drosophila.

Initially, the chemiluminescence based SNO measurement that has been successfully used in Arabidopsis (personal communication from Dr. Byung-Wook Yun) was adopted for the Drosophila SNO measurement. For the original Arabidopsis method, leaves were ground in potassium phosphate buffer (KPi buffer pH 6.5) with a protease inhibitor cocktail (Roche) and centrifuged to precipitate debris. The supernatant was injected into a reducing agent in the reaction chamber. A 0.005 % wt/v CuCl (saturated) and a 1 mM cysteine at 50 ºC (CuCl/Cys) solutions were used as reducing agents. This showed a reducing effect on SNO but not NO_2^- or NO_3^- for the pH values ranging from 6 to 8. NO is released by transnitrosylation from SNOs and subsequently reacts with Cys forming *S*-nitrosocysteine (CysNO). Then, the CysNO is reduced by Cu^+ releasing NO which can be detected by NOA. Cu^{2+} is reduced by Cys to form Cu^+ (Fang et al., 1998; Doctor et al., 2005).

The experiment in Drosophila was carried out as in Arabidopsis with a few modifications. Because of the lack of chemicals maintaining SNOs in the extraction solution, the chelating agents, EDTA and neocuproine, were added to prevent a decomposition of SNOs. In order to prevent protease mediated denitrosylation, SDS was also added to the extraction solution to denature total proteins. To prevent SDS precipitation, the buffer was changed from KPi buffer to NaPi buffer. EDTA, neocuproine and SDS are the chemicals normally used in BST (Forrester et al., 2009). Unexpectedly, when the number of flies added to the extraction buffer was increased the signal decreased (Figure 5-4). We hypothesized either there were inhibitors in the samples that might impair the detection or the CuCl/Cys might have lost its reducing.

To prove this hypothesis, CysNO was synthesized by mixing equimolar concentrations of cysteine (in H_2O) and acidified sodium nitrite ($NaNO_2$ in 1 M hydrochloric acid (HCl) (Gaston et al., 1993), and used as controls. 100 µL of 10 µM CysNO was injected into the reaction chamber before and after injecting of each of the components of the Drosophila extraction buffer to observe whether any of them reduced the detection ability or the reducing capability of the CuCl/Cys. Injection of 500 µL of ground 5 flies in 600 µL of water, 1 x protease inhibitors, 2 mM EDTA, 0.1 mM neocuproine, and 1 % SDS did not affect the amount of CysNO detected (the areas were about 14500 mVolt.min) (Figure 5-5a). Only when 50 mM Tris-Cl pH 7.5 was injected, did the signal from the subsequent CysNO injection greatly reduced (Figure 5-5a) indicating that either Tris-Cl or pH 7.5 was the cause of the impaired detection ability.

To further investigate whether Tris-Cl or pH 7.5 influences the reducing ability of CuCl/Cys, 500 µL of NaPi buffer pH 7.5 was injected after the CysNO injection. This had a similar effect to Tris-Cl pH 7.5 (Figure 5-5b). When 500 µL of NaPi buffer at pH 6.5, instead of pH 7.5, was used a similar effect was observed after three times injection (Figure 5-5c). Therefore, the decrease in the reducing ability of CuCl/Cys was prolonged by injecting the lower pH buffer. This indicates that CuCl/Cys might only have the reducing ability at low pH.

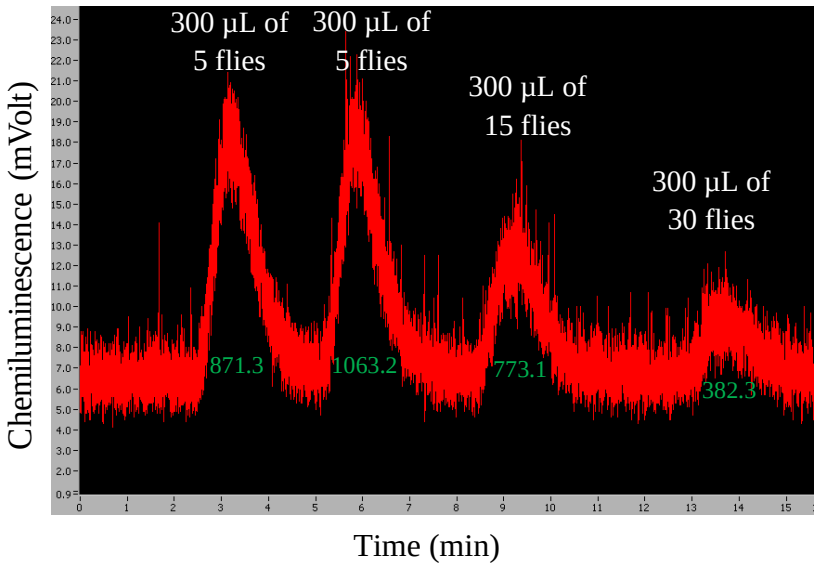

Figure 5-4. The chemiluminescence signal generated by different Drosophila protein concentrations using 10 mL of CuCl/Cys as the reducing agents. Areas under peaks represent the amount of NO released from each sample by the reducing agent. The green numbers indicate area under peaks. Wild-type Drosophila protein extracted in 600 µL extraction buffer (NaPi buffer pH 7.5, EDTA, neocuproine and SDS). 300 µL of each protein extract was injected into the reaction chamber.

(a)

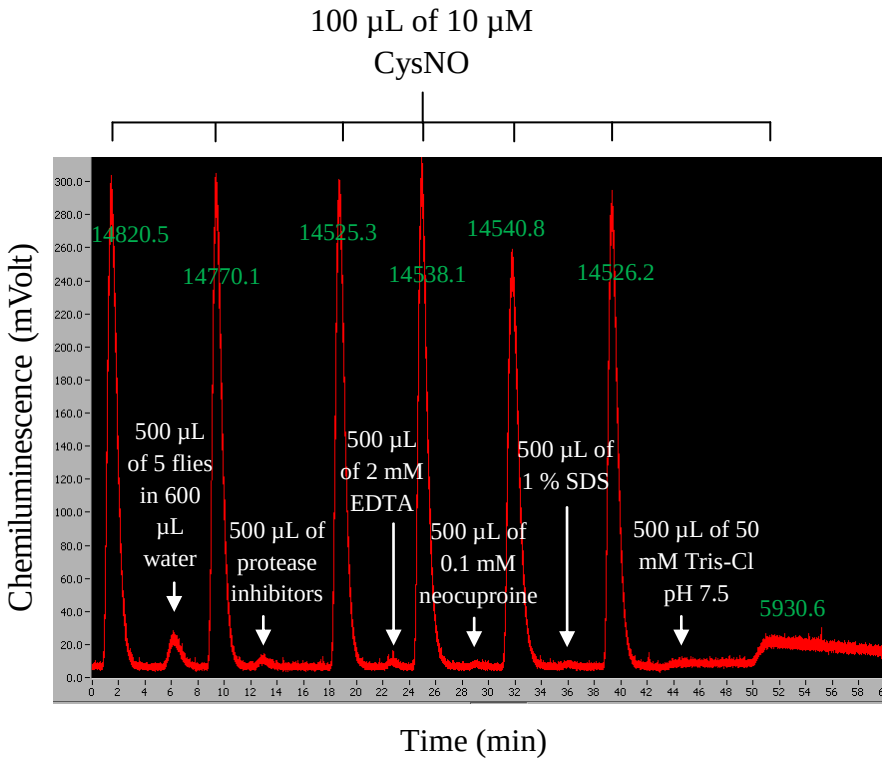
100 µL of 10 µM CysNO
Chemiluminescence (mVolt)
14820.5
14770.1
14525.3
14538.1
14540.8
14526.2
5930.6
500 µL of 5 flies in 600 µL water
500 µL of protease inhibitors
500 µL of 2 mM EDTA
500 µL of 0.1 mM neocuproine
500 µL of 1 % SDS
500 µL of 50 mM Tris-Cl pH 7.5
Time (min)

(b)

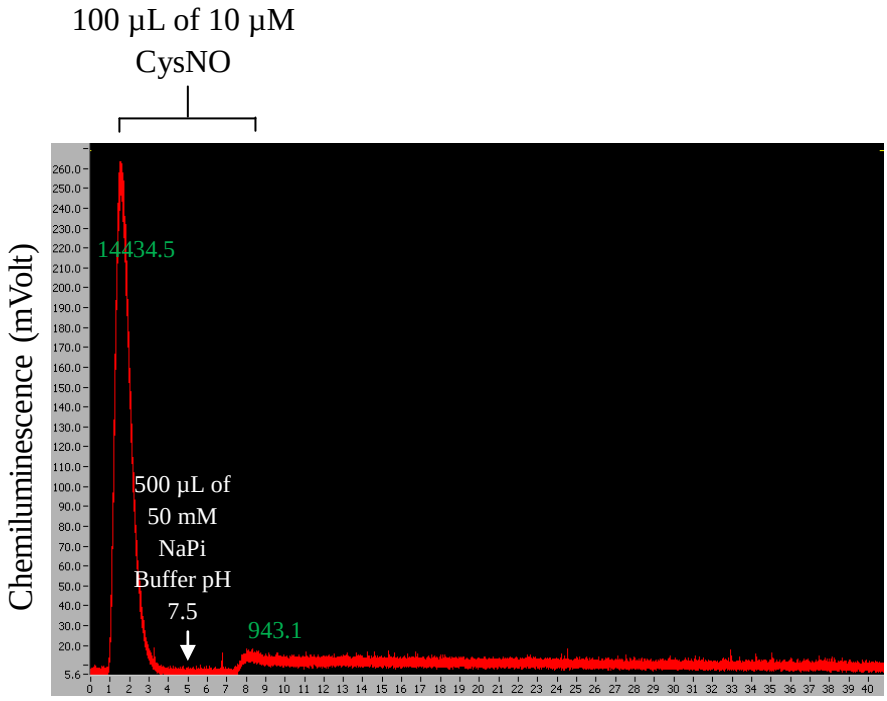
100 µL of 10 µM CysNO
Chemiluminescence (mVolt)
14434.5
943.1
500 µL of 50 mM NaPi Buffer pH 7.5
Time (min)

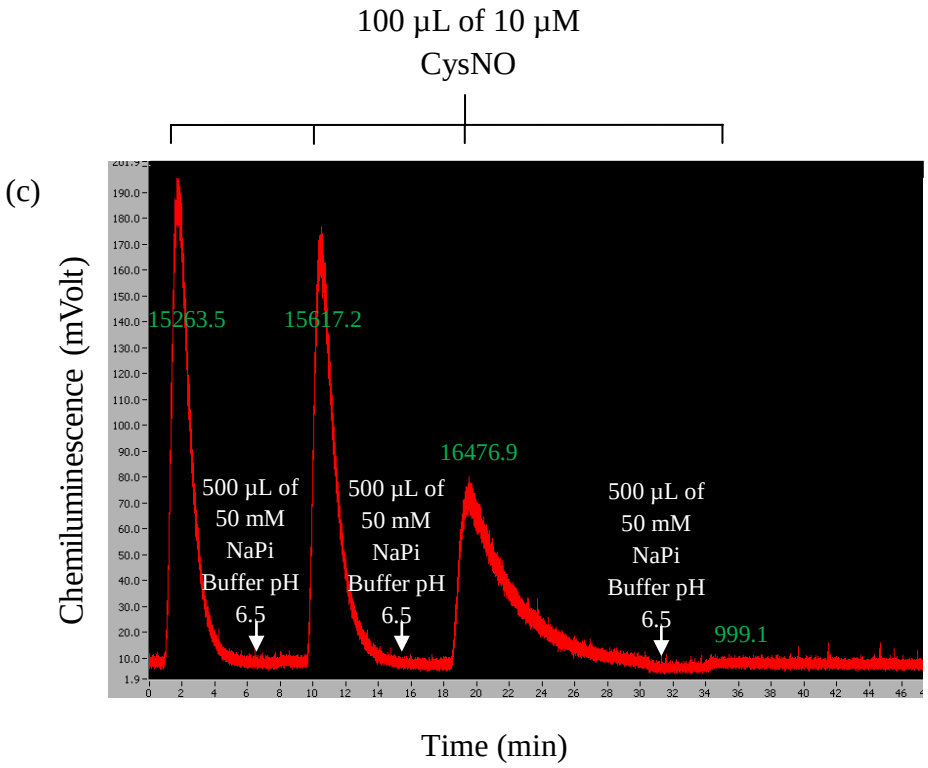

Figure 5-5. The chemiluminescence signal generated by the same amount of chemicals present in the extraction buffer and also other types of buffers to confirm the effect of pH. 100 µL of 10 µM CysNO was injected before and after each chemical. The decrease in the areas under peak of 10 µM CysNO 100 µL indicates the interference from the previous injection. 10 mL of CuCl/Cys was used as the reducing agent. Area under peaks represent the amount of NO released from each sample by the reducing agents. The green numbers indicate area under peaks.

To explain the phenomenon, due to poor solubility and instability of CuCl, Cu^{+} is simply oxidized by O_2 in air to Cu^{2+}. This was observed by the greenish blue colour of the solution (Lide, 2009). We did observe the greenish blue colour in the CuCl/Cys solution. Moreover, when Cu^{+} reduces SNOs or CysNO, it looses an electron and becomes Cu^{2+} (Equation 1; where R is the substrate to be nitrosylated, and X is an unknown intermediate) (Al-Sa'doni and Ferro, 2000). Although Cys or other SH containing molecules can assist recycling of Cu^{2+} to Cu^{+} (Equation 2; where Y is an unknown intermediate) (Al-Sa'doni and Ferro, 2000), the majority of soluble Cu is likely to be Cu^{2+}. The increase of pH by adding the neutral pH buffers encourages the forming of the insoluble $Cu(OH)_2$ (Equation 4) which prevents the recycling of Cu^{+} by Cys and removing Cu out of the reducing solution leading to the loss of reducing capability observed after the neutral pH buffers.

$$\underset{}{Cu^{+}} + \underset{\text{(Cys-S-NO)}}{\text{R-S-NO}} \rightleftarrows \text{X} \rightarrow \underset{\text{(Cys-S-H)}}{\text{R-S}^{\bullet}} + {}^{\bullet}\text{NO} + Cu^{2+} \qquad \text{(Equation 1)}$$

$$\underset{}{Cu^{2+}} + \underset{\text{(Cys-S-H)}}{\text{R-S}^{\bullet}} \rightleftarrows \text{Y} \rightarrow \underset{\text{(Cys-S-H)}}{\text{R-S}^{\bullet}} + Cu^{+} \qquad \text{(Equation 2)}$$

$$\underset{\text{(Cys-S-H)}}{2\ \text{R-S}^{\bullet}} \rightarrow \underset{\text{(Cys-S-S-Cys)}}{\text{R-S-S-R}} \qquad \text{(Equation 3)}$$

$$Cu^{2+} + 2\ OH^{-} \rightarrow \underset{\text{'Insoluble'}}{Cu(OH)_2} \qquad \text{(Equation 4)}$$

We reasoned that the addition of a buffer at pH 3.5 or the change to other reducing agents could overcome this problem.

5.3 The signal obtained from the chemiluminescence method used in Arabidopsis contains nitrite contamination.

Another problem that we observed for the CuCl/Cys was the unwanted NO_2^{-} contaminating the output signal. Although the CuCl/Cys cannot detect NO_2^{-} at pH 6 to pH 8 (Fang et al., 1998), we found using equimolar CysNO and $NaNO_2$ the area

under the graph suggested that CuCl/Cys can detect NO_2^- at the same efficiency as CysNO (Figure 5-6). NO_3^- cannot be detected by CuCl/Cys even at high concentration (100 µL of 100 mM $NaNO_3$) (Figure 5-6).

In order to eliminate the NO_2^- signal contamination, SF was added to the CuCl/Cys. Due to the irreversible reaction with NO_2^- (Figure 5-2), 1 % wt/v SF in CuCl/Cys has been shown to detect serum SNOs without the NO_2^- contamination (Fang et al., 1998). The CuCl/Cys with SF detected CysNO at the similar level with the CuCl/Cys without SF addition (Figure 5-5 and 5-7a); however, SF addition failed to abolish the detection of NO_2^-. The addition of SF to the CuCl/Cys reduced the signal from $NaNO_2$ by about 50 % as compared to the signal from an equimolar amount of CysNO (Figure 5-7a). Possibly, the irreversible reaction between SF and NO_2^- could not completely overcome the conversion of NO_2^- to NO. This effect was not due to the loss of the reducing ability of the reducing agents, because the final 10 µM CysNO injection produced the same under peak area with the initial 10 µM CysNO injection. The final 10 µM CysNO injection was performed as a control in every experiment. Note that low signal gives an inaccurate calculation of an area under peak, for example in Figure 5-7a the area under peak of 100 nM CysNO is not 10 % of the area from 1 µM CysNO.

A new method was adopted instead of using Cys to maintain the level of Cu^+ (Equation 2), ascorbic acid was used (Equation 5) (CuCl/ascorbic acid; Sengupta et al., 2007). Ascorbic acid also reduces and releases NO from SNOs (Equation 6; Z is an unknown intermediate), while Cys is only able to transnitrosylate NO from SNOs to form CysNO which requires Cu^+ to reduce and release NO (Equation 1). Moreover, CuCl/ascorbic acid has been shown to abolish NO_2^- signal contamination (Sengupta et al., 2007). The CuCl/ascorbic acid was able to detect 100 µL of 10 µM CysNO at a similar level as in CuCl/Cys. However, when the 10 µM $NaNO_2$ was injected the NO_2^- was detected at approximately 80 % of the signal detected from 10 µM CysNO. If the appearance of the graph generated from 10 µM CysNO and 10 µM $NaNO_2$ were compared, the signal from 10 µM $NaNO_2$ was detected more slowly (broad peak) compared with 10 µM CysNO (Figure 5-7b) indicating a slow conversion rate from NO_2^- to NO. 1 %wt/v SF was added to CuCl/ascorbic acid in

order to reduce the signal from NO_2^-, but this did not reduce the NO_2^- signal (Figure 5-7c).

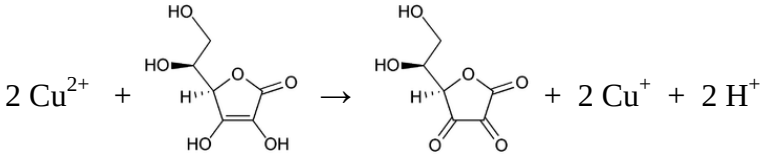

(Equation 5)

Ascorbic acid (reduced form) Dehydroascorbic acid (oxidized form)

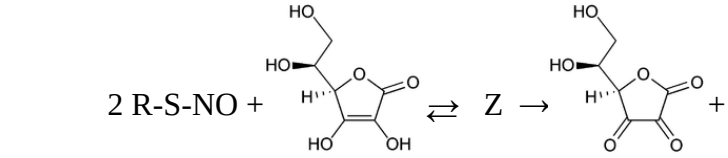

(Equation 6)

Ascorbic acid (reduced form) Dehydroascorbic acid (oxidized form)

We think that the NO_2^- contamination mainly depends on pH. This is because CuCl/ascorbic acid, which was able to detect NO_2^- with the slow NO_2^- to NO conversion rate, has a neutral pH of 7, while the CuCl/Cys which was able to detect NO_2^- with a high conversion rate (the same rate as the detection of CysNO), has an acidic pH of 3.5. There is no evidence that other chemicals in either reducing agent could catalyze the conversion of NO_2^- to NO. From our data, the low pH possibly contributes to the NO_2^- contamination (the conversion of NO_2^- to NO is shown in Equation 7) (Osipov et al., 2007). We think that the reason why the SF was not able to decrease the NO_2^- contamination in the CuCl/ascorbic acid is that SF efficiently reacts with NO_2^- in an acidic condition (Figure 5-2) (Tsikas, 2007). The pH of CuCl/ascorbic acid with SF (pH 6.2) was too high to allow SF to react efficiently with NO_2^- whereas this could occur at the pH of CuCl/Cys with SF (pH 4.6).

$$2\ NO_2^- + H^+ \rightarrow NO_2 + {}^{\bullet}NO + OH^- \qquad \text{(Equation 7)}$$

Instead of using reducing agents which detect SNOs but not NO_2^-, we changed the strategy to eliminate NO_2^- before removing NO from SNOs by reducing agents. Acetic/KI/$CuSO_4$ which has been shown to detect both NO_2^- (Equation 14) (Pinder et al., 2008) and SNOs were used as reducing agents. The SNOs are reduced by triiodide ion (I_3^-) and Cu^+ which are the products of the reaction between I^- and Cu^{2+} (Equation 8 to 11) (Marley et al., 2000). After the reduction, I_2 reacts with I^- to again form I_3^- (Equation 11 to 13) (Marley et al., 2000; Pinder et al., 2008), and Cu^{2+} is recycled according to Equation 2, 8, 9 and 10 (Marley et al., 2000). However, before adopting the SF pre-treatment procedure, we reasoned it would be wise to make certain whether or not SF mixed in reducing agents can completely abolish the NO_2^- signal contamination. The acetic/KI/$CuSO_4$ were mixed with the increased amount of SF at 200 mM (3.44 %) (shown a complete NO_2^- elimination by Nagababu and Rifkind (2007)). The acetic/KI/$CuSO_4$ was able to reduce the 10 µM $NaNO_2$ signal contamination to approximately 80 % of the 10 µM CysNO (Figure 5-7d). We think that even though the SF in the low pH of acetic acid mixture was able to eliminate NO_2^-, the NO_2^- reducing ability of acetic/KI/$CuSO_4$ and high temperature increased the conversion of NO_2^- to NO presenting the high NO_2^- signal contamination.

$$Cu^{2+} + 2\,I^- \rightarrow \underset{\text{'Unstable'}}{CuI_2} \qquad \text{(Equation 8)}$$

$$\underset{\text{'Unstable'}}{2\,CuI_2} \rightarrow 2\,CuI + I_2 \qquad \text{(Equation 9)}$$

$$CuI \rightarrow Cu^+ + I^- \qquad \text{(Equation 10)}$$

$$I_2 + I^- \rightarrow I_3^- \qquad \text{(Equation 11)}$$

$$I_3^- + 2\,\text{R-S-NO} \rightarrow 3\,I^- + \text{R-S-S-R} + 2\,NO^+ \qquad \text{(Equation 12)}$$

$$2\,NO^+ + 2\,I^- + 2\,H^+ \rightarrow 2\,^{\bullet}NO + I_2 + 2\,H_2O \qquad \text{(Equation 13)}$$

$$2\,HNO_2 + 2I^- + 2H^+ \rightarrow 2\,^{\bullet}NO + I_2 + 2\,H_2O \qquad \text{(Equation 14)}$$

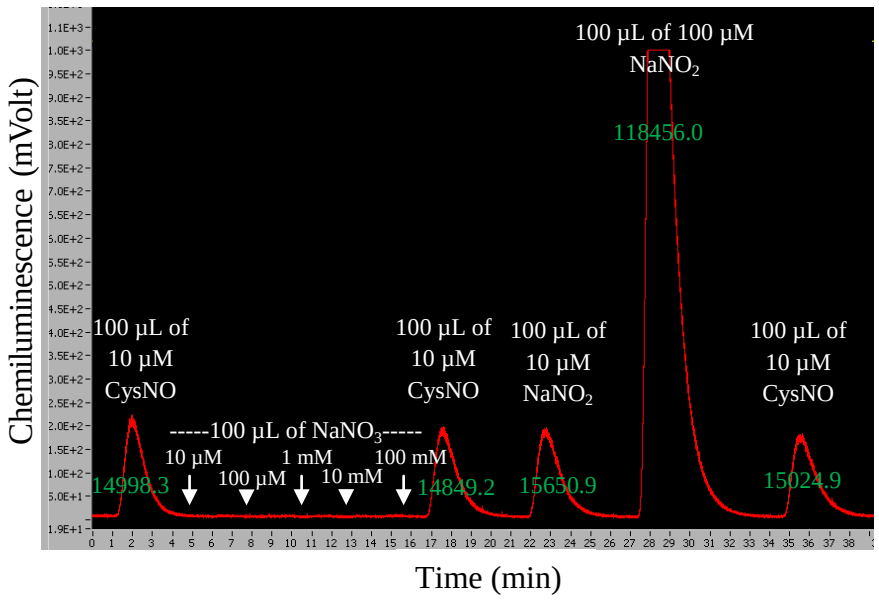

Figure 5-6. The chemiluminescence signal generated by CysNO, $NaNO_2$ and $NaNO_3$ using 10 mL of CuCl/Cys as the reducing agents. Area under peaks represent the amount of NO released from each sample by the reducing agents. The green numbers indicate area under peaks. 100 µL of each sample was injected. The similar first and last injections of 10 µM CysNO 100 µL indicates that the reducing agents still possessed the similar reducing capability throughout the experiment.

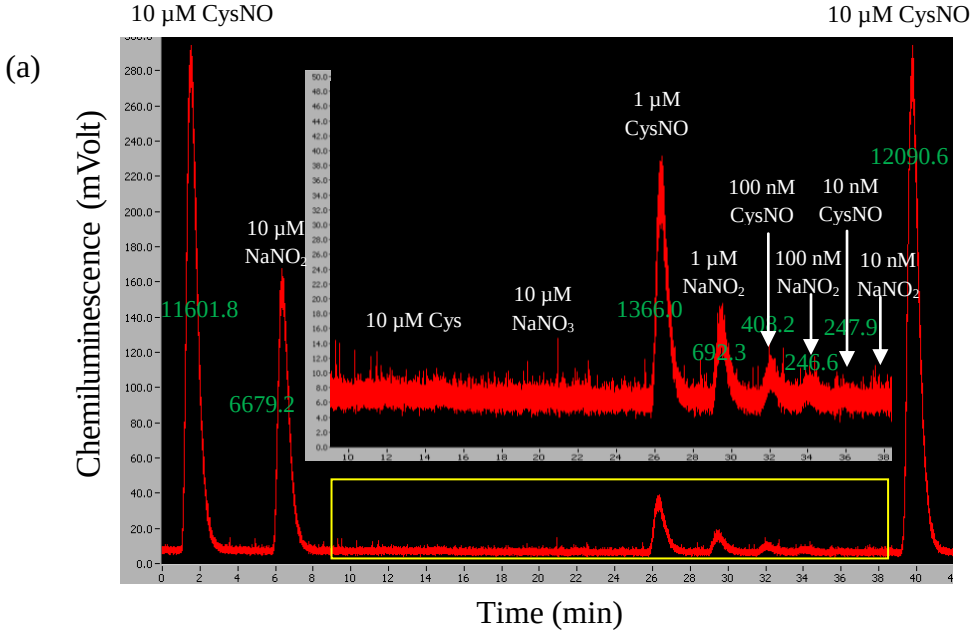

(b)

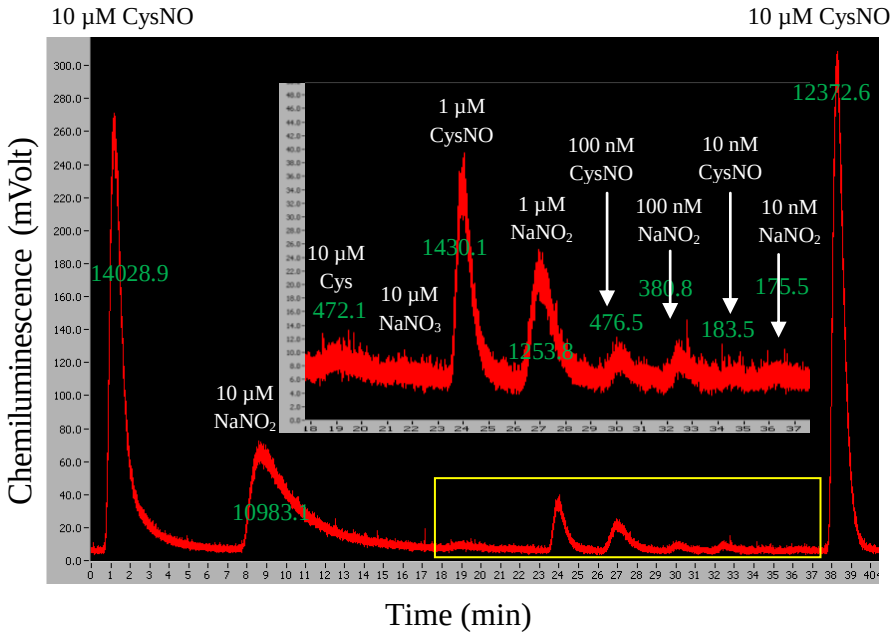
10 µM CysNO
10 µM CysNO
Chemiluminescence (mVolt)
Time (min)
14028.9
10 µM Cys
472.1
10 µM NaNO3
1430.1
1 µM CysNO
10 µM NaNO2
10983.1
1 µM NaNO2
1253.3
100 nM CysNO
476.5
100 nM NaNO2
380.8
10 nM CysNO
183.5
10 nM NaNO2
175.5
12372.6

(c)

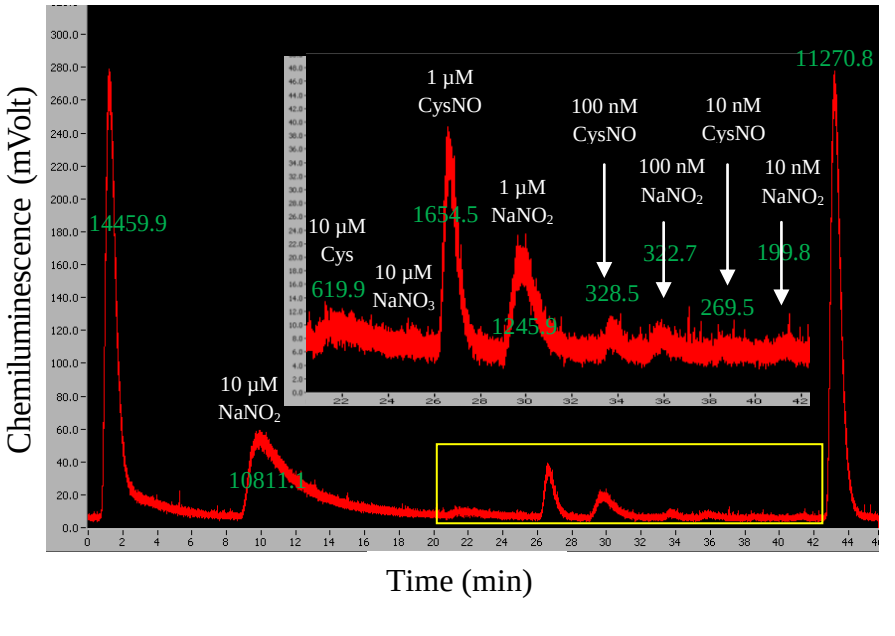
10 µM CysNO
10 µM CysNO
Chemiluminescence (mVolt)
Time (min)
14459.9
10 µM Cys
619.9
10 µM NaNO3
1654.5
1 µM CysNO
10 µM NaNO2
10811.1
1 µM NaNO2
1245.9
100 nM CysNO
328.5
100 nM NaNO2
322.7
10 nM CysNO
269.5
10 nM NaNO2
199.8
11270.8

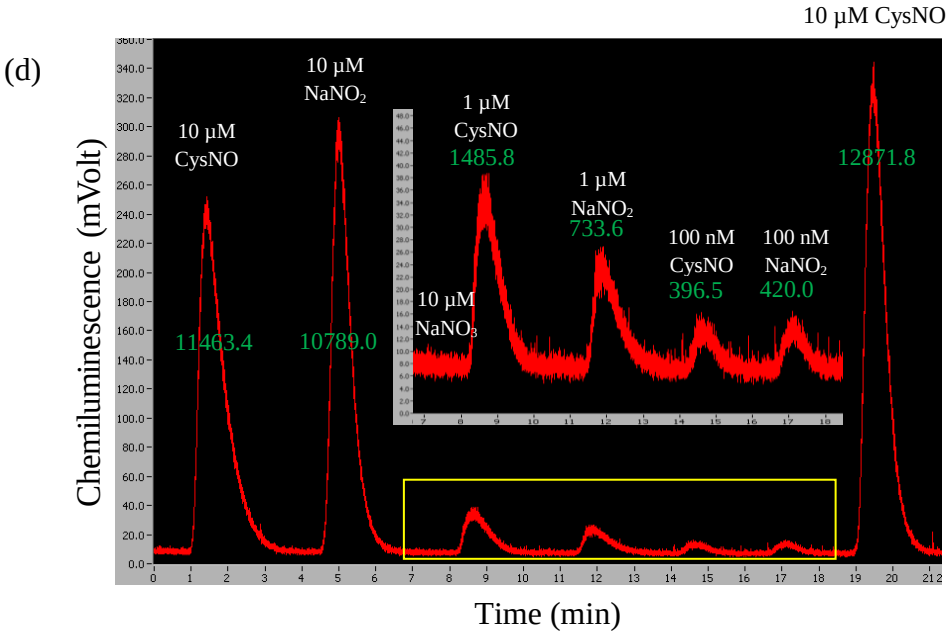

Figure 5-7. The chemiluminescence signal generated by CysNO, $NaNO_2$ and $NaNO_3$ using (**a**) 10 mL of CuCl/Cys with 1 % SF, (**b**) CuCl/Ascorbic acid, (**c**) CuCl/Ascorbic acid with 1 % SF, and (**d**) acetic/KI/$CuSO_4$ with 200 mM SF as the reducing agents. Areas under peaks represent the amount of NO released from each sample by the reducing agents. The green numbers indicate area under peaks. 100 µL of each sample was injected. The similar first and last injections of 10 µM CysNO 100 µL indicates that the reducing agents still possessed similar reducing capability throughout the experiment. The upper graph shows an enlargement of the yellow box.

Due to the unsuccessful NO_2^- signal elimination, the pre-treatment with acidified SF was adopted, regardless of an additional step in measuring SNOs. The final concentration of 0.5 % SF in 0.1 M HCl was used to eliminate NO_2^- (Marley et al., 2000). The 100 µL of NO_2^- concentration at 10 µM was completely removed which is enough for removing NO_2^- from Drosophila samples (Figure 5-8). When this method was used with 100 µL of 10 µM CysNO, the un-reacted NO_2^- was eliminated leaving only NO from CysNO to be detected by the machine. According to our data, the CysNO synthesis by mixing equimolar Cys and $NaNO_2$ in strong acid (Gaston et al., 1993) produced 82.23 ± 2.44 % (a mean ± SD from seven measurements using the same reducing agents and CysNO solution). This experiment also revealedthe high reducing capability of acetic/KI/$CuSO_4$ which was able to withstand 15 time injections of 10 µM CysNO 100 µL without any clear loss of detection ability (Figure 5-8).

The pre-treatment with acidified SF was used with adult Drosophila. In all experiments, flies were ground in 600 µL extraction buffer (50 mM NaPi Buffer at pH 7.5, 2 mM EDTA, 0.1 mM neocuproine and 1 %wt/v SDS). 500 µL of supernatant was collected. If SF treatment was required, the 500 µL supernatant was treated with 100 µL of 3 %wt/v SF in 0.6 M HCl (for measuring XNOs, 30 mM $HgCl_2$ was added together with SF in HCl) to make the final concentration 0.5 %wt/v SF in 0.1 M HCl (5 mM $HgCl_2$). The required volume of the SF-treated fly extract (the maximum of 500 µL) was injected into the reaction chamber.

Acetic/KI/$CuSO_4$ was used to measure SNOs from adult fly extracts with or without the SF pretreatment. Without the SF pretreatment, the protein extract of 5 flies had an area under graph of 770.1 mVolt.min which presumably comprised NO_2^-, SNOs and XNOs. However when the same amount of protein with the SF pretreatment was measured, no signal was detected indicating that the signal from 5 flies without the SF pretreatment was entirely NO_2^- contamination. Although the amount of protein was increased to 500 µL of 15 flies, still no signal was detected. The loss of signal was not due to the loss of reducing capability, because the pre- and post-injection of 10 µM $NaNO_2$ exhibit the equal area under peaks (Figure 5-9).

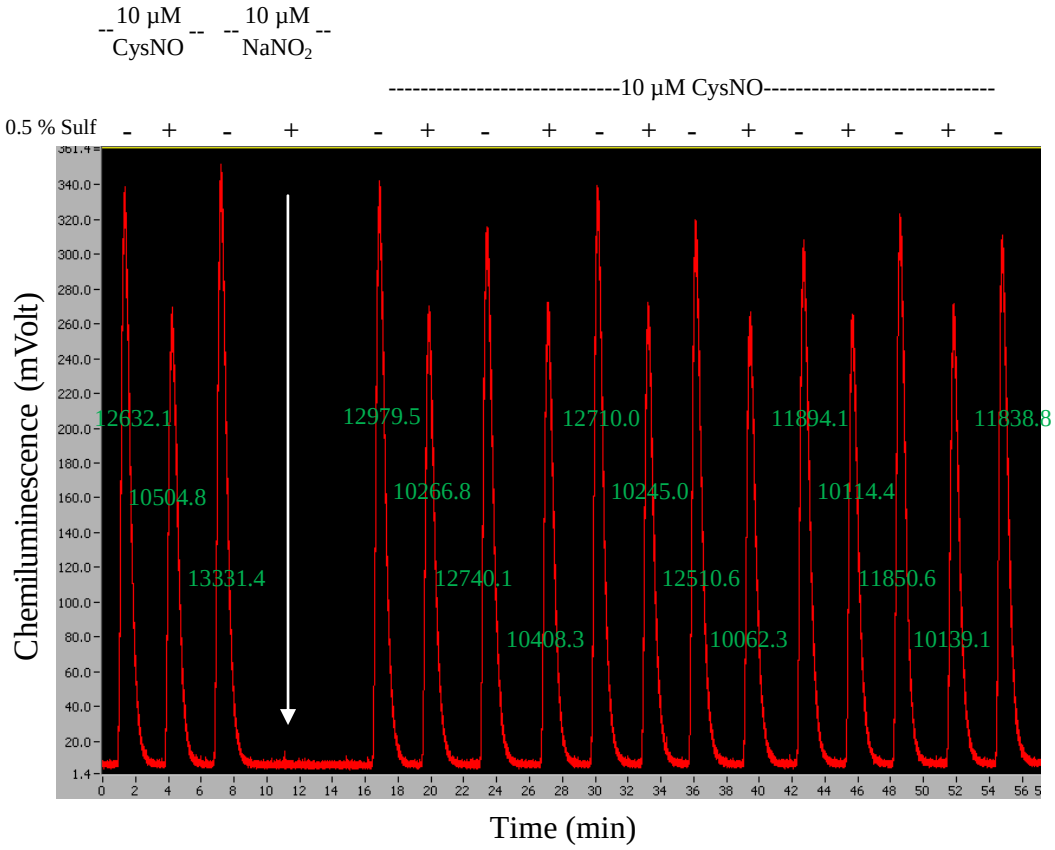

Figure 5-8. The chemiluminescence signal generated by CysNO, $NaNO_2$ and $NaNO_3$ using 10 mL of acetic/KI/$CuSO_4$ as the reducing agents. Area under the peak represents the amount of NO released from each sample by reducing agents. The green numbers indicate area under peaks. 100 µL of each sample was injected. The similar first and last injections of 10 µM CysNO 100 µL indicates that the reducing agents still possessed similar reducing capability throughout the experiment.

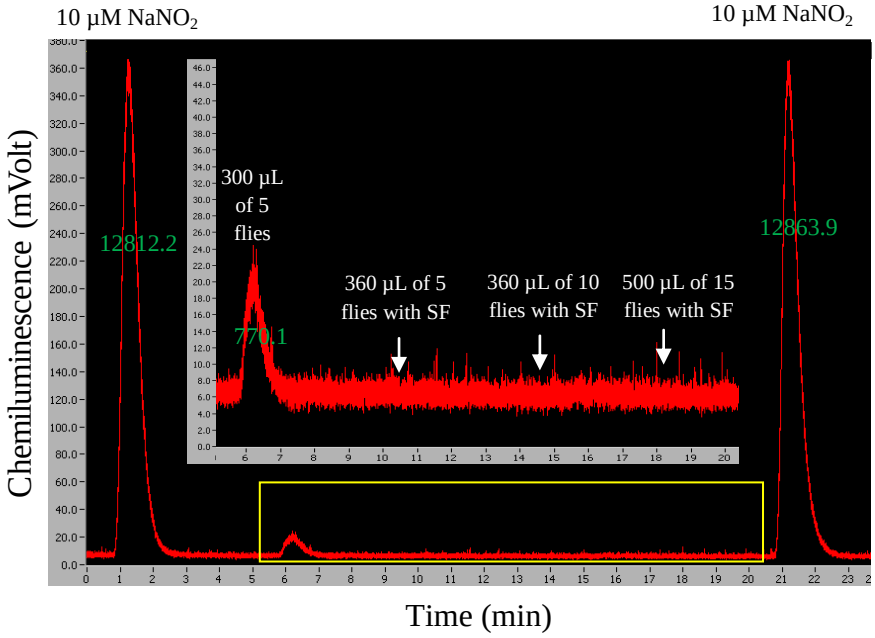

Figure 5-9. The chemiluminescence signal generated by Drosophila protein extracts using 10 mL of acetic/KI/$CuSO_4$ as the reducing agents. Area under peak represents the amount of NO released from each sample by reducing agents. The green numbers indicate area under peaks. Files were ground in 600 µL of the extraction buffer (50 mM NaPi Buffer at pH 7.5, 2 mM EDTA, 0.1 mM neocuproine and 1 %wt/v SDS). The similar first and last injections of 100 µL 10 µM $NaNO_2$ indicates that the reducing agent maintained it reducing capability throughout the experiment.

5.4 Tween-20 prevents protein aggregation from SF pretreatment.

We tried to increase the amount of protein injected by increasing the number of adult flies. When the number was increased to 100 flies, we observed protein aggregation after the SF pretreatment. This effect is possibly because the strong acid HCl used in the SF pretreatment denatures protein and causes the aggregation. To circumvent the problem, we performed a small scale experiment with chemicals previously shown to promote protein solubility (Neagu et al., 2001; Bondos and Bicknell, 2003). The chemicals tested were divided into 1) kosmotropes: sodium sulfate (Na_2SO_4) and NaCl 2) chaotropes: LiCl and RbCl 3) polyhydric alcohols: glycerol 4) detergent: Tween-20. Tween-20 was the only additive that was able to prevent protein aggregation. Although the mixture between glycerol, LiCl, NaCl and RbCl was not able to prevent the aggregation, the mixture produced fine particles of proteins which is compatible with injection (Figure 5-10).

With the addition of Tween-20 to the extraction buffer, the high protein concentration samples were able to be measured. The amount of SNOs and XNOs is extremely low compared with the amount of NO_2^- (the volume of sample with the SF-pretreatment were 10 time larger than samples without the SF-pretreatment) (Figure 5-11).

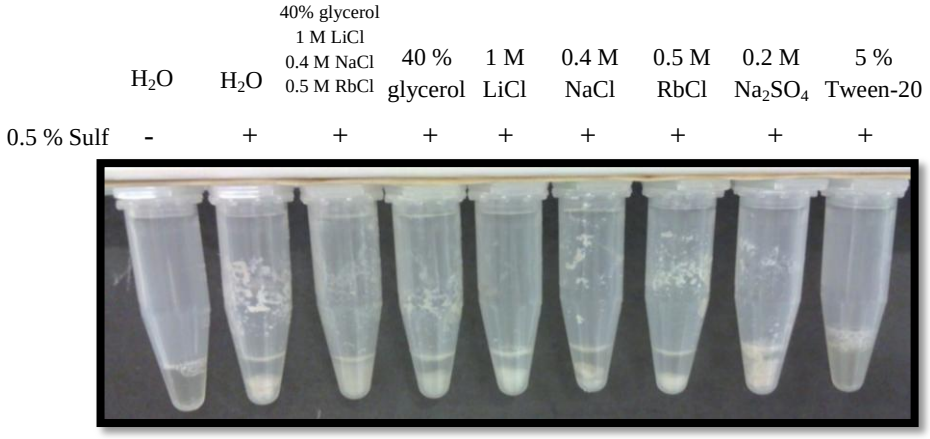

Figure 5-10. The effect of chemical addition in the solubility of high concentration proteins after the SF treatment. Protein aggregation is observed by white precipitate at the bottom of the microcentrifuge tubes. 100 µL of 100 flies extracted in 600 µL of the extraction buffer (NaPi Buffer pH 7.5, EDTA, neocuproine and SDS) with the chemical indicated above was used in each reaction.

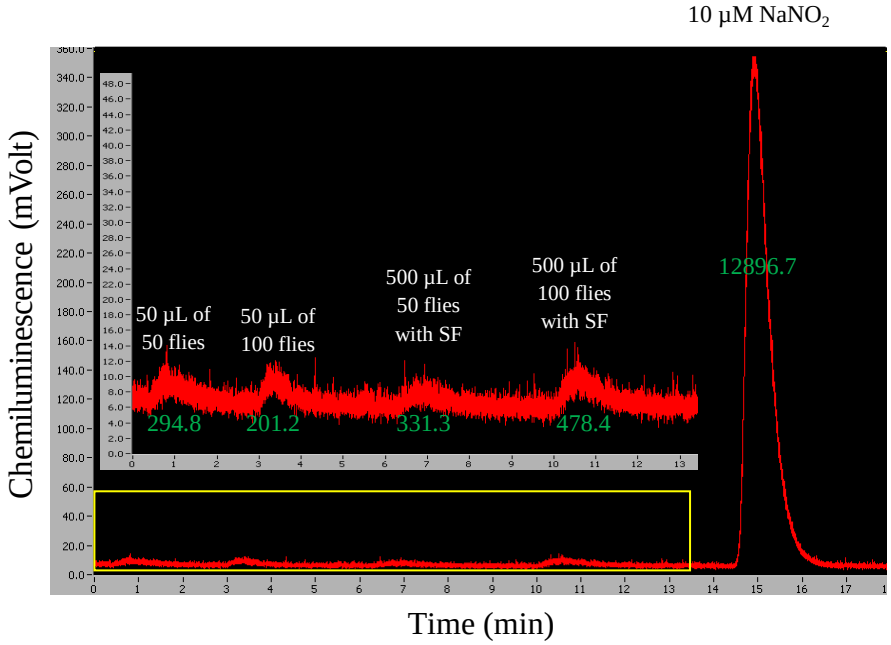

Figure 5-11. The chemiluminescence signal generated by Drosophila protein extract using 10 mL of acetic/KI/$CuSO_4$ as the reducing agents. Area under peak represents the amount of NO released from each sample by reducing agents. The green numbers indicate area under peaks. 50 or 100 files were ground in 600 µL of the extraction buffer (NaPi Buffer pH 7.5, EDTA, neocuproine, SDS and Tween-20). Each sample was divided into 50 µL for measuring without SF treatment and 500 µL for measuring with SF treatment. The last injections of 100 µL 10 µM $NaNO_2$ indicates that the reducing agents still have a reducing capability after the Drosophila SNO measurement.

The individual NO_2^-, SNOs and XNOs can be measured using the acetic/KI/$CuSO_4$ method by three different measurements which are 1) without the SF pretreatment [-], 2) with the SF pretreatment [SF], and 3) with the SF and $HgCl_2$ pretreatment [SF, Hg]. The amount of NO_2^-, SNOs and XNOs was calculated by Equation 15, 16 and 17, respectively. The amount of NO_2^-, SNOs and XNOs of OR adult flies was calculated by [-], [SF] and [SF, Hg] measurements. With similar amount of protein at 500 µL of 100 OR flies, [-] measurement has an area of 1483.85 mVolt.min (160 µL equals 192 µL when compared with [SF] and [SF, Hg]). [SF] and [SF, Hg] have an area of 653.0 and 455.9 mVolt.min, respectively (Figure 5-12). According to Equation 15, 16 and 17, the signal from NO_2^-, SNOs and XNO are 830.85 mVolt.min (57.74 %), 197.1 mVolt.min (13.28 %) and 455.9 mVolt.min (30.72 %), respectively.

$$[NO_2^-] = [-] - [SF] \quad \text{(Equation 15)}$$

$$[SNOs] = [SF] - [SF, Hg] \quad \text{(Equation 16)}$$

$$[XNOs] = [SF, Hg] \quad \text{(Equation 17)}$$

5.5 Potassium ferricyanide ($K_3[Fe(CN)_6]$) can stabilize SNOs.

Because SNOs are a labile protein modification, $K_3[Fe(CN)_6]$ which has been previously shown to preserve SNOs (Mani et al., 2006) was added to the extraction buffer. $K_3[Fe(CN)_6]$ has been proposed to oxidize ferrous-containing proteins, such as deoxyheme-containing proteins which are able to induce transnitrosylation from SNOs to form iron-nitrosyls, to ferri-containing proteins. By the oxidation of ferrous proteins, this process enhances the stability of SNOs (Mani et al., 2006). Addition of $K_3[Fe(CN)_6]$, increased the SNO level by almost 25 % compared to the level without $K_3[Fe(CN)_6]$ (Figure 5-13). The addition of $K_3[Fe(CN)_6]$ did not alter the XNO detection. The level of XNOs was 63 % of the level of SNO and XNO combined (Figure 5-13) which is similar to the level of 69.82 % seen in the previous experiment (Figure 5-12). NEM was also added to the extraction buffer to block free thiols and prevent SNO generation after extraction.

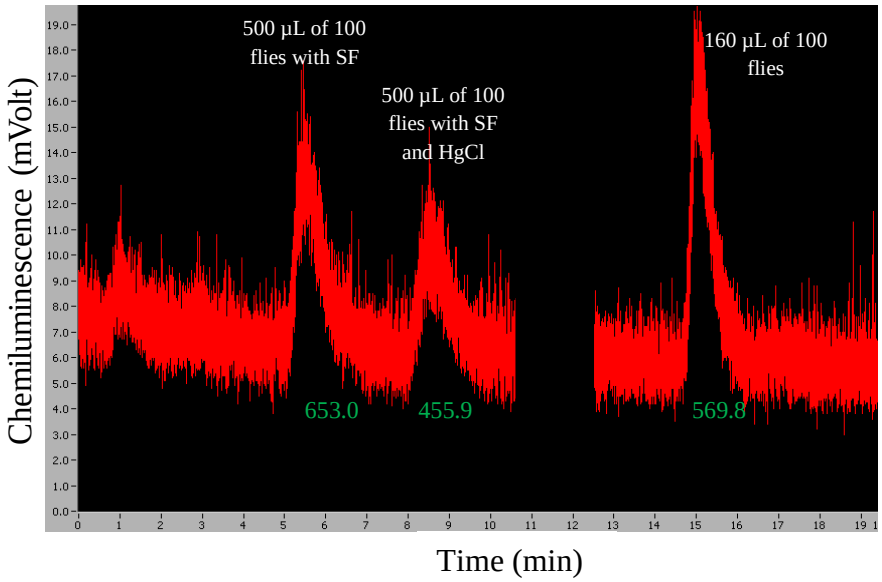

Figure 5-12. The chemiluminescence signal generated from Drosophila protein extracts with SF treatment, with SF and $HgCl_2$ treatment, and without SF treatment. 100 flies ground in 600 µL of the extraction buffer (NaPi Buffer pH 7.5, EDTA, neocuproine, SDS and Tween-20) were used to make the protein extracts. 10 mL of acetic/KI/$CuSO_4$ was used as the reducing agent. A different injection volume (160 µL) was used in the sample without the SF treatment. Area under peak represents the amount of NO released from each sample by the reducing agents. The green numbers indicate area under peaks.

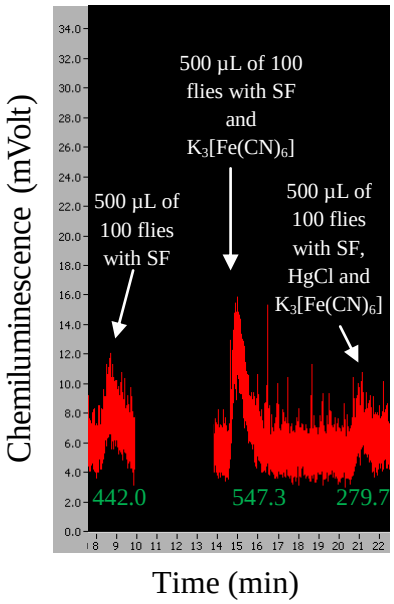

Figure 5-13. The chemiluminescence signal generated from 100 flies were ground in 600 µL of the extraction buffer (NaPi Buffer pH 7.5, EDTA, neocuproine, SDS and Tween-20) with or without $K_3[Fe(CN)_6]$. Drosophila protein extracts were treated with SF or with SF and $HgCl_2$. 500 µL of each sample was injected. 10 mL of acetic/KI/$CuSO_4$ was used as the reducing agent. Area under peak represents the amount of NO released from each sample by reducing agents. The green numbers indicate area under peaks.

5.6 KI and I_2 reducing agents (tri-iodide) with the addition of $K_3[Fe(CN)_6]$ provides better reducing ability.

The final adjustment was performed to the reducing agents. Tri-iodide reducing agents were used instead of acetic/KI/$CuSO_4$ to generate I_3^-. This is because in acetic/KI/$CuSO_4$ I_2 formation is variable depending on the reaction with NO_2^- (Equation 14) (Pinder et al., 2008). Because the amount of I_2 affects the I_3^- formation which is the actual reducing agent (Equation 11), there is variation in the reducing ability in acetic/KI/$CuSO_4$. Tri-iodide has been found to produce more reliable data because of I_2 is directly added to the solution (Pinder et al., 2008).

We added $K_3[Fe(CN)_6]$ to the reducing agent to prevent auto-capturing of NO by ferrous proteins. Anti-foaming agent was also added to prevent foam generate from the high concentration of proteins and Tween-20. The tri-iodide with $K_3[Fe(CN)_6]$ was tested with the extracts of 100 adult flies with SF-pretreatment. We observed an increase in the SNO level and a decrease in background signal. We also tested the extraction of 100 flies by using the conventional buffer (KPi buffer pH 6.5 and protease inhibitors). The novel method that we have developed clearly enhanced the stability of SNOs from adult Drosophila extracts resulting in the higher level of SNO detection (Figure 5-14).

In summary, about 100 flies were ground in the extraction buffer (the components are listed in Table 5-1) avoiding exposure to direct light. Debris was spun down and supernatant was either directly used to measure a NO_2^- level or pre-treated with SF, or SF and Hg, to measure SNO and/or XNO levels. The supernatant was injected into the reaction chamber loaded with the reducing agent (the components are listed in Table 5-2). The area under the peak, which represents NO release from samples, was compared to a standard curve generated by injecting different concentrations of NO_2^- solution. After adjusting for the dilution factors the amount of NO, in moles, released from each sample was calculated and then related to the total protein quantified by the Bradford assay.

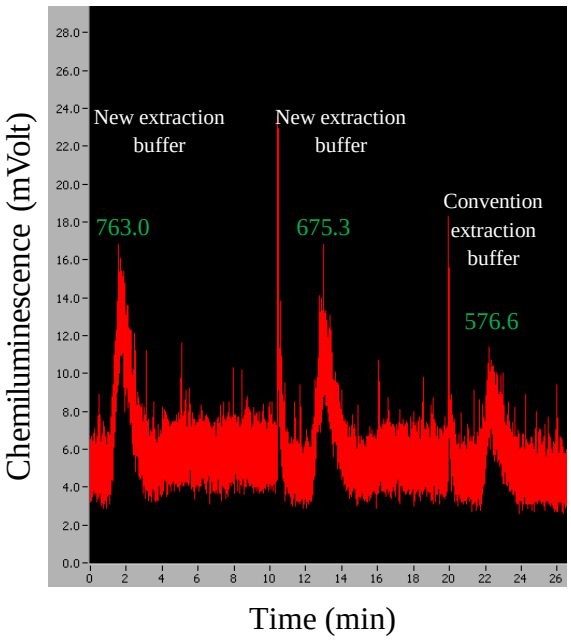

Figure 5-14. The chemiluminescence signal generated from 500 µL of 100 flies extracted in 600 µL of the newly developed extraction buffer (NaPi buffer pH 7.5, EDTA, neocuproine, SDS, Tween-20 and $K_3[Fe(CN)_6]$) or the conventional extraction buffer (KPi buffer pH 6.5 and protease inhibitors). Drosophila protein extracts were treated with SF. 10 mL of tri-iodide was used as the reducing agent. The reducing agent was changed every time after sample injection. Area under peak represents the amount of NO released from each sample by the reducing agents. The green numbers indicate area under peaks.

Table 5-1. The components of the newly developed extraction buffer.

Final concentrations	Chemicals
50 mM	NaPi Buffer pH 7.5
2 mM	EDTA pH 7.5
0.1 mM	Neocuproine
1 % w/v	SDS
5 mM	NEM
5 % v/v	Tween-20
4 mM	$K_3[Fe(CN)_6]$
	HPLC grade water

Table 5-2. The components of the newly developed reducing solution.

Final concentrations	Chemicals
10 mg/mL	KI
6.5 mg/mL	I_2
1:500 dilution	Anti-foaming agent for NOA
25 mM	$K_3[Fe(CN)_6]$
70 % v/v	Acetic acid
	HPLC grade water

This new method for detecting the total SNO level was utilized for measuring the SNO level of the *gsnor* knockout line which due to the loss of GSNOR function might show increases in the total level of SNOs. The total level of SNO (area under graph (mVolt.min)) was compared with the $NaNO_2$ standard in order to obtain moles of NO released from injected SNOs, and then divided by the mg of protein obtained from the Bradford protein quantification.

5.7 *gsnor* flies have similar *S*-nitrosylation level to wild-type.

In Arabidopsis, the total SNO level is elevated in a loss-of-function mutation of *gsnor*. This effect is enhanced by infection. In contrast, GSNOR overexpression lowers the total SNO level (Feechan et al., 2005). The total SNO level of *Df7305*/*Df7306* was examined to investigate whether or not the same is true in Drosophila.

The total SNO level was retested by the newly developed technique to ensure that the new technique gives a consistent result. The ozone-chemiluminescence based assay using tri-iodide as reducing agents with the SF pretreatment with and without $HgCl_2$ were used for measuring SNO and XNO levels of *Pst* infected Arabidopsis leaves extracted by the conventional extraction buffer described in Feechan et al. (2005). The *Pst* infected leaves of wild type, *gsnor* knockout (*gsnor1-3*) and GSNOR overexpression (*gsnor1-1*) were ground in the conventional buffer. The supernatant was divided into two identical groups. The first group was treated with only SF and the second group was treated with SF and $HgCl_2$ before injection into the reaction chamber with tri-iodide solution. Bradford protein quantification assay was performed to measure the total protein injected in order to calculate moles of NO released from SNOs or XNOs per mg protein. Both groups gave similar signals indicating that only XNOs were present. We think that because the protein extraction process was performed by using the conventional extraction buffer without the chelating agents, SDS and $K_3[Fe(CN)_6]$; SNOs were lost during the measurement process. Nonetheless, we think that XNO level might be the same trend as SNO levels. We could not observe the difference when comparing XNO levels of *gsnor1-3* or *gsnor1-1* with wild type. However, there might be different XNO levels in *gsnor1-3* and *gsnor1-1* (Figure 5-15 and 5-16).

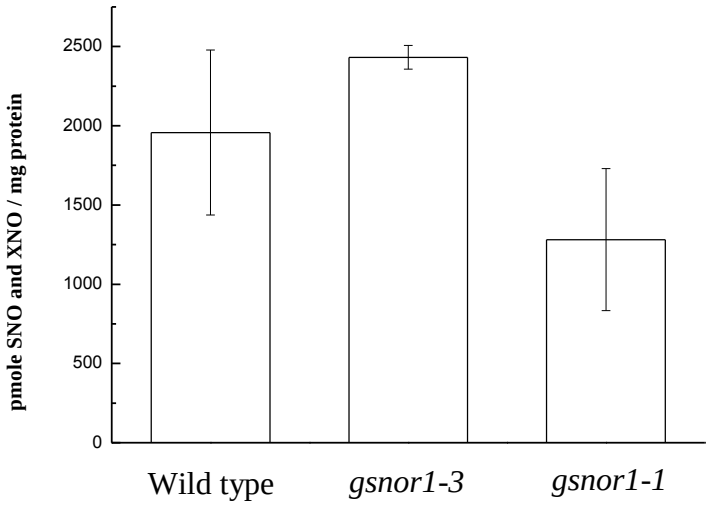

Figure 5-15. SNO and XNO levels of wild type, *gsnor1-3* and *gsnor1-1* Arabidopsis with *Pst* infection for 48 hours. The infected leaves were extracted in the conventional buffer. The ozone-chemiluminescence based assay using tri-iodide as reducing agents with the SF pretreatment (without $HgCl_2$) was performed. The SNO and XNO level (pmole per volume injected) was calibrated and the protein concentration (mg protein per volume) measured by Bradford protein quantification in order to obtain pmole SNO and XNO per mg protein. The values represented are the mean of two independent experiments (±SE).

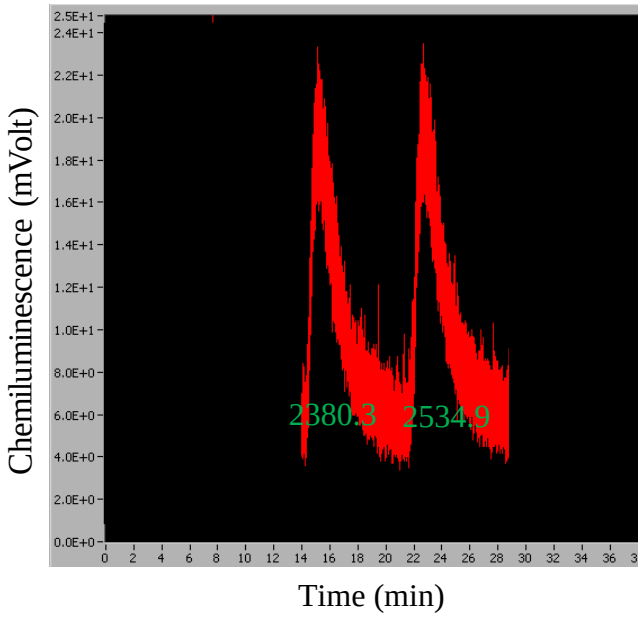

Figure 5-16. Raw data from NOA showing the level of a combination of SNO and XNO level (the first peak) and only XNO level (the second peak) from the similar *gsnor1-3* leaf sample infected with *pst* for 48 hours. The infected leaves were extracted in the conventional buffer. The ozone-chemiluminescence based assay using tri-iodide as reducing agents with the SF pretreatment (without $HgCl_2$) was performed. The area under graph (the numbers) represents the level of SNO and XNO level (the first peak) and only XNO level (the second peak).

The total SNO and XNO level was measured in Drosophila by the newly developed ozone-chemiluminescence based assay using tri-iodide as reducing agents with the SF pretreatment (without $HgCl_2$) was performed. Bradford protein quantification assay was performed to measure the total protein injected in order to calculate pmole SNO and XNO per mg protein. In uninfected flies, the total SNO and XNO levels of OR and *Df7305*/*Df7306* are similar at approximately 3.5 pmole/mg protein which is lower than XNO alone in infected wild-type Arabidopsis (approximately 2000 pmole/mg protein) (Figure 5-15 and 5-17). Then, an infection might be required to observe a difference between OR and *Df7305*/*Df7306* SNO and XNO levels. A time-course experiment was then carried out to determine the time at which OR infected with *B. bassiana* exhibits a significant change in the total SNO and XNO level. No significant difference in XNO and SNO level was seen at any time after infection (Figure 5-18). We thought that possibly the spores from the infection might germinate asynchronously leading to a less robust effect on a change in SNO and XNO level. A new approach was performed using gram-positive bacteria to ensure that the defence response is triggered at the same time in *Df7305*/*Df7306*. A reduction of SNOs and XNOs was observed 15 minutes after the infection with *Micrococcus luteus* that gradually increased back to the normal level within 24 hours. OR was then tested at 15 minutes after the *M. luteus* infection; however, we did not observe a significant difference between OR and *Df7305*/*Df7306* at 15 minutes after the infection (Figure 5-19). Possibly, GSNOR does not function in the total SNO regulation, but may function by regulating specific target proteins.

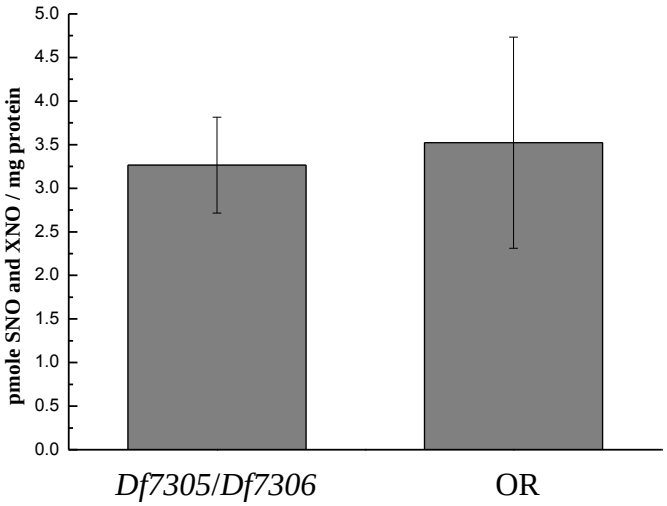

Figure 5-17. SNO and XNO level of OR and *Df7305*/*Df7306* at non-infected condition. Flies were extracted in the newly developed extraction buffer. The ozone-chemiluminescence based assay using tri-iodide as reducing agents with the SF pretreatment (without $HgCl_2$) was performed. The SNO and XNO level (pmole per volume injected) was calibrated with protein concentration (mg protein per volume) measured by the Bradford protein quantification in order to obtain pmole SNO and XNO per mg protein. The values represented are the mean of three independent experiments (±SE).

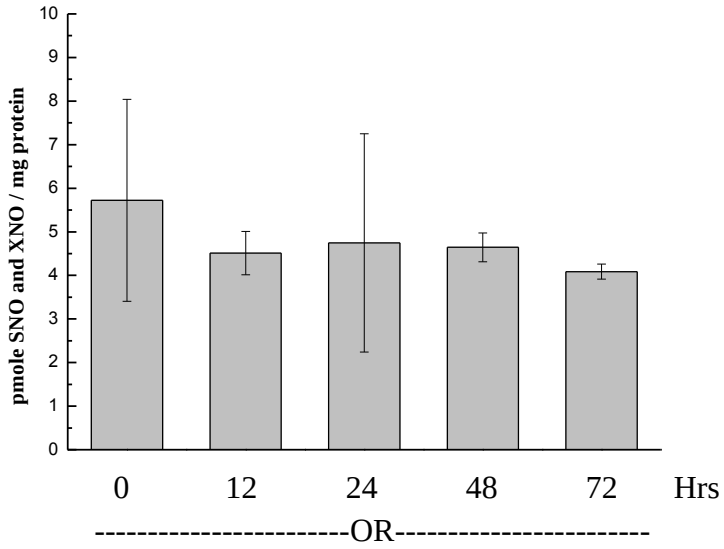

Figure 5-18. SNO and XNO level of OR naturally infected with *B. bassiana* 0 (non-infection), 12, 24, 48 and 72 hours after the infection. Flies were extracted in the newly developed extraction buffer. The ozone-chemiluminescence based assay using tri-iodide as reducing agents with the SF pretreatment (without $HgCl_2$) was performed. The SNO and XNO level (pmole per volume injected) was calibrated with protein concentration (mg protein per volume) measured by the Bradford protein quantification in order to obtain pmole SNO and XNO per mg protein. The values represented are the mean of two independent experiments (±SE).

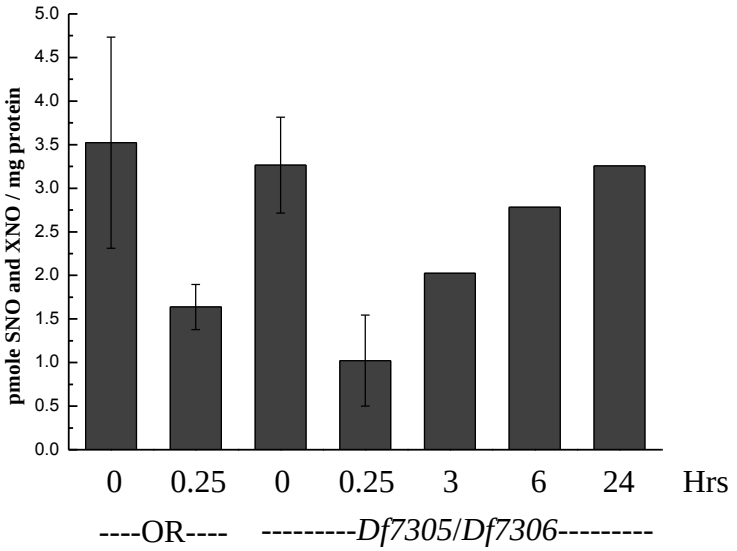

Figure 5-19. SNO and XNO level of OR with a septic *M. luteus* infection at 0 and 15 minutes after the infection, and *Df7305*/*Df7306* with a septic *M. luteus* infection at 0, 15 minutes, 3 hours, 6 hours and 24 hours after the infection. The ozone-chemiluminescence based assay using tri-iodide as reducing agents with the SF pretreatment (without $HgCl_2$) was performed. The SNO and XNO level (pmole per volume injected) was calibrated with protein concentration (mg protein per volume) measured by the Bradford protein quantification in order to obtain pmole SNO and XNO per mg protein. The values at 0 and 15 minutes for OR and *Df7305*/*Df7306* are the mean of two independent experiments (±SE). Only one experiment was done for *Df7305*/*Df7306* at 3, 6 and 24 hours after the infection.

Another approach for detecting a total SNO level was performed by an *in vivo* BST in order to confirm the effect observed by the chemiluminescence method. Instead of detecting individual proteins by Western blot, silver staining was performed to visualize all pulled-down proteins (potential *S*-nitrosylated targets) loaded onto a SDS-PAGE. No significant difference in the number or intensity of bands was seen 24 hour after *B. bassiana* infection when comparing a UV-treated negative control, OR, *Df7305*/*TM6B*, *Df7306*/*TM6B*, *Df7305*/*Df7306*, and *act5c*:*UAS-gsnor*; *Df7305*/*Df7306* (Figure 5-20). This suggests that GSNOR does not function in the regulation of the total SNO level. Also the SNO level in Drosophila is very low (Figure 5-20), so the bands seen could be proteins that bind to the agarose beads and cannot be removed efficiently during washing steps.

5.8 Conclusion

We tried to adopt the chemiluminescence-based method for measuring SNOs in Arabidopsis. The method used in Arabidopsis was unable to detect SNO level in Drosophila due to the weak basic buffer in the Drosophila extraction solution. The basic pH decreases the reducing capability of the CuCl/Cys reducing agents. Another problem is that the CuCl/Cys can detect NO_2^- with the same efficiency as CysNO. We tested many methods to abolish NO_2^- signal contamination. CuCl/Cys with 1 % SF, CuCl/Ascorbic acid, CuCl/Ascorbic acid with 1 % SF, and acetic/KI/$CuSO_4$ with 200 mM SF were not able to eliminate the NO_2^- contamination. We then used the SF pretreatment to eliminate NO_2^- instead of adding SF directly to reducing agents. Pretreatment with SF before reducing SNOs with acetic/KI/$CuSO_4$ was able to abolish NO_2^- signal contamination, gave a reproducible signal, and has high reducing capability.

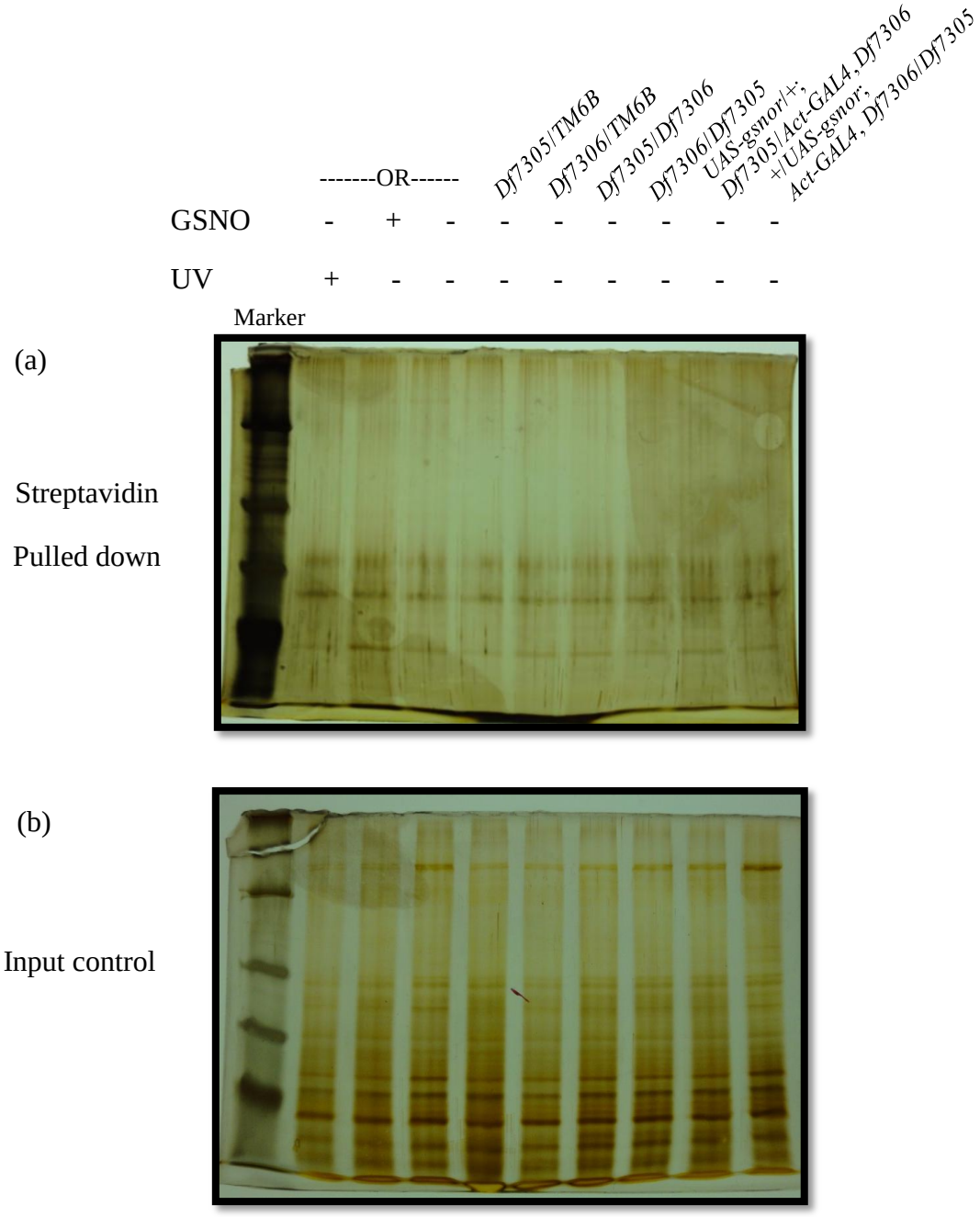

Figure 5-20. (**a**) The total *S*-nitrosylation level measured by BST followed by silver staining. The number and intensity of bands compared with (**b**) the input control indicate the total *S*-nitrosylation level. Each sample is from flies 24 hours after infection with *B. bassiana*. UV-treated protein extract from OR was used as a negative control. GSNO-treated protein extract from OR was used as a positive control.

The SNOs from biological samples were tested. We found that the SNO level in Drosophila is very low, so a high concentration of proteins in samples was measured. However, after SF treatment, the high concentration of protein became denatured and aggregated. The chemicals which have been previously proposed to enhance protein solubility were added to the extraction solution. 5 % Tween-20 was able to prevent protein aggregation after the SF treatment. The addition of $K_3[Fe(CN)_6]$ was able to preserve SNOs in Drosophila protein extracts. We have confirmed that our novel Drosophila SNO measurement method is sensitive and reliable.

The newly developed method was used to measure the total SNO level of wild-type OR and *gsnor* knockout *Df7305*/*Df7306*. We were not able to detect any difference in the total SNO level between non-infected OR and *Df7305*/*Df7306* flies. The time after *B. bassiana* infection was varied in OR; however, there was no difference in SNO level at 0, 12, 24, 48 and 72 hours after infection. A different type of pathogen *M. luteus* was used to infect Drosophila by the septic injury technique. We found that the SNO level of *Df7305*/*Df7306* decreased at 15 minutes after the infection, and then the SNO level gradually increased to the normal level within 24 hours. The SNO level of OR at 15 min after *M. luteus* infection also decreased to about the same level as *Df7305*/*Df7306*. The sensitivity in the SNO response to infection of wild-type and *gsnor* knockout Drosophila may be because our method of NO detection is not sensitive enough to see a difference or because GSNOR does not regulate global SNO level upon infection.

Chapter 6 A Conserved Function of GSNOR in Immunity between Arabidopsis and Drosophila

6.1 Introduction

Drosophila, unlike mammals, lacks adaptive immune responses. They rely on innate immunity to protect themselves from invading pathogens. Innate immunity can be briefly categorized into humoral and cellular defence responses. Both humoral and cellular defence responses work systemically to protect Drosophila from pathogens (Nehme et al., 2011).

6.1.1 Cellular immunity

A Drosophila body is filled with free-circulating and sessile haemocytes. The haemocytes establish cellular defence responses. There are three types of haemocytes: plasmatocytes, lamellocytes and cystal cells (Figure 6-1).

6.1.1.1 Haemocytes

Drosophila haematopoiesis can be divided into two phases: 1) haematopoietic development which starts from the embryonic head mesoderm during embryonic development and 2) the lymph gland released haemocytes. Embryonic haematopoiesis establishes mature circulating haemocytes and the lymph gland haemocytes which reside in the lymph gland in non-immune challenged larvae. When metamorphosis begins, the lymph gland releases a number of plasmatocytes to phagocytose tissue which is unnecessary for adult flies. In adult Drosophila, the lymph gland is empty and no differentiation observed (Lemaitre and Hoffmann, 2007; Grigorian et al., 2011) (Figure 6-1).

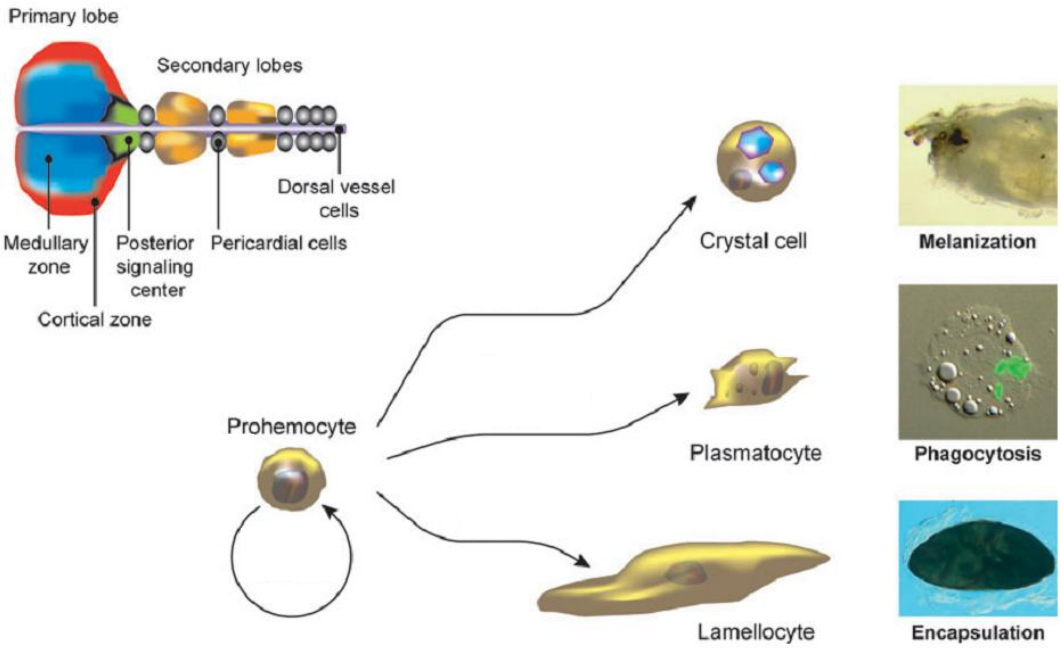

Figure 6-1. Drosophila cellular immunity. The lymph gland that is next to the dorsal aorta contains a large number of prohaemocytes. Its structure is compartmentialized into a medullary zone containing haemocyte precursors, a cortical zone where haemocytes differentiate, a posterior signalling center which acts as an organizer, and the secondary lobes for prohaemocyte storage (shown in the top left figure). Prohaemocytes differentiate into crystal cells for melanization, plasmatocytes for phagocytosis, and lamellocytes for encapsulation. Adapted from Lemaitre and Hoffmann (2007)

6.1.1.2 Phagocytosis

Phagocytosis is a process for removing dead cells and microorganisms. Plasmatocytes which contribute 90-95 % of the total haemocytes are mainly responsible for phagocytosis. The process of phagocytosis begins with the attachment of targets to plasmatocytes by several receptor proteins causing cytoskeleton change, internalization and destruction of the phagocytosed targets (Lemaitre and Hoffmann, 2007). Efficient phagocytosis is assisted by an opsonization mechanism. There are six TEP proteins which have homology with complement alpha2-macroglobulin family. Three of them are induced upon infections (Lagueux et al., 2000).

6.1.1.3 Encapsulation

Encapsulation is mediated by lamellocytes. In healthy Drosophila, lamellocytes are only found in larval stages with the low number of cells. If Drosophila larvae are infected with parasitoid wasps, a large number of lamellocytes can be produced by the lymph gland. After eggs from parasitoid wasps have been laid into larvae, lamellocytes surround the eggs and form multilayer capsules. Melanization of the encapsulated eggs is also observed by the black colour of the encapsulated eggs. The wasp eggs are potentially killed by the by-product ROS generated from melanization process (Nappi et al., 1995; Lemaitre and Hoffmann, 2007).

6.1.1.4 Melanization

Melanization is the process of rapidly producing melanin at sites of wounding or on the surface of parasites in the haemocoel. This contains invading pathogens, physically protects insects from penetration of fungal pathogens, and facilitates wound healing and encapsulation. The main enzyme for melanization is phenol oxidase (PO) which catalyzes phenols to quinines which are required for polymerization to melanin. The by-product of PO reaction is ROS which is toxic to invading microbes. In larvae, PO is produced by crystal cells in an inactive form pro-phenol oxidase (ProPO). This inactive form requires serine protease cascade

MP1/MP2 to process ProPO to PO (Cerenius and Söderhäll, 2004; Tang et al., 2006). PO and proteins controlled by Rel transcription factors are required in melanization. Spn77BA and Spn27A, protease inhibitors of the serpin family, were found to be negative regulators of the MP1/MP2 cascade in trachea and in haemolymph, respectively. Interestingly, local melanization at trachea induces the Toll-independent production of Drs (Tang et al., 2006, 2008).

Study of melanization has revealed the connection between local immunity and systemic immunity. After fungal infection, local melanization at trachea promotes a signal that can pass through a tracheal epithelium layer and systemically induce the production of AMPs by fatbody cells. This yet to be discovered signalling molecule could be metabolites from melanization, ROS, or other melanization induced molecules (Tang et al., 2008).

6.1.1.5 Coagulation

Coagulation is generally similar to blood clotting process in mammals. The roles of coagulation are to prevent the loss of haemolymph, wound healing and disease resistance by immobilizing bacteria (Lemaitre and Hoffmann, 2007). Clotting fibers, such as haemolectin, are generated at the wounding site. The fibers are hardened by crosslink-promoting enzymes including PO and transglutaminase (Scherfer et al., 2004; Bidla et al., 2005).

6.1.2 Humoral immunity

Humoral immunity is the immune responses mediated by secreted AMPs for inhibiting invading pathogens. Many cell types can produce AMPs after pathogen induction, such as haemocytes and epithelial cells; however, the production of AMPs is at local areas. The well-established and important local immunity is the gut immunity. Gut immunity is considered to be a crucial defence layer for Drosophila (Lemaitre and Hoffmann, 2007). Rather than AMPs produced locally from gut epithelia, the microbes in Drosophila guts are also controlled by ROS. ROS is produced from dual oxidase (DUOX) protein located at the cell membrane of the gut epithelium (Ha et al., 2009).

The main production for AMP that acts systemically is by fat body cells. The fat body is a chief organ for AMP secretion into haemolymph. These secreted AMPs function systemically in the whole body of flies (Hoffmann and Reichhart, 2002). Both local and systemic immunity employ similar signalling pathways in order to produce and secrete AMPs. There are two major pathways leading to AMP production in Drosophila: the Toll pathway and the Imd pathway.

6.1.2.1 The Toll pathway

The *Toll* gene and other Toll pathway components, *tube*, *pelle*, *cactus*, and the NF-κB homolog *dorsal* were first identified to be involved in dorsal-ventral patterning in Drosophila embryogenesis (Anderson and Nüsslein-Volhard, 1984). The Toll pathway was linked to insect immunity after the role of NF-κB in mammal immunity was discovered (Sun and Faye, 1992). The Toll pathway was then found to be a signalling pathway for immune responses against fungal infection in Drosophila (Lemaitre et al., 1996). Later on this finding encouraged the discovery of, Toll-like receptors (TLRs), the innate immunity receptors, in humans (Valanne et al., 2011).

Unlike mammals, where Toll directly recognizes pathogens, Drosophila Toll recognized only Spz. There must therefore be pathogen recognition receptors (PRRs) locating upstream of Spz (Figure 6-2).

6.1.2.1.1 Pathogen sensing of the Toll pathway

6.1.2.1.1.1 Gram-positive bacteria detection

Peptidoglycan receptor proteins (PGRPs) are conserved in insects and mammals (Kang et al., 1998). In *D. melanogaster* there are 17 PGRPs which can be divided into long (L) and short (S) forms. Long PGRPs are part of the Imd pathway and are predicted to be membrane bound, intercellular and intracellular proteins. Short PGRPs are part of the Toll pathway and are all predicted to be secreted into haemolymph. All PGRPs contain a PGRP conserved domain for peptidoglycan (PGN) recognition and RIP (receptor-interacting protein) homotypic interaction motif (RHIM)-like motif for signalling. However, they have different functions in immunity (Werner et al., 2000; Michel et al., 2001).

By studying a mutant *semmelweis* (*seml*), the haemolymph localized PGRP-SA was the first Toll pathway PRR to be identified (Michel et al., 2001). PGRP-SA has L,D-carboxypeptidase activity for diaminopimelic acid type PGN (DAP-PGN) produced from gram-negative bacteria. It was hypothesized that PGRP-SA may act as a negative regulator of the Imd pathway by degradation of DAP-PGN or as a positive regulator by producing monomeric DAP-PGN for PGRP-LC to recognize and initiate the Imd response (Chang et al., 2004). PGRP-SA binds to both lysine-type PGN (Lys-PGN) from gram-positive and DAP-PGN from gram-negative bacteria with different affinities depending on bacteria species (Wang et al., 2006; Chang et al., 2004).

Gram-negative bacteria binding protein 1 (GNBP-1) binds to only gram-positive bacteria PGN *M. luteus* and *Enterococcus faecalis*, but not for *Staphylococcus aureus*, and *Bacillus subtilis*. GNBP-1 can also hydrolyze *M. luteus* PGN. The presence of both PGRP-SA and GNBP-1 increases the efficiency in hydrolyzing *M. luteus* PGN *in vitro* (Wang et al., 2006). Wang et al. (2006) proposed that PGRP-SA and GNBP1 form 1:1 molar ratio complex. Without PGN, PGRP-SA loosely binds with GNBP1; therefore, no signal is generated. When PGN is presented, it is recognized by the PGRP-SA and GNBP1 complex. Forming this tripartite complex allows PGN to be hydrolyzed faster by GNBP-1. When small-sized hydrolyzed PGN is formed, it binds with a high affinity to PGRP-SA and then induces a conformational change of PGRP-SA allowing it to bind firmly with GNBP1. At this stage, this complex can convey the signal by triggering downstream serine protease cascade.

In contrast, Buchon et al. (2009) proposed that because full-length GNBP1 has no activity *in vitro*, GNBP1 may just play a role as a linker between PGRP-SA and a modular serine protease (Mod-SP).

Mutants in *PGRP-SD* are sensitive to some gram-positive bacteria and increase the sensitivity of *PGRP-SA* and *GNBP1* loss-of-function mutants suggests that PGRP-SD is within the Toll pathway (Bischoff et al., 2004). In order to perceive and exhibit proper Toll responses, PGRP-SA, GNBP1 and PGRP-SD work together as a complex via protein-protein binding providing versatility to PGN recognition.

The utilization of these three components in this complex is different depending on species of bacteria. For example, all three components are required to exhibit proper Toll responses against *Staphylococcus aureus* (Wang et al., 2008). However for *M. luteus* and *S. saprophyticus*, only two components are required in the signalling (PGRP-SA and GNBP1 for *M. luteus*, and PGRP-SD and GNBP1 for *S. saprophyticus*) (Leone et al., 2008; Wang et al., 2008).

6.1.2.1.1.2 Fungal detection

Drosophila fungal receptors were screened from ethylmethane sulfonate (EMS) mutagenesis by Levashina et al. (1999). This screening revealed the negative regulator of Toll pathway Necrotic (Nec). Nec is a serine protease inhibitor of the Serpin family and this mutant can be rescued by expressing the *serpin* gene, *Spn43Ac*. This mutant constitutively expresses the anti-microbial peptides Mtk and Drs which results from up-regulation of the Toll pathway. *Nec* mutants also exhibit a constitutively high level of melanization. A few years later Ligoxygakis et al. (2002) did an EMS mutagenesis screen to search for suppressors of the Nec phenotype. This identified mutations in *persephone* (*psh*). These rescue the necrotic phenotype of Nec mutants and block the Toll signaling pathway. From epistasis studies, Ligoxygakis et al. (2002) concluded that Psh is located upstream of *Spz*, and from fungal infection assays that Psh is necessary for Drosophila to combat fungal pathogens. Psh is a haemolymph serine protease with a CLIP-prodomain, a disulfide-knotted region for protein-protein interaction, on the N-terminus. Serine proteases can be organized in a cascade. Initially, the proteases are produced as inactive zymogens with an N-terminal prodomain and a C-terminal catalytic site. Activation requires upstream proteolytic cleavage by proteases (Krem and Di Cera, 2002). However, the predicted Psh structure does not suggest that it has a fungal cell wall binding property; therefore, there were possibly undiscovered fungal receptors.

D. melanogaster GNBP proteins are good candidates as a fungal receptor protein, because they are members of GNBP/ β-glucan recognition proteins (βGRP) family. There are three GNBPs in Drosophila: GNBP1, GNBP2 and GNBP3 (Kim et al., 2000), and of these, GNBP3 has the highest similarity to lepidopteran β-(1,3)-glucan recognition proteins. GNBP3 has been therefore tested and shown to bind *in*

vitro with β-(1,3)-glucan of fungal cell walls. Moreover, GNBP3 also triggers the Toll pathway by the activation of Spz and is required for resistance against fungal infections. This supports the idea that GNBP3 is the receptor for fungal recognition (Gottar et al., 2006; Mishima et al., 2009).

However, epistasis analysis of Psh and GNBP3 indicated that they are not in the same signalling pathway, even though they both induce the activation of Spz and downstream Toll responses. This raises a question "What is the Psh-dependent pathway for?" Entomopathogenic hyphomycete fungi have been shown to secrete proteases and chitinases to digest insect's protective exoskeleton allowing them to penetrate into the insect body cavity (Clarkson and Charnley, 1996). The insect fungal pathogens *B. bassiana* and *M. anisopliae* produce PR1 subtilisins (a subclass of serine protease), from appressorium structures that quickly degrade protein in the cuticle, while they try to penetrate into a cuticle layer (Bagga et al., 2004). Gottar et al. (2006) have found that PR1 subtilisins can initiate Toll signalling resulting in Drs production, and this signal can be blocked by the loss-of-function *Psh*. Furthermore, PR1 subtilisins can directly cleave Psh *in vitro*. These results indicate that Psh plays a role in sensing the fungal virulence factor PR1. Psh is pivotal to fight against insect fungal *B. bassiana*. Without functioning Psh, *D. melanogaster* is sensitive to fungal infection because AMP production is compromised, even though there is still GNBP3 to sense the fungal cell wall. This phenomenon suggests that *B. bassiana* has evolved an inhibitor(s) targeting GNBP3 (Gottar et al., 2006).

Psh can also sense proteases or gram-positive bacterial virulence factors from virulent gram-positive bacteria, such as *B. subtilis* and *E. faecalis* (Chamy et al., 2008).

6.1.2.1.2 Spaetzle activation by serine protease cascades

After pathogen recognition, the signal is amplified by serine protease cascades. Starting with ModSP, it integrates the signals from GNBP3, and the PGRP-SA and GNBP1. Because on its own ModSP has high autoproteolytic activity *in vitro*, in order to convey signals these receptors recruit ModSP to create a high local concentration and enhance its autoactivation ability carrying on the signals to Grass.

Interestingly, ModSP does not directly cleave Grass, another serine protease which was identified to respond to gram-positive bacteria and fungi, so presumably there are other components involved with Glass proteolytic cleavage (Chamy et al., 2008; Buchon et al., 2009). There are four other serine proteases: Spirit, Spheroide, and Sphinx1/2 which were found to be also involved with the responses to gram-positive bacteria and fungi by Toll pathway (Kambris et al., 2006). The signal from Psh also requires Spirit, Spheroide, or Sphinx1/2 to convey Toll signalling, however where exactly these two cascade join together is still unclear (Kambris et al., 2006) (Figure 6-2).

The serine protease cascades end with Spaetzle processing enzyme (SPE) which is required for a Spz cleavage (Jang et al., 2006). Spz is an endogenous cytokine ligand which interacts with Toll receptors on the cell membrane. However, before the interaction occurs, Spz has to be processed by SPE to remove the Spz prodomain that prevents the interact with Toll (Arnot et al., 2010). Interestingly after the removal of the Spz prodomain, which is pivotal for Spz secretion and folding, this prodomain still attaches to processed Spz until the binding of this complex to Toll receptors. It has been proposed that, after the binding between Toll and Spz, the Spz prodomain is released (Figure 6-2) and then acts as a negative regulator of Toll signalling by inhibiting the upstream protease cascades (Weber et al., 2007).

6.1.2.1.3 The core of Toll signalling

After Spz binds to Toll receptors, Toll passes the signal through the Toll and interleukin-1 receptor (TIR)-domain and death-domain containing adapter protein dMyD88, death-domain containing protein (two distinct surfaces) Tube, and death-domain containing kinase Pelle (Figure 6-2).

dMyD88 at normal cellular conditions binds to phosphatidylinositol bisphosphate or phosphatidylinositol phosphate, the phospholipid components of the plasma membrane, with C-terminal extension (CTE). This binding interaction translocates this protein to the cell membrane where Toll resides. Because dMyD88 also binds with Tube through interaction of the death-domain of both proteins, Tube is brought to the plasma membrane together with dMyD88 (Marek and Kagan,

2012). This increases binding between the death domains of Tube and Pelle. The interaction between the death domains of dMyD88, Tube and Pelle leads to formation of a heterotrimeric complex that interacts with Toll via the TIR of Toll and dMyD88 (Horng and Medzhitov, 2001; Sun et al., 2002; Moncrieffe et al., 2008) (Figure 6-2).

Pelle is a serine/threonine kinase that contains an N-terminal death domain and is a homolog of the human IL-1R-associated kinase (IRAK). Pelle has to be autophosphorylated to be able to transphosphorylate its targets. This autophosphorylation of Pelle is in a concentration-dependent manner (Shen and Manley, 2002). Because dMyD88, Tub and Pelle form a heterotrimeric complex which binds to the Toll receptor at the plasma membrane (Moncrieffe et al., 2008), it is likely that autophosphorylation of Pelle occurs when Spz dimers bind to Tolls resulting in bringing two Toll receptors together (Gangloff et al., 2008). Dimerization of Tolls, which already bind with the heterotrimeric complex, increases the local concentration of Pelle resulting in increased autophosphorylation. After the autophosphorylation, Pelle is able to transphosphorylate its targets, Tube, Toll and Cactus (Inhibitor of NF-κB (IκB)) (Whalen and Steward, 1993; Shen and Manley, 1998, 2002) (Figure 6-2). Once phosphorylated Pelle has transphosphorylated Tube and Toll, the complex disassociates (about five-fold decrease in binding affinity (Edwards et al., 1997)). This mechanism acts as a feedback loop to control the immune response (Towb et al., 2001; Shen and Manley, 2002).

Autophosphorylation of Pelle permits Pellino to bind at the N-terminal kinase domain of Pelle (Figure 6-2). Pellino is a conserved protein among animal kingdom (Grosshans et al., 1999), and is required in Drosophila immunity. The *Pellino* null-allele flies are susceptible to the gram-positive bacteria *M. luteus*. Interestingly, after *M. luteus* infection of flies overexpressing Pellino the level of Drs induction is higher than wild-type flies. Pellino is therefore categorized as a positive regulator of Toll pathway (Haghayeghi et al., 2010). The molecular mechanism by which Pellino acts as a positive regulator in Drosophila is still unclear. All mammalian Pellinos contain CHC2CHC2 RING-like motif which groups them into E3-ligase enzyme category (Schauvliege et al., 2006).

Under normal conditions, IκB Cactus binds to NF-κB Dorsal and Dif preventing them from entering the nucleus and initiating transcription of NF-κB responsive genes. In pathogen-induced condition, phosphorylated Pelle induces Cactus degradation by phosphorylation and Lys-48 ubiquitination at one of two distinct phosphorylation sites in the N-terminal region (Wu and Anderson, 1998; Fernandez et al., 2001) (Figure 6-2). The degradation of Cactus releases Dorsal and Dif to translocate into the nucleus to stimulate transcription of NF-κB responsive genes, such as AMP genes. From a dsRNA screen for all possible kinase and phosphatase, Pelle seem to be the only kinase relating with immune responses (Huang et al., 2010); however, Pelle is unable to fulfill the requirement for Cactus phosphorylation (Hetru and Hoffmann, 2009).

Dif or Dorsal-related immune factor was discovered after Dorsal as a NF-κB responded to Toll signalling. Dif and Dorsal have both redundant and specific functions. Dif does not have a role in dorsoventral patterning as Dorsal does, but has a role in larval and adult immunity as a responsive NF-κB in the Toll signalling pathway (Ip et al., 1993). Dif influences adult immunity toward fungi and gram-positive bacteria by controlling the production of Drs and Def, but not Mtk (antifungal AMP) (details of AMPs will be described in the Section 6.1.2.3), whereas in larvae Dif and Dorsal act redundantly to allow Toll induced AMP production (Manfruelli et al., 1999; Rutschmann et al., 2000).

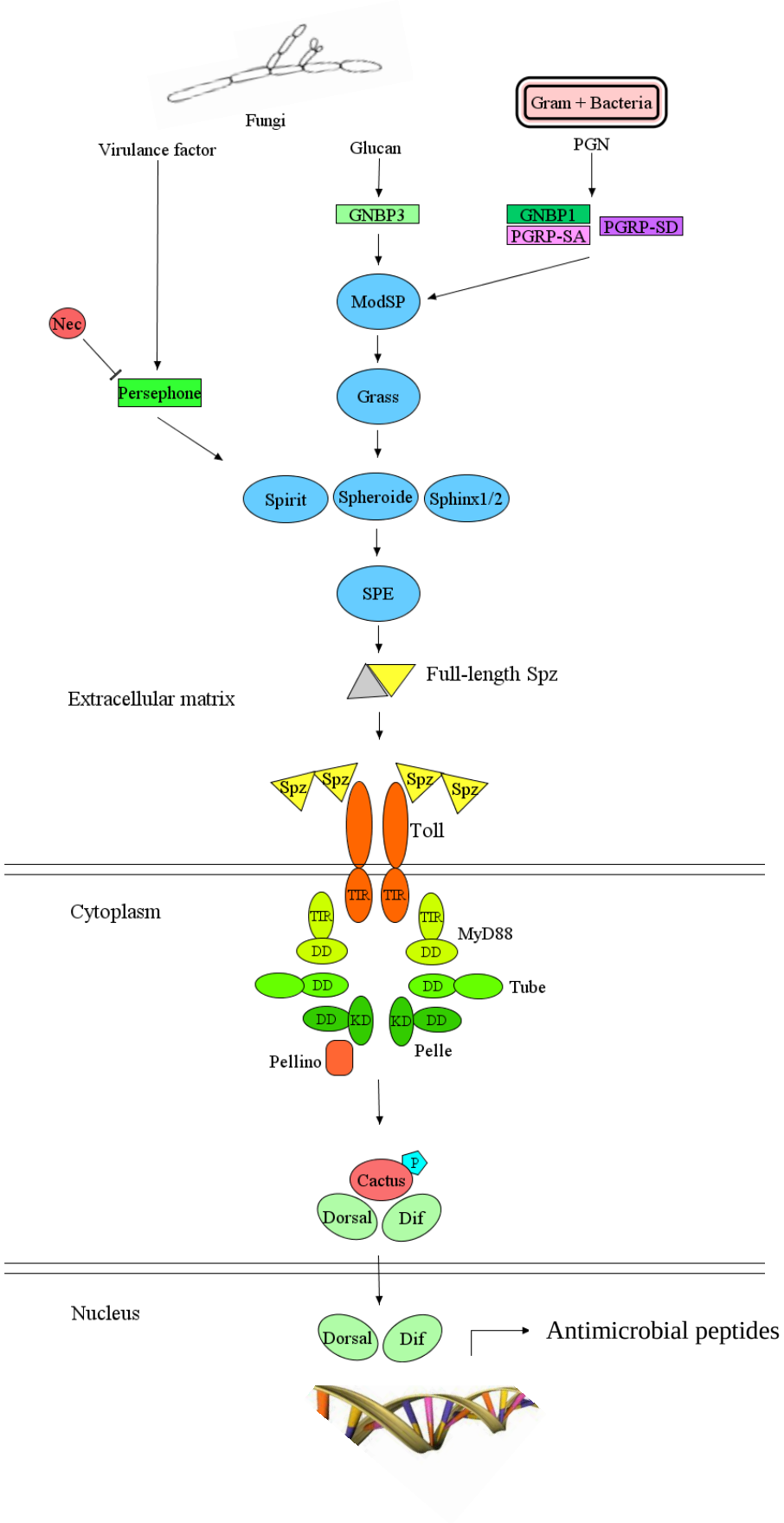
Fungi
Gram + Bacteria
Virulance factor
Glucan
PGN
GNBP3
GNBP1
PGRP-SA
PGRP-SD
ModSP
Nec
Persephone
Grass
Spirit
Spheroide
Sphinx1/2
SPE
Full-length Spz
Extracellular matrix
Spz
Spz
Spz
Spz
Toll
TIR
TIR
TIR
TIR
Cytoplasm
MyD88
DD
DD
DD
DD
Tube
DD
KD
KD
DD
Pellino
Pelle
P
Cactus
Dorsal
Dif
Nucleus
Dorsal
Dif
Antimicrobial peptides

Figure 6-2. The Toll signalling pathway. The Toll pathway is initiated from fungi or gram-positive bacteria via the specific recognition between glucan, virulent factors or PGN, and their receptors. The recognition activates the protease cascade resulting in the proteolytic activation of Spz. Spz dimers then binds to the toll receptors at the plasma membrane leading to the autophosphorylation of Pelle by the dimerization of the heterocomplexs (formed by the interaction between Toll, dMyD88, Tube and Pelle via interleukin-1 receptor domain (TIR) and death domain (DD)). The autophosphorylated Pelle allows the binding of Pellino to kinase domain (KD) of Pelle for positively regulating the Toll pathway, and phosphorylates Cactus triggering the degradation of Cactus. Once Cactus is degraded, Dorsal and Dif are released and able to transcribe the Toll pathway responsive genes, such as AMPs.

6.1.2.2 The Imd pathway

The Imd pathway was identified by the *immune deficiency* (*imd*) mutant which is sensitive to gram-negative bacteria infection, but resistant to fungal and gram-positive infection. The sensitivity to gram-negative bacteria is due to the impaired production of AMP transcripts against gram-negative bacteria, such as Drosocin (Dro), Diptericin (Dpt) and Cecropin (Cec) (Lemaitre et al., 1995; Lemaitre and Hoffmann, 2007)

6.1.2.2.1 Pathogen sensing of the Imd pathway

Unlike the Toll receptors, the Imd pathway receptors located on the cell membrane directly recognize PGN. The long form of PGRPs is responsible for the recognition of DAP-PGN from gram-negative bacteria and the Imd signalling initiation. Gram-negative bacteria are recognized by PGRP-LC and PGRP-LE (Gottar et al., 2002; Kaneko et al., 2006). PGRP-LC has a transmembrane domain allowing it to bind with the plasma membrane. Due to alternative splicing, PGRP-LC has three isoforms: PGRP-LCa, PGRP-LCx, and PGRP-LCy (Werner et al., 2000). PGRP-LCx has an ability to bind with polymeric DAP-PGN, and once induced by DAP-PGN, the clustering of PGRP-LCx occurs (Mellroth et al., 2005). PGRP-LCa has no PGN binding ability and has to form a heterodimer with PGRP-LCx to be able to recognize monomeric DAP-PGN (Chang et al., 2005; Mellroth et al., 2005). The function of PGRP-LCy is still unknown. PGRP-LE does not have a transmembrane domain, so it localizes in the cytosol. The role of PGRP-LE in recognizing monomeric DAP-PGN is required synergistically with PGRP-LC (Takehana et al., 2004). Although PGRP-LE is an intracellular protein, it is required for defence signalling in certain cell types, such as malphigian tubules, which can import small fragments of PGN (Kaneko et al., 2006). The PGRP domain of PGRP-LE (PGRP-LE^{pg}) can be found in the extracellular fluid. PGRP-LE^{pg} alone cannot induce the expression of *Dpt* in S2 cells, however together with PGRP-LC, it enhances the *Dpt* expression. Therefore, PGRP-LE^{pg} has been proposed to bind with monomeric DAP-PGN and carry the DAP-PGN to cell surface where it interacts with PGRP-LC (Kaneko et al., 2006). PGRP-LF is a negative regulator of the Imd pathway through its interaction with PGRP-LCx (Maillet et al., 2008; Basbous et al., 2011).

6.1.2.2.2 Signal transduction in the Imd pathway

After DAP-PGN recognition, the recruitment of Imd, DREDD and FADD to the receptors has been proposed. DREDD is a caspase-8-like protein and FADD is the adaptor of DREDD. Both DREDD and FADD are required for the Imd cleavage (Paquette et al., 2010). Cleavage of Imd causes exposure of IAP-binding motif to the outer environment. This motif can interact with the BIR domain of the Drosophila inhibitor of apoptosis 2 (DIAP2) protein leading to the ubiqintination of the cleaved Imd by the E3-ubiquintin ligase activity of the RING-finger domain at C-terminal of DIAP2 (Vaux and Silke, 2005). Together with three E2-ubiquitin-conjugating enzymes Uev1a (Zhou et al., 2005) , Ubc13 (bendless) (Zhou et al., 2005) and Effete (a homolog of human Ubc5) (Paquette et al., 2010), the cleaved Imd is only ubiquintinated at Lys 63 to produce Lys 63-polyubiqitinated Imd (Zhou et al., 2005; Paquette et al., 2010) (Figure 6-3). Lys 63-polyubiqitination has been proposed to function in signalling rather than the proteosome-mediated degradation (Chiu et al., 2009). Interestingly, unanchored Lys 63 polyubiquintin alone is enough to activate the downstream kinases TAK1 and IKK (Xia et al., 2009). The Lys 63 polyubiquintin may function as a scaffold for recruiting the TAK1 and IKK together to generate a suitable microenvironment for TAK1 to be able to phosphorylate IKK (Paquette et al., 2010). The binding of TAK1 and IKK to Lys 63 polyubiquintin is predicted to be mediated by TAB2, which has Lys 63-polyubiquintin binding domain, to form a complex (Kaneko et al., 2006) with TAK1 and IKK (Ea et al., 2006; Zhuang et al., 2006). Normal expression of defence genes via the Imd pathway requires both phosphorylation of Relish by phosphorylated IKK, allowing it to recruit RNA polymerase II and cleavage of Relish by DREDD, to allow it to enter the nucleus (Ertürk-Hasdemir et al., 2009) (Figure 6-3).

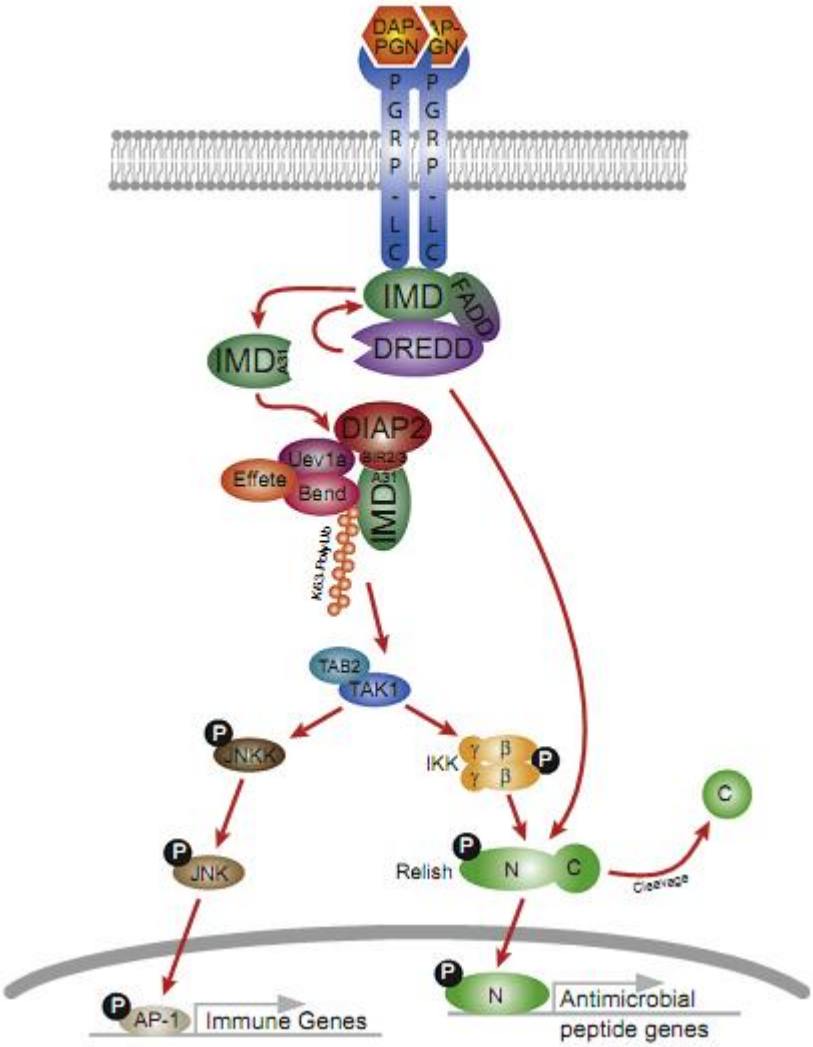

Figure 6-3. The Imd pathway. The Imd signalling is initiated from DAP-PGN binding to the receptor PGRP-LC. This recruits Imd, FADD and DREDD complex generating cleaved Imd. The cleaved Imd is then Lys 63 polyubiquintinated by the assistance of DIAP2, Uev1a, Bendless and Effete. This Lys 63 polyubiquintin activates the downstream kinases leading the expression through NF-κB or c-Jun N-terminal kinases (JNK). This figure is taken from Paquette et al. (2010).

6.1.2.3 Antimicrobial peptide (AMP) production

The Toll and Imd signalling pathways induce expression of defence-related genes. AMP genes for inhibiting invading pathogens are expressed after infection. AMPs can be divided into four groups based on a Toll and Imd pathway mutant analysis.

1. AMPs that are mainly regulated by Toll pathway: Drs (Lemaitre et al., 1996)
2. AMPs that are mainly regulated by Imd pathway: Dpt and Dro (Lemaitre et al., 1996)
3. AMPs that require both Toll and Imd pathways: Cec A, attacin and Def (Lemaitre et al., 1996)
4. AMPs that require either Toll or Imd pathways: Mtk (Levashina et al., 1998)

The NF-κBs, Dorsal, Dif, Relish and the cleaved form of Relish, form both homo and heterodimer *in vitro* and *in vivo* (Gross et al., 1996; Tanji et al., 2010). In cell culture, the Dif-Relish heterodimer can trigger higher Drs production compared with Dif alone or the Dif-Dif homodimer. In adult flies, the heterodimer of Dif and Relish is able to activate AMPs from both the Toll and Imd pathways (Tanji et al., 2010). This is supported by the identification of Dif-Relish heterodimer specific binding (Senger et al., 2004). Moreover, this is an excellent example of crosstalk between the Toll and Imd pathways.

6.1.2.3.1 The specificity toward microbes of AMPs

Each type of AMP has a specific inhibitory effect toward different types of microbes. In general, each AMP can be characterized by its main function, such as anti-gram-positive, anti-gram-negative, and/or anti-fungal AMPs; however, the functions of AMPs also depend on species of microbe. The inhibitory properties of AMPs against different types of microbes that have been published are described in Table 6-1.

From Table 6-1, it can be generally summarized that Drs is very effective against fungi. Mtk has antifungal and also anti-gram-positive bacteria properties. Def is only effective against gram-positive bacteria. Dro is both anti-gram-negative and

anti-gram-positive bacteria AMP. Att and Dpt are mainly for protecting against gram-negative bacteria. Cec is a broad range AMP. The anti-microbial ability of Cec can inhibit certain types of fungi, gram positive and gram-negative bacteria.

Table 6-1. List of microbes that have been tested against each AMP for an inhibitory effect.

Types of AMPs	Sensitivity	Filamentous fungi	Yeast	Gram-positive bacteria	Gram-negative bacteria
Drosomysin (Drs)	Sensitive microbes	*Neurospora crassna*[1, 2, 3], *Geotrichum candidum*[2, 3], *Alternaria brassicola*[2], *Alternaria longipes*[2], *Ascochyta pisi*[2], *Botrytis cinerea*[2], *Fusarium culmorum*[2], *Fusarium oxysporum*[2], *Nectria haematococca*[2]	*Saccharomyces cerevisiae*[2, 3]	-	-
	Insensitive microbes	-	-	*Micrococcus luteus*[1]	*Escherichia coli* D31[1]
Metchnikowin (Mtk)	Sensitive microbes	*Neurospora crassna*[1]	-	*Micrococcus luteus*[1]	-
	Insensitive microbes	-	-	-	*Escherichia coli* D31[1]
Defensin (Def)	Sensitive microbes	-	-	*Micrococcus luteus*[1,8]	-
	Insensitive microbes	*Neurospora crassna*[1]	-	-	*Escherichia coli* D31[1]
Diptericin (Dpt)	Sensitive microbes	-	-	-	*Escherichia coli* D31[7]
	Insensitive microbes	-	-	*Micrococcus luteus*[7], *Bacillus subtilis*[7], *Bacillus thuringiensis*[7]	*Enterobacter cloacae* β12[7], *Pseudomonas aeruginosa* OT97[7]
Drosocin (Dro)	Sensitive microbes	-	-	*Micrococcus luteus*[1]	*Escherichia coli* D31[1], *Escherichia coli* D31[9],
	Insensitive microbes	*Neurospora crassna*[1]	-	-	-
Attacin (Att)	Sensitive microbes	-	-	-	*Escherichia coli* DH5α[5], *Escherichia coli* D31[6], *Escherichia coli* D21[6], *Escherichia coli* D22[6], *Pseudomonas maltophilia*[6], *Acinetobacter calcoaceticus*[6]
	Insensitive microbes	-	-	*Bacillus megaterium*[6], *Bacillus subtilis* Bs11[6], *Streptococcus fecalis* AD-4[6], *Sarcina lutea* ATCC-9341[6], *Micrococcus luteus* Ml11[6],	*Enterobacter cloacae*[6] , *Pseudomonas aeruginosa* OT97[6] ,
Cecropin (Cec)	Sensitive microbes	*Neurospora crassa*[4]	-	*Bacillus megaterium*[4], *Micrococcus luteus*[4]	*Agrobacterium tumefaciens*[4], *Enterobacter cloacae* β12[4], *Escherichia coli* SBS 363[4], *Escherichia coli* D31[4], *Escherichia coli* D22[4], *Erwinia carotovora carotovora*[4], *Pseudomonas aeruginosa*[4], *Salmonella typhimurium*[4]
	Insensitive microbes	*Aspergillus fumigatus*[4]	*Candida albicans*[4], *Candida glabrata*[4], *Cryptococcus neoformans*[4], *Saccharomyces cerevisiae*[4]	*Staphylococcus aureus*[4], *Streptococcus pyogenes*[4]	*Serratia marcescens*[4]

[1] (Levashina et al., 1995)

[2] (Fehlbaums et al., 1994)

[3] (Tian et al., 2008)

[4] (Rabel et al., 2004)

[5] (Wang et al., 2010)

[6] (Hultmark et al., 1983) (based on Att of *Hyalophora cecropia*)

[7](Dimarcq et al., 1988) (based on Dpt of *Phorrnia terranovae*)

[8](Dimarcq et al., 1994)

[9](Bulets et al., 1993)

6.2 GSNOR is important for Arabidopsis disease resistance.

GSNOR is required for all three main layers of plant disease resistance (basal, *R* gene-mediated, and non-host disease resistance) (Feechan et al., 2005). The role of GSNOR in basal disease resistance was confirmed by *Pst* leaf inoculation followed by a colony count. Wild-type and *gsnor* loss of function *gsnor1-3* Arabidopsis leaves were infected with *Pst*. After 2 days, the leaves were punched to an equal leaf area and ground. The supernatant was diluted to an appropriate dilution before spreading to petridishes with bacterial culture media and selective antibiotics. Colonies were counted and calculated to colony forming unit per cm^2 leaf tissue. A similar result to Feechan et al. (2005) was observed (Figure 6-4).

6.3 GSNOR is not essential for immunity against gram-negative bacteria infection.

In order to test whether GSNOR is required for gram-negative bacteria infection which is known to trigger the Imd pathway (Lemaitre et al., 1995), the overlapping deficiency *Df7305*/*Df7306* was challenged by gram-negative bacteria via septic infection. A tungsten needle previously disinfected by 70 % ethanol and then dipped in a freshly prepared pellet of *E. coli* MG1655 of 10 mL overnight culture at 37˚ C was used to administer bacteria into the fly's body cavity by puncturing the thorax. This method of infection is called 'septic infection' in this thesis. Infected flies were then observed twice a day over ten days. The survival of *Df7305*/*Df7306* and *Df7306*/*Df7305* flies was reduced to about 80 percent in 100 hours, whereas the survival of OR, *Df7305*/*TM6B* and *Df7306*/*TM6B* remained constant at 100 percent. Flies mutant for *imd* or *Relish*, which have been previously shown to be sensitive to gram-negative bacteria (Lemaitre et al., 1995; Hedengren et al., 1999), were used as positive controls for this assay (Figure 6-5a). However, *Df7305*/*Df7306* and *Df7306*/*Df7305* showed approximately the same loss of viability (at about 80 percent in 100 hours and 85 percent in 100 hour, respectively) when punctured with a sterile needle dipped in LB (Figure 6-5b). This suggests that GSNOR does not play a role in the immunity triggered by *E. coli* septic infection, because the observed effect on survival was also seen after administration of LB

broth. *Relish* and *imd* flies survived LB treatment. This rules out the possibility of bacterial contamination. If contamination was involved, *Relish* and *imd* flies would be more sensitive. Therefore, the sensitivity of the *gsnor* knockout in LB treatment might be due to wound healing. In addition, *Spaetzle* flies do not show susceptibility in septic infection with *E. coli* suggesting that the Toll pathway is not required for resistance against gram-negative bacterial infection. Furthermore, melanization of the wound was observed in *Df7305*/*Df7306* (Figure 6-5c) suggesting that melanization, which is a part of insect defence machinery, was not affected by the loss of GSNOR in *Df7305*/*Df7306* flies.

After the discovery that *gsnor* knockout does not increase the susceptibilities of flies to *E. coli* septic infection, we decided to test a different route of infection to confirm that GSNOR does not have a role in immunity against gram-negative bacteria.

*Ecc*15 is a plant pathogenic bacterium strain containing Erwinia virulence factor (Evf) permitting this bacteria to survive and propagate in the Drosophila gut, and then to use flies as an obligate host for transmitting the disease (Quevillon-Cheruel et al., 2009). *Ecc*15 can cause lethality in Drosophila at high concentration. In this experiment, 500 mL LB was inoculated with 10 mL *Ecc*15 overnight culture (about 50 fold dilution). The bacteria pellet was collected, and the volume estimated in a 15 mL falcon tube. An equal volume of 10 % sucrose was mixed with the pellet to make about a half of pellet concentration in 5 % sucrose. The *Ecc*15 suspension was fed to flies which had been previously starved for 2 hours.

With *Ecc*15 oral infection *Df7305*/*Df7306* did not show a clear difference in survival with OR, *Df7305*/*TM6B* and *Df7306*/*TM6B*. Although *imd* flies exhibit a similar survival pattern with OR, *Relish* flies showed a clear decrease in survival confirming that the Imd pathway is required for resistance to gram-negative bacteria oral infection (Figure 6-6). This observation supports our conclusion that GSNOR does not play a role in immunity against gram-negative bacteria and presumably the Imd pathway may not be affected by the loss of GSNOR.

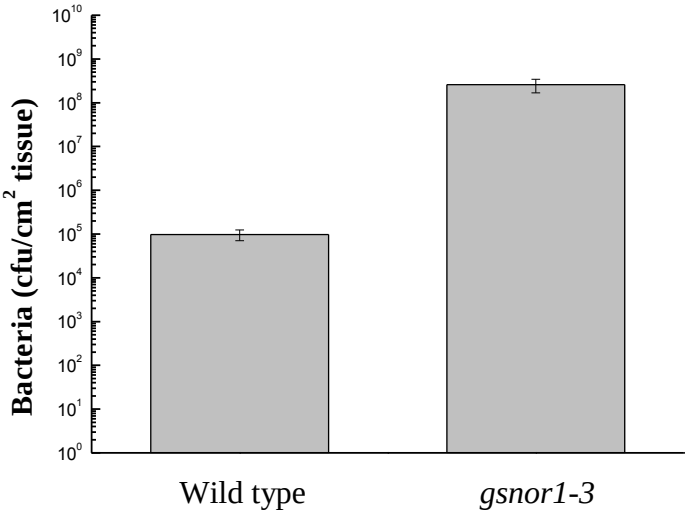

Figure 6-4. *gsnor1-3* increases susceptibility to the virulent bacterial pathogen *Pst*. *Pst* at 0.0002 OD was infiltrated into leaves of wild type and *gsnor1-3* Arabidopsis. After five days, the number of *Pst* colonies were counted by plating appropriate dilutions of ground inoculated leaves. Data represent the mean from eight independent experiments (±SE).

(a)

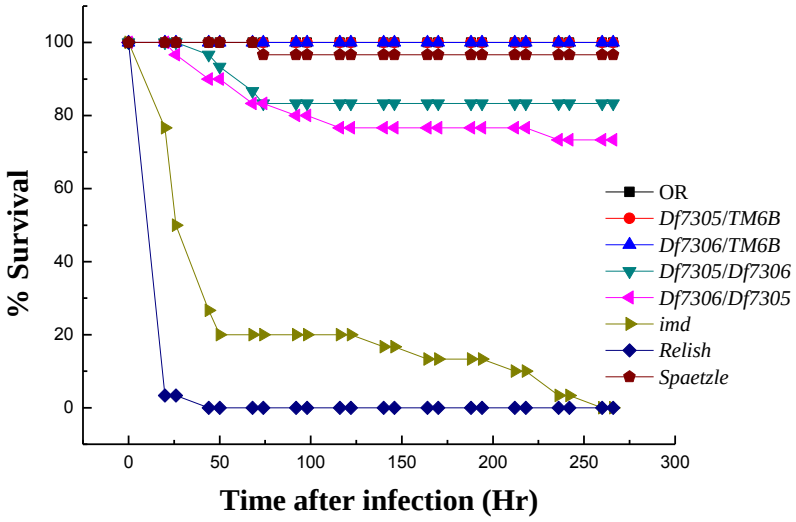
% Survival
Time after infection (Hr)
OR
Df7305/TM6B
Df7306/TM6B
Df7305/Df7306
Df7306/Df7305
imd
Relish
Spaetzle

(b)

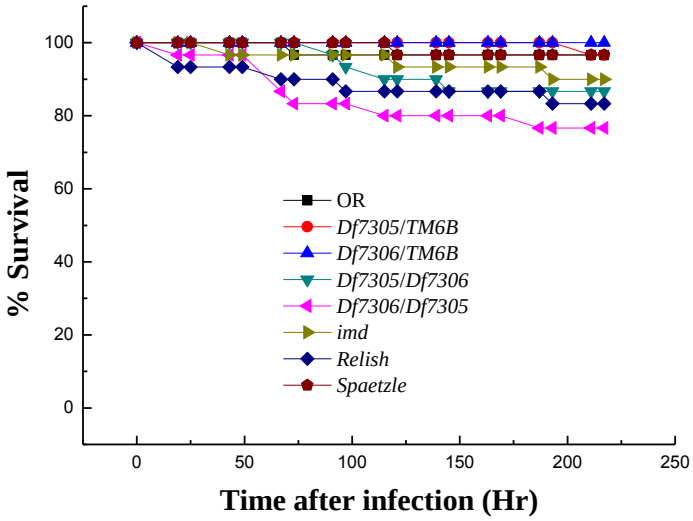
% Survival
Time after infection (Hr)
OR
Df7305/TM6B
Df7306/TM6B
Df7305/Df7306
Df7306/Df7305
imd
Relish
Spaetzle

(c)

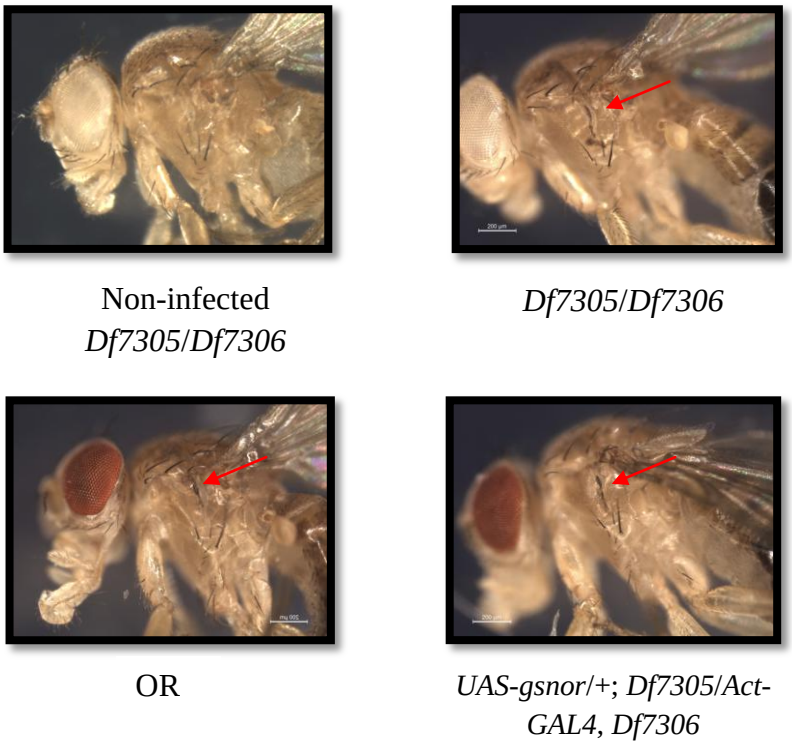

Figure 6-5. Percentage survival of Drosophila after (**a**) *E. coli* MG1655 septic infection and (**b**) LB administration. (**c**) After *E. coli* infection, melanization can still occur at the infection sites (indicates by red arrows).

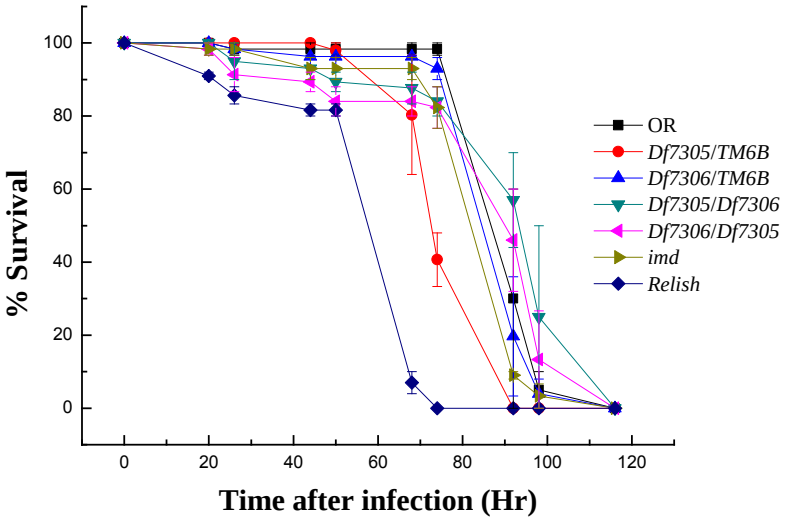

Figure 6-6. Percent survival of Drosophila after *Ecc15* oral administration. The data represent the mean of two independent experiments (±SE).

6.4 GSNOR is required for immunity against fungal infection.

In order to investigate whether GSNOR is important for immunity against fungal infection which is known to trigger the Toll pathway (Ligoxygakis et al., 2002), an insect pathogenic fungus *B. bassiana*, which has been previously shown to be pathogenic for Drosophila (Gillespie et al., 2000), was used to infect *gsnor* knockout flies. 30 flies were shaken with *B. bassiana* spores in a 2 mL microcentrifuge tube for two minutes and incubated at 29℃. The survival of *Df7305*/*Df7306* and *Df7306*/*Df7305* to *B. bassiana* infection was below that of OR, *Df7305*/*TM6B*, *Df7306*/*TM6B* and of flies with the Toll pathway impaired by a *Spaetzle* mutant. *imd* and *Relish* showed a similar response to wild-type OR indicating that the Imd pathway is not involved in immunity against *B. bassiana*. The *Df7305*/*Df7306* susceptible phenotype can be totally rescued by GSNOR overexpression from *act5c*:*UAS-gsnor*; *Df7305*/*Df7306* and *act5c*:*UAS-gsnor*; *Df7306*/*Df7305*. Rescue of the disease phenotype in GSNOR overexpression flies confirms that GSNOR is required for immunity against fungal infection. However from our results so far, it is unclear where exactly GSNOR functions in immunity. GSNOR could function in systemic, local (such as epidermal immunity), and/or cellular immune responses against fungal infection.

Interestingly, the susceptibility of *Df7305*/*Df7306* flies was observed within 24 hours after the infection, while at this time *Spaetzle* flies were not affected until approximately 100 hours after infection. Subsequently, their survival dropped to almost the same level as *Df7305*/*Df7306* (Figure 6-7a and 6-7b). If GSNOR functions in the Toll pathway, the early rapid response of *Df7305*/*Df7306* might suggest that GSNOR functions at an early stage of the Toll pathway, probably before Spz. GSNOR could also function in an unknown pathway which rapidly responds to fungal infection.

Shaking flies with spores in a 2 mL tube might wound them and generate a false positive phenotype. In order to confirm that the method of infection did not contribute to the observed phenotype, flies were treated in the same way but with inactive *B. bassiana* spores. The result shows that the observed susceptibility was not from wounding which may only cause a slight reduction in survival (Figure 6-7d).

Expression of GSNOR from the endogenous promoter (*EP-gsnor*/*EP-gsnor*; *Df7305*/*Df7306*) did not restore the wild-type response (Figure 6-7c), even though it could complement the tergite phenotype (Figure 3-19). This might suggest that each biological process requires a different level of *S*-nitrosylation controlled by GSNOR.

6.5 GSNOR is important for expression of anti-fungal antimicrobial peptide genes after fungal infection.

Drosophila does not have an adaptive immune response. It relies on an array of AMPs to fight directly against invading pathogens. The production of AMPs is crucial for Drosophila immunity, and it indicates a level of disease resistance (Lemaitre and Hoffmann, 2007). There are many types of AMPs. In terms of function, each AMP has both redundant and unique properties (Table 6-1). We have tested a transcription level of four different AMPs: *Dpt*, *Def*, *Drs* and *Mtk* in order to confirm whether or not *gsnor* knockout affects AMP expression after *B. bassiana* infection but not after *E. coli* septic infection.

The mRNA level of *Dpt*, an AMP against gram-negative bacteria produced by the Imd pathway, was measured in order to confirm that GSNOR is not essential for the Imd pathway of systemic immune responses. Total RNA was extracted and reverse transcribed to cDNA. The copy number of AMP cDNA was quantified by qRT-PCR and normalized with the copy number of *Rp49* cDNA. The normalized data indicate expression of AMPs. As expected with *E. coli* infection, there is no significant different among *Df7305*/*Df7306*, OR, *Df7305*/*TM6B*, *Df7306*/*TM6B* and the complementation in *Dpt* transcription level (Figure 6-8).

(a)

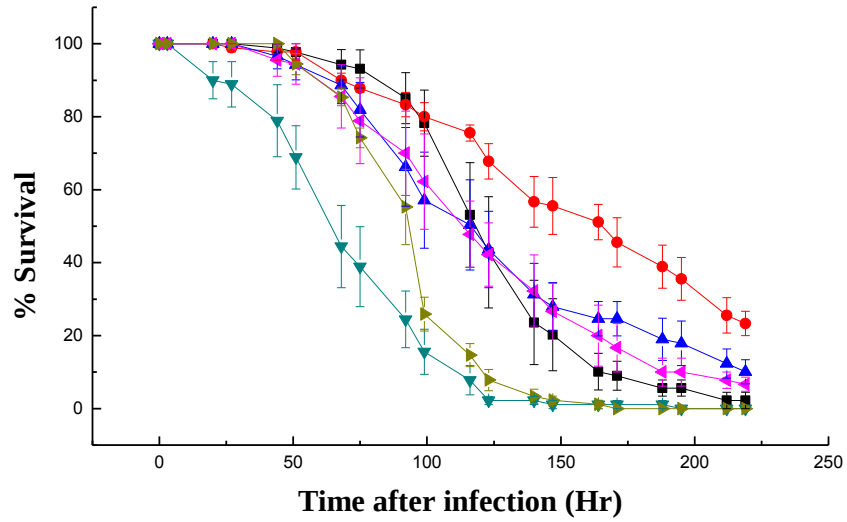

OR
Df7305/TM6B
Df7306/TM6B
Df7306/Df7305
+/UAS-gsnor; Act-GAL4, Df7306/Df7305
Spaetzle

(b)

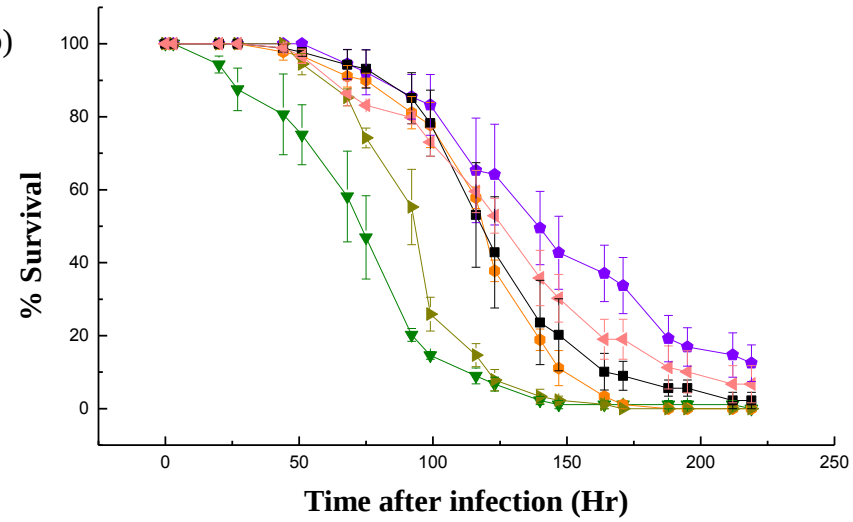

OR
imd
Relish
Df7305/Df7306
UAS-gsnor/+; Df7305/Act-GAL4, Df7306
Spaetzle

(c)

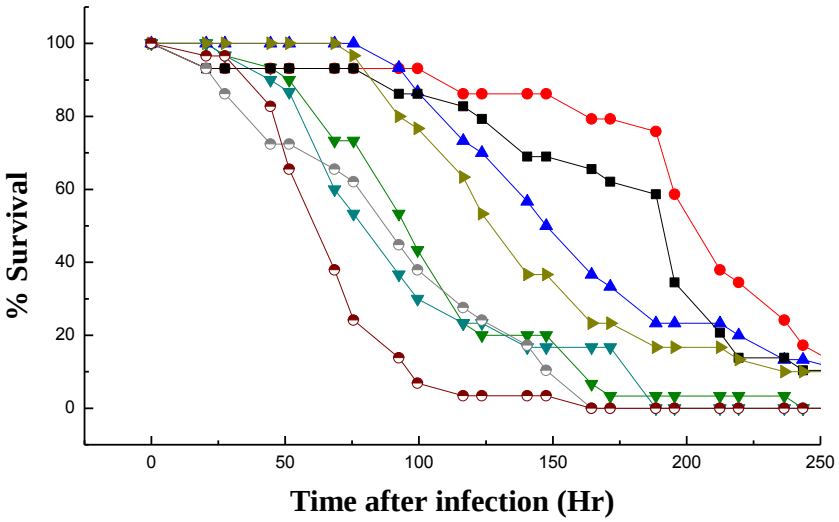

OR
Df7305/TM6B
Df7306/TM6B
Df7305/Df7306
Df7306/Df7305
EP-gsnor/EP-gsnor; Df7305/Df7306
EP-gsnor/EP-gsnor; Df7306/Df7305
Spaetzle

(d)

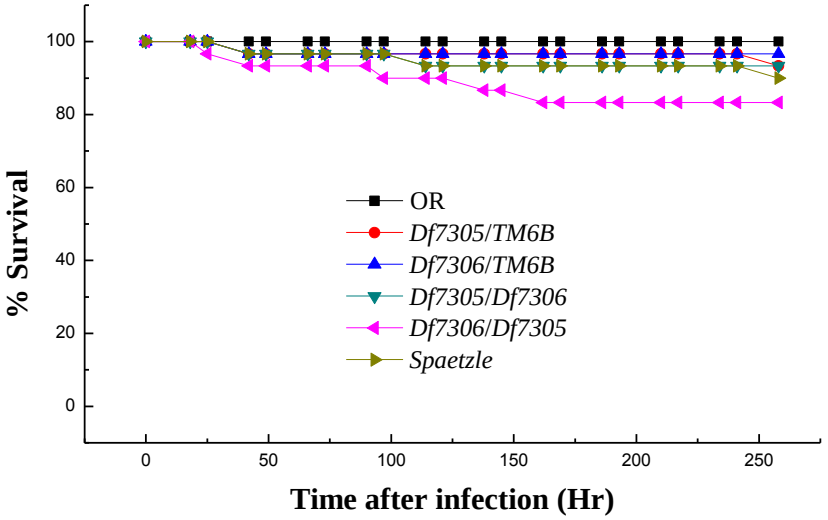

(e)

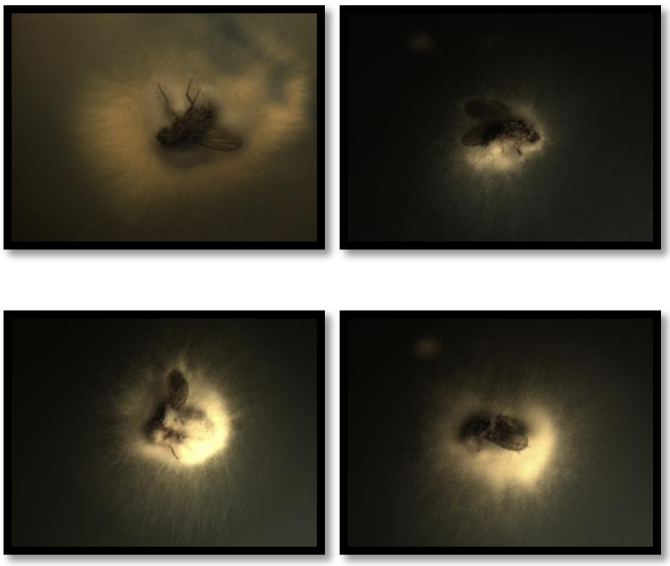

Figure 6-7. Percent survival of Drosophila (**a, b and c**) after *B.bassiana* infection and (**d**) after inactive *B. bassiana* infection. The data represent the mean of three independent experiments (±SE) (a, b) and one experiment (c, d). The data from Figure a and b was obtained from the same experiment. OR and *Spaetzle* data were replotted in Figure b as a negative and positive controls, respectively. (**e**) After infection, dead flies were placed on a PDA plate with chloramphenicol to observe fungal growth in order to ensure that the death of flies was a result of the fungal infection. Drosophila genotype does not affect the growth of fungi (All figures show *Df7305*/*Df7306* flies).

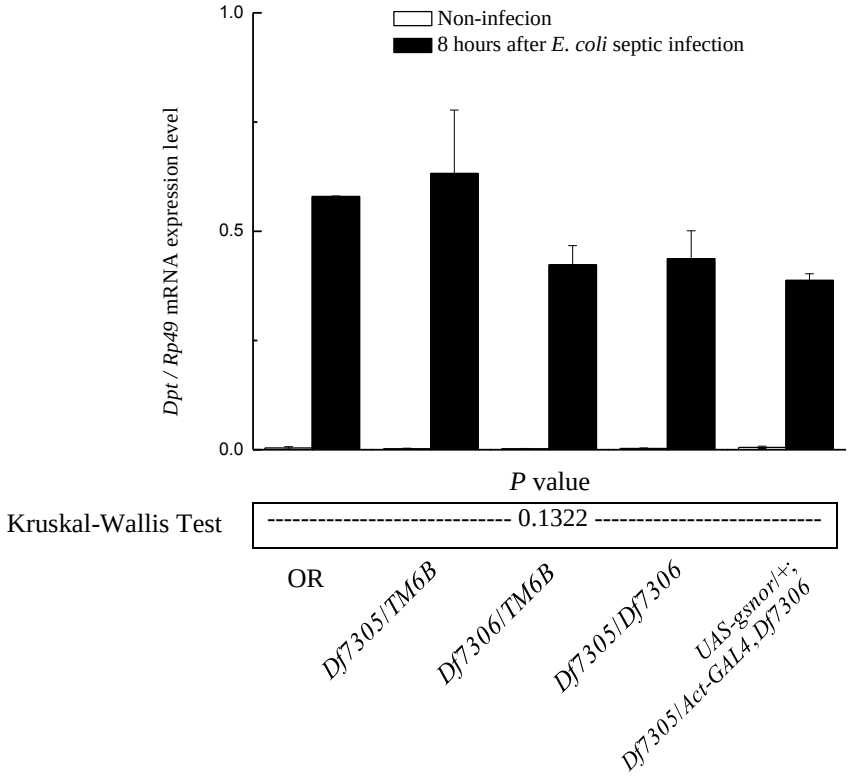

Figure 6-8. qRT-PCR quantifying level of *Dpt* mRNA in Drosophila 8 hours after *E. coli* septic infection or without infection. The *Dpt* transcript level was normalized to the level of *Rp49* mRNA. mRNA level increases after infection but does so to the same extent to each genotype. The data represent the mean from at least three independent experiments (±SE). The *P* value is calculated from Kruskal-Wallis test to determine the probability that all infected samples come from the same population. Statistically significant differences are indicated by * ($P < 0.05$).

In order to observe AMP expression from gram-positive bacteria septic infection, the gram-positive bacteria *M. luteus* which has been shown to trigger AMP production without the effect on survival (Romeo and Lemaitre, 2008) was used to septic infect flies. mRNA level of *Def*, the anti-gram-positive bacteria AMP produced by the Toll pathway (Levashina et al., 1995), was measured. Unexpectedly, with *M. luteus* infection the expression of *Def* in *Df7305*/*Df7306* was significantly higher than OR, *Df7305*/*TM6B* and *Df7306*/*TM6B*. The complementation decreased *Def* expression back to *Df7305*/*TM6B*, but not as similar as OR or *Df7306*/*TM6B* (Figure 6-9b). This might indicate that GSNOR is a negative regulator of *Def* expression, or the *gsnor* knockout could not control *M. luteus* propagation leading to increased expression of *Def*.

The production of *Def* was not induced with *B. bassiana* infection in all genotypes tested (Figure 6-9a). This is very interesting because the Toll signalling from fungal and gram-positive infection converges into the same signalling pathway (Figure 6-2). Therefore, either fungal or gram-positive bacteria infection, the production of final products (AMPs) should be similar. This phenomenon might suggest an unknown mechanism that controls the specificity of defence responses toward different groups of pathogens. In this case, Def is an anti-gram-positive bacteria AMP, but not anti-fungal AMP, so this unknown mechanism might assist Drosophila to concentrate energy to produce only anti-fungal AMPs. Although it has been shown that Drosophila can discriminate between different classes of pathogens (this specificity is decided by whether a pathogen is perceived by Toll or Imd pathways) (Lemaitre et al., 1997), this is the first evidence indicating possible specificity in the same pathway toward different groups of pathogen. However, it has been shown by northern blot that *Def* is slightly induced by *B. bassiana* septic infection (Lemaitre et al. 1997). We thinks that our results are more reliable because the qRT-PCR which has more accuracy for quantification was performed, and we applied the fungal spores to fly's cuticle by shaking flies with spores in a microcentrifuge tube. This method of infection possibly generates less *Def* induction than the septic infection method which gave a noticeable increase in *Def* production (Lemaitre et al., 1997). However, another reason why there was no induction of *Def*

production upon *B. bassiana* infection might also be due to the ability of *B. bassiana* in suppressing Drosophila immunity (Gottar et al., 2006).

The transcript level of anti-fungal AMPs *Drs* and *Mtk* (Levashina et al., 1995; Zhang and Zhu, 2009) were measured in order to observe any effect of GSNOR on the systemic production of anti-fungal AMPs. With *B. bassiana* infection, the level of *Drs* mRNA in *Df7305*/*Df7306* was reduced significantly when compared with OR and *Df7305*/*TM6B* (Figure 6-10a). The complementation *act5c*:*UAS-gsnor*; *Df7305*/*Df7306* was able to rescue the *Drs* mRNA level back to the wild-type level (Figure 6-10a). We also observed this effect with *M. luteus* infection, but the reduction of *Drs* expression in *Df7305*/*Df7306* was less than with fungal infection (Figure 6-10b). Then when we looked at the transcript level of *Mtk*, this provided additional evidence about the production of anti-fungal AMPs in *gsnor* knockout mutants. The level of *Mtk* was significantly reduced after *B. bassiana* infection in *Df7305*/*Df7306* when compared with OR, *Df7305*/*TM6B* and *Df7306*/*TM6B* (Figure 6-11b). Complementation of the *gsnor* deletion by *act5c*:*UAS-gsnor* was able to rescue the *Mtk* mRNA level back to the wild-type level (Figure 6-11b). The reduction of *Mtk* expression level could not be observed in *M. luteus* infection with statistical significance (Figure 6-11c). This suggests that GSNOR is required to trigger anti-fungal systemic immune response. The defence pathway affected is likely to be the Toll pathway which is the main defence against fungal infection. However, the effect of *gsnor* knockout flies observed in *B. bassiana* infection assay (Figure 6-7a and b) could be due to the defect solely in systemic immune responses or in combination with local immune responses, and/or cellular immune responses.

The effects observed in the transcript level of *Drs* and *Mtk* are very interesting, because Drosophila uses the Toll pathway in order to respond to both fungi and gram-positive bacteria infections. The *Drs* and *Mtk* mRNA levels of *gsnor* knockout flies are more impaired in response to fungal infection than to gram-positive bacteria infection. This indicates that the role of GSNOR in the Toll pathway might be at the beginning of the fungal infection signalling, but before a signal from fungal infection and a signal from gram-positive bacteria infection converge together (Figure 6-2).

(a)

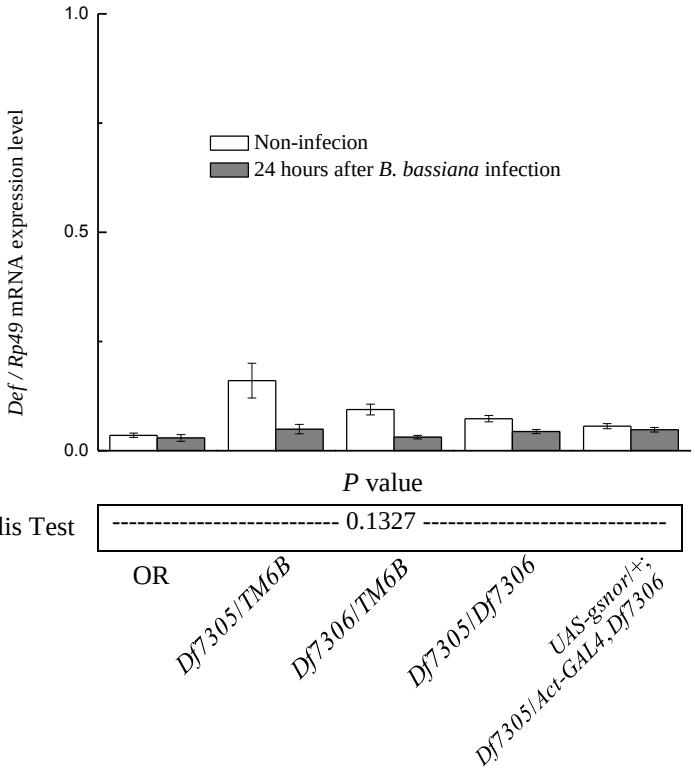

P value

Kruskal-Wallis Test	0.1327			
OR	*Df7305/TM6B*	*Df7306/TM6B*	*Df7305/Df7306*	*UAS-gsnor/+; Df7305/Act-GAL4,Df7306*

(b)

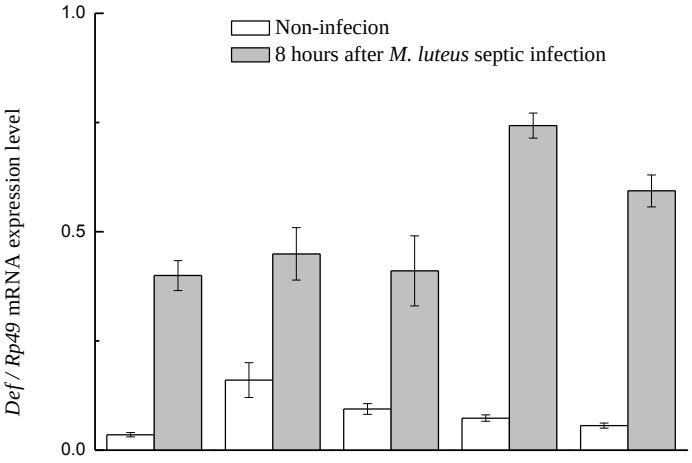

P value

Kruskal-Wallis Test	0.0048*				
Mann-Whitney U Test	OR	--	--	0.0119*	0.0119*
	Df7305/TM6B	--	--	0.0119*	0.0833
	Df7306/TM6B	--	--	0.0119*	0.0476*
	OR	*Df7305/TM6B*	*Df7306/TM6B*	*Df7305/Df7306*	*UAS-gsnor/+; Df7305/Act-GAL4,Df7306*

Figure 6-9. qRT-PCR quantifying level of *Def* mRNA in Drosophila (**a**) 24 hours after *B. bassiana* infection or without infection, or (**b**) 8 hours after *M. luteus* infection or without infection. The *Def* transcript level was normalized to the level of *Rp49* mRNA. (a) mRNA level does not increase after *B. bassiana* infection. (b) mRNA level increases after *M. luteus* infection but does so to the same extent to each genotype. The data represent the mean from at least three independent experiments (±SE). The table gives the *P* value from Kruskal-Wallis test to determine the probability that all infected samples come from the same population and Mann-Whitney U test for comparison of the *Def*/*Rp49* ratio for infected flies of each genotype compared with the value for infected OR (row one), *Df7305*/*TM6B* (row two) and *Df7306*/*TM6B* (row three). -- indicates insufficient data to do the test. Statistically significant differences are indicated by * ($P < 0.05$).

(a)

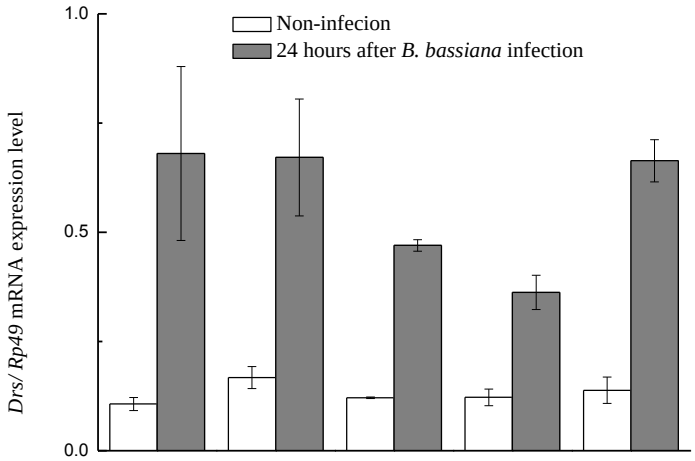

P value

Kruskal-Wallis Test	---------- 0.0082* ----------				
Mann-Whitney U Test	OR		--	--	0.0476*	0.2738
	Df7305/TM6B	--		--	0.0119*	0.3571
	Df7306/TM6B	--	--		0.1310	0.0119*

OR *Df7305/TM6B* *Df7306/TM6B* *Df7305/Df7306* *UAS-gsnor/+; Df7305/Act-GAL4,Df7306*

(b)

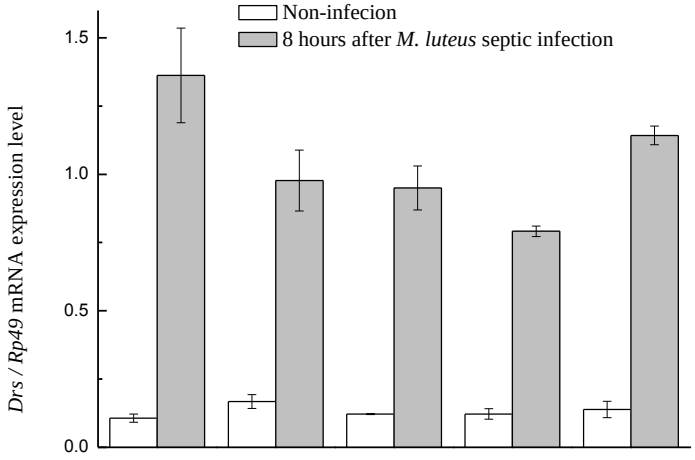

P value

Kruskal-Wallis Test	---------- 0.0081* ----------				
Mann-Whitney U Test	OR		--	--	0.0119*	0.1905
	Df7305/TM6B	--		--	0.0833	0.1310
	Df7306/TM6B	--	--		0.0833	0.0238*

OR *Df7305/TM6B* *Df7306/TM6B* *Df7305/Df7306* *UAS-gsnor/+; Df7305/Act-GAL4,Df7306*

Figure 6-10. qRT-PCR quantifying level of *Drs* mRNA in Drosophila (**a**) 24 hours after *B. bassiana* infection or without infection, or (**b**) 8 hours after *M. luteus* infection or without infection. The *Drs* transcript level was normalized to the level of *Rp49* mRNA. mRNA level increases after infection but does so to the same extent to each genotype. The data represent the mean from at least three independent experiments (±SE). The table gives the *P* value from Kruskal-Wallis test to determine the probability that all infected samples come from the same population and Mann-Whitney U test for comparison of the *Drs*/*Rp49* ratio for infected flies of each genotype compared with the value for infected OR (row one), *Df7305*/*TM6B* (row two) and *Df7306*/*TM6B* (row three). -- indicates insufficient data to do the test. Statistically significant differences are indicated by * ($P < 0.05$).

Mtk has been previously shown to be induced by either gram-negative bacteria or by fungi (Levashina et al., 1998). Crosstalk from the Imd pathway to the Toll pathway was examined by measuring *Mtk* mRNA levels in *E. coli* infected Drosophila. The *Mtk* level was not significantly different between the genotype tested (Figure 6-11a). This suggests that GSNOR might not be required for activation of *Mtk* by gram-negative bacteria and presumably the Toll pathway is responsible to gram-negative bacteria. The crosstalk between the Toll and Imd pathways is still inconclusive; however currently, there is an increasing amount of evidence regarding this crosstalk. Crosstalk has been discovered at more than one level from the beginning of the Toll pathway. The gram-positive bacterial receptors PGRP-SA and PGRP-SD were shown to have an affinity for DAP-type PGN from gram-negative bacteria (Wang et al., 2006; Leone et al., 2008). At the regulatory sequence of *Mtk*, there are three NF-κβ sites. One of them can bind to both Dif and Relish, while the other two can bind only to Relish (Busse et al., 2007). Therefore, if the crosstalk starts from PGRP-SA and PGRP-SD, it will suggest that GSNOR functions at the beginning of fungal infection signalling before the signals from fungal and gram-positive infection converge (Figure 6-2). Together with the data from fungal and gram-positive infections, GSNOR is very likely to regulate GNBP3, Psh and/or Nec.

(a)

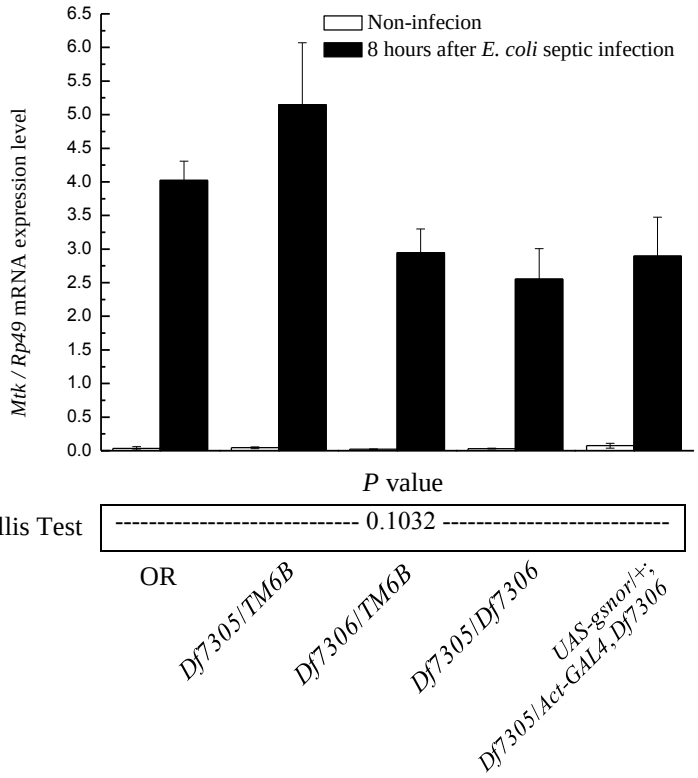

P value

Kruskal-Wallis Test	---------- 0.1032 ----------

OR

Df7305/TM6B

Df7306/TM6B

Df7305/Df7306

UAS-gsnor/+; Df7305/Act-GAL4,Df7306

(b)

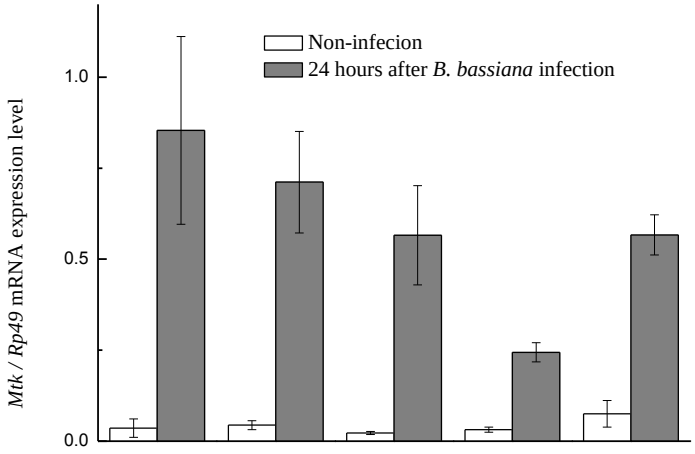

P value

Kruskal-Wallis Test	---------- 0.0137* ----------				
Mann-Whitney U Test OR		--	--	0.0119*	0.2738
Df7305/TM6B	--		--	0.0119*	0.1310
Df7306/TM6B	--	--		0.0238*	0.4524

OR

Df7305/TM6B

Df7306/TM6B

Df7305/Df7306

UAS-gsnor/+; Df7305/Act-GAL4,Df7306

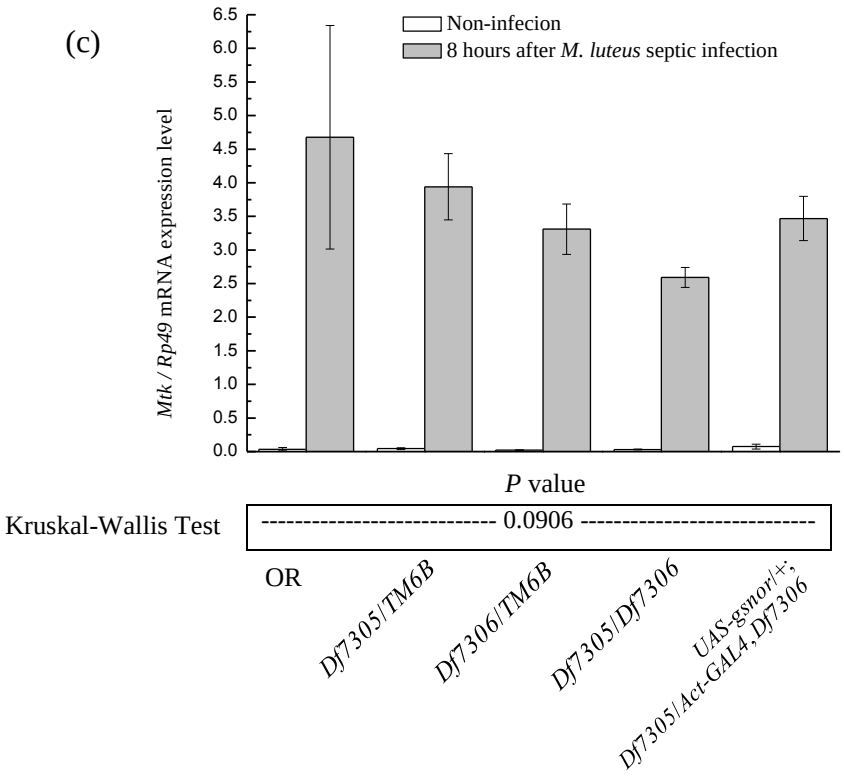

Figure 6-11. qRT-PCR quantifying level of *Mtk* mRNA in Drosophila (**a**) 8 hours after *E. coli* septic infection or without infection, (**b**) 24 hours after *B. bassiana* infection or without infection, or (**c**) 8 hours after *M. luteus* infection or without infection. The *Mtk* transcript level was normalized to the level of *Rp49* mRNA. mRNA level increases after infection but does so to the same extent to each genotype. The data represent the mean from at least three independent experiments (±SE). The table gives the *P* value from Kruskal-Wallis test to determine the probability that all infected samples come from the same population and Mann-Whitney U test for comparison of the *Mtk*/*Rp49* ratio for infected flies of each genotype compared with the value for infected OR (row one), *Df7305*/*TM6B* (row two) and *Df7306*/*TM6B* (row three). -- indicates insufficient data to do the test. Statistically significant differences are indicated by * ($P < 0.05$).

6.6 Conclusion

In Arabidopsis, GSNOR has been previously demonstrated to be important for all layers of plant disease resistance (Feechan et al., 2005). However *gsnor* knockout Drosophila did not show any increased susceptibility to septic infection by the gram-negative bacteria *E. coli* or oral infection by *Ecc*15. Melanization of the site of septic infection was not affected in *gsnor* knockout flies, suggesting this process is also not affected by the loss of *gsnor*. Interestingly for the Toll pathway, *gsnor* knockout exhibited an increased sensitivity observed from the early time points to the *B. bassiana* infection pointing out the possibility of the importance of GSNOR in the Toll pathway.

The role of GSNOR in the Imd and Toll pathway was further confirmed by the qRT-PCR measuring the transcript levels of AMPs which are the end products of these pathways. As expected the level of RNA of *Dpt*, an AMP induced by gram-negative bacteria, was similar in wild-type and *gsnor* knockout flies after *E.coli* infection. Interestingly, the *gsnor* knockout overproduced the anti-gram-positive bacteria *Def* after *M. luteus* infection. This phenomenon suggests that the GSNOR may be a negative regulator of *Def* production, or *gsnor* knockout Drosophila has the higher amount of the bacteria leading to the higher production of *Def* mRNA. Unexpectedly, there is no induction of *Def* after *B. bassiana* infection in all flies tested. This might be the first evidence indicating the specificity toward different kinds of pathogens that are responded through the Toll pathway. By producing only AMPs required for each type of infection, this possibly enhances efficiency of defence responses. Another possibility of the absence of *Def* induction might be due to the suppression of defence responses by *B. bassiana*. The quantification of anti-fungal AMPs *Drs* and *Mtk* demonstrates an important role of GSNOR for producing a normal level of *Drs* and *Mtk* after *B. bassiana* infection. This suggests that GSNOR might be required for the normal function of the fungi-triggered Toll signalling in systemic immune responses. Because GSNOR is less required for producing *Drs* and *Mtk* after *M. luteus* infection, we think that the role of GSNOR in gram-positive bacteria infection might not be as important as in the fungal infection. Because *Mtk* was also shown to be induced by gram-negative bacteria (Levashina et al., 1998), the

Mtk level after *E. coli* infection was measured to examine crosstalk between the Toll and Imd pathways.

While the results presented in this thesis show that GSNOR is required for Toll mediated response to *B. bassiana* infection. It is possible that it may also be required for other immune responses to fungal infection. Another possibility that GSNOR may be involved in alternative pathways is supported by our observation that after fungal infection *gsnor* knockout flies die much faster than *Spaetzle*, the component of the Toll pathway.

The difference between the anti-fungal AMP production in gram-positive bacteria and fungal infection may suggest where in the Toll pathway GSNOR may function. Because both gram-positive bacteria and fungi are responded through the Toll pathway, the role of GSNOR may be required before the convergence of the both signals at the fungal receptor level. The *Mtk* level of gram-negative bacteria infected flies was not altered in the *gsnor* knockout mutant indicating that GSNOR is not required for signalling from the perception of gram-negative bacteria to the cross of the signal to the Toll pathway which results in the production of Toll specific AMPs. If the signal crosses to the Toll pathway at PGRP-SA and PGRP-SD (Wang et al., 2006; Leone et al., 2008), this might suggest that GSNOR might function at the fungal receptor level. The possible candidates were GNBP3, Psh and/or Nec.

Chapter 7 Psh is a Potential *S*-Nitrosylation Target Regulated by GSNOR.

7.1 Introduction

The results in Chapter 6 indicate lower induction of *Drs* and *Mtk* mRNA after *B. bassiana* infection in *gsnor* mutant flies as compared to wild-type, whereas there is only a slight effect on induction after infection with *M. luteus*. Since both fungi and gram-positive bacteria trigger the Toll pathway, we believe that GSNOR might function somewhere between the initiation of defence signalling due to fungal infection and before the signal combined with a signal generated from gram-positive bacteria. Therefore GNBP3, Psh and/or Nec might be controlled by GSNOR (Figure 6-2). The amino acid sequences of these three proteins were checked to see whether there is any cysteine residue. Psh, a serine protease, was the only protein which has cysteines.

Psh contains 17 cysteines in a sequence of 394 amino acids. It is initially produced as a zymogen which contains a CLIP-prodomain for protein-protein interaction on the N-terminus and a serine protease domain on the C-terminus (Ligoxygakis et al., 2002). It has been proposed that Psh autocleaves its CLIP domain and the autocleaved Psh serves as a sentinel for sensing PR1 protease produced by invading *B. bassiana*. If PR1 is present, it cleaves Psh leading to the activation of the Toll signalling pathway (Gottar et al., 2006). Moreover, in Arabidopsis the serine protease ClpP has been shown to be *S*-nitrosylated *in vitro* (Romero-Puertas et al., 2008).

7.2 GSNOR might function in a denitrosylation process of Psh.

We have modeled the Psh 3D structure using web-based program ‘Phyre2’ (Kelley and Sternberg, 2009) in order to identify cysteines that may be solvent exposed cysteines. We have identified 11 potential surface cysteines which are

potentially targets for being *S*-nitrosylated (Cys 30, 40, 46, 67, 77, 78, 83, 84, 125, 335 and 366) (Figure 7-1).

BST followed by Western blot using antibody against Psh was performed in order to detect protein specific *in vivo S*-nitrosylation of Psh. *S*-Nitrosylation was detected at a low level in OR without any infection. This preliminary result suggests that Psh is *S*-nitrosylated at a normal condition. At nine hours after *B. bassiana* infection, the *S*-nitrosylation level was elevated to an equal level in all genotypes tested (OR, *Df7305*/*Df7306* and *act5c*:*UAS-gsnor*; *Df7305*/*Df7306*). At 24 hours after the infection, defence responses against fungi have already initiated resulting in AMPs production (Figure 6-10a and 6-11b). In OR and *act5c*:*UAS-gsnor*; *Df7305*/*Df7306*, the *S*-nitrosylation level decreased to below the basal level (because the input control of *act5c*:*UAS-gsnor*; *Df7305*/*Df7306* was higher than the others, the actual *S*-nitrosylation level should be lower than the present band). However for *Df7305*/*Df7306*, the *S*-nitrosylation level was still maintained with a slight reduction (Figure 7-3a). This phenomenon suggests an important role of GSNOR in a protein specific denitrosylation process of Psh protein which possibly involves with elicitation of proper immune responses, and this is also the first evidence demonstrating that Drosophila Psh is *S*-nitrosylated.

We also examined other protein targets previously shown to be *S*-nitrosylated. Glyceraldehyde-3-phosphate dehydrogenase (GAPDH) is one of the most used housekeeping genes in comparisons of gene expression. It is commonly known for catalyzing the sixth step of glycolysis by converting glyceraldehyde 3-phosphate to D-glycerate 1,3-bisphosphate. In Arabidopsis and mammals, GAPDH has been shown to be *S*-nitrosylated resulting in an inhibition of its activity (Padgett and Whorton, 1995; Mohr et al., 1996; Lindermayr et al., 2005). Because it is a highly conserved protein and the cysteine shown to be *S*-nitrosylated is conserved between plants, Drosophila and humans (Figure 7-2), GAPDH is very likely to be *S*-nitrosylated in Drosophila. Moreover, because of GAPDH cellular abundance (Sawa et al., 1997), *S*-nitrosylated GAPDH might represent a global *S*-nitrosylation level.

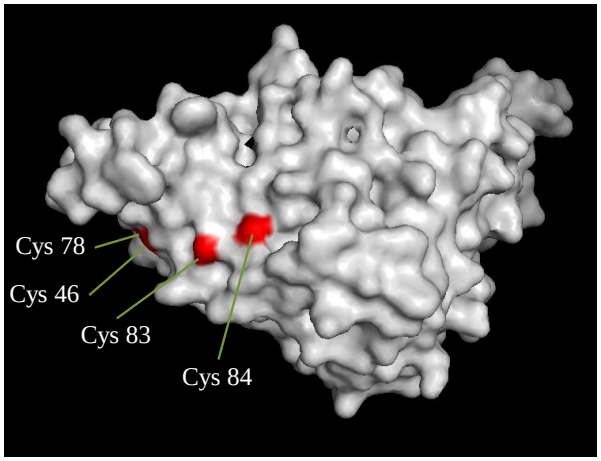
Cys 78
Cys 46
Cys 83
Cys 84

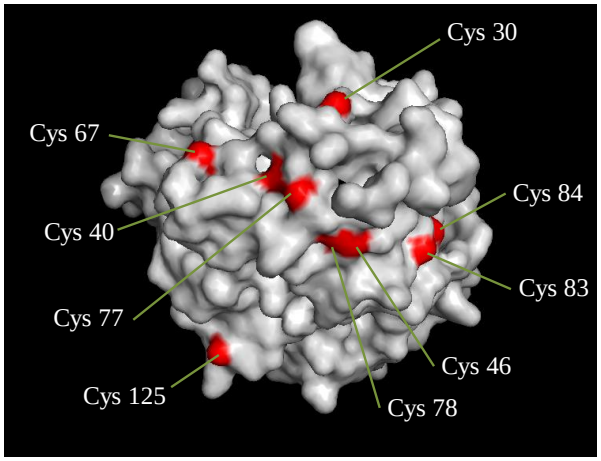
Cys 30
Cys 67
Cys 84
Cys 40
Cys 83
Cys 77
Cys 46
Cys 125
Cys 78

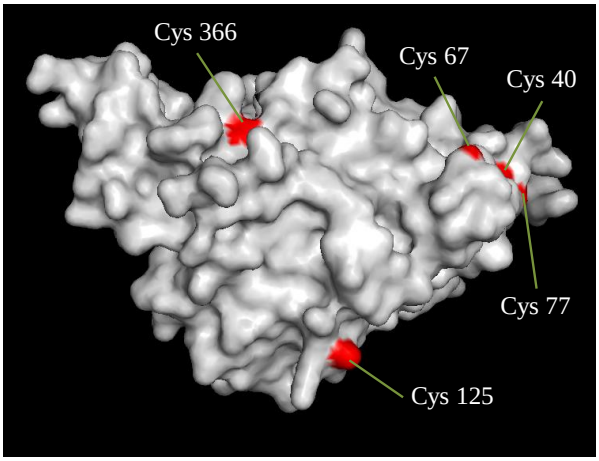
Cys 366
Cys 67
Cys 40
Cys 77
Cys 125

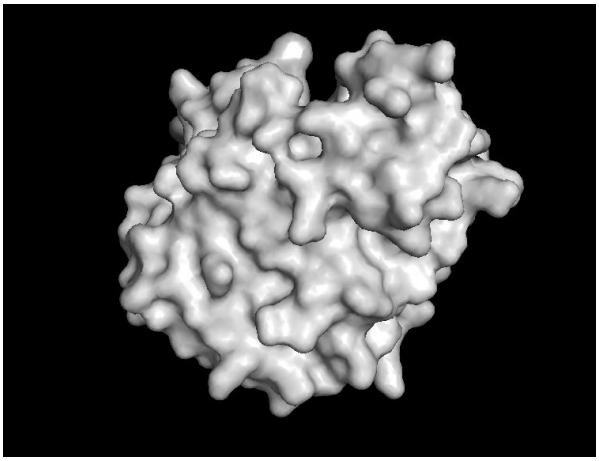

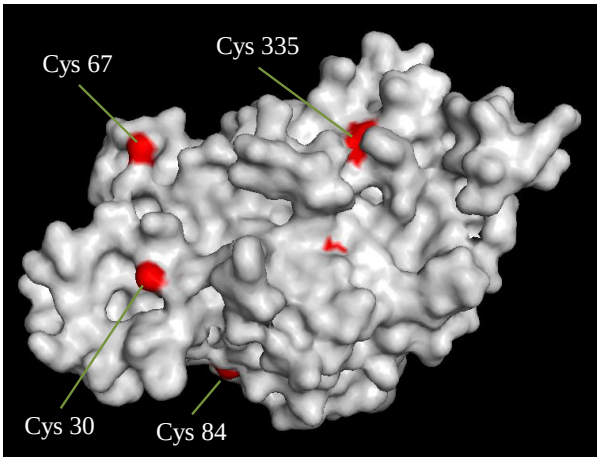
Cys 67
Cys 335
Cys 30
Cys 84

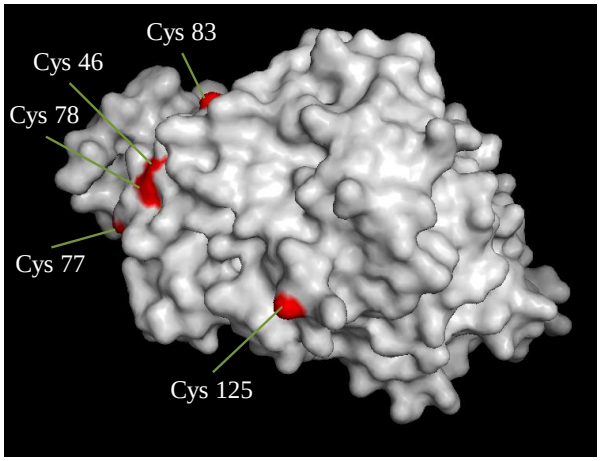
Cys 83
Cys 46
Cys 78
Cys 77
Cys 125

Figure 7-1. Psh 3D structure predicted by Phyre2 (Kelley and Sternberg, 2009) with 94% of residues modelled at >90% confidence. Red colour labels solvent exposed sulfer atoms of cysteines which are potentially targets for S-nitrsylation. The numbers indicate the position of cysteines in the Psh peptide chain. Each figure represents different viewing positions of Psh illustrated by highlighted areas of the adjacent boxes.

```
DmGAPDH MS------------------------------------------------------------KIGINGFGRIGRLVLRAA 20
HsGAPDH MG------------------------------------------------------------KVKVGVNGFGRIGRLVTRAA 22
AtGAPDH MASVTFSVPKGFTEFSGLRSSSASLPFGKKLSSDEFVSIVSFQTSAMGSSGGYRKGVTEAKLKVAINGFGRIGRNFLRCW 80
        *.                                                          *:.:******** . *.

DmGAPDH I---DKG-ASVVAVNDPFIDVNYMVYLFKFDSTHGRFKGTVAAEGG-FLVVNGQKITVFSERDPANINWASAGAEYVVES 95
HsGAPDH F---NSGKVDIVAINDPFIDLNYMVYMFQYDSTHGKFHGTVKAENG-KLVINGNPITIFQERDPSKIKWGDAGAEYVVES 98
AtGAPDH HGRKDSP-LDIIAINDTG-GVKQASHLLKYDSTLGIFDADVKPSGETAISVDGKIIQVVSNRNPSLLPWKELGIDIVIEG158
            :.   .::*:**.  .::   :::::*** * *.. * ...   : ::*: * :..:*:*: : * . * : *:*.
                                                          ↓  ↓
DmGAPDH TGVFTTIDKASTHLKGGAKKVIISAPS-ADAPMFVCGVNLDAYSPDMKVVSNASCTTNCLAPLAKVINDNFEIVEGLMTT174
HsGAPDH TGVFTTMEKAGAHLQGGAKRVIISAPS-ADAPMFVMGVNHEKYDNSLKIISNASCTTNCLAPLAKVIHDNFGIVEGLMTT177
AtGAPDH TGVFVDREGAGKHIEAGAKKVIITAPGKGDIPTYVVGVNADAYSHDEPIISNASCTTNCLAPFVKVLDQKFGIIKGTMTT238
        ****.  : *. *::.***:***:**. .* * :* *** : *. .  ::************:.**:.::* *::* ***

DmGAPDH VHATTATQKTVDGPSGKLWRDGRGAAQNIIPAATGAAKAVGKVIPALNGKLTGMAFRVPTPNVSVVDLTVRLGKGATYDE254
HsGAPDH VHAITATQKTVDGPSGKLWRDGRGALQNIIPASTGAAKAVGKVIPELNGKLTGMAFRVPTANVSVVDLTCRLEKPAKYDD257
AtGAPDH THSYTGDQRLLDASHRDL-RRARAAALNIVPTSTGAAKAVALVLPNLKGKLNGIALRVPTPNVSVVDLVVQVSKKTFAEE317
        .*: *. *: :*..  .* * .*.*  **:*::*******. *:* *:***.*:*:****.*******. :: * :  ::

DmGAPDH IKAKVEEASKGPLKGILGYTDEEVVSTDFFSDTHSSVFDAKAGISLNDKFVKLISWYDNEFGYSNRVIDLIKYMQ-SKD 332
HsGAPDH IKKVVKQASEGPLKGILGYTEHQVVSSDFNSDTHSSTFDAGAGIALNDHFVKLISWYDNEFGYSNRVVDLMAHMA-SKE 335
AtGAPDH VNAAFRDSAEKELKGILDVCDEPLVSVDFRCSDFSTTIDSSLTMVMGDDMVKVIAWYDNEWGYSQRVVDLADIVANNWK 396
        ::  ..::::  *****.  :. :** ** .. .*:.:*:   : :.*.:**:*:*****:***:**:**   :  . .
```

Figure 7-2. Amino acid sequence alignment of *D. melanogaster* GAPDH (DmGAPDH), human GAPDH (HsGAPDH), and *A. thaliana* GAPDH (AtGAPDH). Cysteines are marked in red. The red arrow indicates cysteine residues previously shown to be *S*-nitrosylated (a cysteine at position 152 of HsGAPDH). The black arrow indicates cysteines found to be conserved among compared peptides. For the degree of similarity, (*) indicates positions which have a single, fully conserved residue, (:) indicates where one of the 'strong' groups (STA, NEQK, NHQK, NDEQ, QHRK, MILV, MILF, HY and FYW) is fully conserved, (.) indicates where one of the 'weaker' groups (CSA, ATV, SAG, STNK, STPA, SGND, SNDEQK, NDEQHK, NEQHRK, FVLIM and HFY) is fully conserved. The alignment was generated from T-Coffee sequence alignment program (Notredame et al., 2000).

When the BST together with Western blot using GAPDH antibody was performed, *in vivo S*-nitrosylation was detected in every sample; however, no significant difference was detected between each sample (Figure 7-3c). This preliminary result suggests that GSNOR might not function in regulating *S*-nitrosylation of GAPDH, and this is the first evidence demonstrating that Drosophila GAPDH is *S*-nitrosylated. Although the UV-treated negative control did not give a band with a lower intensity, the rest of the samples should represent the level of *S*-nitrosylation of GAPDH. We think that UV-treated sample does not work efficiently in *in vivo* BST, because different SNOs have a different wavelength for NO cleavage (Gow et al., 2007) (from a personal communication with Dr. Steven Spoel, without ascorbate serves as a better negative control).

In humans, the DNA binding ability of NF-κB has been shown to be inhibited by *S*-nitrosylation. This reduces NF-κB dependent promoter activity, and NF-κB dependent gene transcription (Marshall et al., 2004). There are total of five NF-κBs in humans which can be divided into two groups. 1) p105 and p100 which are NF-κBs containing Rel homology domain (RHD) and inhibitory ankyrin repeats. 2) p65, RelB and c-Rel which are NF-κBs containing RHD and transactivation sequence. RHD is important for DNA binding, IκB binding, dimerization and nuclear localization. In the first group, the ankyrin repeats fold back and inhibit the RHD. To release NF-κB from IκB, proteolytic processing is required. For the second group, NF-κBs are bound and inhibited by IκBs which contain ankyrin repeats. IκBs have to be phosphorylated leading to ubiquitin-mediated proteosome degradation in order to release active NF-κBs (Gilmore and Ip, 2005). Before performing BST for detecting Drosophila NF-κBs, amino acid sequences from humans and Drosophila were aligned in order to observe whether the previously reported *S*-nitrosylated cysteines (a cysteine at position 62 of p105 and a cysteine at position 38 of p65 (Marshall et al., 2004)) are conserved in Drosophila. Comparison of the amino acid sequences of p105, p100 and Relish, shows that the cysteine at position 62 of p105 is not conserved in Drosophila Relish; however, the other two cysteines have been found to be conserved in these proteins (Figure 7-4a). The cysteine at position 38 of p65 is conserved in RelB, c-Rel, Dif and Dorsal. There are an additional four conserved cysteines in these proteins (Figure 7-4b). *S*-Nitrosylated Relish and Dorsal were then

measured by BST followed by Western blot using Relish and Dorsal antibodies. We cannot detect any signal from Western blot even in positive controls. Because Relish and Dorsal can be detected at low level in input controls, their protein amount is probably too low to be detected after BST.

IκB is another candidate which we would like to examine the *S*-nitrosylation of this protein. Even though IκB has not been shown to be *S*-nitrosylated in all organisms, its function in binding and inhibiting NF-κB may reveal a potential of *S*-nitrosylation in IκB probably by transnitrosylation from NF-κB to IκB. After performing BST followed by Western blot using Cactus (Drosophila IκB) antibody, *in vivo S*-nitrosylation was detected in every samples, but the difference among each sample was not clear (Figure 7-3b and d). These preliminary results suggest that GSNOR again might not have a role in regulating *S*-nitrosylation of IκB *in vivo*. Nonetheless, this is the first evidence indicating that the IκB protein is *S*-nitrosylated.

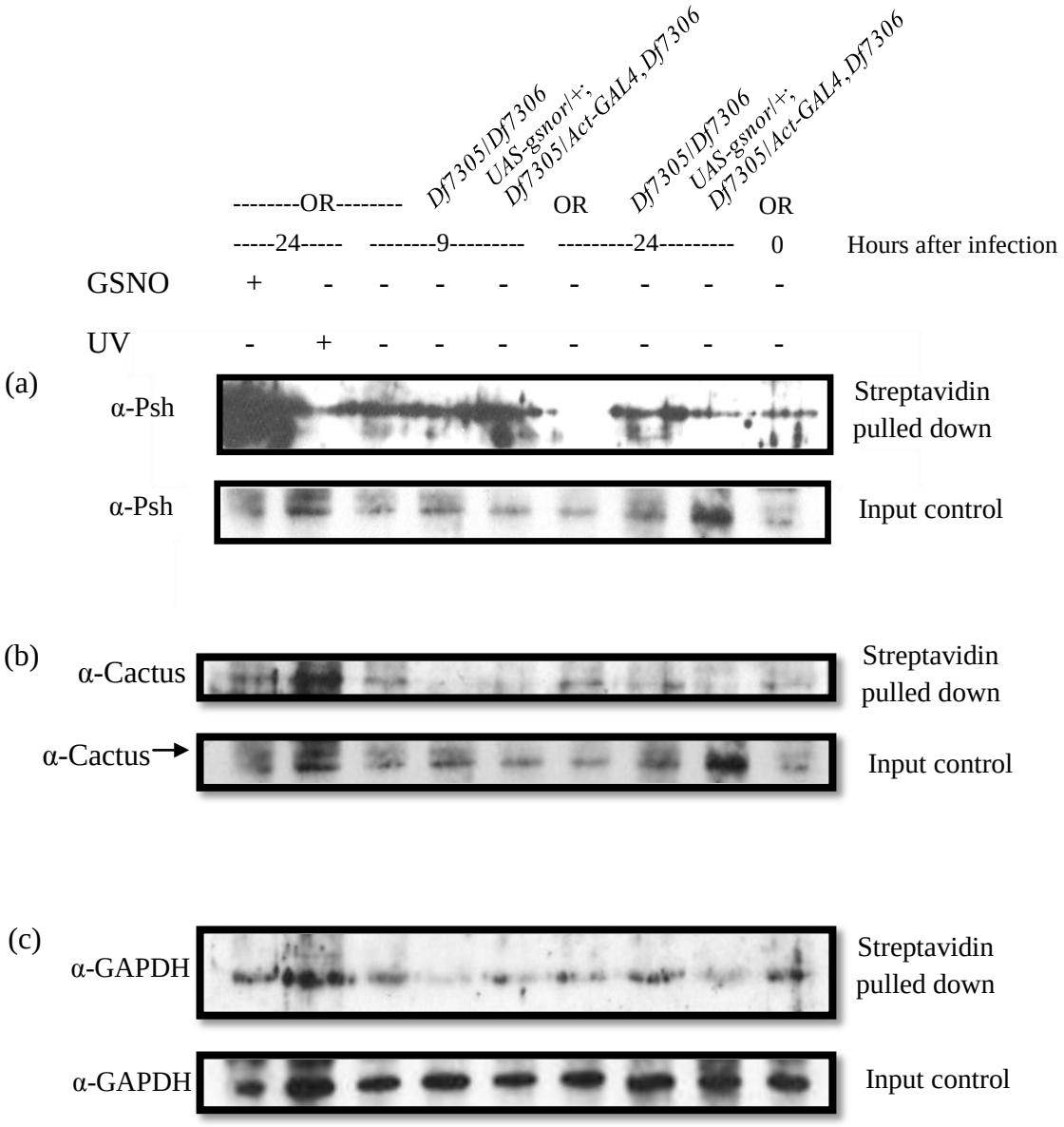
Df7305/Df7306
UAS-gsnor/+;
Df7305/Act-GAL4,Df7306
Df7305/Df7306
UAS-gsnor/+;
Df7305/Act-GAL4,Df7306
--------OR--------
OR
OR
-----24-----
--------9---------
---------24---------
0
Hours after infection
GSNO
+ - - - - - - - -
UV
- + - - - - - - -
(a)
α-Psh
Streptavidin pulled down
α-Psh
Input control
(b)
α-Cactus
Streptavidin pulled down
α-Cactus
Input control
(c)
α-GAPDH
Streptavidin pulled down
α-GAPDH
Input control

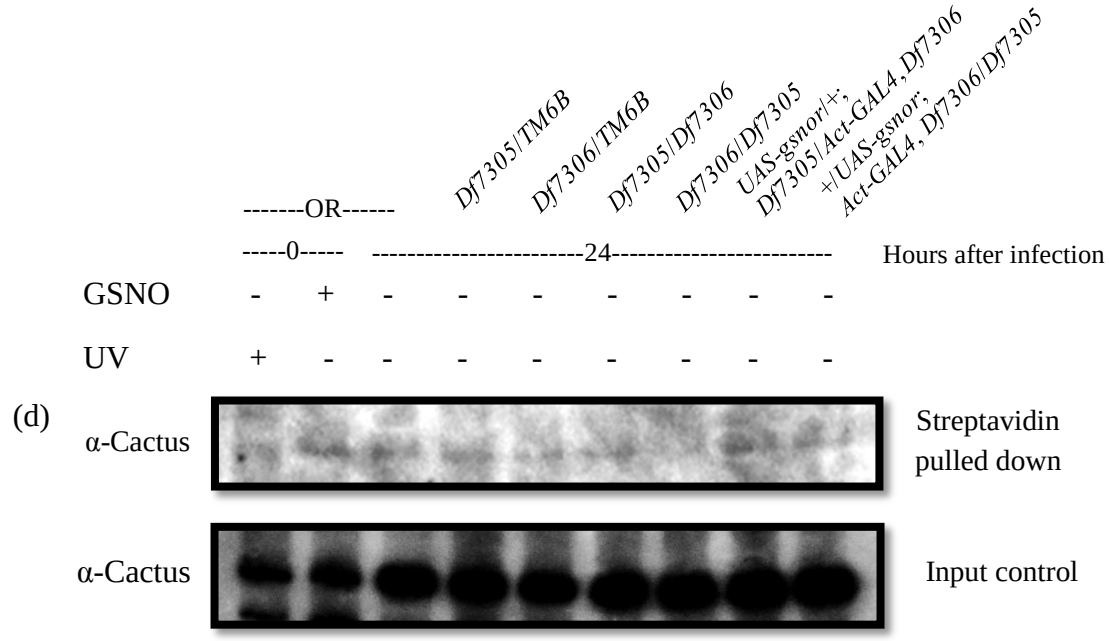

Figure 7-3. BST followed by Western blot using specific antibodies to quantify *S*-nitrosylation level of Psh (a), Cactus (b and d) and GAPDH (c). The numbers (0, 9 and 24) indicate sample collecting time point after *B. bassiana* infection. Samples treated with GSNO were used as positive controls and samples treated with UV which specifically remove NO out of SNO groups were used as negative controls.

(a)

```
Relish LNNGGICQLGATNLINSTGVSFGVANVTSFGNMYMDHQYFVPAPATVPPSQNFGYHQNGLASDGDIKHVPQLRIVEQPVE 160
p100   ------------------------------------------------------------------TADGPYLVIVEQPKQ 48
p105   ------------------------------------------------------------------TADGPYLQILEQPKQ 53
                                                                          . * * *:*** :

Relish K-FRFRYKSEMHGTHGSLNGANSKRTPKTFPEVTLCNYDGPAVIRCSLFQTNLD--SPHSHQLVVRKD-DRDVCDPHDLH 236
p100   RGFRFRYGCEG-PSHGGLPGASSEKGRKTYPTVKICNYEGPAKIEVDLVT-HSDPPRAHAHSLVGKQCSELGICAVS--- 123
p105   RGFRFRYVCEG-PSHGGLPGASSEKNKKSYPQVKICNYVGPAKVIVQLVT-NGKNIHLHAHSLVGKHC-EDGICTVT--- 127
       : ***** .*   :**.* **.*::  *::* *.:*** *** :  .*.  : .    *:*.** ::  : .:*
```

(b)

```
Dorsal G------------QQSLNYNGLPAQ-----QQQQLA--QSTKNVRKKPYVKITEQPAGKALRFRYECEGRSAGSIPGVNS 79
Dif    GAVGGGGAAHHILSQSTSLPVMPSHIPLHLQNQNMNQNLPEPSARSGPHLRIVEEPTSNIIRFRYKCEGRTAGSIPGMNS 110
p65    ------------------FPLIFPA---------------EPAQASGPYVEIIEQPKQRGMRFRYKCEGRSAGSIPGERS 51
RelB   PRLVSRGAAS--LSTVTLGPVAPPATPPPWGCPLGRLVSPAPGPGPQPHLVITEQPKQRGMRFRYECEGRSAGSILGESS 157
C-Rel  ----------------------------------------SGAYNPYIEIIEQPRQRGMRFRYKCEGRSAGSIPGEHS 40
                                                 *:: * *:*  . :****:****:**** *  *

Dorsal -TPENKTYPTIEIVGYKGRAVVVVS--CVTKDTPYRPHPHNLVGKE---GCKKGVCTLEINSET-MRAVFSNLGIQCVKK 152
Dif    SSETGKTFPTIEVCNYDGPVIIVVS--CVTSDEPFRQHPHWLVSKEEADACKSGIYQKKLPPEE-RRLVLQKVGIQCAKK 187
p65    -TDTTKTHPTIKINGYTGPGTVRIS--LVTKDPPHRPHPHELVGKD----CRDGFYEAELCPDR-CIHSFQNLGIQCVKK 123
RelB   -TEASKTLPAIELRDCGGLREVEVTACLVWKDWPHRVHPHSLVGKD----CTDGICRVRLRPHVSPRHSFNNLGIQCVRK 232
C-Rel  -TDNNRTYPSIQIMNYYGKGKVRIT--LVTKNDPYKPHPHDLVGKD----CRDGYYEAEFGQER-RPLFFQNLGIRCVKK 112
        :   :* *:*:: .  *   : ::   * .: *.: *** **.*:    * .*    .:  .      :.::**:*.:*

Dorsal KDIEAALKAREEIRVDPFKTGFSHRFQPSSIDLNSVRLCFQVFMESEQKGRFTSPLPPVVSEPIFDKKA--MSDLVICRL 230
Dif    LEMRDSLVERERRNIDPFNAKFDHKDQIDKINRYELRLCYQAFITV---GNSKVPLDPIVSSPIYGKS----SELTITRL 260
p65    RDLEQAISQRIQTNNNPFQVPIEE--QRGDYDLNAVRLCFQVTVRD-PSGRP-LRLPPVLSHPIFDNRAPNTAELKICRV 199
RelB   KEIEAAIERKIQLGIDPYNAGSLK--NHQEVDMNVVRICFQASYRD-QQGQM-RRMDPVLSEPVYDKKSTNTSELRICRI 308
C-Rel  KEVKEAIITRIKAGINPFNVPEKQLNDIEDCDLNVVRLCFQVFLPD-EHGNLTTALPPVVSNPIYDNRAPNTAELRICRV 191
        ::. ::  : .   :*::.   .  :  . :   :*:*:*.       *.    : *::* *::.:     ::* * *:

Dorsal CSCSATVFGNTQIILLCEKVAKEDISVRFFEEK-NGQSVWEAFGDFQHTDVHKQTAITFKTPRYHTLDITEPAKVFIQLR 309
Dif    CSCAATANGGDEIIMLCEKIAKDDIEVRFYETDKDGRETWFANAEFQPTDVFKQMAIAFKTPRYRNTEITQSVNVELKLV 340
p65    NRNSGSCLGGDEIFLLCDKVQKEDIEVYFTG------PGWEARGSFSQADVHRQVAIVFRTPPYADPSLQAPVRVSMQLR 273
RelB   NKESGPCTGGEELYLLCDKVQKEDISVVFSR------ASWEGRADFSQADVHRQIAIVFKTPPYEDLEIVEPVTVNVFLQ 382
C-Rel  NKNCGSVRGGDEIFLLCDKVQKDDIEVRFVL------NDWEAKGIFSQADVHRQVAIVFKTPPYCK-AITEPVTVKMQLR 264
          ...  *. :: :**:*: *:**.* *          * . . *. :**.:* **.*:** *    :  .. * : *
```

Figure 7-4. Amino acid sequence alignment of (**a**) NF-κBs containing RHD and ankyrin repeats and (**b**) NF-κBs containing RHD and transactivation domain. Cysteines are marked as red. Red arrows indicate cysteine residuals previously shown to be *S*-nitrosylated (a cysteine at position 62 of p105 (a) and a cysteine at position 38 of p65 (b)). Black arrows indicate all cysteines found to be conserved among compared proteins. For the degree of similarity, (*) indicates positions which have a single, fully conserved residue, (:) indicates where one of the 'strong' groups (STA, NEQK, NHQK, NDEQ, QHRK, MILV, MILF, HY and FYW) is fully conserved, (.) indicates where one of the 'weaker' groups (CSA, ATV, SAG, STNK, STPA, SGND, SNDEQK, NDEQHK, NEQHRK, FVLIM and HFY) is fully conserved. The alignment was generated from T-Coffee sequence alignment program (Notredame et al., 2000).

7.3 Proposed model for regulation of *S*-nitrosylation of Psh

From the BST and total SNO level, the results suggest that *S*-nitrosylation is possibly regulated specifically at the level of individual proteins. We have shown that GSNOR regulates Psh, but not Cactus and GAPDH (Figure 7-3). After the fungal infection, the fluctuation of the *S*-nitrosylation level of Psh was observed (Figure 7-3a). This fluctuation resembles the free NO pattern produced from Drosophila infected with parasitoid wasps that free NO concentration is increased rapidly after the parasitoid infection and then decreased to below the initial level. Carton et al. (2009) have proposed that NO and NO derivatives, which have cytotoxic and cytoprotective abilities, are rapidly produced in order to act as an early response toward invading pathogens. The decrease of the free NO to below the initial level is proposed to act as a signal for later defence responses (Carton et al., 2009).

We think that the fluctuation of *S*-nitrosylation level in Psh might be a result from the immediate production of NO for the direct toxicity after the infection, and the regulation of this nitrosative stress for preventing host cell damage and generating defence signalling. We proposed that under normal non-infected conditions *S*-nitrosylation level of Psh might be maintained at a certain level (Figure 7-3a). Production of free NO after infection is not only toxic to pathogens, but also possibly *S*-nitrosylates its protein targets as detected in the increment of Psh *S*-nitrosylation level after nine hours after the fungal infection (Figure 7-3a). However, cells cannot maintain high NO levels for a long time because NO is toxic to host cells as well. Drosophila requires a mechanism for removing NO. GSNOR is one of the mechanisms that indirectly removes NO via GSNO intermediate without returning NO back to the cellular environment. This might decrease NO in both free form and the protein-bound form. The decrease in protein *S*-nitrosylation might initiate the defence signal transduction. One of the defence signals is possibly the decrease in *S*-nitrosylation Psh in wild-type flies, but not Psh in *gsnor* knockout. We believe that this reduction in the *S*-nitrosylation level of Psh might be essential for the proper Toll immune responses to produce AMPs against the fungal infection (Figure 7-5). We also believe that there might be target specificity in each denitrosylation system and that possibly explain why there is a difference in *S*-

nitrosylation level between Psh in wild-type files and *gsnor* knockout flies, but not between Cactus or GAPDH in wild-type files and *gsnor* knockout flies. Possibly other denitrosylation systems, such as thioredoxin/thioredoxin reductase system or glutathione peroxidase system, are responsible for Cactus and/or GAPDH *S*-nitrosylation.

7.4 Conclusion

Before each candidate was examined, the total *S*-nitrosylation level was measured. We cannot detect any significant difference between *gsnor* knockout and wild type as reported in Arabidopsis (Feechan et al., 2005). The three candidates were checked whether they have a possibility for being a target for *S*-nitrosylation by checking on an availability of cysteines. We found that only Psh have cysteines. The amino acid sequence of Psh was predicted for a 3D structure. We found that 11 out of 17 cysteines are the solvent exposed cysteines which are the potential cysteines for being *S*-nitrosylated. The *in vivo* BST followed by Western blots was adopted to examine Psh and other potential targets for *S*-nitrosylation (Cactus and GAPDH). Although *gsnor* knockout Drosophila exhibited the same level of Cactus *S*-nitrosylation as in wild type, this is the first evidence indicating that Cactus is nitrosylated *in vivo* which might involve in the function of this protein. Similar to mammalian GAPDH, the *S*-nitrosylation of Drosophila GAPDH was observed, however, there is no difference between wild type and *gsnor* knockout Drosophila. This suggests that GSNOR might not involve in the regulation of *S*-nitrosylation levels of Cactus and GAPDH.

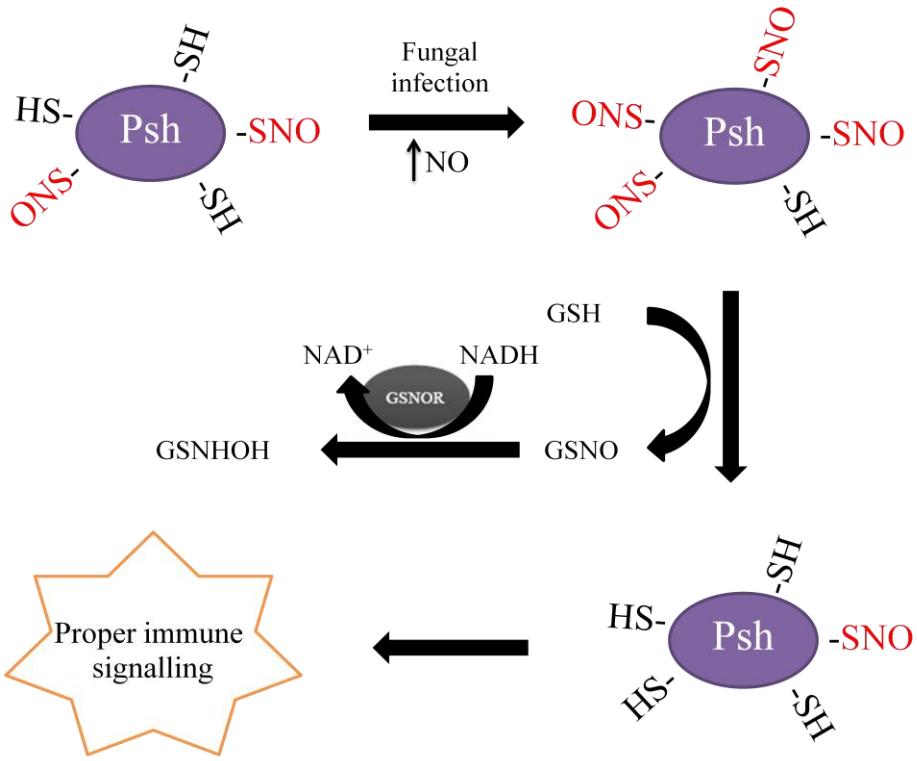

Figure 7-5. A diagram demonstrating how *S*-nitrosylation level of Psh might be regulated. Under normal condition, *S*-nitrosylation level of Psh is possibly maintained at a certain level. After an infection Psh might be heavily *S*-nitrosylated due to the production of NO. In order to convey a normal immune signalling, Psh possibly has to be denitrosylated by GSNOR until the *S*-nitrosylation level of Psh is below the initial level.

We have shown that Psh is *S*-nitrosylated *in vivo* and there is a potential that GSNOR regulates the *S*-nitrosylation level of Psh due to the difference in *S*-nitrosylation level between wild type and *gsnor* knockout at 24 hours after *B. bassiana* infection. From this study, we have proposed the model of the *S*-nitrosylation of Psh regulated by GSNOR. Psh is possibly *S*-nitrosylated at a normal condition. After fungal infection, the *S*-nitrosylation level of Psh might be increased potentially by the increased NO production required for the direct toxicity toward pathogens (Carton et al., 2009). In order to exhibit proper immune responses, GSNOR is possibly required to indirectly denitrosylate Psh via GSNO intermediate. When the *S*-nitrosylation level of Psh is below the level at the normal condition, the appropriate immune responses could be subsequentially triggered. However, if GSNOR is absent as in *gsnor* knockout, Psh might not be able to be denitrosylated (as observed in 24 hours after fungal infection (Figure 7-3a)). This defect in denitrosylation possibly impairs the defence signalling leading to the susceptible phenotype as observed in *gsnor* knockout after B. *bassiana* infection.

Chapter 8 General Discussion

8.1 The overlapping deficiency *Df7305*/*Df7306* Drosophila is a *gsnor* knockout exhibiting absent and/or deformed tergites.

Overexpression of GSNOR under control of the *actin* promoter linked with *GAL4* (*act5c*:*UAS-gsnor*; *Df7305*/*Df7306*) restores GSNOR activity. We have shown that *Df7305*/*Df7306* Drosophila, and flies from the reciprocal cross (*Df7306*/*Df7305*) are *gsnor* deficient, due to loss of *gsnor* genomic DNA, *gsnor* mRNA, GS-FDH activity and GSNOR activity. Moreover, the *gsnor* with the endogenous upstream and downstream non-coding regions (*EP-gsnor*/*EP-gsnor*; *Df7305*/*Df7306*) expressed GSNOR activity below that displayed by wild type. *gsnor* loss of function Drosophila shows three distinct phenotypes, namely tergite development, female fertility, and immunity to fungal infection. All or some of the phenotypic effects observed in *gsnor* loss of function Drosophila could be the effects of loss of GS-FDH activity, but not GSNOR activity.

gsnor knockout Drosophila exhibit a deformed tergite phenotype (70-80 % in females and 60 % in males). Their phenotype is complemented by *act5c*:*UAS-gsnor*; *Df7305*/*Df7306* and *EP-gsnor*/*EP-gsnor*; *Df7305*/*Df7306* indicating that the effect on tergites of *gsnor* knockout flies is due to the loss of GSNOR activity. Interestingly, *EP-gsnor*/*EP-gsnor*; *Df7305*/*Df7306* flies recover the wild-type phenotype more efficiently than *act5c*:*UAS-gsnor*; *Df7305*/*Df7306*, even though this line express very low GSNOR activity. However, *EP-gsnor*/*EP-gsnor*; *Df7305*/*Df7306* flies cannot complement the disease phenotype of *Df7305*/*Df7306* flies. Interestingly, this may suggest that different biological processes may require different GSNOR activity, and as a consequence, different *S*-nitrosylation levels and status for each biological process to function as normal.

NO has been proposed as a cell proliferation inhibitor (Sharma et al., 1999; Pervin et al., 2001; Wedgwood and Black, 2003). Drosophila treated with NO inhibitors shows oversized legs, tergites, sternites, genital structures, and wings. In contrast, ectopic expression of a mouse NOS reduces the size of limbs in adult flies

(Enikolopov et al., 1999). In *gsnor* knockout flies, the absence and malformation of tergites may be due to increased NO levels due to GSNOR activity. However, the phenotype is only observed in tergites. This is possibly due to the specificity of the denitrosylation process by GSNOR. The specificity may occur by transnitrosylation between SNO proteins and NO recipient molecules, or GSNOR might require an adapter protein to control the specific denitrosylation process. The GSNOR might denitrosylate only protein required for tergite formation, but not for others which shape independent developmental processes.

8.2 GSNOR is required for fertility in female Drosophila.

GSNOR activity is also required for female fertility in Drosophila. Interestingly, this phenomenon has also been observed in Arabidopsis, This may suggest a conserved function for GSNOR activity in fertility between plants and animals. A low hatching frequency and egg retention phenotypes were observed in *gsnor* knockout Drosophila. The low hatching frequency might be due to a defect in cell proliferation of follicle cells. This is because the follicle cells which produce the eggshell are defective in *gsnor* knockout Drosophila. The egg retention phenotype might be because GSNOR is involved in neurotransmission steps required to induce oviduct contraction and relaxation required for egg laying. Alternatively, this might be a consequence of defective follicle cell formation that can occur when expression of M6 protein is decreased (Zappia et al., 2011).

Follicle cell formation is a critical process in oogenesis and these cells are required in many important egg development processes. Because NO can function as a cell proliferation inhibitor (Villalobo, 2006), the GSNOR system might remove *S*-nitrosylated proteins through a specific denitrosylation process. These denitrosylated proteins could be required for proper function of follicle cell proliferation, but not for other cell type proliferation. It is also speculated a similar mechanism may be required for the loss and malformed tergite phenotype.

8.3 GSNOR is required for immunity against fungal infection and anti-fungal AMP expression.

GSNOR in Drosophila functions in immunity against *B. bassiana* infection, but not *E. coli* septic or *Ecc*15 oral infection. In Arabidopsis, GSNOR has been also shown to be important for all three major layers of plant disease resistance (basal, R gene-mediated, and non-host disease resistance) (Feechan et al., 2005). This phenomenon may suggest a conserved function for GSNOR between plants and animals.

We could not detect any significant difference in the transcript level of *Dpt*, which is an AMP against gram-negative bacteria, between *gsnor* knockout, the complementation, OR, *Df7305*/*TM6B*, and *Df7306*/*TM6B*, comfirming that GSNOR does not function in the Imd pathway. Although we did not test the survival of *gsnor* knockout flies with gram-positive bacteria infection, the qRT-PCR data suggests that the *gsnor* knockout can still produce *Def* indicating a normal response to gram-positive bacterial infection. This is because the transcript level of *Def*, which is an AMP against gram-positive bacteria, is significantly higher in the *M. luteus* infected *gsnor* knockout Drosophila than OR, *Df7305*/*TM6B* and *Df7306*/*TM6B*. Moreover, after *M. luteus* infection the transcript level of *Mtk*, which is an AMP against gram-positive bacteria and fungi, is not affected by the loss of *gsnor*. The increase of *Def* transcript level after *M. luteus* infection in *gsnor* knockout Drosophila might suggest a potential role of GSNOR as a negative regulator of *Def* expression. However, another possibility that could explain the increase of *Def* transcript production after *M. luteus* infection in *gsnor* knockout flies is that *gsnor* knockout flies could not control the propagation of *M. luteus*. The increased number of the bacteria leads to the increased *Def* mRNA production observed in *Df7305*/*Df7306*. Therefore, *gsnor* knockout flies might still be susceptible to gram-positive bacteria.

The qRT-PCR supports an important role for GSNOR during fungal infection. Induction of *Drs* and *Mtk* RNA is significantly reduced in *gsnor* knockout Drosophila after *B. bassiana* infection, but just slightly decreased in *gsnor* knockout after *M. luteus* infection. As Drosophila produces AMPs for fungal and gram-positive bacteria infection through the Toll pathway, we hypothesize that the

function of GSNOR is possibly at the fungal receptors at the upper stages of the pathway (before the convergence of the both signals). Further investigated revealed that only Psh has cysteines residues and this observation lead us to investigate the possibility that Psh is modified by *S*-nitrosylation.

Toll receptors are conserved between plants, insects and mammals, with many also providing a conserved immune-related function (Takeda and Akira, 2003). Our discovery that GSNOR function is important for only the Toll pathway in Drosophila but not for the Imd pathway, could possibly suggest a common feature of the primitive immune system. Evolution appears to have conserved the Toll pathway across animals and plants, and with it, an importance for proper GSNOR function.

8.4 GSNOR regulates protein specific *S*-nitrosylation levels after infection, but not global *S*-nitrosylation.

We have developed a chemiluninescence-based method for detecting SNOs present in Drosophila total protein extracts. Using this method, we could not detect a difference between the ambient SNO levels of wild-type and *gsnor* knockout flies, even if flies had previously been infected with pathogen. A similar result showing low and equal SNO levels between wild-type and *gsnor* knockout flies was also observed using BST followed by silver staining.

This could be explained if GSNOR controls *S*-nitrosylation at a protein-specific level instead of the global *S*-nitrosylation. Modificiation by *S*-nitrosylation of Psh, Cactus and GAPDH was observed in our preliminary experiment, however, only Psh showed a difference between *gsnor* knockout and wild-type Drosophila.

Upon fungal infection, two parallel signalling pathways are activated. GNBP3 recognizes fungal cell wall, and Psh recognizes PR1 (the fungal protease). This dual activation resembles the model in mammals. Specifically, mammals use Toll-like receptors to sense extracellular microbial determinants, Nod-like receptors to sense intracellular microbial determinants, and protease-activated receptor 2 (PAR2) for some proteases secreted from pathogens, which often leads to the production and secretion of AMPs and inflammatory cytokines (Shpacovitch et al., 2007; Chamy et al., 2008).

It is speculated that Psh not only senses proteases, but might also perceive (via *S*-nitrosylation) an increase in NO abundance after infection. Protein specific denitrosylation of Psh dependent on GSNOR might be required in order to convey defence signalling. Just how *S*-nitrosylation affects the function of Psh still remains to be determined. We hypothesize that *S*-nitrosylated Psh might enhance the inhibition by Nec, or inhibit the protease activity or the proteolytic activation of Psh. These events might block signal progression to downstream proteases.

In Drosophila immunity, GSNOR may not be the key regulator of global cellular *S*-nitrosylation upon infection as is the case in Arabidopsis. Alternatively, GSNOR may function in the regulation of *S*-nitrosylation at a protein specific level. In *gsnor* knockout mice, the SNO level in blood increases concomitantly with arterial pressure pointing to a role of NO in regulating blood flow. However, in liver, where GSNOR activity is high, SNO levels in *gsnor* knockout mice are similar to the wild type. A difference only exists after an intraperitoneal injection of the extremely high amount of LPS (Liu et al., 2004). The reason there is no significant difference between *gsnor* knockout and wild-type Drosophila might be because in this study protein was extracted from the whole body, so if SNO levels are different in each organ of Drosophila, this may not be detected with an acceptable level of accuracy. Differing SNO level in the mouse liver only occurs with a high amount of LPS, which is beyond the normal LPS level of infection, so this might not represent realistic SNO levels from infection. This infers that in nature, GSNOR might not regulate the global SNO level after infection.

Asthma has been shown to be closely associated with GSNOR activity. Results of bronchoalveolar lavage of asthma patients demonstarate that GSNOR activity increases and correlates with SNO levels (Que et al., 2009). Moreover, *gsnor* knockout mice exposed to the allergen ovalbumin exhibit increased SNO levels in lungs tissue (Que et al., 2005). It would be interesting to ascertain whether *gsnor* knockout Drosophila also exhibit increased SNO levels in trachea.

8.5 Implication

It was observed that the *gsnor* knockout has increased egg retention. This may suggest that neurotransmission is affected. In humans, NO functions as a co-transmitter (Garthwaite et al., 1989; Duncan and Heales, 2005), and the same may be true for oviduct relaxation. Moreover, in Drosophila, GSNOR has been shown to be required in visual pattern memory (Hou et al., 2011) emphasizing the involvement of GSNOR in neurotransmission. We believe that the study of *gsnor* knockout in Drosophila might pave the way for better understanding the function of GSNOR in neurotransmission.

As the *gsnor* knockout results specifically in an absent and deformed tergite phenotype, and a presumed defect in follicle cell formation, but not in other tissues, suggests a role for GSNOR as a tissue-specific positive regulator of cell proliferation. It is speculated that the specificity of GSNOR is possibly due to specific transnitrosylation between SNO proteins and GSH, but not other NO acceptors, or that denitrosylation by GSNOR requires specific adapter proteins resembling mammalian nNOS (Fang et al., 2000). NO has been shown to induce cell cycle arrest of human breast cancer cell culture (Pervin et al., 2001) raising the possibility that the recently discovered inhibitors of mammalian GSNOR (Sanghani et al., 2009) might be used to specifically suppressed cancer cells without interference with non-target cells.

Drosophila has been widely used as a model organism to study human diseases and a number of studies in Drosophila innate immunity have been applied to humans, such as the discovery of the Toll receptors (Lemaitre et al., 1996). Our study might reveal a conserved role of GSNOR in human innate immunity. Possibly, GSNOR might also regulate PAR2, which is used for sensing pathogen proteases in humans (Shpacovitch et al., 2007; Chamy et al., 2008).

8.6 Conclusion and future prospects

The integrity of follicle cells in each stage of oogenesis and muscle cells of oviducts could be observed through confocal microscopy, and we could test whether

the hatching frequency phenotype could be complemented by tissue-specific expression of GSNOR in the follicle cells by using the GAL4/UAS system. If this approach can complement the phenotype, it will confirm that GSNOR is required in follicle cells to generate complete development eggs. Furthermore if defective follicle cell formation is involved in the egg retention phenotype as observed in decreased expression of M6 protein (Zappia et al., 2011), the complement flies should also lay more eggs.

We could examine whether the egg retention phenotype of *gsnor* knockout Drosophila is due to the defective neurotransmission, by measuring oviduct contraction and relaxation (in accordance to the methods described in Rodríguez-Valentín et al. (2006)) which is controlled by neurotransmission of innervating nerve cells. If the muscle can still contract and relax normally after electrical stimulation of nerve cells, it may be concluded that GSNOR is not involved in the regulation of neurotransmission controlling oviduct muscles.

GSNOR is essential for immunity against fungal infection. *gsnor* loss-of-function Drosophila reduced the transcript levels of *Drs* and *Mtk*, the two main AMPs against fungi. We have proposed that GSNOR might regulate *S*-nitrosylation at the protein specific level. Psh was shown to be *S*-nitrosylated after fungal infection and GSNOR might be required for denitrosylation of Psh which is possibly to trigger immune responses.

In order to obtain a clear explanation of how GSNOR regulates denitrosylation of Psh, protein-tagged Psh will be transformed into *psh* and *gsnor* double knockout Drosophila. *S*-Nitrosylation of Psh will be observed by BST followed by western blot with specific antibody to the tag protein. We expect to see an enhanced signal from western blot with lower background, because monoclonal antibody for the tag protein is used instead of the polyclonal anti-Psh antibody. The tagged Psh can be also used to detect cellular localization of Psh, because Psh is predicted to be in extracellular matrix, but no one has shown the actual localization.

Identification of *S*-nitrosylated cysteines in Psh is important to predict the effect of *S*-nitrosylation on the protein properties. Recombinant tagged Psh protein

could be produced from bacteria. The protein could be *S*-nitrosylated *in vitro* by adding GSNO followed by BST to exchange SNOs with S-biotins. The biotinylated cysteine will be identified by mass spectrometry (Wang et al., 2009a). The recombinant Psh with or without *in vitro S*-nitrosylation could be tested of the auto- and PR1-mediated proteolytic activation, and protease activity assay described in Harcum and Bentley (1993).

The transcript level of *gsnor* after fungal infection could be determined in order to observe whether there is a correlation between *gsnor* transcript and the *S*-nitrosylation level of Psh (or not). As Psh is an extracellular protein, demonstration that GSNOR also presents in extracellular matrix could provide stronger evidence supporting our proposed Psh model.

GSNOR shows conserved functions in fertility and immunity between Arabidopsis and Drosophila suggesting that the regulation of *S*-nitrosylation by GSNOR is a pivotal mechanism underlying fertility and immunity of plants and animals. This mechanism could also be applied to humans for deeper understanding of human fertility and immunity.

Chapter 9 Bibliography

Al-Sa'doni, H., and Ferro, A. (2000). *S*-Nitrosothiols: a class of nitric oxide-donor drugs. Clinical Science 98, 507–520.

Anderson, K. V., and Nüsslein-Volhard, C. (1984). Information for the dorsal–ventral pattern of the Drosophila embryo is stored as maternal mRNA. Nature 331, 223–227.

Andreou, A. M., and Tavernarakis, N. (2009). SUMOylation and cell signalling. Biotechnology Journal 4, 1740–1752.

Appleby, C. A. (1984). Leghemoglobin and rhizobium respiration. Annual Review of Plant Physiology and Plant Molecular Biology 35, 443–478.

Arancio, O., Kiebler, M., Lee, C. J., Lev-Ram, V., Tsien, R. Y., Kandel, E. R., and Hawkins, R. D. (1996). Nitric oxide acts directly in the presynaptic neuron to produce long-term potentiation in cultured hippocampal neurons. Cell 87, 1025–1035.

Arnot, C. J., Gay, N. J., and Gangloff, M. (2010). Molecular mechanism that induces activation of Spätzle, the ligand for the Drosophila Toll receptor. The Journal of Biological Chemistry 285, 19502–19509.

Bagga, S., Hu, G., Screen, S. E., and St. Leger, R. J. (2004). Reconstructing the diversification of subtilisins in the pathogenic fungus *Metarhizium anisopliae*. Gene 324, 159–169.

Barton, H. (2008). M.Sc. Thesis.

Basbous, N., Coste, F., Leone, P., Vincentelli, R., Royet, J., Kellenberger, C., and Roussel, A. (2011). The Drosophila peptidoglycan-recognition protein LF interacts with peptidoglycan-recognition protein LC to downregulate the Imd pathway. EMBO Reports 12, 327–333.

Bateman, R. L., Rauh, D., Tavshanjian, B., and Shokat, K. M. (2008). Human carbonyl reductase 1 is an *S*-nitrosoglutathione reductase. The Journal of Biological Chemistry 283, 35756–35762.

Belenghi, B., Romero-Puertas, M. C., Vercammen, D., Brackenier, A., Inzé, D., Delledonne, M., and Van Breusegem, F. (2007). Metacaspase activity of *Arabidopsis thaliana* is regulated by *S*-nitrosylation of a critical cysteine residue. The Journal of Biological Chemistry 282, 1352–1358.

Benhar, M., Forrester, M. T., and Stamler, J. S. (2009). Protein denitrosylation: enzymatic mechanisms and cellular functions. Nature Reviews Molecular Cell Biology 10, 721–732.

Berg, C. A. (2005). The Drosophila shell game: patterning genes and morphological change. Trends in Genetics 21, 346–355.

Bethke, P. C., Badger, M. R., and Jones, R. L. (2004). Apoplastic synthesis of nitric oxide by plant tissues. The Plant Cell 16, 332–341.

Bidla, G., Lindgren, M., Theopold, U., and Dushay, M. S. (2005). Hemolymph coagulation and phenoloxidase in Drosophila larvae. Developmental and Comparative Immunology 29, 669–679.

Bischof, J., Maeda, R. K., Hediger, M., Karch, F., and Basler, K. (2007). An optimized transgenesis system for Drosophila using germ-line-specific phi C31 integrases. Proceedings of the National Academy of Sciences of the United States of America 104, 3312–3317.

Bischoff, V., Vignal, C., Boneca, I. G., Michel, T., Hoffmann, J. A., and Royet, J. (2004). Function of the drosophila pattern-recognition receptor PGRP-SD in the detection of gram-positive bacteria. Nature Immunology 5, 1175–1180.

Bogart, K., and Andrews, J. (2006). CGB technical report 2006-10: extraction of total RNA from Drosophila. (Bloomington, Indiana).

Bondos, S. E., and Bicknell, A. (2003). Detection and prevention of protein aggregation before, during, and after purification. Analytical Biochemistry 316, 223–231.

Bonfoco, E., Krainc, D., Ankarcrona, M., Nicotera, P., and Lipton, S. A. (1995). Apoptosis and necrosis: two distinct events induced, respectively, by mild and intense insults with *N*-methyl-D-aspartate or nitric oxide/superoxide in cortical cell cultures. Proceedings of the National Academy of Sciences of the United States of America 92, 7162–7166.

Boucher, J. L., Genet, A., Vadon, S., Delaforge, M., Henry, Y., and Mansuy, D. (1992a). Cytochrome P450 catalyzes the oxidation of N^{ω}-hydroxy-L-arginine by NADPH and O_2 to nitric oxide and citrulline. Biochemical and Biophysical Research Communications 187, 880–886.

Boucher, J. L., Genet, A., Vadon, S., Delaforge, M., and Mansuy, D. (1992b). Formation of nitrogen oxides and citrulline upon oxidation of N^{ω}-hydroxy-L-arginine by hemeproteins. Biochemical and Biophysical Research Communications 184, 1158–1164.

Bownes, M. (1986). Expression of the genes coding for vitellogenin (yolk protein). Annual Review of Entomology 31, 507–531.

Bright, J., Desikan, R., Hancock, J. T., Weir, I. S., and Neill, S. J. (2006). ABA-induced NO generation and stomatal closure in Arabidopsis are dependent on H_2O_2 synthesis. The Plant Journal 45, 113–122.

Broderick, K. E., Feala, J., McCulloch, A., Paternostro, G., Sharma, V. S., Pilz, R. B., and Boss, G. R. (2006). The nitric oxide scavenger cobinamide profoundly improves survival in a *Drosophila melanogaster* model of bacterial sepsis. The FASEB Journal 20, 1865–1873.

Bryan, N. S., and Grisham, M. B. (2007). Methods to detect nitric oxide and its metabolites in biological samples. Free Radical Biology and Medicine 43, 645–657.

Buchon, N., Poidevin, M., Kwon, H.-M., Guillou, A., Sottas, V., Lee, B.-L., and Lemaitre, B. (2009). A single modular serine protease integrates signals from pattern-recognition receptors upstream of the Drosophila Toll pathway.Buchon, N., Poidevin, M., Kwon, H.-M., Guillou, A., Sottas, V., Lee, B.-L., and Lemaitre, B. (2009). A single modular serine pro. Proceedings of the National Academy of Sciences of the United States of America 106, 12442–12447.

Bulets, P., Dimarcqs, J., Hetru, C., Lagueux, M., Charlet, M., Hegy, G., Van Dorsselaer, A., and Hoffmann, J. A. (1993). A novel inducible antibacterial peptide of Drosophila carries an O-glycosylated substitution. The Journal of Biological Chemistry 268, 14893–14897.

Busse, M. S., Arnold, C. P., Towb, P., Katrivesis, J., and Wasserman, S. A. (2007). A kappaB sequence code for pathway-specific innate immune responses. The EMBO Journal 26, 3826–3835.

Carton, Y., Frey, F., and Nappi, A. J. (2009). Parasite-induced changes in nitric oxide levels in *Drosophila paramelanica*. The Journal of Parasitology 95, 1134–1141.

Carvalho, A. T. P., Swart, M., van Stralen, J. N. P., Fernandes, P. A., Ramos, M. J., and Bickelhaupt, F. M. (2008). Mechanism of thioredoxin-catalyzed disulfide reduction. Activation of the buried thiol and role of the variable active-site residues. The Journal of Physical Chemistry B 112, 2511–2523.

Cerenius, L., and Söderhäll, K. (2004). The prophenoloxidase-activating system in invertebrates. Immunological Reviews 198, 116–126.

Chamy, L. E., Leclerc, V., Caldelari, I., and Reichhart, J.-M. (2008). Sensing of "danger signals" and pathogen-associated molecular patterns defines binary signaling pathways "upstream" of Toll. Nature Immunology 9, 1165–1170.

Chang, C.-I., Ihara, K., Chelliah, Y., Mengin-Lecreulx, D., Wakatsuki, S., and Deisenhofer, J. (2005). Structure of the ectodomain of Drosophila peptidoglycan-recognition protein LCa suggests a molecular mechanism for pattern recognition. Proceedings of the National Academy of Sciences of the United States of America 102, 10279–10284.

Chang, C.-I., Pili-Floury, S., Hervé, M., Parquet, C., Chelliah, Y., Lemaitre, B., Mengin-Lecreulx, D., and Deisenhofer, J. (2004). A Drosophila pattern recognition receptor contains a peptidoglycan docking groove and unusual L,D-carboxypeptidase activity. PLoS Biology 2, E277.

Chevallet, M., Luche, S., and Rabilloud, T. (2006). Silver staining of proteins in polyacrylamide gels. Nature Protocols 1, 1852 – 1858.

Chiu, Y., Zhao, M., and Chen, Z. J. (2009). Ubiquitin in NF-KB signaling. Chemical Reviews 109, 1549–1560.

Ciani, E., Severi, S., Contestabile, A., Bartesaghi, R., and Contestabile, A. (2004). Nitric oxide negatively regulates proliferation and promotes neuronal differentiation through N-Myc downregulation. Journal of Cell Science 117, 4727–4737.

Clarkson, J. M., and Charnley, A. K. (1996). New insights into the mechanisms of fungal pathogenesis in insects. Trends in Microbiology 4, 197–203.

Cole, S. H., Carney, G. E., McClung, C. A., Willard, S. S., Taylor, B. J., and Hirsh, J. (2005). Two functional but noncomplementing Drosophila tyrosine decarboxylase genes: distinct roles for neural tyramine and octopamine in female fertility. The Journal of Biological Chemistry 280, 14948–14955.

Coleman, J. W. (2001). Nitric oxide in immunity and inflammation. International Immunopharmacology 1, 1397–1406.

Cooney, R. V, Harwood, P. J., Custer, L. J., and Franke, A. A. (1994). Light-mediated conversion of nitrogen dioxide to nitric oxide by carotenoids. Environmental Health Perspectives 102, 460–462.

Corpas, F. J., Chaki, M., Fernández-Ocaña, A., Valderrama, R., Palma, J. M., Carreras, A., Begara-Morales, J. C., Airaki, M., del Río, L. A., and Barroso, J. B. (2008). Metabolism of reactive nitrogen species in pea plants under abiotic stress conditions. Plant & Cell Physiology 49, 1711–1722.

Cui, X., Zhang, J., Ma, P., Myers, D. E., Goldberg, I. G., Sittler, K. J., Barb, J. J., Munson, P. J., Cintron, A. D. P., McCoy, J. P., et al. (2005). cGMP-independent nitric oxide signaling and regulation of the cell cycle. BMC genomics 6, 151.

Danielsson, O., Atrian, S., Luque, T., Hjelmqvist, L., Gonzàlez-Duarte, R., and Jörnvall, H. (1994). Fundamental molecular differences between alcohol dehydrogenase classes. Proceedings of the National Academy of Sciences of the United States of America 91, 4980–4984.

David, R. F. L. (1994). Long DNA palindromes, cruciform structures, genetic instability and secondary structure repair. BioEssays 16, 893–900.

Davies, S.-A. (2000). Nitric oxide signalling in insects. Insect Biochemistry and Molecular Biology 30, 1123–1138.

Delledonne, M., Zeier, J., Marocco, A., and Lamb, C. (2001). Signal interactions between nitric oxide and reactive oxygen intermediates in the plant hypersensitive disease resistance response. Proceedings of the National Academy of Sciences of the United States of America 98, 13454–13459.

Dimarcq, J., Hoffmann, D., Meister, M., Bulet, P., Lanot, R., Reichhart, J., and Hoffmann, J. A. (1994). Characterization and transcriptional profiles of a Drosophila gene encoding an insect defensin A study in insect immunity. European Journal of Biochemistry 221, 201–209.

Dimarcq, J., Keppi, E., Dunbar, B., Lambert, J., Rankine, S. M., Fothergill, J. E., and Hoffmann, J. A. (1988). Insect immunity Purification and characterization of a family of novel inducible antibacterial proteins of the predominant member, diptericin A. European Journal of Biochemistry 171, 17–22.

Doctor, A., Platt, R., Sheram, M. L., Eischeid, A., McMahon, T., Maxey, T., Doherty, J., Axelrod, M., Kline, J., Gurka, M., et al. (2005). Hemoglobin conformation couples erythrocyte *S*-nitrosothiol content to O_2 gradients. Proceedings of the National Academy of Sciences of the United States of America 102, 5709–5714.

Dordas, C., Rivoal, J., and Hill, R. D. (2003). Plant haemoglobins, nitric oxide and hypoxic stress. Annals of Botany 91, 173–178.

Duffy, J. B. (2002). GAL4 system in Drosophila: a fly geneticist's Swiss army knife. Genesis 34, 1–15.

Duncan, A. J., and Heales, S. J. R. (2005). Nitric oxide and neurological disorders. Molecular Aspects of Medicine 26, 67–96.

Durner, J., Wendehenne, D., and Klessig, D. F. (1998). Defense gene induction in tobacco by nitric oxide, cyclic GMP, and cyclic ADP-ribose. Proceedings of the National Academy of Sciences of the United States of America 95, 10328–10333.

Ea, C.-K., Deng, L., Xia, Z.-P., Pineda, G., and Chen, Z. J. (2006). Activation of IKK by TNFalpha requires site-specific ubiquitination of RIP1 and polyubiquitin binding by NEMO. Molecular Cell 22, 245–257.

Edwards, D. N., Towb, P., and Wasserman, S. A. (1997). An activity-dependent network of interactions links the Rel protein Dorsal with its cytoplasmic regulators. Development 124, 3855–3864.

Eklund, H., and Ramaswamy, S. (2008). Medium- and short-chain dehydrogenase/reductase gene and protein families. Cellular and Molecular Life Sciences 65, 3907–3917.

Eleftherianos, I., Felföldi, G., Ffrench-Constant, R. H., and Reynolds, S. E. (2009). Induced nitric oxide synthesis in the gut of *Manduca sexta* protects against oral infection by the bacterial pathogen *Photorhabdus luminescens*. Insect Molecular Biology 18, 507–516.

Enikolopov, G., Banerji, J., and Kuzin, B. (1999). Nitric oxide and Drosophila development. Cell Death and Differentiation 6, 956–963.

Ertürk-Hasdemir, D., Broemer, M., Leulier, F., Lane, W. S., Paquette, N., Hwang, D., Kim, C.-H., Stöven, S., Meier, P., and Silverman, N. (2009). Two roles for the Drosophila IKK complex in the activation of Relish and the induction of antimicrobial peptide genes. Proceedings of the National Academy of Sciences of the United States of America 106, 9779–9784.

Erwin, P. A., Lin, A. J., Golan, D. E., and Michel, T. (2005). Receptor-regulated dynamic *S*-nitrosylation of endothelial nitric-oxide synthase in vascular endothelial cells. The Journal of Biological Chemistry 280, 19888–19894.

Fang, K., Ragsdale, N. V, Carey, R. M., MacDonald, T., and Gaston, B. (1998). Reductive assays for *S*-nitrosothiols: implications for measurements in biological systems. Biochemical and Biophysical Research Communications 252, 535–540.

Fang, M., Jaffrey, S. R., Sawa, A., Ye, K., Luo, X., and Snyder, S. H. (2000). Dexras1: a G protein specifically coupled to neuronal nitric oxide synthase via CAPON. Neuron 28, 183–193.

Feechan, A., Kwon, E., Yun, B.-W., Wang, Y., Pallas, J. A., and Loake, G. J. (2005). A central role for *S*-nitrosothiols in plant disease resistance. Proceedings of the National Academy of Sciences of the United States of America 102, 8054–8059.

Fehlbaums, P., Bulets, P., Michauts, L., Lagueuxs, M., Broekaerto, W. F., Hetrus, C., and Hoffmannh, J. A. (1994). Septic injury of Drosophila induces the synthesis of a potent antifungal peptide with sequence homology to plant antifungal peptides. Insect Immunity 269, 33159–33163.

Fernandez, N. Q., Grosshans, J., Goltz, J. S., and Stein, D. (2001). Separable and redundant regulatory determinants in Cactus mediate its dorsal group dependent degradation. Development 128, 2963–2974.

Finocchietto, P. V, Franco, M. C., Holod, S., Gonzalez, A. S., Converso, D. P., Antico Arciuch, V. G., Serra, M. P., Poderoso, J. J., and Carreras, M. C. (2009). Mitochondrial nitric oxide synthase: a masterpiece of metabolic adaptation, cell growth, transformation, and death. Experimental Biology and Medicine 234, 1020–1028.

Flores-Pérez, U., Sauret-Güeto, S., Gas, E., Jarvis, P., and Rodríguez-Concepción, M. (2008). A mutant impaired in the production of plastome-encoded proteins uncovers a mechanism for the homeostasis of isoprenoid biosynthetic enzymes in Arabidopsis plastids. The Plant Cell 20, 1303–1315.

Foley, E., and O'Farrell, P. H. (2003). Nitric oxide contributes to induction of innate immune responses to gram-negative bacteria in Drosophila. Genes & Development 17, 115–125.

Forrester, M. T., Foster, M. W., Benhar, M., and Stamler, J. S. (2009). Detection of protein *S*-nitrosylation with the biotin-switch technique. Free Radical Biology & Medicine 46, 119–126.

Gangloff, M., Murali, A., Xiong, J., Arnot, C. J., Weber, A. N., Sandercock, A. M., Robinson, C. V, Sarisky, R., Holzenburg, A., Kao, C., et al. (2008). Structural insight into the mechanism of activation of the Toll receptor by the dimeric ligand Spätzle. The Journal of Biological Chemistry 283, 14629–14635.

Garcês, H., Durzan, D., and Pedroso, M. C. (2001). Mechanical stress elicits nitric oxide formation and DNA fragmentation in *Arabidopsis thaliana*. Annals of Botany 87, 567–574.

Garthwaite, J., Garthwaite, G., Palmer, R. M. J., and Moncada, S. (1989). NMDA receptor activation induces nitric oxide synthesis from arginine in rat brain slices. European Journal of Pharmacology 172, 413–416.

Gas, E., Flores-Pérez, U., Sauret-Güeto, S., and Rodríguez-Concepción, M. (2009). Hunting for plant nitric oxide synthase provides new evidence of a central role for plastids in nitric oxide metabolism. The Plant cell 21, 18–23.

Gaston, B., Reilly, J., Drazen, J. M., Fackler, J., Ramdev, P., Arnelle, D., Mullins, M. E., Sugarbaker, D. J., Chee, C., and Singel, D. J. (1993). Endogenous nitrogen oxides and bronchodilator *S*-nitrosothiols in human airways. Proceedings of the National Academy of Sciences of the United States of America 90, 10957–10961.

Ghalayini, I. F. (2004). Nitric oxide-cyclic GMP pathway with some emphasis on cavernosal contractility. International Journal of Impotence Research 16, 459–469.

Gillespie, J. P., Bailey, A. M., Cobb, B., and Vilcinskas, A. (2000). Review fungi as elicitors of insect immune responses. Archives of Insect Biochemistry and Physiology 44, 49–68.

Gilmore, T. D., and Ip, Y. T. (2005). Signal transduction pathways in development and immunity: Rel pathways. Encyclopedia of Life Sciences, 1–8.

Glozak, M. A., Sengupta, N., Zhang, X., and Seto, E. (2005). Acetylation and deacetylation of non-histone proteins. Gene 363, 15–23.

Goretski, J., and Hollocher, T. C. (1988). Trapping of nitric oxide produced during denitrification by extracellular hemoglobin. The Journal of Biological Chemistry 263, 2316–2323.

Gottar, M., Gobert, V., Matskevich, A. A., Reichhart, J.-M., Wang, C., Butt, T. M., Belvin, M., Hoffmann, J. A., and Ferrandon, D. (2006). Dual detection of fungal infections in Drosophila via recognition of glucans and sensing of virulence factors. Cell 127, 1425–1437.

Gottar, M., Gobert, V., Michel, T., Belvin, M., Duyk, G., Hoffmann, J. A., Ferrandon, D., and Royet, J. (2002). The Drosophila immune response against Gram-negative bacteria is mediated by a peptidoglycan recognition protein. Nature 416, 640–644.

Gow, A., Doctor, A., Mannick, J., and Gaston, B. (2007). *S*-Nitrosothiol measurements in biological systems. Journal of Chromatography B 851, 140–151.

Grigorian, M., Mandal, L., and Hartenstein, V. (2011). Hematopoiesis at the onset of metamorphosis: terminal differentiation and dissociation of the Drosophila lymph gland. Development Genes and Evolution 221, 121–131.

Gross, I., Georgel, P., Kappler, C., Reichhart, J. M., and Hoffmann, J. A. (1996). Drosophila immunity: a comparative analysis of the Rel proteins dorsal and Dif in the induction of the genes encoding diptericin and cecropin. Nucleic Acids Research 24, 1238–1245.

Grosshans, J., Schnorrer, F., and Nüsslein-Volhard, C. (1999). Oligomerisation of Tube and Pelle leads to nuclear localisation of Dorsal. Mechanisms of Development 81, 127–138.

Guikema, B., Lu, Q., and Jourd'heuil, D. (2005). Chemical considerations and biological selectivity of protein nitrosation: implications for NO-mediated signal transduction. Antioxidants & Redox Signaling 7, 593–606.

Guo, F.-Q., Okamoto, M., and Crawford, N. M. (2003). Identification of a plant nitric oxide synthase gene involved in hormonal signaling. Science 302, 100–103.

Gustafson, K., and Boulianne, G. L. (1996). Distinct expression patterns detected within individual tissues by the GAL4 enhancer trap technique. Genome 39, 174–182.

Ha, E.-M., Lee, K.-A., Park, S. H., Kim, S.-H., Nam, H.-J., Lee, H.-Y., Kang, D., and Lee, W.-J. (2009). Regulation of DUOX by the Gαq-phospholipase Cβ-Ca^{2+} pathway in Drosophila gut immunity. Developmental Cell 16, 386–397.

Haghayeghi, A., Sarac, A., Czerniecki, S., Grosshans, J., and Schöck, F. (2010). Pellino enhances innate immunity in Drosophila. Mechanisms of Development 127, 301–307.

Hanahan, D. (1983). Studies on transformation of *Escherichia coli* with plasmids. Journal of Molecular Biology 166, 557–580.

Harcum, S. W., and Bentley, W. E. (1993). Detection, quantification, and characterization of proteases in recombinant *Escherichia coli*. Biotechnology Techniques 7, 441–447.

Harrison, R. (2002). Structure and function of xanthine oxidoreductase: where are we now? Free Radical Biology and Medicine 33, 774–797.

Hart, T. W. (1985). Some observations concerning the *S*-nitroso and *S*-phenylsulphonyl derivatives of L-cysteine and glutathione. Tetrahedron Letters 26, 2013–2016.

Hedengren, M., Bengt, A., Dushay, M. S., Ando, I., Ekengren, S., Wihlborg, M., and Hultmark, D. (1999). Relish , a central factor in the control of humoral but not cellular immunity in Drosophila. Molecular cell 4, 827–837.

Hess, D. T., Matsumoto, A., Kim, S.-O., Marshall, H. E., and Stamler, J. S. (2005). Protein *S*-nitrosylation: purview and parameters. Nature Reviews Molecular Cell Biology 6, 150–166.

Hetru, C., and Hoffmann, J. A. (2009). NF-kappaB in the immune response of Drosophila. Cold Spring Harbor Perspectives in Biology 1, 1–6.

Hoffmann, J. A., and Reichhart, J.-M. (2002). Drosophila innate immunity: an evolutionary perspective. Nature Immunology 3, 121–126.

Hogg, N. (2002). The biochemistry and physiology of *S*-nitrosothiols. Annual Review of Pharmacology and Toxicology 45, 585–600.

Horng, T., and Medzhitov, R. (2001). Drosophila MyD88 is an adapter in the Toll signaling pathway. Proceedings of the National Academy of Sciences of the United States of America 98, 12654–12658.

Hornyák, I., Marosi, K., Kiss, L., Gróf, P., and Lacza, Z. (2012). Increased stability of *S*-nitrosothiol solutions via pH modulations. Free Radical Research 46, 214–225.

Hou, Q., Jiang, H., Zhang, X., Guo, C., Huang, B., Wang, P., Wang, T., Wu, K., Li, J., Gong, Z., et al. (2011). Nitric oxide metabolism controlled by formaldehyde dehydrogenase (*fdh*, homolog of mammalian *GSNOR*) plays a crucial role in visual pattern memory in Drosophila. Nitric Oxide 24, 17–24.

Hou, Y., Guo, Z., Li, J., and Wang, P. G. (1996). Seleno compounds and glutathione peroxidase catalyzed decomposition of *S*-nitrosothiols. Biochemical and Biophysical Research Communications 228, 88–93.

Huang, C. Y., Ken, C. F., Wen, L., and Lin, C. T. (2009). An enzyme possessing both glutathione-dependent formaldehyde dehydrogenase and *S*-nitrosoglutathione reductase from *Antrodia camphorata*. Food Chemistry 112, 795–802.

Huang, H.-R., Chen, Z. J., Kunes, S., Chang, G.-D., and Maniatis, T. (2010). Endocytic pathway is required for Drosophila Toll innate immune signaling. Proceedings of the National Academy of Sciences of the United States of America 107, 8322–8327.

Huang, S., Kerschbaum, H. H., Engel, E., and Hermann, A. (1997). Biochemical characterization and histochemical localization of nitric oxide synthase in the nervous system of the snail, *Helix pomatia*. Journal of Neurochemistry 69, 2516–2528.

Hultmark, D., Engström, A., Andersson, K., Steiner, H., Bennich, H., and Boman, H. G. (1983). Insect immunity. Attacins, a family of antimicrobial proteins from *Hyalophora cecropia*. The EMBO Journal 2, 571–576.

Into, T., Inomata, M., Nakashima, M., Shibata, K.-I., Häcker, H., and Matsushita, K. (2008). Regulation of MyD88-dependent signaling events by S nitrosylation retards Toll-like receptor signal transduction and initiation of acute-phase immune responses. Molecular and Cellular Biology 28, 1338–1347.

Ip, Y. T., Reach, M., Engstrom, Y., Kadalayil, L., Cai, H., González-Crespo, S., Tatei, K., and Levine, M. (1993). *Dif*, a *dorsal*-related gene that mediates an immune response in Drosophila. Cell 75, 753–763.

Jaffrey, S. R., Erdjument-Bromage, H., Ferris, C. D., Tempst, P., and Snyder, S. H. (2001). Protein *S*-nitrosylation: a physiological signal for neuronal nitric oxide. Nature Cell Biology 3, 193–197.

Jang, I.-H., Chosa, N., Kim, S.-H., Nam, H.-J., Lemaitre, B., Ochiai, M., Kambris, Z., Brun, S., Hashimoto, C., Ashida, M., et al. (2006). A Spätzle-processing enzyme required for toll signaling activation in Drosophila innate immunity. Developmental Cell 10, 45–55.

Jensen, D. E., Belka, G. K., and Bois, G. C. D. (1998). *S*-Nitrosoglutathione is a substrate for rat alcohol dehydrogenase class III isoenzyme. Biochem. J. 331, 659–668.

Jensen, O. N. (2004). Modification-specific proteomics: characterization of post-translational modifications by mass spectrometry. Current Opinion in Chemical Biology 8, 33–41.

Jourd'heuil, D., Laroux, F. S., Miles, A. M., Wink, D. A., and Grisham, M. B. (1999). Effect of superoxide dismutase on the stability of *S*-nitrosothiols. Archives of Biochemistry and Biophysics 361, 323–330.

Kambris, Z., Brun, S., Jang, I.-H., Nam, H.-J., Romeo, Y., Takahashi, K., Lee, W.-J., Ueda, R., and Lemaitre, B. (2006). Drosophila immunity: a large-scale in vivo RNAi screen identifies five serine proteases required for Toll activation. Current Biology 16, 808–813.

Kaneko, T., Yano, T., Aggarwal, K., Lim, J.-H., Ueda, K., Oshima, Y., Peach, C., Erturk-Hasdemir, D., Goldman, W. E., Oh, B.-H., et al. (2006). PGRP-LC and PGRP-LE have essential yet distinct functions in the drosophila immune response to monomeric DAP-type peptidoglycan. Nature Immunology 7, 715–723.

Kang, D., Liu, G., Lundstrom, A., Gelius, E., and Steiner, H. (1998). A peptidoglycan recognition protein in innate immunity conserved from insects to humans. Immunology 95, 10078–10082.

Kelley, L. A., and Sternberg, M. J. E. (2009). Protein structure prediction on the web: a case study using the Phyre server. Nature Protocols 4, 363–371.

Kerscher, O., Felberbaum, R., and Hochstrasser, M. (2006). Modification of proteins by ubiquitin and ubiquitin-like proteins. Annual Review of Cell and Developmental Biology 22, 159–180.

Kim, Y. S., Ryu, J. H., Han, S. J., Choi, K. H., Nam, K. B., Jang, I. H., Lemaitre, B., Brey, P. T., and Lee, W. J. (2000). Gram-negative bacteria-binding protein, a pattern recognition receptor for lipopolysaccharide and β-1,3-glucan that mediates the signaling for the induction of innate immune genes in *Drosophila melanogaster* cells. The Journal of Biological Chemistry 275, 32721–32727.

King, M., Gildemeister, O., Gaston, B., and Mannick, J. B. (2005). Assessment of *S*-nitrosothiols on diaminofluorescein gels. Analytical Biochemistry 346, 69–76.

King, R. C., Aggarwal, S. K., and Aggarwal, U. (1968). The development of the female Drosophila reproductive system. Journal of Morphology 124, 143–166.

Koch, E. A., and King, R. C. (1966). The origin and early differentiation of the egg chamber of *Drosophila melanogaster*. Journal of Morphology 119, 283–303.

Koganezawa, M., and Shimada, I. (2002). Novel odorant-binding proteins expressed in the taste tissue of the fly. Chemical Senses 27, 319–332.

Krem, M. M., and Di Cera, E. (2002). Evolution of enzyme cascades from embryonic development to blood coagulation. Trends in Biochemical Sciences 27, 67–74.

Lagueux, M., Perrodou, E., Levashina, E. A., Capovilla, M., and Hoffmann, J. A. (2000). Constitutive expression of a complement-like protein in Toll and JAK gain-of-function mutants of Drosophila. Proceedings of the National Academy of Sciences of the United States of America 97, 11427–11432.

Lee, H.-G., Seong, C.-S., Kim, Y.-C., Davis, R. L., and Han, K.-A. (2003). Octopamine receptor OAMB is required for ovulation in *Drosophila melanogaster*. Developmental Biology 264, 179–190.

Leipe, D. D., Wolf, Y. I., Koonin, E. V, and Aravind, L. (2002). Classification and evolution of P-loop GTPases and related ATPases. Journal of Molecular Biology 317, 41–72.

Lemaitre, B., and Hoffmann, J. (2007). The host defense of *Drosophila melanogaster*. Annual Review of Imunology 25, 697–743.

Lemaitre, B., Kromer-Metzger, E., Michaut, L., Nicolas, E., Meister, M., Georgel, P., Reichhart, J. M., and Hoffmann, J. A. (1995). A recessive mutation, immune deficiency (*imd*), defines two distinct control pathways in the Drosophila host defense. Proceedings of the National Academy of Sciences of the United States of America 92, 9465–9469.

Lemaitre, B., Nicolas, E., Michaut, L., Reichhart, J.-M., and Hoffmann, J. A. (1996). The dorsoventral regulatory gene cassette *spätzle*/*Toll*/*cactus* controls the potent antifungal response in Drosophila adults. Cell 86, 973–983.

Lemaitre, B., Reichhart, J. M., and Hoffmann, J. A. (1997). Drosophila host defense: differential induction of antimicrobial peptide genes after infection by various classes of microorganisms. Proceedings of the National Academy of Sciences of the United States of America 94, 14614–14619.

Leone, P., Bischoff, V., Kellenberger, C., Hetru, C., Royet, J., and Roussel, A. (2008). Crystal structure of Drosophila PGRP-SD suggests binding to DAP-type but not lysine-type peptidoglycan. Molecular Immunology 45, 2521–2530.

Levashina, E. A., Langley, E., Green, C., Gubb, D., Ashburner, M., Hoffmann, J. A., and Reichhart, J.-M. (1999). Constitutive activation of Toll-mediated antifungal defense in Serpin-deficient Drosophila. Science 285, 1917–1919.

Levashina, E. A., Ohresser, S., Bulet, P., Reichhart, J. M., Hetru, C., and Hoffmann, J. A. (1995). Metchnikowin, a novel immune-inducible proline-rich peptide from Drosophila with antibacterial and antifungal properties. European Journal of Biochemistry 233, 694–700.

Levashina, E. A., Ohresser, S., Lemaitre, B., and Imler, J. L. (1998). Two distinct pathways can control expression of the gene encoding the Drosophila antimicrobial peptide metchnikowin. Journal of Molecular Biology 278, 515–527.

Lide, D. R. (2009). CRC handbook of chemistry and physics 89th ed. D. R. Lide, ed. (Boca Raton, FL: CRC Press/Taylor and Francis).

Ligoxygakis, P., Pelte, N., Hoffmann, J. A., and Reichhart, J.-M. (2002). Activation of Drosophila Toll during fungal infection by a blood serine protease. Science 297, 114–116.

Lillig, C. H., and Holmgren, A. (2007). Thioredoxin and related molecules - From biology to health and disease. Antioxidants & Redox Signaling 9, 25–47.

Lima, B., Forrester, M. T., Hess, D. T., and Stamler, J. S. (2010). *S*-Nitrosylation in cardiovascular signaling. Circulation Research 106, 633–646.

Lindermayr, C., Saalbach, G., and Durner, J. (2005). Proteomic identification of *S*-nitrosylated proteins in Arabidopsis. Plant Physiology 137, 921–930.

Liu, L., Yan, Y., Zeng, M., Zhang, J., Hanes, M. A., Ahearn, G., McMahon, T. J., Dickfeld, T., Marshall, H. E., Que, L. G., et al. (2004). Essential roles of *S*-nitrosothiols in vascular homeostasis and endotoxic shock. Cell 116, 617–628.

Lucas, K. A., Pitari, G. M., Kazerounian, S., Ruiz-Stewart, I., Park, J., Schulz, S., Chepenik, K. P., and Waldman, S. A. (2000). Guanylyl cyclases and signaling by cyclic GMP. Pharmacological Reviews 52, 375–414.

Lundberg, J. O., and Weitzberg, E. (2005). NO generation from nitrite and its role in vascular control. Arteriosclerosis, Thrombosis, and Vascular Biology 25, 915–922.

Luque, T., Atrian, S., Danielsson, O., Jörnvall, H., and Gonzàlez-Duarte, R. (1994). Structure of the *Drosophila melanogaster* glutathione-dependent formaldehyde dehydrogenase/octanol dehydrogenase gene (class III alcohol dehydrogenase). Evolutionary pathway of the alcohol dehydrogenase genes. European Journal of Biochemistry 225, 985–993.

López-Otín, C., and Overall, C. M. (2002). Protease degradomics: a new challenge for proteomics. Nature Reviews. Molecular Cell Biology 3, 509–519.

MacArthur, P. H., Shiva, S., and Gladwin, M. T. (2007). Measurement of circulating nitrite and *S*-nitrosothiols by reductive chemiluminescence. Journal of Chromatography B 851, 93–105.

Madden, T. (2002). The BLAST sequence analysis tool. In The NCBI Handbook [Internet], M. J and O. J, eds. (Bethesda (MD): National Center for Biotechnology Information (US)), pp. 1–15.

Maillet, F., Bischoff, V., Vignal, C., Hoffmann, J., and Royet, J. (2008). The Drosophila peptidoglycan recognition protein PGRP-LF blocks PGRP-LC and IMD/JNK pathway activation. Cell Host & Microbe 3, 293–303.

Manfruelli, P., Reichhart, J. M., Steward, R., Hoffmann, J. A., and Lemaitre, B. (1999). A mosaic analysis in Drosophila fat body cells of the control of antimicrobial peptide genes by the Rel proteins Dorsal and DIF. The EMBO Journal 18, 3380–3391.

Mani, A. R., Ebrahimkhani, M. R., Ippolito, S., Ollosson, R., and Moore, K. P. (2006). Metalloprotein-dependent decomposition of *S*-nitrosothiols: studies on the stabilization and measurement of *S*-nitrosothiols in tissues. Free Radical Biology & Medicine 40, 1654–1663.

Mannick, J. B., Hausladen, A., Liu, L., Hess, D. T., Zeng, M., Miao, Q. X., Kane, L. S., Gow, A. J., and Stamler, J. S. (1999). Fas-induced caspase denitrosylation. Science 284, 651–654.

Marek, L. R., and Kagan, J. C. (2012). Phosphoinositide binding by the Toll adaptor dMyD88 controls antibacterial responses in Drosophila. Immunity 36, 612–622.

Margaritis, L. H., Kafatos, F. C., and Petri, W. H. (1980). The eggshell of *Drosophila melanogaster*. I. Fine structure of the layers and regions of the wild-type eggshell. Journal of Cell Science 43, 1–35.

Margis, R., Dunand, C., Teixeira, F. K., and Margis-Pinheiro, M. (2008). Glutathione peroxidase family - an evolutionary overview. The FEBS Journal 275, 3959–3970.

Margolis, J., and Spradling, A. (1995). Identification and behavior of epithelial stem cells in the Drosophila ovary. Development 121, 3797–3807.

Mariño, K., Bones, J., Kattla, J. J., and Rudd, P. M. (2010). A systematic approach to protein glycosylation analysis: a path through the maze. Nature Chemical Biology 6, 713–723.

Markstein, M., Pitsouli, C., Villalta, C., Celniker, S. E., and Perrimon, N. (2008). Exploiting position effects and the gypsy retrovirus insulator to engineer precisely expressed transgenes. Nature Genetics 40, 476–483.

Marley, R., Feelisch, M., Holt, S., and Moore, K. (2000). A chemiluminescense-based assay for *S*-nitrosoalbumin and other plasma *S*-nitrosothiols. Free Radical Research 32, 1–9.

Marshall, H. E., Hess, D. T., and Stamler, J. S. (2004). *S*-Nitrosylation: physiological regulation of NF-kappaB. Proceedings of the National Academy of Sciences of the United States of America 101, 8841–8842.

McComb, R. B., Bond, L. W., Burnett, R. W., Keech, R. C., and Bowers, G. N. (1976). Determination of the molar absorptivity of NADH. Clinical Chemistry 22, 141–150.

McNeil, G. P., Smith, F., and Galioto, R. (2004). The Drosophila RNA-binding protein Lark is required for the organization of the actin cytoskeleton and Hu-li tai shao localization during oogenesis. Genesis 40, 90–100.

Mellroth, P., Karlsson, J., Håkansson, J., Schultz, N., Goldman, W. E., and Steiner, H. (2005). Ligand-induced dimerization of Drosophila peptidoglycan recognition proteins *in vitro*. Proceedings of the National Academy of Sciences of the United States of America 102, 6455–6460.

Michel, T., Reichhart, J. M., Hoffmann, J. A., and Royet, J. (2001). Drosophila Toll is activated by gram-positive bacteria through a circulating peptidoglycan recognition protein. Nature 414, 756–759.

Middleton, C. A., Nongthomba, U., Parry, K., Sweeney, S. T., Sparrow, J. C., and Elliott, C. J. H. (2006). Neuromuscular organization and aminergic modulation of contractions in the Drosophila ovary. BMC Biology 4, 17.

Miguel, A. R. M., Alberto, M., Alicia Rodriguez, H., and Gustafson, J. P. (2003). Glutathione peroxidase genes in Arabidopsis are ubiquitous and regulated by abiotic stresses through diverse signaling pathways. The Plant Journal 36, 602–615.

Mishima, Y., Quintin, J., Aimanianda, V., Kellenberger, C., Coste, F., Clavaud, C., Hetru, C., Hoffmann, J. A., Latgé, J.-P., Ferrandon, D., et al. (2009). The N-terminal domain of Drosophila gram-negative binding protein 3 (GNBP3) defines a novel family of fungal pattern recognition receptors. The Journal of Biological Chemistry 284, 28687–28697.

Modolo, L. V, Augusto, O., Almeida, I. M. G., Magalhaes, J. R., and Salgado, I. (2005). Nitrite as the major source of nitric oxide production by *Arabidopsis thaliana* in response to *Pseudomonas syringae*. FEBS Letters 579, 3814–3820.

Mohr, S., Stamler, J. S., and Brüne, B. (1996). Posttranslational modification of glyceraldehyde-3-phosphate dehydrogenase by *S*-nitrosylation and subsequent NADH attachment. The Journal of Biological Chemistry 271, 4209–4214.

Monastirioti, M. (2003). Distinct octopamine cell population residing in the CNS abdominal ganglion controls ovulation in *Drosophila melanogaster*. Developmental Biology 264, 38–49.

Moncrieffe, M. C., Gu, J., and Gay, N. J. (2008). Assembly of oligomeric death domain complexes during Toll receptor signaling. The Journal of Biological Chemistry 283, 33447–33454.

Moreau, M., Lee, G. I., Wang, Y., Crane, B. R., and Klessig, D. F. (2008). AtNOS/AtNOA1 is a functional *Arabidopsis thaliana* cGTPase and not a nitric-oxide synthase. The Journal of Biological Chemistry 283, 32957–32967.

Nadolski, M. J., and Linder, M. E. (2007). Protein lipidation. The FEBS Journal 274, 5202–5210.

Nagababu, E., and Rifkind, J. M. (2007). Measurement of plasma nitrite by chemiluminescence without interference of *S*-, *N*-nitroso and nitrated species. Free Radical Biology and Medicine 42, 1146–1154.

Naito, Y., Yamada, T., Matsumiya, T., Ui-Tei, K., Saigo, K., and Morishita, S. (2005). dsCheck: highly sensitive off-target search software for double-stranded RNA-mediated RNA interference. Nucleic Acids Research 33, W589–W591.

Nappi, A. J., and Vass, E. (1998). Hydrogen peroxide production in immune-reactive *Drosophila melanogaster*. Journal of Parasitology 84, 1150–1157.

Nappi, A. J., Vass, E., Frey, F., and Carton, Y. (2000). Nitric oxide involvement in Drosophila immunity. Nitric oxide: Biology and Chemistry 4, 423–430.

Nappi, A., Vass, E., Frey, F., and Carton, Y. (1995). Superoxide anion generation in Drosophila during melanotic encapsulation of parasites. European Journal of Cell Biology 68, 450–456.

Neagu, A., Neagu, M., and Dér, A. (2001). Fluctuations and the Hofmeister effect. Biophysical Journal 81, 1285–1294.

Nehme, N. T., Liegeois, S., Kele, B., Giammarinaro, P., Pradel, E., Hoffmann, J. A., Ewbank, J. J., and Ferrandon, D. (2007). A model of bacterial intestinal infections in *Drosophila melanogaster*. Plos Pathogens 3, 1694–1709.

Nehme, N. T., Quintin, J., Cho, J. H., Lee, J., Lafarge, M.-C., Kocks, C., and Ferrandon, D. (2011). Relative roles of the cellular and humoral responses in the Drosophila host defense against three gram-positive bacterial infections. PloS One 6, e14743.

Nilson, L. A., and Schüpbach, T. (1998). Localized requirements for *windbeutel* and *pipe* reveal a dorsoventral prepattern within the follicular epithelium of the Drosophila ovary. Cell 93, 253–262.

Notredame, C., Higgins, D. G., and Heringa, J. (2000). T-Coffee: a novel method for fast and accurate multiple sequence alignment. Journal of Molecular Biology 302, 205–217.

Nowotny, M., and Yang, W. (2009). Structural and functional modules in RNA interference. Current Opinion in Structural Biology 19, 286–293.

Osipov, A. N., Borisenko, G. G., and Vladimirov, Y. A. (2007). Biological activity of hemoprotein nitrosyl complexes. Biochemistry (Moscow) 72, 1491–1504.

Osterwalder, T., Yoon, K. S., White, B. H., and Keshishian, H. (2001). A conditional tissue-specific transgene expression system using inducible GAL4. Proceedings of the National Academy of Sciences of the United States of America 98, 12596–12601.

Padgett, C. M., and Whorton, A. R. (1995). *S*-Nitrosoglutathione reversibly inhibits GAPDH by *S*-nitrosylation. The American Journal of Physiology 269, 739–749.

Paik, W. K., Paik, D. C., and Kim, S. (2007). Historical review: the field of protein methylation. Trends in Biochemical Sciences 32, 146–152.

Paquette, N., Broemer, M., Aggarwal, K., Chen, L., Husson, M., Ertürk-Hasdemir, D., Reichhart, J.-M., Meier, P., and Silverman, N. (2010). Caspase-mediated cleavage, IAP binding, and ubiquitination: linking three mechanisms crucial for Drosophila NF-kappaB signaling. Molecular Cell 37, 172–182.

Park, S. W., Huq, M. D. M., Hu, X., and Wei, L.-N. (2005). Tyrosine nitration on p65: a novel mechanism to rapidly inactivate nuclear factor-kappaB. Molecular & cellular proteomics 4, 300–309.

Parks, A. L., Cook, K. R., Belvin, M., Dompe, N. A., Fawcett, R., Huppert, K., Tan, L. R., Winter, C. G., Bogart, K. P., Deal, J. E., et al. (2004). Systematic generation of high-resolution deletion coverage of the *Drosophila melanogaster* genome. Nature Genetics 36, 288–292.

Perazzolli, M., Dominici, P., Romero-puertas, M. C., Zago, E., Sonoda, M., Lamb, C., and Delledonne, M. (2004). Arabidopsis nonsymbiotic hemoglobin AHb1 modulates nitric oxide bioactivity. The Plant Cell 16, 2785–2794.

Pervin, S., Singh, R., and Chaudhuri, G. (2001). Nitric oxide-induced cytostasis and cell cycle arrest of a human breast cancer cell line (MDA-MB-231): potential role of cyclin D1. Proceedings of the National Academy of Sciences of the United States of America 98, 3583–3588.

Pfeiffer, S., Janistyn, B., Jessner, G., Pichorner, H., and Ebermann, R. (1994). Gaseous nitric oxide stimulates guanosine-3′,5′-cyclic monophosphate (cGMP) formation in spruce needles. Pharmacological Reviews 36, 259–262.

Pinder, A. G., Rogers, S. C., Khalatbari, A., Ingram, T. E., and James, P. E. (2008). The measurement of nitric oxide and its metabolites in biological samples by ozone-based chemiluminescence. In Redox-Mediated Signal Transduction: Methods and Protocols, J. T. Hancock, ed. (New York: Humana Press, a part of Springer Science+Business Media), pp. 10–27.

Planchet, E., and Kaiser, W. M. (2006). Nitric oxide (NO) detection by DAF fluorescence and chemiluminescence: a comparison using abiotic and biotic NO sources. Journal of Experimental Botany 57, 3043–3055.

Poluha, W., Schonhoff, C. M., Harrington, K. S., Lachyankar, M. B., Crosbie, N. E., Bulseco, D. A., and Ross, A. H. (1997). A novel, nerve growth factor-activated pathway involving nitric oxide, p53, and p21 WAF1 regulates neuronal differentiation of PC12 cells. The Journal of Biological Chemistry 272, 24002–24007.

Que, L. G., Liu, L., Yan, Y., Whitehead, G. S., Gavett, S. H., Schwartz, D. A., and Stamler, J. S. (2005). Protection from experimental asthma by an endogenous bronchodilator. Science 308, 1618–1621.

Que, L. G., Yang, Z., Stamler, J. S., Lugogo, N. L., and Kraft, M. (2009). *S*-Nitrosoglutathione reductase: an important regulator in human asthma. American Journal of Respiratory and Critical Care Medicine 180, 226–231.

Quevillon-Cheruel, S., Leulliot, N., Muniz, C. A., Vincent, M., Gallay, J., Argentini, M., Cornu, D., Boccard, F., Lemaître, B., and van Tilbeurgh, H. (2009). Evf, a virulence factor produced by the Drosophila pathogen *Erwinia carotovora*, is an *S*-palmitoylated protein with a new fold that binds to lipid vesicles. The Journal of Biological Chemistry 284, 3552–3562.

Rabel, D., Charlet, M., Ehret-Sabatier, L., Cavicchioli, L., Cudic, M., Otvos, L., and Bulet, P. (2004). Primary structure and *in vitro* antibacterial properties of the *Drosophila melanogaster* attacin C Pro-domain. The Journal of Biological Chemistry 279, 14853–14859.

Reynaert, N. L., Ckless, K., Korn, S. H., Vos, N., Guala, A. S., Wouters, E. F. M., van der Vliet, A., and Janssen-Heininger, Y. M. W. (2004). Nitric oxide represses inhibitory kappaB kinase through *S*-nitrosylation. Proceedings of the National Academy of Sciences of the United States of America 101, 8945–8950.

Richard, D. S., Gilbert, M., Crum, B., Hollinshead, D. M., Schelble, S., and Scheswohl, D. (2001). Yolk protein endocytosis by oocytes in *Drosophila melanogaster*: immunofluorescent localization of clathrin, adaptin and the yolk protein receptor. Journal of Insect Physiology 47, 715–723.

Rodríguez-Valentín, R., López-González, I., Jorquera, R., Labarca, P., Zurita, M., and Reynaud, E. (2006). Oviduct contraction in Drosophila is modulated by a neural network that is both, octopaminergic and glutamatergic. Journal of Cellular Physiology 198, 183–198.

Romeo, Y., and Lemaitre, B. (2008). Methods for monitoring the activity of Toll and Imd signaling pathways. In Methods in Molecular Biology, vol. 415, J. Ewbank and E. Vivier, eds. (Totowa: Humana Press), pp. 379–394.

Romero-Puertas, M. C., Campostrini, N., Mattè, A., Righetti, P. G., Perazzolli, M., Zolla, L., Roepstorff, P., and Delledonne, M. (2008). Proteomic analysis of *S*-nitrosylated proteins in *Arabidopsis thaliana* undergoing hypersensitive response. Proteomics 8, 1459–1469.

Romero-Puertas, M. C., Laxa, M., Mattè, A., Zaninotto, F., Finkemeier, I., Jones, A. M. E., Perazzolli, M., Vandelle, E., Dietz, K.-J., and Delledonne, M. (2007). *S*-Nitrosylation of peroxiredoxin II E promotes peroxynitrite-mediated tyrosine nitration. The Plant Cell 19, 4120–4130.

Rustérucci, C., Espunya, M. C., Díaz, M., Chabannes, M., and Martínez, M. C. (2007). *S*-Nitrosoglutathione reductase affords protection against pathogens in Arabidopsis, both locally and systemically. Plant Physiology 143, 1282–1292.

Rutschmann, S., Jung, A. C., Hetru, C., Reichhart, J., Hoffmann, J. A., and Ferrandon, D. (2000). The Rel protein DIF mediates the antifungal but not the antibacterial host defense in Drosophila. Immunity 12, 569–580.

Ryu, J.-H., Kim, S.-H., Lee, H.-Y., Bai, J. Y., Nam, Y.-D., Bae, J.-W., Lee, D. G., Shin, S. C., Ha, E.-M., and Lee, W.-J. (2008). Innate immune homeostasis by the homeobox gene caudal and commensal-gut mutualism in Drosophila. Science 319, 777–782.

Saito, S., Yamamoto-Katou, A., Yoshioka, H., Doke, N., and Kawakita, K. (2006). Peroxynitrite generation and tyrosine nitration in defense responses in tobacco BY-2 cells. Plant & Cell Physiology 47, 689–697.

Samouilov, A., and Zweier, J. L. (1998). Development of chemiluminescence-based methods for specific quantitation of nitrosylated thiols. Analytical Biochemistry 258, 322–330.

Sanghani, P. C., Davis, W. I., Fears, S. L., Green, S.-L., Zhai, L., Tang, Y., Martin, E., Bryan, N. S., and Sanghani, S. P. (2009). Kinetic and cellular characterization of novel inhibitors of *S*-nitrosoglutathione reductase. The Journal of Biological Chemistry 284, 24354–24362.

Saville, B. (1958). A scheme for the colorimetric determination of microgram amounts of thiols. Analyst 83, 670–672.

Sawa, A., Khan, A. A., Hester, L. D., and Snyder, S. H. (1997). Glyceraldehyde-3-phosphate dehydrogenase: nuclear translocation participates in neuronal and nonneuronal cell death. Proceedings of the National Academy of Sciences of the United States of America 94, 11669–11674.

Schauvliege, R., Janssens, S., and Beyaert, R. (2006). Pellino proteins are more than scaffold proteins in TLR/IL-1R signalling: a role as novel RING E3-ubiquitin-ligases. FEBS Letters 580, 4697–4702.

Scherfer, C., Karlsson, C., Loseva, O., Bidla, G., Goto, A., Havemann, J., Dushay, M. S., and Theopold, U. (2004). Isolation and characterization of hemolymph clotting factors in *Drosophila melanogaster* by a pullout method. Current Biology 14, 625–629.

Schmidt, K., Pfeiffer, S., and Mayer, B. (1998). Reaction of peroxynitrite with HEPES or MOPS results in the formation of nitric oxide donors. Free Radical Biology & Medicine 24, 859–862.

Schopfer, F. J., Baker, P. R. S., and Freeman, B. A. (2003). NO-dependent protein nitration: a cell signaling event or an oxidative inflammatory response? Trends in Biochemical Sciences 28, 646–654.

Senger, K., Armstrong, G. W., Rowell, W. J., Kwan, J. M., Markstein, M., and Levine, M. (2004). Immunity regulatory DNAs share common organizational features in Drosophila. Molecular Cell 13, 19–32.

Sengupta, R., Ryter, S. W., Zuckerbraun, B. S., Tzeng, E., Billiar, T. R., and Stoyanovsky, D. A. (2007). Thioredoxin catalyzes the denitrosation of low-molecular mass and protein *S*-nitrosothiols. Biochemistry 46, 8472–8483.

Seth, D., and Stamler, J. S. (2011). The SNO-proteome: causation and classification. Current Opinion in Chemical Biology 15, 129–136.

Sexton, D. J., Muruganandam, A., McKenney, D. J., and Mutus, B. (1994). Visible light photochemical release of nitric oxide from *S*-nitrosoglutathione: potential photochemotherapeutic applications. Photochemistry and Photobiology 59, 463–467.

Sharma, R. V, Tan, E., Fang, S., Gurjar, M. V, and Bhalla, R. C. (1999). NOS gene transfer inhibits expression of cell cycle regulatory molecules in vascular smooth muscle cells NOS gene transfer inhibits expression of cell cycle regulatory molecules in vascular smooth muscle cells. American Journal of Physiology - Heart and Circulatory Physiology 276, H1450–H1459.

Shen, B., and Manley, J. L. (2002). Pelle kinase is activated by autophosphorylation during Toll signaling in Drosophila. Development 129, 1925–1933.

Shen, B., and Manley, J. L. (1998). Phosphorylation modulates direct interactions between the Toll receptor, Pelle kinase and Tube. Development 125, 4719–4728.

Shishido, S. M., Seabra, A. B., Loh, W., and Ganzarolli de Oliveira, M. (2003). Thermal and photochemical nitric oxide release from *S*-nitrosothiols incorporated in Pluronic F127 gel: potential uses for local and controlled nitric oxide release. Biomaterials 24, 3543–3553.

Shpacovitch, V., Feld, M., Bunnett, N. W., and Steinhoff, M. (2007). Protease-activated receptors: novel PARtners in innate immunity. Trends in Immunology 28, 541–550.

Sik Lee, Y., and Carthew, R. W. (2003). Making a better RNAi vector for Drosophila: use of intron spacers. Methods 30, 322–329.

Sliskovic, I., Raturi, A., and Mutus, B. (2005). Characterization of the *S*-denitrosation activity of protein disulfide isomerase. The Journal of Biological Chemistry 280, 8733–8741.

Song, F. M., and Goodman, R. M. (2001). Activity of nitric oxide is dependent on, but is partially required for function of, salicylic acid in the signaling pathway in tobacco systemic acquired resistance. Molecular Plant-Microbe Interactions 14, 1458–1462.

Spradling, A. (1993). The Development of *Drosophila melanogaster*. In Volume 1, M. Bate and A. M. Arias, eds. (New York: Cold Spring Harbor Laboratory Press), pp. 2–6.

Staab, C. A., Hellgren, M., and Höög, J.-O. (2008). Medium- and short-chain dehydrogenase/reductase gene and protein families: dual functions of alcohol dehydrogenase 3: implications with focus on formaldehyde dehydrogenase and *S*-nitrosoglutathione reductase activities. Cellular and Molecular Life Sciences 65, 3950–3960.

Stamler, J. S. (1994). Redox signaling: nitrosylation and related target interactions of nitric oxide. Cell 78, 931–936.

Stoyanovsky, D. A., Tyurina, Y. Y., Tyurin, V. A., Anand, D., Mandavia, D. N., Gius, D., Ivanova, J., Pitt, B., Billiar, T. R., and Kagan, V. E. (2005). Thioredoxin and lipoic acid catalyze the denitrosation of low molecular weight and protein *S*-nitrosothiols. Journal of the American Chemical Society 127, 15815–15823.

Sudhamsu, J., Lee, G. I., Klessig, D. F., and Crane, B. R. (2008). The structure of YqeH. An AtNOS1/AtNOA1 ortholog that couples GTP hydrolysis to molecular recognition. The Journal of Biological Chemistry 283, 32968–32976.

Sun, H., Bristow, B. N., Qu, G., and Wasserman, S. A. (2002). A heterotrimeric death domain complex in Toll signaling. Proceedings of the National Academy of Sciences of the United States of America 99, 12871–12876.

Sun, S., and Faye, I. (1992). Cecropia immunoresponsive factor, an insect immunoresponsive factor with DNA-binding properties similar to nuclear-factor KB. European Journal of Biochemistry 204, 885–892.

Tada, Y., Spoel, S. H., Pajerowska-Mukhtar, K., Mou, Z., Song, J., Wang, C., Zuo, J., and Dong, X. (2008). Plant immunity requires conformational changes [corrected] of NPR1 via *S*-nitrosylation and thioredoxins. Science 321, 952–956.

Takeda, K., and Akira, S. (2003). Toll receptors and pathogen resistance. Cellular Microbiology 5, 143–153.

Takehana, A., Yano, T., Mita, S., Kotani, A., Oshima, Y., and Kurata, S. (2004). Peptidoglycan recognition protein (PGRP)-LE and PGRP-LC act synergistically in Drosophila immunity. The EMBO Journal 23, 4690–4700.

Tang, H., Kambris, Z., Lemaitre, B., and Hashimoto, C. (2008). A serpin that regulates immune melanization in the respiratory system of Drosophila. Developmental Cell 15, 617–626.

Tang, H., Kambris, Z., Lemaitre, B., and Hashimoto, C. (2006). Two proteases defining a melanization cascade in the immune system of Drosophila. The Journal of Biological Chemistry 281, 28097–28104.

Tanji, T., Yun, E.-Y., and Ip, Y. T. (2010). Heterodimers of NF-κB transcription factors DIF and Relish regulate antimicrobial peptide genes in Drosophila. Proceedings of the National Academy of Sciences 107, 14715–14720.

Tarrant, M. K., and Cole, P. A. (2009). The chemical biology of protein phosphorylation. Annual Review of Biochemistry 78, 797–825.

Tian, C., Gao, B., Rodriguez, M. D. C., Lanz-Mendoza, H., Ma, B., and Zhu, S. (2008). Gene expression, antiparasitic activity, and functional evolution of the drosomycin family. Molecular Immunology 45, 3909–3916.

Torreilles, J. (2001). Nitric oxide: one of the more conserved and widespread signaling molecules. Frontiers in Bioscience 6, d1161–1172.

Towb, P., Bergmann, A., and Wasserman, S. A. (2001). The protein kinase Pelle mediates feedback regulation in the Drosophila Toll signaling pathway. Development 128, 4729–4736.

Trujillo, M., Alvarez, M. N., Peluffo, G., Freeman, B. A., and Radi, R. (1998). Xanthine oxidase-mediated decomposition of *S*-nitrosothiols. The Journal of Biological Chemistry 273, 7828–7834.

Tsikas, D. (2007). Analysis of nitrite and nitrate in biological fluids by assays based on the Griess reaction: appraisal of the Griess reaction in the l-arginine/nitric oxide area of research. Journal of Chromatography B 851, 51–70.

Tsikas, D., Sandmann, J., Rossa, S., Gutzki, F. M., and Frölich, J. C. (1999). Gas chromatographic-mass spectrometric detection of *S*-nitroso-cysteine and *S*-nitroso-glutathione. Analytical Biochemistry 272, 117–122.

Uicker, W. C., Schaefer, L., Koenigsknecht, M., and Britton, R. A. (2007). The essential GTPase YqeH is required for proper ribosome assembly in *Bacillus subtilis*. Journal of Bacteriology 189, 2926–2929.

Ursini, F., Maiorino, M., Brigelius-Flohé, R., Aumann, K. D., Roveri, A., Schomburg, D., and Flohé, L. (1995). Diversity of glutathione peroxidases. Methods in Enzymology 252, 38–48.

Valanne, S., Wang, J.-H., and Rämet, M. (2011). The Drosophila Toll signaling pathway. Journal of Immunology 186, 649–656.

Vaux, D. L., and Silke, J. (2005). IAPs, RINGs and ubiquitylation. Nature Reviews. Molecular Cell Biology 6, 287–297.

Villalobo, A. (2006). Nitric oxide and cell proliferation. The FEBS Journal 273, 2329–2344.

Voelker, R. A., Langley, C. H., Brown, A. J., Ohnishi, S., Dickson, B., Montgomery, E., and Smith, S. C. (1980). Enzyme null alleles in natural populations of *Drosophila melanogaster*: frequencies in a North Carolina population. Proceedings of the National Academy of Sciences of the United States of America 77, 1091–1095.

Walsh, C. T., Garneau-Tsodikova, S., and Gatto, G. J. (2005). Protein posttranslational modifications: the chemistry of proteome diversifications. Angewandte Chemie International Edition 44, 7342–7372.

Wang, L., Gilbert, R. J. C., Atilano, M. L., Filipe, S. R., Gay, N. J., and Ligoxygakis, P. (2008). Peptidoglycan recognition protein-SD provides versatility of receptor formation in Drosophila immunity. Proceedings of the National Academy of Sciences of the United States of America 105, 11881–11886.

Wang, L., Weber, A. N. R., Atilano, M. L., Filipe, S. R., Gay, N. J., and Ligoxygakis, P. (2006). Sensing of gram-positive bacteria in Drosophila: GNBP1 is needed to process and present peptidoglycan to PGRP-SA. The EMBO Journal 25, 5005–5014.

Wang, L.-N., Yu, B., Han, G.-Q., and Chen, D.-W. (2010). Molecular cloning, expression in *Escherichia coli* of Attacin A gene from Drosophila and detection of biological activity. Molecular Biology Reports 37, 2463–2469.

Wang, Y., Liu, T., Wu, C., and Li, H. (2009a). A strategy for direct identification of protein *S*-nitrosylation sites by quadrupole time-of-flight mass spectrometry. Journal of The American Society for Mass Spectrometry 19, 1353–1360.

Wang, Y.-Q., Feechan, A., Yun, B.-W., Shafiei, R., Hofmann, A., Taylor, P., Xue, P., Yang, F.-Q., Xie, Z.-S., Pallas, J. A., et al. (2009b). *S*-Nitrosylation of AtSABP3 antagonizes the expression of plant immunity. The Journal of Biological Chemistry 284, 2131–2137.

Watts, R. A., Hunt, P. W., Hvitved, A. N., Hargrove, M. S., Peacock, W. J., and Dennis, E. S. (2001). A hemoglobin from plants homologous to truncated hemoglobins of microorganisms. Proceedings of the National Academy of Sciences of the United States of America 98, 10119–10124.

Weber, A. N. R., Gangloff, M., Moncrieffe, M. C., Hyvert, Y., Imler, J.-L., and Gay, N. J. (2007). Role of the Spatzle Pro-domain in the generation of an active toll receptor ligand. The Journal of Biological Chemistry 282, 13522–13531.

Wedgwood, S., and Black, S. M. (2003). Molecular mechanisms of nitric oxide-induced growth arrest and apoptosis in fetal pulmonary arterial smooth muscle cells. Nitric Oxide 9, 201–210.

Werner, T., Liu, G., Kang, D., Ekengren, S., Steiner, H., and Hultmark, D. (2000). A family of peptidoglycan recognition proteins in the fruit fly *Drosophila melanogaster*. Proceedings of the National Academy of Sciences of the United States of America 97, 13772–13777.

Whalen, A. M., and Steward, R. (1993). Dissociation of the dorsal-cactus complex and phosphorylation of the dorsal protein correlate with the nuclear localization of dorsal. The Journal of Cell Biology 123, 523–534.

Winter, D., Vinegar, B., Nahal, H., Ammar, R., Wilson, G. V, and Provart, N. J. (2007). An electronic fluorescent pictograph browser for exploring and analyzing large-scale biological data sets. PloS One 2, e718.

Wolfner, M. F. (2011). Precious essences: female secretions promote sperm storage in Drosophila. PLoS Biology 9, e1001191.

Worsfold, M., Marshall, M. J., and Ellis, E. B. (1976). Enzyme detection using phenazine methosulphate and tetrazolium salts: interference by oxygen. Analytical Biochemistry 79, 152–156.

Wu, L. P., and Anderson, K. V (1998). Drosophila immune response. Nature 392, 93–97.

Wu, X., Tanwar, P. S., and Raftery, L. A. (2008). Drosophila follicle cells: morphogenesis in an eggshell. Seminars in Cell & Developmental Biology 19, 271–282.

Xia, Z.-P., Sun, L., Chen, X., Pineda, G., Jiang, X., Adhikari, A., Zeng, W., and Chen, Z. J. (2009). Direct activation of protein kinases by unanchored polyubiquitin chains. Nature 461, 114–119.

Xue, Y., Liu, Z., Gao, X., Jin, C., Wen, L., Yao, X., and Ren, J. (2010). GPS-SNO: computational prediction of protein *S*-nitrosylation sites with a modified GPS algorithm. PloS One 5, e11290.

Yamasaki, H., Sakihama, Y., and Takahashi, S. (1999). An alternative pathway for nitric oxide production in plants: new features of an old enzyme. Trends in Plant Science 4, 128–129.

Zaman, K., Carraro, S., Doherty, J., Henderson, E. M., Lendermon, E., Liu, L., Verghese, G., Zigler, M., Ross, M., Park, E., et al. (2006). *S*-Nitrosylating agents: a novel class of compounds that increase cystic fibrosis transmembrane conductance regulator expression and maturation in epithelial cells. Molecular Pharmacology 70, 1435–1442.

Zappia, M. P., Brocco, M. A., Billi, S. C., Frasch, A. C., and Ceriani, M. F. (2011). M6 membrane protein plays an essential role in Drosophila oogenesis. PloS One 6, e19715.

Zemojtel, T., Kolanczyk, M., Kossler, N., Stricker, S., Lurz, R., Mikula, I., Duchniewicz, M., Schuelke, M., Ghafourifar, P., Martasek, P., et al. (2006). Mammalian mitochondrial nitric oxide synthase: characterization of a novel candidate. FEBS Letters 580, 455–462.

Zhang, C., Czymmek, K. J., and Shapiro, A. D. (2003). Nitric oxide does not trigger early programmed cell death events but may contribute to cell-to-cell signaling governing progression of the Arabidopsis hypersensitive response. Molecular Plant-Microbe Interactions 16, 962–972.

Zhang, Z.-T., and Zhu, S.-Y. (2009). Drosomycin, an essential component of antifungal defence in Drosophila. Insect Molecular Biology 18, 549–556.

Zhou, R., Silverman, N., Hong, M., Liao, D. S., Chung, Y., Chen, Z. J., and Maniatis, T. (2005). The role of ubiquitination in Drosophila innate immunity. The Journal of Biological Chemistry 280, 34048–34055.

Zhuang, Z.-H., Sun, L., Kong, L., Hu, J.-H., Yu, M.-C., Reinach, P., Zang, J.-W., and Ge, B.-X. (2006). Drosophila TAB2 is required for the immune activation of JNK and NF-kappaB. Cellular Signalling 18, 964–970.

Zottini, M., Costa, A., De Michele, R., Ruzzene, M., Carimi, F., and Lo Schiavo, F. (2007). Salicylic acid activates nitric oxide synthesis in Arabidopsis. Journal of Experimental Botany 58, 1397–1405.